UNIVERSITAT POLITÈCNICA DE CATALUNYA BARCELONATECH

The role of superplasticizers and their degradation products on radionuclide mobility

David Manuel García Cobos

UNIVERSITAT POLITÈCNICA DE CATALUNYA
BARCELONATECH

THE ROLE OF SUPERPLASTICIZERS AND THEIR DEGRADATION PRODUCTS ON RADIONUCLIDE MOBILITY

David Manuel García Cobos

A thesis submitted in fulfilment of the requirements for degree of

Doctor of Philosophy

at the

Universitat Politècnica de Catalunya

Supervised by

Dra. Mireia Grivé

Dra. Lara Duro

Barcelona

2018

“Nothing in life is to be feared, it is only to be understood.

Now is the time to understand more, so that we may fear less.”

Marie Curie

Abstract

Nowadays, the long-term management of radioactive waste materials is envisaged in several countries (Belgium, France, Sweden, etc.) through the disposal of those wastes in deep disposal facilities. Such installations should ensure the safety of the waste disposal and additionally minimize a possible external waste perturbation. Concrete or concrete-based materials are widespread in those facilities, mainly used as a construction material but also in some specific cases used as an inert waste matrix or even as a safety barrier. Among other concrete components, superplasticizers (a type of organic polymer), are by default included in those facilities in huge quantities.

The hyperalkaline conditions developed in cementitious environments, can cause chemical transformations of polymeric materials (degradation, aging, etc.) with the subsequent production of organic compounds with new chemical properties. It is well recognized that, in general, organic compounds have a powerful capacity to form stable complexes with some radionuclides. It is thus expected that organics can play an important role in transporting radionuclides through the near and far field of a radioactive waste repository. Therefore, the understanding on the nature and strength of the interactions between radionuclides and organic admixtures present in the concrete formulations (and their degradation products) is of outmost importance.

Overall the work presented in this thesis tries to discern whether the presence of polycarboxylic ether-based (PCE) superplasticizers coming from the concrete used to build-up the deep disposal repository, may have some impact in the mobility of radionuclides. Additionally, the stability of these materials towards temperature, radiolysis and hydrolysis degradation processes has been studied to ensure the integrity of superplasticizers in the expected repository conditions.

As mentioned before, superplasticizers added into cement can degrade due to hydrolytic, thermal, radiolytic and microbial effects. This work presents a state-of-the-art of the degradation process of superplasticizers and a thermodynamic study on the effect of model compounds, considered as proxy superplasticizer degradation products, have on the mobility of several radionuclides (Ni, Eu, U). Short-chain organic compounds such as acetate, phthalate, oxalate, phenol, urea, etc., have been confirmed as possible superplasticizers degradation products. Our results indicate that the complexation capacity of the proxy superplasticizers degradation products considered (i.e. acetate, phthalate, phenol and urea) towards Ni Eu and U is almost negligible in alkaline conditions, while relatively important in the near-neutral pH range. In parallel, the degradation of polycarboxylate ether-based (PCE) superplasticizers (SPs) has been investigated in this work. Our results indicate that the studied SPs remain unaltered when exposed to hydrolysis processes. In the other hand, when these materials are exposed to high temperatures or radiation doses, important changes in the SPs structure have been observed although the main chemical groups remain unaltered.

The effect of superplasticizers on nickel hydroxide solubility has been evaluated in this work. The experiments have been performed in the following solutions a) synthetic cement porewater and b) concrete

leachates including a commercial polycarboxylate superplasticizer, namely Glenium®27, as an addition, and avoiding the presence this superplasticizer in solution. Results presented in this work indicate that once the Glenium®27 is added to water and then mixed with cement, this polymeric material is stabilized (e.g. adsorbed into the cement phases) and not released back to the aqueous solution, with negligible effects on the mobility of nickel. Contrary to that, when added directly into synthetic cement porewater samples at dosages producing total organic carbon values of $3 \cdot 10^{-3}$ mol·L^{-1} in solution an important effect is observed on nickel behaviour, increasing its solubility almost two/three orders of magnitude. Thermodynamic calculations indicate that the effect of such component on Ni is likely the effect that other organics (i.e. isosaccharinate, gluconate, oxalate) could have over this radionuclide, indicating that these organics may be good surrogates for understanding superplasticizer complexation capacity.

Agraïments

En primer lloc vull agrair a Amphos 21, i especialment a la Dra. Mireia Grivé i a la Dra. Lara Duro, per confiar en mi i donar-me l'oportunitat de realitzar aquesta tesis i de formar part de l'equip professional d'Amphos 21. Aquest treball no hauria estat possible sense la seva persistència i confiança, gràcies.

Special thanks are due to Ondraf-Niras, and specially for Dr. Stéphane Brassinnes, who has been both financially and technically supporting this study. It has been a pleasure working with you.

Vull agrair també a la UPC i al CTM, i especialment al Dr. Joan de Pablo i al Dr. Miquel Rovira, totes les facilitats que m'han donat per poder realitzar les tasques experimentals emmarcades en aquest treball. Gràcies per no tenir mai un no com a resposta i per la vostra gran predisposició a col·laborar en tots els àmbits d'aquest treball.

No puc oblidar-me de tota la gent que ha compartit amb mi, encara que hagi sigut per un temps molt breu, aquesta etapa des del CTM. A la gent de l'àrea de medi ambient Marta Viladés, Judith, Lydia, David, Cristina, Miriam, Marta "Speddy" Gonzaléz, Laura, Isabel, Jose, Frederic, Irene, Albert i com no Neus. Gràcies a tots per suportar-me durant els anys que vaig passar amb vosaltres i per contribuir d'una manera o d'un altre a realitzar tota aquesta feina. I would like to acknowledge Jony for her encourage and her smiles, you were in CTM for a short period but I will never forget the very nice time we pass together. Gràcies també a tota la gent de l'àrea de materials i a la de gestió interna que ha contribuït a la realització d'aquesta feina.

Aquest treball tampoc hagués estat possible sense la col·laboració de diferents departaments de la UPC. Dra. Susanna Valls i Dr. Diego Ocampo, del departament d'Enginyeria de la Construcció, gràcies per ajudar-me durant la preparació de les provetes de formigó i amb la caracterització dels materials de partida. Dr. Jordi Bou i Dra. Alexandra Espriu, del departament d'Enginyeria Química de l'ETSEIB, per l'ajuda durant la caracterització de les mostres orgàniques. Jordi sense la teva inestimable guia hagués sigut impossible entendre la química d'aquestes mostres. Gràcies també a l'INTE i especialment a la Dra. Mª Amor Duch per l'ajuda dispensada durant la radiòlisi d'algunes mostres orgàniques.

People from Subatech and the ARRONAX facility are also acknowledge for is commitment with the radiolytic investigations carried out in this work. Special thanks for Dra. Catherine Landessman, Dr. Guillaume Blain and Dr. Massoud Fattahi-Vanani. I would like to mention here all the people from the cement-organics working group we set-up in the pass between Loughborough University, RWM, Subatech, Andra, Ondraf-Niras and Amphos 21. We had very

fruitful and interesting meetings sharing our advances. Thanks to Mathew, Amy, Rebecca, David, Yulia, Catherine, Andrei, Pierre, Eric, Stéphane, Benny, Lara and Mireia.

Eric, wherever you are. I will never forget you, I will never forget your advices, I will never forget your passion for work, I will never forget your passion science…I will never forget you.

I la gent d'Amphos…que, us pensàveu que m'oblidava? Doncs no, no m'oblido de vosaltres. A tot l'equip de Gestió de Residus liderat per la Mireia: GRÀCIES. Seré breu, o almenys ho intentaré. Eli gràcies per ajudar-me en tot el que he necessitat durant aquest procés, has sigut clau per mi en molts moments de la feina i un gran suport. Olga, moltes gràcies per aguantar totes les meves tonteries i palles mentals sense enviar-me a fregir espàrrecs. Alba, gràcies, gràcies per estar sempre disposada a escoltar-me encara que només digués bajanades i per ajudar-me en tot el que he necessitat. Durant aquests anys hem passat molts bons moments però també moments molt complicats, la vida ens ha colpejat de diverses maneres però sempre has estat allà per mi quan t'he necessitat i mai ho oblidaré. Isaac, gracias por ayudarme con todo lo que he necesitado y por estar siempre dispuesto a discutir y escuchar mis extraños razonamientos. Gracias por aconsejarme y sobre todo gracias por ser como has sido durante estos últimos años. Marta, ay Marta, eres con la que menos tiempo he compartido de la tesis, pero quizás con una de las que más he discutido sobre las mil historias que iban saliendo. Muchas gracias por tu paciencia conmigo y por desprender y compartir esa energía tan positiva que tienes. Javi, gracias por la mano que me echaste con las probetas, sin tu ayuda no las hubiera mezclado, moldeado ni curado, gracias. Maria Rosa, tot i que ja no estàs Amphos, i que ets gairebé inclassificable he decidit posar-te en aquest bloc. Gràcies per tota la ajuda dispensada i el suport llunyà que em vas enviar des d'Alemanya. He d'anar escurçant així que, sense voler oblidar-me de cap company, gràcies a la resta de gent d'Amphos que d'una forma o d'un altre mà donat un cop de mà amb la feina realitzada.

Mireia, gràcies per confiar en mi no només durant el temps que ha durat la tesis sinó durant tot el temps que portem treballant plegats. Sense el teu suport i confiança no hagués evolucionat mai i mai hagués sigut capaç de créixer. Has sigut un suport professional i emocional molt important per mi durant aquests anys de muntanya russa d'emocions que he viscut i vull que sàpigues que sempre estaré en deute amb tu. Gràcies de tot cor.

I la família i amics, que sempre van els últims però potser son els més importants ja que han d'aguantar les paranoies mentals del doctorand. Gràcies als amics de la uni (i els que no) que sempre han estat allà després de tots aquests anys i que han sigut una part molt important de la meva vida. Aquesta tesi no hagués sigut possible sense el vostre suport: Sonia, Xevi, Marta, Jose,

Ester, Berto, Raquel. Laurent, gracias también a ti que, desde la distancia que nos separa, siempre te has preocupado y me has ayudado cuando lo he necesitado.

Hermanitos ¿quién os iba a decir que íbamos a llegar hasta aquí? Pues mirad aquí estáis. Gracias a los tres Antonio, Juan y Javi por haberme ayudado desde bien pequeño a ser la persona que soy, por indicarme el camino a seguir y por ayudarme a seguirlo. El pitu ha crecido, pero en el fondo sigue siendo el mismo con el que jugabais hace ya muchos años, aunque no se callará ni debajo del agua. Mama y papa, a los dos, gracias por educarme con los valores que me educasteis y gracias por darme todo lo que he necesitado siempre sin recibir nada a cambio. Los hijos somos muy desagradecidos y hasta que no tienes uno no eres capaz de abrir los ojos mirar atrás y ver lo injusto que fuiste muchas veces con tus padres. Los dos habéis sido y seguís siendo un ejemplo de lucha para mí, viniendo como vinisteis de una familia cordobesa humilde y trabajando con tesón para poder darle a vuestros hijos las oportunidades que vosotros no tuvisteis. Ojalá algún día yo os haga sentir igual de orgullosos de lo que yo me siento por teneros como padres. Senyora Montserrat i Txell, gràcies per aguantar totes les meves tonteries i per cuidar d'en Biel per que jo tingui temps d'escriure aquestes coses rares que faig. A mi suegro que des de allá donde está estoy seguro de que me da fuerzas para escribir las últimas líneas de esta tesis y le da fuerzas a toda la familia para cuidar de Biel, nuestro pequeño tesoro. El tiempo pasa, pero el recuerdo siempre persiste.

Anna gràcies per ajudar-me, des de que ens van conèixer a la universitat, a ser la persona que sóc. Has sigut un suport molt important per mi en les bones i en les dolentes, i mai et podré agrair suficient tot el que has fet per mi. La teva comprensió i la teva paciència es mereixen molt més del que jo he sigut capaç de donar-te durant aquests anys, però espero retornar-t'ho durant les etapes futures que ens esperen plegats. Biel carinyo, el meu tete. Ets l'alegria de casa, la coseta més maca que ha existit mai i el destroyer més gran que haguem conegut. Vas arribar a les nostres vides fa dos anys i les vas omplir d'entropia...i mira que jo era d'energia lliure... Tot el que fem i farem és per tu, espero que algun dia, quan siguis gran puguis mirar enrere i estar orgullós del teus pares. Us estimo un mol (d'àtoms) a tots dos.

David

TABLE OF CONTENTS

List of figures

List of tables

Glossary of terms

AAS	Atomic Absorption Spectroscopy
BSE	Back-Scattered Electrons
C_6H_5OH	Phenol
$C_2H_3O_2^-$	Acetate
$C_8H_4O_4^{2-}$	Phthalate
EDX	Energy-Dispersive X-ray
H_4N_2CO	Urea
GPC	Gel Permeation Chromatography
GC-MS	Gas Chromatography – Mass Spectrometry
H-NMR	H-Nuclear Magnetic Resonance
IC	Ionic Chromatography
ICP-MS	Inductively Coupled Plasma – Mass Spectrometry
ICP-OES	Inductively Coupled Plasma – Optical Emission Spectroscopy
IR	Infrared
NMR	Nuclear Magnetic Rresonance
PCE	Polycarboxylate ether-based
SEM-SEI	Scanning Electron Microscopy- Secondary Electron Imaging
SMF	Sulfonated Melamine Formaldehyde
SN	Sulfonated Naphthalene
SNF	Sulfonated Naphthalene Formaldehyde
SNFC	Sulfonated Naphthalene Formaldehyde Condensate
SP/SPs	Superplasticizer
TIC	Total Inorganic Carbon
TOC	Total Organic Carbon
TGA/DSC	ThermoGravimetric Analysis / Differential Scanning Calorimetry
UV-Vis	Ultraviolet-Visible
XRD	X-Ray Diffraction

Chapter 1: INTRODUCTION

1 Introduction

Radioactive waste materials have been generated during the last century in a considerable amount due to anthropogenic activities, i.e. energy production, medical uses, academic investigations. The hazard of those wastes to human kind is notably high because of the ionizing radiations produced by the presence of radionuclides in their composition. Moreover, for some specific radionuclides as ^{99}Tc or ^{237}Np (half-life of 220.000 and 2 million of years, respectively), those radiations may last for millions of years. Thus, an efficient and safe strategy to manage these waste materials is required to ensure the safety of present and future generations.

Several strategies have been discussed worldwide in the past to manage radioactive waste, being the most accepted the disposal of the waste in deep underground facilities located in stable geological environments (mainly in clay, granite or saline formations). Several countries such as Finland, Sweden or France, adopted this option and the construction of the facilities (Figure 1-1) are at different stages of development depending on the country [64]. In Belgium, the *Organisme National des Déchets RaDioactifs et des matières Fissiles enrichies* (ONDRAF, in English acronym NIRAS), which is responsible for the final disposal of radioactive waste materials by a mandatory law, agreed in following the same strategy and is currently investigating the feasibility of building such facility in a Belgian clay formation [16].

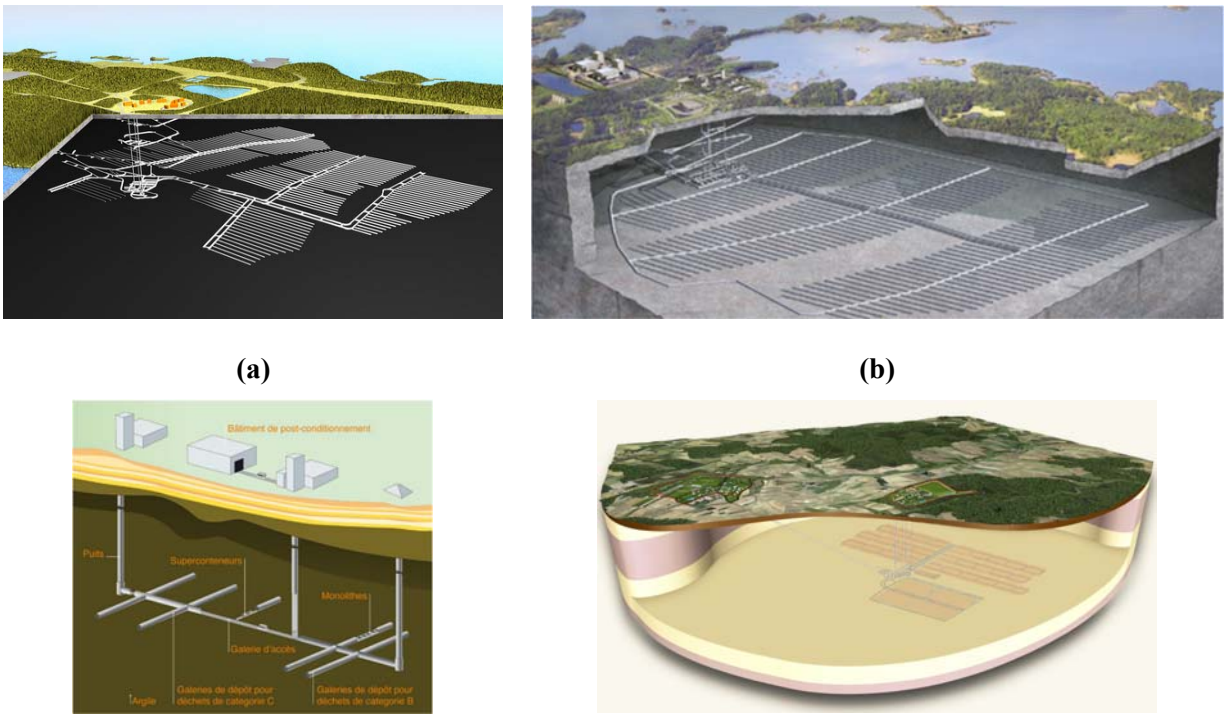

Figure 1-1. Different sketches from future radioactive waste disposal facilities as defined by the different national agencies, a) POSIVA OY from Finland (*http://www.posiva.fi/*), b) SKB from Sweden (*http://www.skb.com/*), c) Ondraf/Niras from Belgium (*https://www.ondraf.be/*) and d) ANDRA from France (*http://www.xn--cigo-dpa.com/en/*).

Cementitious materials are present in important amounts in most planned designs of radioactive waste disposal facilities. An example of this are galleries, shafts and/or the main repository structure which will be mainly build with those materials. Even for some specific wastes cementitious materials are used as immobilization matrices [16].

Superplasticizers are a type of organic chemical admixtures used by manufacturers to improve dispersion, hydration and workability properties of concrete [89]. Therefore, the presence of superplasticizers as a concrete component in nuclear waste disposal facilities is considered. The range of superplasticizer compositions is wide, although, in general those compounds are characterized by a long hydrophobic carbon back-bone with different hydrophilic end-members. During the last century, superplasticizer formulations have been continuously evolving in a search for improvement of concrete performance. Overall, four different superplasticizer categories (Figure 1-2) can be defined: (a) naphthalene-sulfonate based superplasticizers [93], (b) melamine-sulfonate based superplasticizers [4], (c) lignosulfonate based superplasticizers [57], and (d) polycarboxylate ether-based superplasticizers.

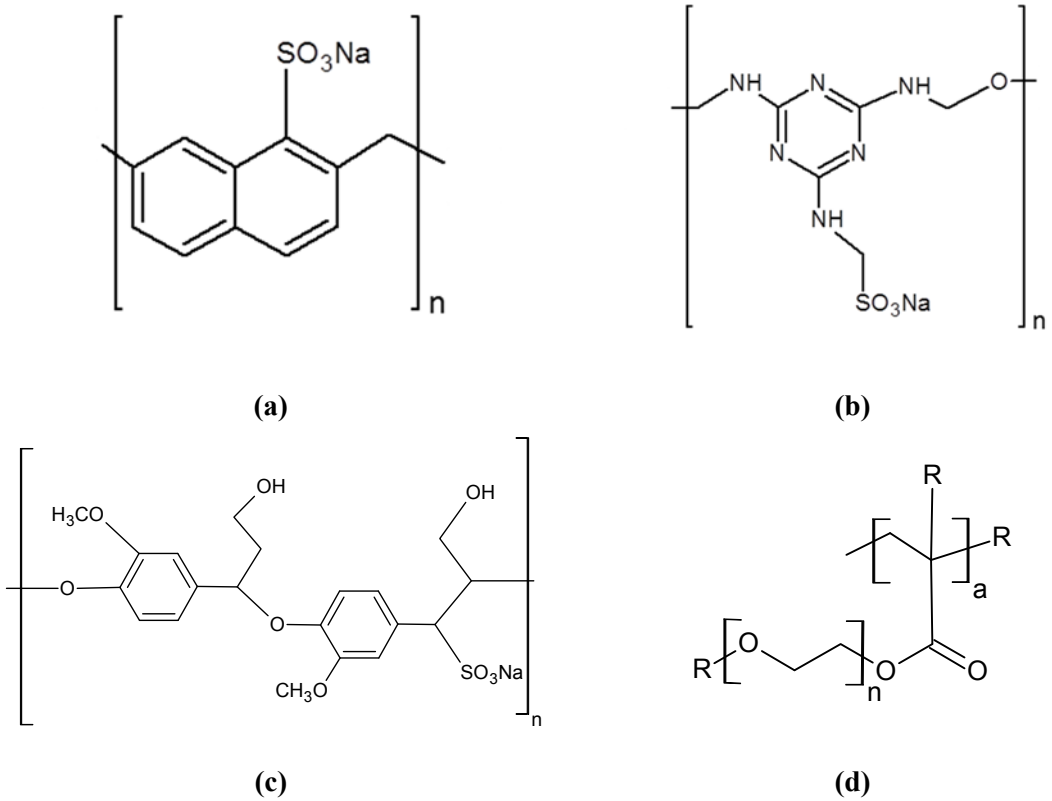

Figure 1-2. a) Naphthalene sulfonate SPs type structure, b) Melamine sulfonate SPs type structure, c) lignosulfonate, and d) polycarboxylate ether-based SPs type structure.

(a), (b), and (c) superplasticizers type were widely used in the past century being also named as 1st and 2nd generation superplasticizers. (d) superplasticizers type was described in the 90's, the so called 3rd generation superplasticizers, being currently widely used in the cement industry. In contrast with the older superplasticizer generations this kind of superplasticizers improves the dispersion of cement particles by electro-steric repulsions (Figure 1-3).

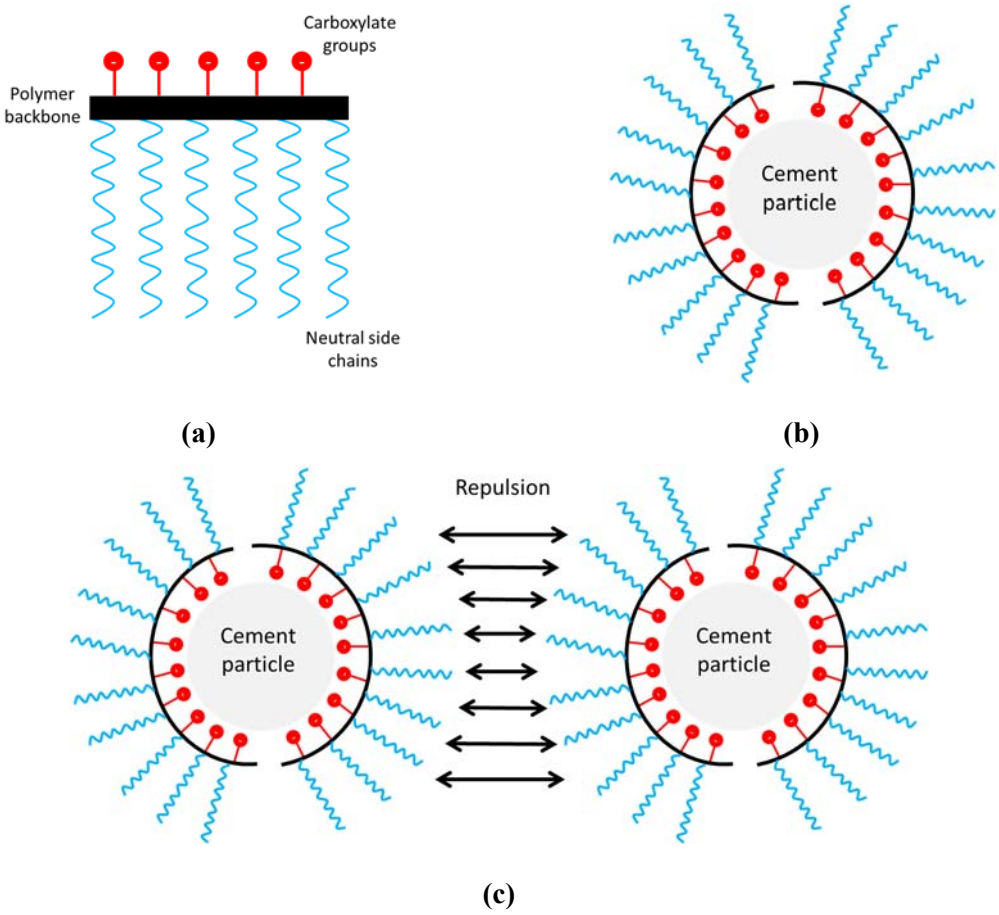

Figure 1-3. a) Simplified sketch of a polycarboxylate ether-based superplasticizers, b) representation of cement particle and polycarboxylate ether-based superplasticizers interaction, and c) repulsion between cement particles surrounded by polycarboxylate ether-based superplasticizers.

Under deep repository conditions different factors may favour superplasticizers degradation through thermal, irradiation or chemical (i.e. hydrolysis) processes [8]. As later explained in *Chapter* 3 , those processes may lead to the generation of small organic compounds which in turn may influence the behaviour of radionuclides present in the wastes, through different complexation mechanisms [8, 32, 106]. The current state of knowledge regarding the degradation of SPs in such systems is poor [33], although the understanding of this topic is crucial to assess the safety of nuclear waste disposal [106]. Therefore, the study of the nature of SPs degradation mechanisms as well as their degradation products deserves specific investigations.

The main objective of the present work is to study the stability of cement superplasticizers under repository relevant conditions and to assess the effect of the presence of complexing organic materials from cement on radionuclide behaviour. To do so, to sub-objectives have been pursued in this thesis:

- To gain knowledge on superplasticizer degradation products generated in deep disposal conditions through different mechanism (temperature, hydrolytic and irradiation induced degradation), and

- To study the effect of a commercial superplasticizer on the behaviour of a selected radionuclide, nickel, under relevant deep disposal conditions.

Chapter 2: METHODOLOGY

2 Methodology

The work presented in this thesis has been divided in two blocks:

a) the study of the degradation of cement superplasticizers under repository relevant conditions, and

b) the study of the effect of cement superplasticizers onto radionuclides behaviour (e.g. Nickel).

The approach followed to study the degradation of superplasticizers has been based in a two-step process. In a first step, an extensive literature review has been carried out to decipher possible superplasticizer degradation products and a desk study was done to analyse the effect of those products on selected radionuclide behaviour. *Chapter* 3 and Appendix II of the present document are entirely devoted to this topic. In a second step, based on the information gathered from the literature review, an experimental study has been done to analyse the degradation of a commercial polycarboxylate ether-based (PCE) superplasticizer (Glenium®27) and an in-house synthesized PCE superplasticizer. To this aim selected superplasticizers have been treated with different treatments likely to accelerate their degradation, i.e. hydrolysis, temperature and radiolysis. The resulting products have been analysed with several techniques. All the information related with this subject has been compiled in *Chapter* 4 of the present document.

A solubility study has been performed in this work to discern the possible effect of superplasticizers on the behaviour of selected radionuclides (nickel). Over and under-saturation experiments with nickel hydroxide have been carried out in the presence of concrete leachates and concrete synthetic porewater. Additionally, experiments with superplasticizer spikes in solution have been performed to complement system understanding. The experimental details of this study as well as the results gathered from these experiences are presented in *Chapter* 5 of this thesis.

The different raw materials, the in-house prepared samples and the analytical techniques used in this thesis are described below. The results on materials characterisation are detailed in Appendix I.

2.1 Cementitious materials

Cementitious materials have been supplied by NIRAS (Figure 2-1).

Figure 2-1. Raw materials as received at CTM.

The materials and amounts are shown in Figure 2-2 and detailed below:

- CEM I 42.5 (Manufactured by Holcim Dannes) - 25 kg
- Limestone filler (Manufactured by Premiacal) - 25 kg
- Sand 0/4 (particle size from 0 to 4 mm) - 25 kg
- Aggregates 2/6 and 6/14 (particle size from 2 to 6 and from 6 to 14 mm, respectively) - 25 kg each
- Glenium®27 (Manufactured by BASF) - 1 kg

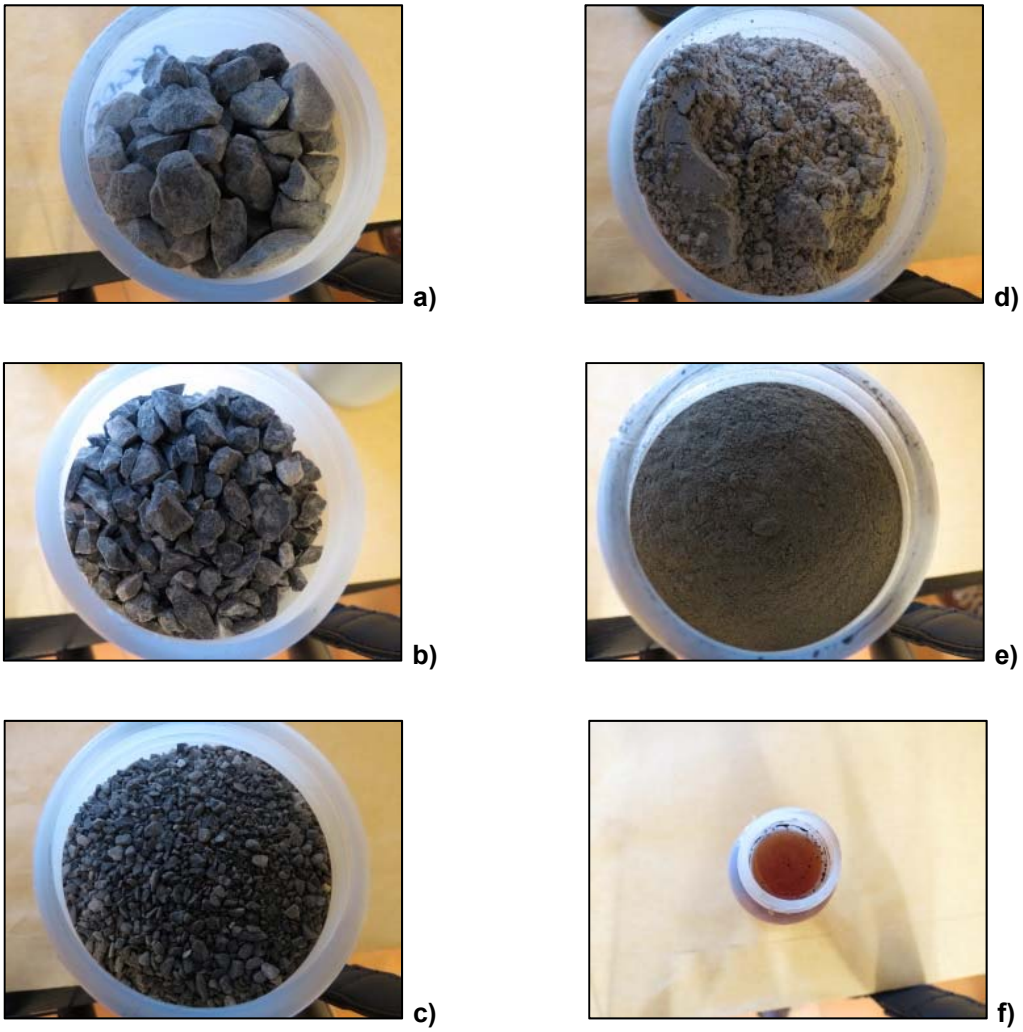

Figure 2-2. Raw materials as received. a) Aggregates 6/14,b) aggregates 2/6, c) sand 0/4, d) filler, e) CEM I and f) Glenium® 27.

Solid samples have been characterised by X-Ray Diffraction (XRD) (see *Section* 2.5.16 for experimental details) and acid digestions (HF and Aqua Regia) followed by ICP-OES (see *Section* 2.5.7 for experimental details) and ICP-MS (see *Section* 2.5.6 for experimental details) metals analysis.

Different techniques have been used to characterise raw Glenium®27 (Figure 2-2f):

- pH measurement, see *Section* 2.5.9 for experimental details.
- Total Organic Carbon, TOC, see *Section* 2.5.13 for experimental details.
- UltraViolet Visible spectroscopy, UV-vis, see *Section* 2.5.15 for experimental details.
- InfraRed spectroscopy, IR, see *Section* 2.5.8 for experimental details.
- High-Pressure Liquid-Chromatography High-Resolution Mass-Spectrometry, HPLC-HRMS, see *Section* 2.5.8 for experimental details.

Additionally, one part of Glenium®27 superplasticizer has been freeze-dried (see Figure 2-3) to allow for solid analyses. The freeze-dried sample was analysed with the following techniques:

- InfraRed spectroscopy, IR, see *Section* 2.5.8 for experimental details.
- ThermoGravimetric Analysis, TGA, see *Section* 2.5.14 for experimental details.
- Nuclear Magnetic Resonance of H, H-NMR, see *Section* 2.5.4 for experimental details.

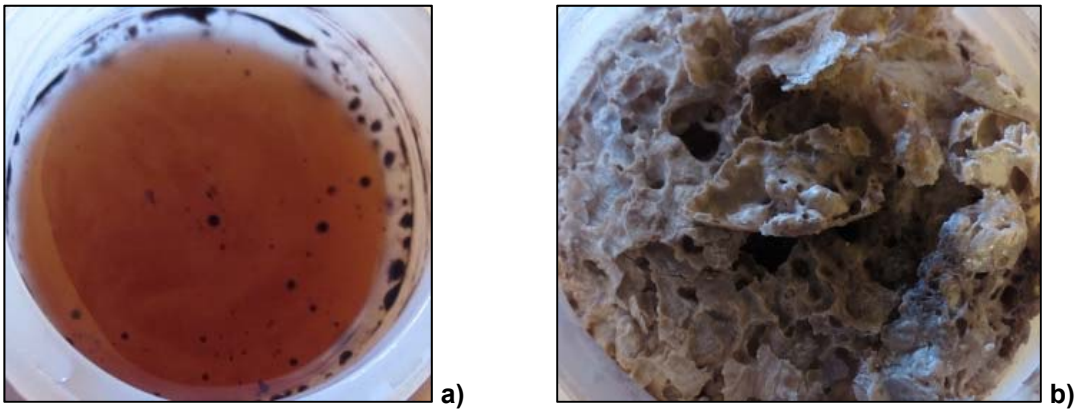

Figure 2-3. Visual aspect of a) raw superplasticizer, and b) the freeze-dried superplasticizer.

The complete set of characterisation results is detailed in Appendix I.

2.2 Concrete samples preparation

Concrete blocks have been prepared following the European standard UNE-EN 196-1 [2]. Briefly, raw materials (Table 2-1) have been mixed and left to a solidification period of 24 hours under atmospheric conditions (open atmosphere). Two different series have been produced one containing Glenium®27 (G samples) and another one without Glenium®27 (WG samples). For each of the series, 9 cast of ~ 4 kg per sample have been produced. After the solidification period, samples have been unmoulded and stored for curing in a climatic chamber for 28 days at 25ºC and 100% of humidity (Figure 2-4).

Table 2-1. Amounts of materials used in the sample preparation. Note that two different series were produced one containing Glenium®27 (G samples) and another one without Glenium®27 (WG samples).

	kg of used material	
	Sample series 1 (WG)	**Sample series 2 (G)**
Cement	5.3	5.3
Filler	1.5	1.5
Aggregate 0/4	10.6	12.7
Aggregate 2/6	8.0	5.1
Aggregate 6/14	8.5	8.5
Glenium® 27	-	0.1
Water	2.8	2.1
Water/Cement ratio (W/C)	0.5	0.4

Figure 2-4. Pictures from the concrete samples preparation and curation process.

Once the curing process was finished, samples have been hand-crushed and sieved at two different size fractions, between 1-4 mm and <1 mm (Figure 2-5). Contamination of the samples with metal particles from the crushing materials has been prevented in order to avoid unwanted experimental artefacts in the experiments. The samples have been characterised by using XRD and SEM-EDX (see *Section* 2.5 for details) and room stored prior to their use. Characterisation results are presented in Appendix I.

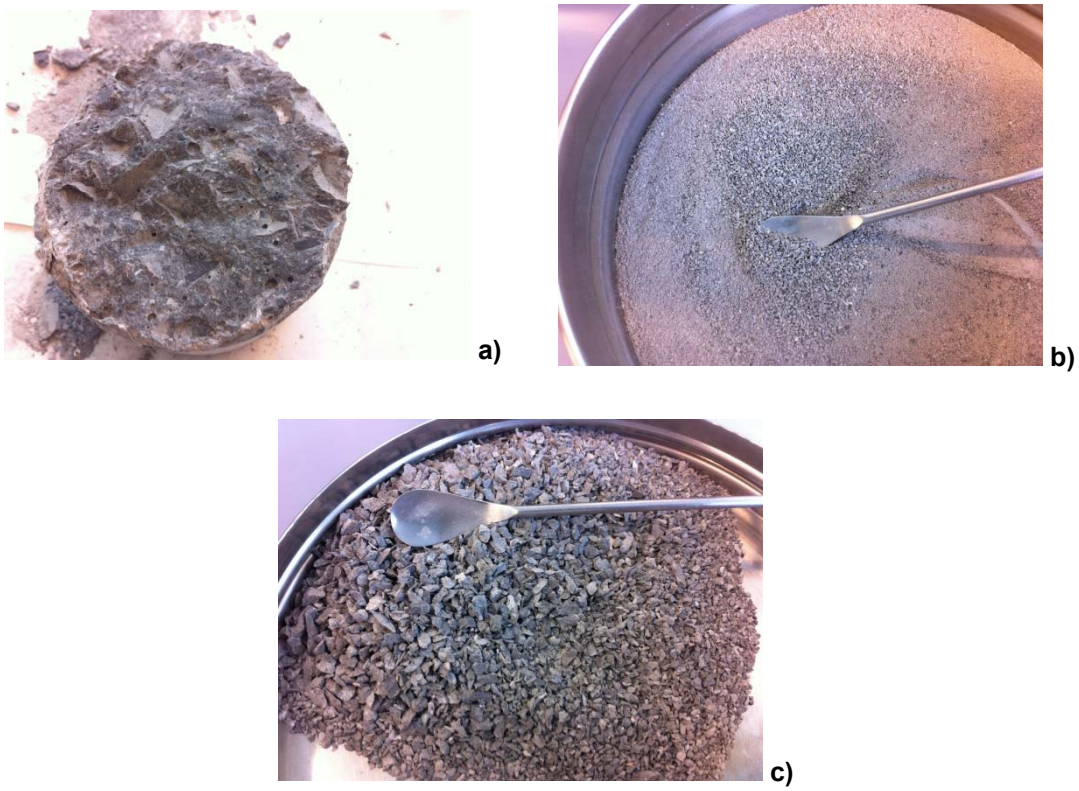

Figure 2-5. Pictures from the concrete samples crushing and sieving process.

2.3 Concrete porewaters preparation

Concrete synthetic porewater (CSPW) has been prepared according to [87]. Briefly, the necessary amounts of KOH (Scharlau, Extra pure), NaOH (Scharlau, Extra pure), $Na_2SiO_3 \cdot 9H_2O$ (Sigma, 98% pure), Calcite (Scharlau, Extra pure) and Portlandite (Scharlau, Extra pure) have been mixed and left in orbital agitation for 3 weeks. After that time, the solution has been filtered through 0.22µm Nylon filters suitable for use in alkaline conditions. Finally, Na_2SO_4 (Scharlau, reagent grade) and $Al_2(SO_4)_3 \cdot 10H_2O$ (Scharlau, Extra pure) have been added to the solution. All handling during CSPW preparation has been done in glove box conditions (Jacomex, GP[Concept]-II-S) to avoid $CO_2(g)$ presence.

Concrete leachates with and without Glenium®27 (G and WG leachates) have been obtained after i) drying samples at 60ºC during one hour in the oven, ii) placing samples in a desiccator for 24 hours, and, finally iii) contacting the hand-crushed concrete (1-4 mm and <1 mm fractions) with MilliQ water for 30 days (Figure 2-6) at a fixed solid/liquid ratio of 10 $g \cdot L^{-1}$ according to the granular material leaching standard UNE-EN 12457-2 [1].

Figure 2-6. Crushed concrete samples contacted with MilliQ water in continuous agitation.

All prepared waters (Table 5-2), CSPW and real leachates generated in this work, have been characterised in terms of pH, cations (ICP-OES and ICP-MS), anions (IC), Total Inorganic Carbon (TIC) and Total Organic Carbon (TOC). For additional experimental details related with the measurements the reader is refereed to *Section* 2.4. Concrete and leachates compositions detailed in Table 2-2 were in the range of values reported in the literature for similar systems [23]. Ni concentrations in all prepared initial waters were below the limit of detection. As shown in Table 2-2, no differences in leachate compositions have been observed as a function of the samples grinding size and thus the effect of this parameter in the studied conditions will not be further discussed.

Table 2-2. CSPW and real concrete leachates compositions obtained in this work. Note that CSPW, WG and G stand for Concrete Synthetic PoreWater, concrete leachates without Glenium®27 and concrete leachates with Glenium®27 respectively. For each of the leachates two different compositions have been reported as a function of the grinding size (<1 mm and 1-4 mm).

	CSPW	WG <1 mm	WG 1-4 mm	G <1 mm	G 1-4 mm
pH	13.3	12.4	12.4	12.5	12.4
			$mol \cdot L^{-1}$		
TIC	<LOD*	$1.7 \cdot 10^{-5}$	$3.2 \cdot 10^{-5}$	$1.7 \cdot 10^{-5}$	$2.3 \cdot 10^{-5}$
TOC	-	$5.2 \cdot 10^{-5}$	$4.7 \cdot 10^{-5}$	$1.2 \cdot 10^{-4}$	$1.2 \cdot 10^{-4}$
Na	$1.2 \cdot 10^{-1}$	$1.2 \cdot 10^{-4}$	$1.0 \cdot 10^{-4}$	$1.2 \cdot 10^{-4}$	$9.4 \cdot 10^{-5}$
K	$8.2 \cdot 10^{-2}$	$4.6 \cdot 10^{-4}$	$4.2 \cdot 10^{-4}$	$4.3 \cdot 10^{-4}$	$3.7 \cdot 10^{-4}$
Ca	$1.4 \cdot 10^{-3}$	$7.5 \cdot 10^{-3}$	$6.6 \cdot 10^{-3}$	$6.1 \cdot 10^{-3}$	$7.7 \cdot 10^{-3}$
SO_4	$1.8 \cdot 10^{-3}$	$5.9 \cdot 10^{-6}$	$7.7 \cdot 10^{-6}$	$8.2 \cdot 10^{-6}$	$8.3 \cdot 10^{-6}$
Fe	<LOD	<LOD	<LOD	<LOD	<LOD
Al	$7.7 \cdot 10^{-6}$	<LOD	$4.8 \cdot 10^{-6}$	<LOD	$4.8 \cdot 10^{-6}$
Cl	-	$2.1 \cdot 10^{-4}$	$2.3 \cdot 10^{-4}$	$1.7 \cdot 10^{-4}$	$1.5 \cdot 10^{-4}$
Si	$6.2 \cdot 10^{-6}$	<LOD	<LOD	<LOD	<LOD
Ni	<LOD	<LOD	<LOD	<LOD	<LOD

* <LOD. Below limit of detection

2.4 Synthesis of a reference PCE superplasticizer

A PCE reference superplasticizer (Figure 2-7) has been prepared following the recipe in [76]. Briefly, the necessary quantities of Poly(ethylene glycol) methyl ether methacrylate (PEGMA) (Sigma-Aldrich, average M_n 360), sodium methacrylate (Sigma-Aldrich, 99%), methallyl sulfonic acid (MASA) (Sigma-Aldrich 98%) and sodium persulfate (Sigma-Aldrich, Bioxtra >98%) have been placed in a spherical round bottom flask. The mixture has been stirred and heated up to 80ºC for 2 hours (Figure 2-8).

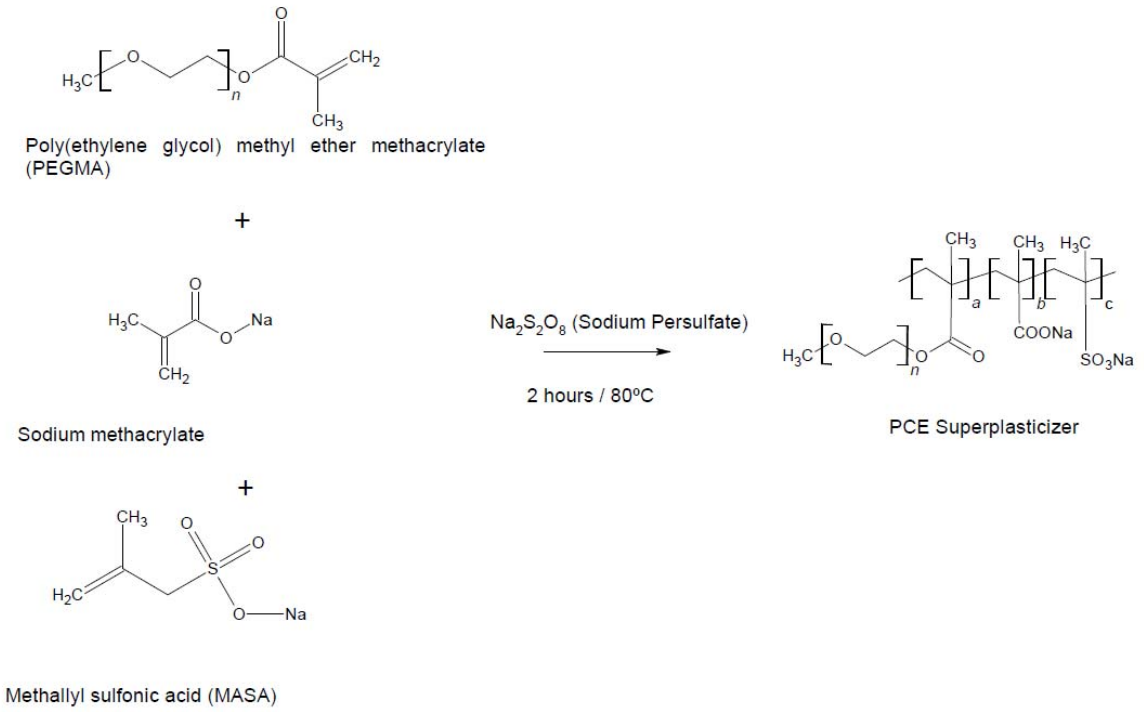

Figure 2-7. Synthesis reaction followed in this work for the reference PCE.

Once the reaction is completed, the superplasticizer has been purified through a three-step dialysis process. First, the sample has been introduced in a Slide-A-Lyzer™ Dialysis Flask (Thermo Scientific). The flask has been sealed and immersed in a MilliQ water solution (buffer solution) for three hours with continuous stirring (Figure 2-9). After that time, the buffer has been renewed and the flask again immersed in the buffer solution for three hours. Three hours later the buffer has been renewed again and the flask containing the synthesized superplasticizer has been left in this solution overnight. Finally, the purified superplasticizer has been collected from the flaks with a syringe and preserved in the glovebox until being freeze-dried. The final product has been characterised by using H-MNR (see *Section* 2.5.4 for experimental details) and IR (see *Section* 2.5.8 for experimental details) spectroscopies; results are presented in Appendix I.

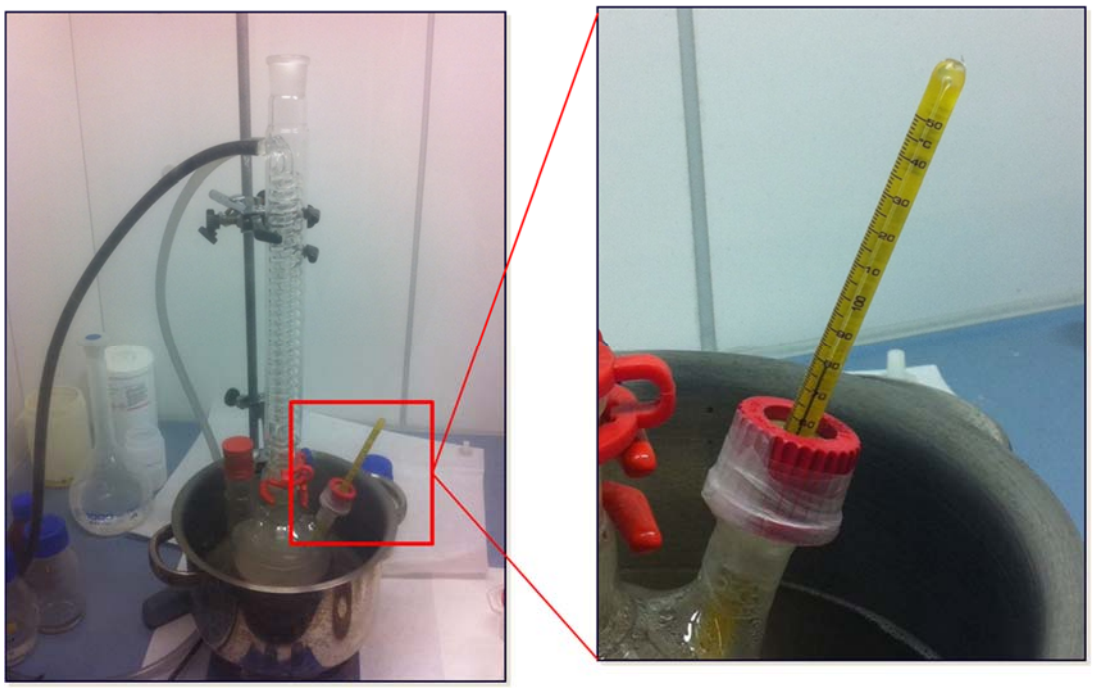

Figure 2-8. Detail of the PCE synthesis, heating process up to 80ºC.

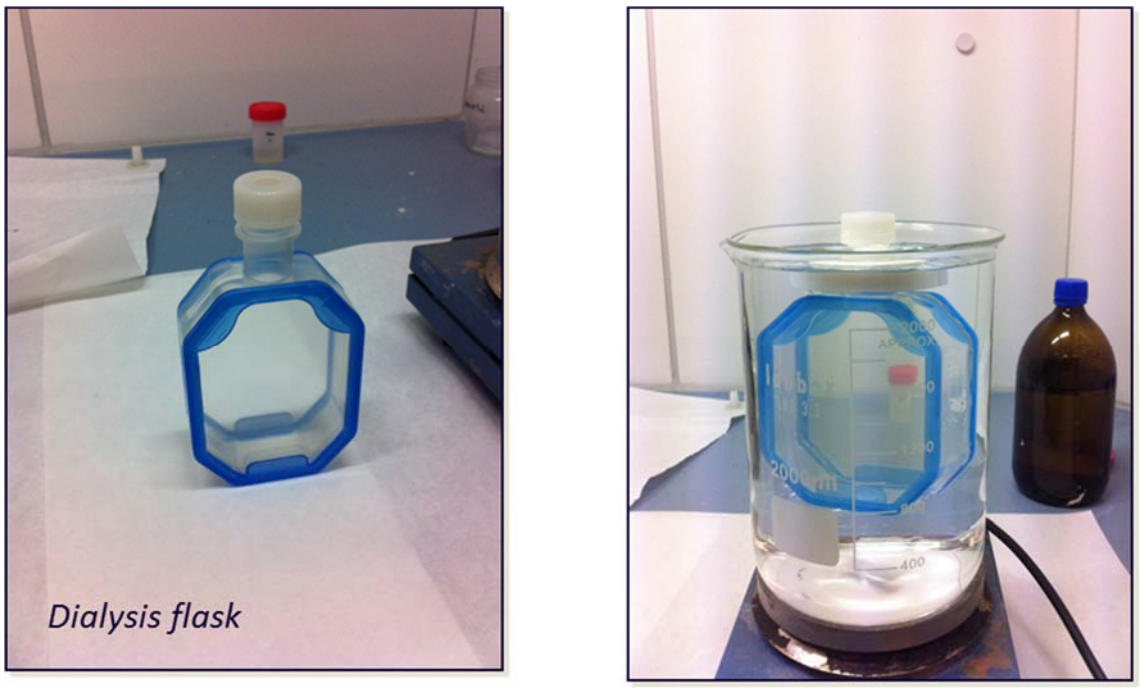

Figure 2-9. Detail of the PCE purification, dialysis process.

2.5 Analytical techniques

2.5.1 AAS

Atomic Absorption Spectroscopy (AAS) (model AA-6200 manufactured by Shimadzu) has been performed by diluting samples in 1M HCl solutions (Scharlau Extrapure) with 10% lanthanum addition (La_2O_3, Scharlau Extrapure, in 1M HCl solution) as interference suppressor. This technique has been used to analyse Calcium, Sodium and Potassium dissolved concentrations.

2.5.2 GPC

Gel permeation chromatography (GPC) (Agilent Infinity 1260) has been performed by dissolving samples in a phosphate buffer (pH = 7.4). Sample concentration was 2 $mg \cdot mL^{-1}$ and the injection loop was charged with 100 µL of solution each time. The mobile phase was a phosphate buffer (0.05 $mol \cdot L^{-1}$, pH = 7.4) with a 0.8 $mL \cdot min^{-1}$ flux. The chromatographic column was a Aquagel manufactured by Polymer Laboratories. A UV and a refraction detector have been used. Equipment calibration has been done with poly(ethylene oxide) samples.

2.5.3 H-NMR

Proton-Nuclear Magnetic Resonance (NMR) has been done with a AMX 300 Fourier Transform equipment manufactured by Bruker working at 300 MHz. Samples have been dissolved in deuterated water (D_2O) at a 20 $mg \cdot mL^{-1}$ ratio and placed in the corresponding vials. Around 128 pulses have been acquired for each sample. This technique has been employed to characterise the superplasticizers studied in this work.

2.5.4 HPLC-HRMS

High-Pressure Liquid-Chromatography High-Resolution Mass-Spectrometry (HPLC-HRMS) has been performed with a LQT Orbitap Velos manufactured by Thermofisher Scientific. A Luna C18, 5 microns, 150x2mm chromatographic column has been used under variable mobile phase gradient using two mobile phases (A: H_2O, 0.1% formic acid; B: MeCN, 0.1% formic acid). The flux has been fixed at 0.3 $mL \cdot min^{-1}$ and the injection loop has been charged with 10 µL of solution each time. Mass spectrometry ionization has been done with an electrospray (ESI) in both positive and negative polarity. This technique has been employed to characterise the raw Glenium®27 in aqueous solution.

2.5.5 IC

Ionic Chromatography (IC) (ICS-2000 system, manufactured by Dionex) has been performed by diluting samples in MilliQ water. This technique has been employed to determine and monitor the concentration of Sodium, Potassium, Sulphate and Chloride in aqueous solution.

2.5.6 ICP-MS

Inductively Coupled Plasma – Mass Spectrometry (ICP-MS) (model 7500cx, manufactured by Agilent Technologies Inc.) has been done by diluting samples in 2% HNO_3 solutions (ppb-trace analysis grade, Scharlau). Through ICP-MS Ni and other cations concentration in solution has been analysed.

2.5.7 ICP-OES

Inductively Coupled Plasma – Optical Emission Spectroscopy (ICP-OES) (model iCap 6000 series, manufactured by Thermo Scientific) has been done by diluting samples in 2% HNO_3 solutions (ppb-trace

analysis grade, Scharlau). Through ICP-OES metal and semi-metal concentrations in solution have been analysed.

2.5.8 IR

InfraRed (IR) spectroscopy has been carried out with two different equipments:

- Spectrum BX manufactured by Perkin Elmer. Spectra have been acquired in attenuated reflectance mode (ATR) by using a ZnSe holder.
- Jasco FTIR 4100. Spectra have been acquired in attenuated reflectance mode (ATR) by using a MKII Gloden manufactured by Specac.

This technique has been used to characterise main functional groups within Glenium®27.

2.5.9 pH

The pH-meter employed was a Crison model GLP 22 with 52-22 electrode, the system has an associate error of ≤0.1. The equipment has been calibrated with buffer solutions at pH 11 (Scharlab, Boric acid/Sodium hydroxide/Potassium chloride), 12 (Scharlab, di-Sodium hydrogen phosphate/Sodium hydroxide) and 13 (Scharlab, Potassium chloride/Sodium hydroxide). The pH has been analysed in all solubility and degradation experiments as well as in some raw materials (i.e. Gelenium®27).

2.5.10 SEM-SEI / EDX / BSE

Scanning Electron Microscopy (SEM) has been used to obtain topographic images (SEI) of samples surface as well as different chemical composition displayed on a specific surface (EDX). This technique offers rather information of the materials micro-texture and composition. The analysis of samples has been performed using a Field Emission Scanning Electron Microscope (FE-SEM - ZEISS Ultraplus) which has an EDX (Energy Dispersive X-ray Spectroscopy) analyser for semi-quantitative chemical composition analysis (X-Max EDX detector, from OXFORD Instruments). Images have been taken using different electron detectors: (a) SE2, secondary electrons detector which provides topographic images and (b) In-Lens, High resolution, detector for SE1 electron detection in HV mode (90º Vertical). Surface of the dried samples has been metalized with a thin layer of Au/Pd.

2.5.11 Raman

Raman spectroscopy has been done by using a i-Raman®Plus model manufactured by BWTEK. Two different methodologies have been used depending on the sample state. Solid samples have been located on a Raman microscope (BAC151B, BWTEK) for analysis while liquid samples measurements have been done by using a Raman Cuvette holder (BCR100A, BWTEK). Raman spectra have been acquired in approx. 10 minutes. As in the case of the IR, this technique has been used to characterise main functional groups within Glenium®27.

2.5.12 TIC

A model Multi N/C 3100 manufactured by Analytik Jena has been employed to determine the Total Inorganic Carbon (TIC) in the studied solutions. Samples and standards have been diluted in MilliQ water.

2.5.13 TOC

Total Organic Carbon (TOC) in the studied solutions has been analysed by using a Shimadzu 5050 equipment. Samples and standards have been diluted in MilliQ water.

2.5.14 TGA / DSC

Sample weight change has been measured with a simultaneous TGA/DSC thermal analyser model StrareE manufactured by Mettler Toledo. The working temperature lapse comprised 30 to 1000 ºC with a heating rate of 10 $ºC \cdot min^{-1}$. Approximate 10 mg of samples have been placed into ceramic holder for its analysis. With this technique, besides the water content of the samples, the different compositional trends have been analysed.

2.5.15 UV-Vis

UltraViolet Visible (UV-Vis) spectroscopy has been done with a model UV-2450 manufactured by Shimadzu. Samples have been located in appropriate quartz holders and if necessary diluted with MilliQ water. This technique has been used to characterise main functional groups within Glenium®27.

2.5.16 XRD

Samples crystalline and semi-crystalline phase composition has been determined in an X-Ray diffractometer (PANalytical X'Pert PRO MPD Alpha1) with an X-Ray generator formed by a Copper anode and a Wolfram cathode which worked at 40-45 kV and 40 mA. PIXcel and X'Celerator detectors have been used for the different samples using monochromator in continuous scanning within a 2-theta range from 4 to 100 degrees.

Chapter 3: THE POTENTIAL ROLE OF SUPERPLASTICIZERS AND THEIR DEGRADATION PRODUCTS ON RADIONUCLIDE MOBILIZATION

"The work presented in this Chapter has been submitted for publication in Applied Geochemistry, 16th International Conference on the Chemistry and Migration Behaviour of Actinides and Fission Products in the Geosphere, Special Issue Volume, and is included in Appendix III of this thesis"

3 The potential role of superplasticizers and their degradation products on radionuclide mobilization

3.1 Superplasticizers in nuclear waste disposal environments

As already presented in the introductory chapter on this thesis, in nuclear waste disposal facilities concrete is used as a construction material (construction and stabilisation of galleries and tunnels shotcrete), as a confinement matrix to immobilize some type of wastes but also as a safety barrier to reduce the potential mobility of radionuclides in the eventual scenario of radionuclide release [12]. Superplasticizers, see *Chapter* 1 for a detailed explanation on the definition and the chemistry of those components, are an important concrete component.

Little information is available regarding the degradation of SPs in cementitious systems [33], although the interest on this topic has recently increased [106]. It is well recognized that hyperalkaline conditions developed in cementitious environments can cause chemical transformations of organic substances, i.e. polymeric SPs, (degradation, aging, etc.) with the subsequent production of small organic compounds with new chemical properties [38, 39, 109].

The role of SPs degradation processes and their corresponding degradation products on radionuclide mobility through the near and far field of a radioactive waste repository is therefore a matter of concern for performance assessment of radioactive waste repositories. The work presented in this chapter aims at investigating to which extent the degradation products of SPs may affect radionuclide behaviour in concrete environments.

3.2 Superplasticizers degradation: Literature survey

In this section, a literature research focused on SPs hydrolytic, thermal, radiological and microbial degradation is provided. Overall there is an important lack of SPs degradation studies. To complement the literature research, studies focused on main organic SPs groups' (i.e. naphthalene, melamine, etc.) degradation have been also reviewed.

To the best of our knowledge studies dealing with the degradation of PCE SPs are not available yet. Therefore, specific degradation products from PCE SPs degradation have not been found.

3.2.1 Hydrolytic degradation

Cementitious environments promote highly alkaline systems due to the dissolution-precipitation processes occurring within a cementitious matrix in contact with water. Overall, four pH ranges may be defined depending on the cement degradation state: (i) fresh or degradation state I, characterised by a high alkaline pH range (> 13) produced by the dissolution of Na and K alkalis, (ii) degradation state II, in where portlandite ($Ca(OH)_2$) dissolution controls the evolution of the system, buffering the pH around values of 12.5, (iii) degradation state III, after total dissolution of portlandite, C-S-H gels dissolve buffering the

system from pH 12.3 to 10.5 as a function of the Ca/Si ratio within the C-S-H gel, and, finally (iv) degradation state IV, where the formation of calcite within the cement matrix buffers the system pH at values < 10 [89]. For the current research, only those studies at pH > 10.5 have been considered in order to magnify SPs hydrolysis.

Yilmaz and co-workers [109] studied the degradation of Sulfonated Naphthalene Formaldehyde (SNF) and Sulfonated Melamine Formaldehyde (SMF) SPs. According to their results, SNF SPs were not altered in alkaline solutions (1 $mol \cdot L^{-1}$ KOH) while solid precipitation was observed in SMF solutions at similar pH values. Analysis of the precipitated product confirmed the alteration of the original SMF chemistry. However, the chemical characterisation of the precipitated solid was not entirely clear and thus the authors did not report conclusive SPs degradation pathways.

Naphthalene degradation was studied by Lair and co-workers [56]. The authors investigated different parameters affecting naphthalene degradation, among others the system pH (from 2 to 12). From their results Lair and co-workers [56] concluded that an increase of the system pH increased the degradation rate of naphthalene. A possible explanation for this phenomenon reported by the authors is that the increase of OH^- ions in solution increase the presence of $OH^{\bullet}$ radicals favouring naphthalene degradation. Intermediate degradation products were determined by GC-MS (Gas Chromatography – Mass Spectrometry) analyses; dozens of compounds were identified being 2-formylcinnamaldehyde and 1-naphtalenol the most abundant (see Appendix II).

Melamine Formaldehyde-Acrylic coatings degradation were studied by English et al. [28] with different analytical techniques (^{13}C NMR, IR). Under standard weathering conditions, only accounting for hydrolysis at atmospheric conditions, the degradation reaction reported by the authors was r. 1. This reaction involved the substitution of the terminal methyl by water releasing formaldehyde. No modifications of the melamine back-bone were found by the authors. Later Gerlock et al. [35], confirmed the same degradation pathway by using photo-enhanced hydrolysis.

$$\text{Melamine-}CH_2OCH_3 + H_2O \Leftrightarrow \text{Melamine-}CH_2OH + CH_3OH \qquad \textbf{r. 1}$$

3.2.2 Thermal degradation

Temperature elevations (around 100ºC) in the surroundings of a high-level waste repository are expected due to the presence of the exothermic wastes [15, 36]. In order to minimize the effect of temperature on the repository performance, in the current facilities waste management organizations designed repositories to ensure a temperature below 100ºC in the internal package surfaces and below 90ºC in the host rock [9]. Thermal organic polymer degradation mostly occurs at temperatures above 100ºC [47] and thus for a better temperature degradation analysis in the following survey studies at higher temperatures (>100ºC) have been also included.

Lair and co-workers [56], studied the effect of temperature (from 10 to 40ºC) on naphthalene degradation. They could not draw clear conclusions on the temperature effect, as volatilization of naphthalene could affect the results. Nevertheless, in agreement with what was mentioned in *Section* 2.1, the authors identified 2-formylcinnamaldehyde and 1-naphtalenol as the most abundant intermediates during naphthalene degradation (see Appendix II).

Onwudili and Williams [66], investigated the reaction mechanisms of phenanthrene and naphthalene hydrothermal degradation from 350 to 380ºC. The authors used sealed reactors reaching highly pressurized systems (170-225 bar). Weak naphthalene decomposition was reported to occur after 1 h at 380ºC, as 90% of naphthalene remained in solution. The presence of a large excess of oxidant in solution favours naphthalene degradation under those temperature conditions. Naphthalene decomposition products were determined by GC-MS. The reaction path mechanism shown in Figure 3-1 was proposed for the oxidative degradation of naphthalene.

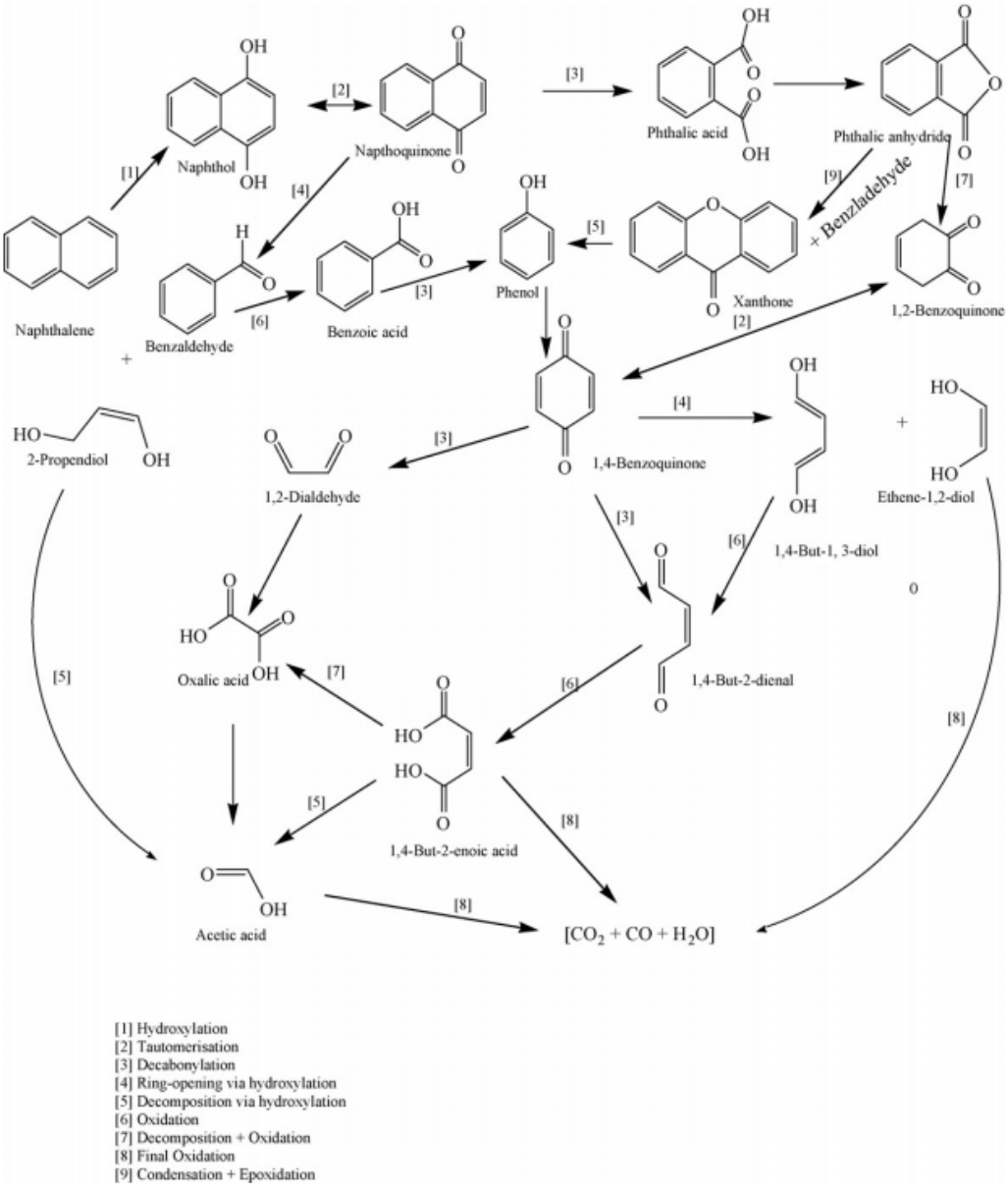

Figure 3-1. Naphthalene degradation reaction mechanism proposed by [66] under hydrothermal conditions.

Brebu and Vasile [22], published a literature survey on lignin thermal degradation products. Those authors reported lignin degradation to start between 200 and 275ºC, the main process occurring around 400ºC, yielding a variety of organic compounds (i.e. aromatic hydrocarbons, phenolics, hydroxyphenolics and guaiacyl/syringil-type compounds). Pyrolysis up to 340ºC of three different lignin-based compounds (lignosulfonate among others) was done by Brebu and co-workers [21]. Degradation products were characterised by thermogravimetric and chromatographic analysis. The authors reported the formation of ammonia and sulphur dioxide around 250ºC (see Appendix II) followed by derivatives of the structural compounds in lignin (i.e. phenols derivatives as pyrocatechol).

Deamination followed by condensation was reported by Costa and Camino [26] in their melamine thermal study. According to their thermogravimetric results, the authors suggests the formation of ammonia in a temperature range between 350-400ºC. Analysis of the residual product by IR showed the presence of

unreacted solid, melamine, and the formation of a water-insoluble product coming from melamine condensation. The identification of this water-insoluble product was not clearly defined in the study although the authors claimed the formation of "melem", an organic molecule formed by different cyameluric rings [31, 94].

3.2.3 Radiolytic or radiolytic induced degradation

Ionizing radiation released by nuclear waste may lead to the alteration of the different elements present in storage conditions (i.e. water radiolysis and subsequent generation of $OH^{\bullet}$).

Palmer and Fairhall [70], examined the production of gas due to the irradiation of small OPC cylinders and blast furnace slag grouts containing sulfonated naphthalenes formaldehyde condensates (Na-SNFC) and sulfonated melamine formaldehyde condensate (SMFC) SPs. The radiation field was 104 $Gy \cdot hr^{-1}$ and total dose applied over the samples was up to 9 MGy. The results showed that both CO_2 (g) and H_2 (g) were generated by irradiation (up to 6.7 mL $gas \cdot g^{-1}$ superplasticizer). The authors commented that the radiation did not appear to affect the strength or stability of the grout.

Naphthalene degradation was accounted for by Kanodia and co-workers [53] by means of radiolitically produced $OH^{\bullet}$ radicals. An oxidative process was then favoured yielding the conversion of naphthalene to naphthalenol. The same degradation product was found by Balakrishnan and Reddy [11] in aqueous γ irradiated solutions containing naphthalene at high temperatures (see Appendix II).

3.2.4 Microbial degradation

Microbiology within nuclear waste disposal has been a matter of important studies during the last five decades. Biogeochemical effects on the chemistry and the long-term evolution of repository materials as well as on the transport of radionuclides have been extensively studied [60, 74, 105]. Among other processes mediated by microbes, biodegradation of bituminized waste forms [104] yielding small organic compounds, is a case comparable to the one studied here, involving SPs biodegradation.

Haveman and co-workers [46], studied Disal (a naphthalene based SPs) degradation in the presence of *Pseudonomas* bacteria. The authors reported an increase of bacteria population in anaerobic conditions and in the presence of nitrate as electron acceptor. The degradation of naphthalene under denitrifying conditions or coupled to sulphate reduction have been reported by others [14, 61, 62, 81, 86]. In all those studies [14, 61, 62, 81, 86] naphthalene mineralization is observed but some authors [14] also reported naphthalenol as an intermediate product during naphthalene degradation (see Appendix II). Ruckstuhl and co-workers [83], studied the leaching and biodegradation of SN and SNFC from concrete materials used in tunnel constructions. Those authors reported that in-situ biodegradation, mediated by the microorganism presents in the studied samples, was the most effective mechanism to remove SNFC components from groundwater. Total depletion of mono-sulfonated monomers was quickly observed while the di-sulphonated analogues were proven to be persistent. Unfortunately, information about possible degradation products was not detailed by the authors, which may indicate a possible total mineralization of the original SPs.

Pseudomonas sp. HOB1 bacterium was used by Pathak and co-authors [73] in their naphthalene degradation studies. The authors reported total naphthalene mineralization indicating that temperatures about 35-37ºC and alkaline pH favoured naphthalene degradation. No intermediate products were detected by those authors.

The metabolism of melamine degradation by *Klebsiella terragena* was studied in detail by Shelton et al. [85]. The authors reported a deamination pathway (Figure 3-2) of the triazine ring through hydrolytic reactions mediated by the studied bacteria yielding the following degradation products: ammeline, ammelide, cyanuric acid, biuret and urea (see Appendix II). Early in the 80's, Jutzi et al [52] proposed a similar degradative pathway using *Pseudonomas sp. Strain A.2* bacteria.

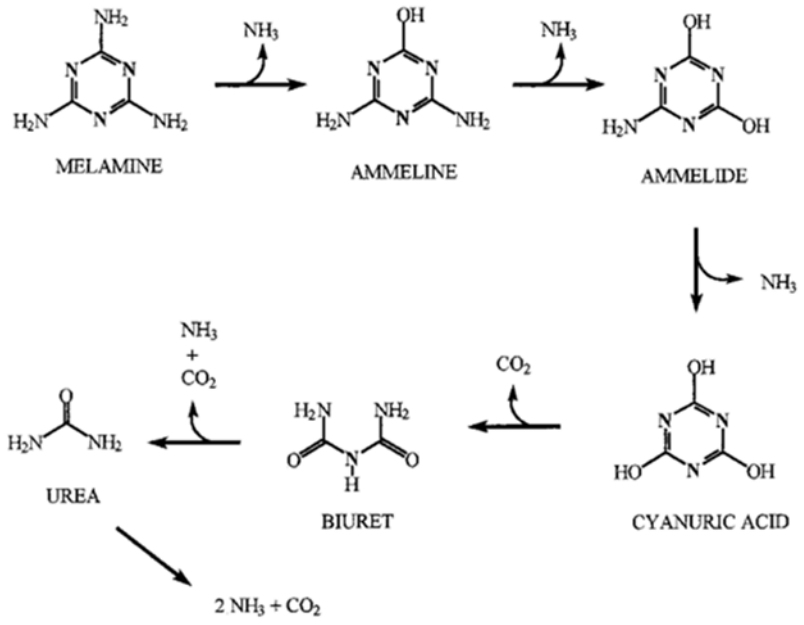

Figure 3-2. Melamine degradation reaction mechanism proposed by [85] under microbial mediated conditions.

The degradation of lignin through the fungus *Formes annosus* was studied in the 80's by Haars and Hüttermann [45]. Although not much detail is provided in that work phenolic derivatives were detected by the authors in the presence of the so-called fungus. Early in the 70's, Watkins [103] reported that lignosulfonates were more resistant than lignin to microbial decomposition due to a) the sulphonation of side chains of aromatic monomers, and b) the hydrolysis of the ether linkages and the formation of new carbon-carbon bonds between aromatic rings.

The list of possible superplasticizer degradation products detailed in Appendix II could be divided in three categories: i) aromatic compounds, ii) aliphatic compounds, and iii) inorganic species. The first (i) and the second (ii) categories include degradation products derived from naphthalene and melamine based SPs, while in the third (iii) category species derived from lignosulfonate and/or melamine based SPs degradation are included. Overall, aromatic compounds are more reactive than aliphatic species. However,

the presence of carboxylic terminations in the aliphatic compounds included in Appendix II may increase the reactivity of those species, producing thus quite reactive aliphatic degradation products.

Although no specific degradation studies on PCE SPs have been found in the literature, aliphatic organic compounds previously specified can be taken as a proxy for PCE SPs degradation products.

3.3 Discussion

In the previous *Section* 3.2 an extensive list of possible SPs degradation products has been compiled based on independent literature reported data (see Appendix II). Four degradation products have been selected to further study their possible effect on radionuclides aqueous chemistry, including both aromatic and aliphatic organic compounds, representative of possible PCE SPs degradation:

- Phthalic and acetic acids, formed during naphthalene (proxy for SNF structure) hydrothermal degradation. It is well recognized that both acids have a powerful capacity to interact with a variety of radionuclides [17, 65, 71, 80, 96, 108]. Given that those species are generated through a thermal process, the formation of those species is expected to occur during the temperature transient period (~100 years) under repository conditions.
- Phenol, formed during the biodegradation of both lignin and naphthalene (proxy for SMF and SNF structures, respectively). In general little is known about phenol interaction with radionuclides although some authors reported strong affinity towards actinides [13, 69, 84]. The formation of this species in deep repository conditions through SPs polymers degradation is expected to occur only through microbial-mediated mechanisms. In deep repository conditions microbes will be first fed by small organics, already present in the system from other sources, and later by big polymers like SPs. Thus, phenol formed due to lignin or naphthalene biodegradation is expected to appear in the repository in a long-time scale.
- Urea, formed during melamine (proxy for a SMF structure) biodegradation. The interaction between lanthanides and urea has recently been a matter of concern and some authors reported relatively weak affinities among them [48, 68]. Like phenol, urea generated due to melamine biodegradation is expected to appear in the repository in the long-term.

Ni (II), Eu(III) and U(VI) have been selected as radionuclides of interest for this exercise. Nickel is a constituent of repository construction materials (i.e. stainless steel) and its corresponding activation products are expected to be encountered in the deep disposal conditions studied in this work. Eu(III), as representative of the trivalent lanthanides, constitute the major fraction of the minor lanthanides/actinides present in the high-level liquid waste generated during the reprocessing of spent nuclear fuel and thus the understanding of its chemical interactions with organics is of utmost importance to ensure the repository safety. Finally, U(VI) constitutes the major component of spent fuel, being a good representative of heavy actinides.

In order to study the possible effect of those organics on radionuclides chemistry, it is of the outmost importance to have a consistent and reliable set of thermodynamic data. Thus, before performing specific thermodynamic calculations a data selection has been done and is presented in the following section.

3.3.1 Thermodynamic data selection

3.3.1.1 Phthalic and acetic acid

ThermoChimie database [37] provides trustworthy data on the stability of the species formed between radionuclides and those organics. The database is available at https://www.thermochimie-tdb.com/. ThermoChimie database was created by the French National Waste Management agency (ANDRA) to address geochemical modelling and performance assessment tasks; being the included thermodynamic data self-consistent and reliable.

Thermodynamic data for Ni, Eu and U complexation with both organics, acetate ($C_2H_3O_2^-$) and phthalate ($C_8H_4O_4^{2-}$), included in ThermoChimie and considered in this work are listed in Table 3-1.

3.3.1.2 Phenol

There is a general lack of data for the complexation of phenol with rare earth elements [58]. The only data on the complexation of uranyl (VI) ion with phenol come from the potentiometric titrations of Bartušek and Sommer [13]. The authors suggested the formation of 1:1 metal-ligand complex in acidic conditions (pH< 3), which is easily hydrolysed to polynuclear species at pH 4-5. The Log *K* value calculated by the authors according to r. 2 is -3.56 ± 0.1 (I = 0.1 mol·L^{-1} $NaClO_4$), and is the one selected in this work (Table 3-1).

$$UO_2^{2+} + C_6H_5OH \leftrightarrow UO_2(C_6H_5O)^+ + H^+ \qquad \textbf{r. 2}$$

To the best of our knowledge, thermodynamic data for the complexation of phenol with Ni and Eu are not available in the open literature.

3.3.1.3 Urea

As in the case of phenol, little is known about the complexation of urea with Ni, Eu and U. Osman and co-workers [67, 68], studied the complexation of urea and uric acid with uranium in acid conditions (pH< 4), and proposed the formation of a 1:1 week complex ($UO_2(H_4N_2CO)^{2+}$). The authors reported a stability constant of 2.12 ± 0.18 (I = 0.1 mol·L^{-1} $NaClO_4$) according to r. 3.

$$UO_2^{2+} + H_4N_2CO \leftrightarrow UO_2(H_4N_2CO)^{2+} \qquad \textbf{r. 3}$$

Similarly, Heller and co-workers [48], studied the complexation of trivalent Eu and Cm with urea in aqueous solution. The authors reported stability constants for two Eu – urea weak complexes (r. 4 and r. 5), $Eu(H_4N_2CO)^{3+}$ and $Eu(OH)(H_4N_2CO)^{2+}$, -0.12 ± 0.05 and -6.86 ± 0.15 (I = 0.1 mol·L^{-1} $NaClO_4$) respectively.

$Eu^{3+} + H_4N_2CO \leftrightarrow Eu(H_4N_2CO)^{3+}$ **r. 4**

$Eu^{3+} + H_4N_2CO + H_2O \leftrightarrow Eu(OH)(H_4N_2CO)^{2+} + H^+$ **r. 5**

To the best of our knowledge, thermodynamic data for the complexation of urea with Ni are not available in the open literature. Selected data for the studied urea – radionuclide systems is detailed in Table 3-1.

Table 3-1. Relevant thermodynamic data used in this work.

Reaction	Log K^0	Reference
$Ni^{2+} + C_2H_3O_2^- \leftrightarrow Ni(C_2H_3O_2)^+$	1.34 ± 0.11	ThermoChimie database [37]
$Eu^{3+} + C_2H_3O_2^- \leftrightarrow Eu(C_2H_3O_2)^{2+}$	2.90 ± 0.50	
$Eu^{3+} + 2C_2H_3O_2^- \leftrightarrow Eu(C_2H_3O_2)_2^+$	4.80 ± 0.20	
$Eu^{3+} + 3C_2H_3O_2^- \leftrightarrow Eu(C_2H_3O_2)_3(aq)$	5.60 ± 0.20	
$Ni^{2+} + C_8H_4O_4^{2-} \leftrightarrow Ni(C_8H_4O_4)(aq)$	3.00 ± 1.00	
$Eu^{3+} + C_8H_4O_4^{2-} \leftrightarrow Eu(C_8H_4O_4)^+$	4.96 ± 0.30	
$Eu^{3+} + 2C_8H_4O_4^{2-} \leftrightarrow Eu(C_8H_4O_4)_2^-$	7.34 ± 0.50	
$UO_2^{2+} + C_6H_5OH \leftrightarrow UO_2(C_6H_5O)^+ + H^+$	-3.77* ± 0.10	[13]
$UO_2^{2+} + H_4N_2CO \leftrightarrow UO_2(H_4N_2CO)^{2+}$	2.12* ± 0.18	[68]
$Eu^{3+} + H_4N_2CO \leftrightarrow Eu(H_4N_2CO)^{3+}$	-0.12* ± 0.05	[48]
$Eu^{3+} + H_4N_2CO + H_2O \leftrightarrow Eu(OH)(H_4N_2CO)^{2+} + H^+$	-7.28* ± 0.15	

*Values corrected to I=0 using Davies ionic strength corrections.

3.4 Thermodynamic calculations

Calculations presented in this section have been done with the PhreeqC geochemical code [72]. As mentioned in the previous section, thermodynamic data used in the calculations have been taken from ThermoChimie database and from other literature sources if not available in ThermoChimie. All calculations were performed at 25ºC and ionic strength corrections have been applied by using the Davies approach [42]. In agreement with the solid phase selection in Albrecht et al. [5], the effect of the organic complexes has been calculated on the solubility of the following solid phases: $Ni(OH)_2(s)$, $Eu(OH)_3(s)$ and $CaU_2O_7 \cdot 3H_2O(s)$.

Solubility diagrams obtained in the presence of acetate as a function of pH are shown in Figure 3-3, Figure 3-4 and Figure 3-5. The underlying chemical speciation of each element is shown in the same figures. According to these results, organic ligand concentrations higher than 10^{-4} mol·L^{-1} are required to see some effects on Ni and Eu chemistry (Figure 3-3 and Figure 3-4). For both elements, acetate complexation only occurs from pH 8 to 9.5, increasing 25% the solubility of both $Ni(OH)_2(s)$ and $Eu(OH)_3(s)$. In alkaline pH conditions, the hydrolysis of Ni and Eu is strong enough to avoid the binding with acetate up to organic concentrations of 10^{-2} mol·L^{-1}. Increasing the acetate concentration up to 10^{-2} mol·L^{-1} does not affect the aqueous chemistry of U in the whole studied pH range (8 – 13) (Figure 3-5). Unrealistic acetate concentrations as high as $10^{-0.3}$ mol·L^{-1} (see Appendix II), are needed to observe an important effect on U behaviour in near neutral pH conditions. The same is true for phthalate (see Figure 3-5 and Appendix II). As with acetate, phthalate affects Ni and Eu chemistry only at concentrations over 10^{-2} mol·L^{-1} (Figure 3-3 and Figure 3-4). Phthalate complexation with Ni and Eu is relatively stronger than acetate complexation, prevailing up to pH ~ 10. This is notorious in near neutral pH conditions, where the solubility of both $Ni(OH)_2(s)$ and $Eu(OH)_3(s)$ increase more than one order of magnitude when increasing phthalate aqueous concentration from 10^{-2} mol·L^{-1} to 10^{-4} mol·L^{-1}. Overall, the effect of acetate and phthalate on the chemistry of Ni, Eu and U will be negligible in the alkaline pH region but certainly important in near-neutral conditions (i.e. clay barriers or clay host-rock present in some repository designs) (see Appendix II). It is worth mentioning that in clay conditions the effect of carbonate, a major system species, will partially hinder the effect of acetate and phthalate on radionuclides behaviour.

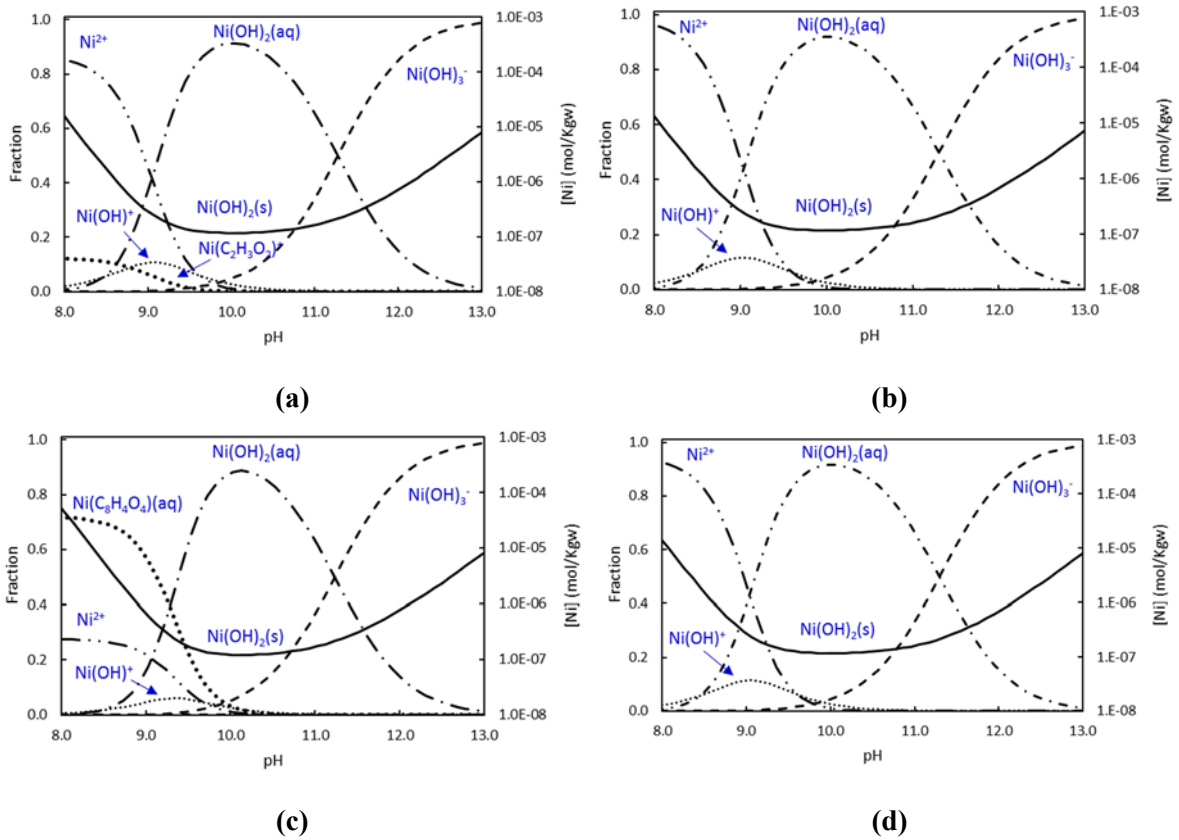

Figure 3-3. Solubility curve (black solid line) calculated for $Ni(OH)_2(s)$ in the presence of acetate (a – b) and phthalate (c – d) as a function of pH. Dashed lines stand for the speciation of Ni in equilibrium with the solid phase. Organic concentration fixed as 10^{-2} mol·L^{-1} (a – c) and 10^{-4} mol·L^{-1} (b – d). Calcium concentration fixed in all diagrams as 10^{-3} mol·L^{-1} in agreement with the expected Ca concentrations in state II cement degradation conditions.

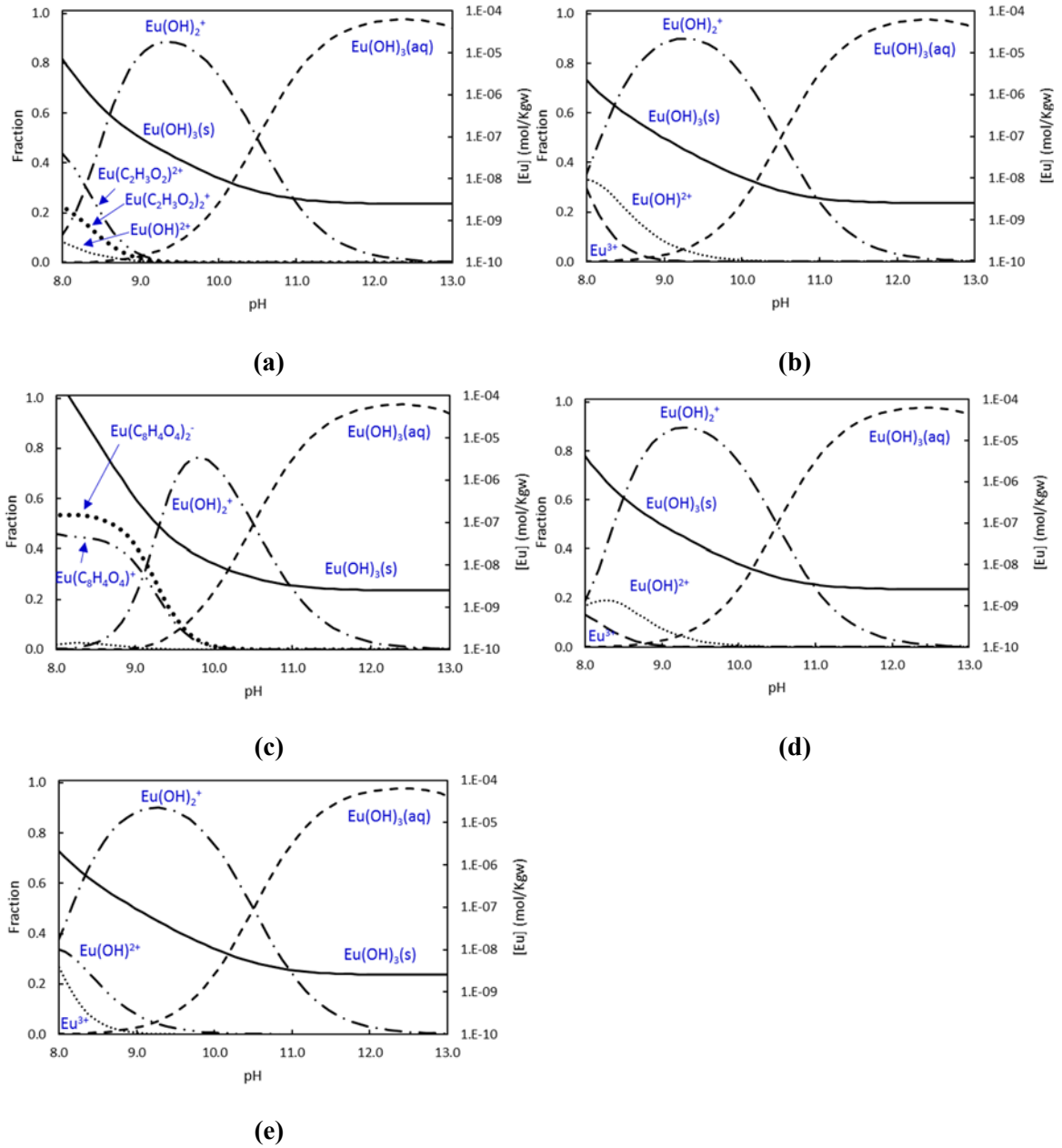

Figure 3-4. Solubility curve (black solid lines) calculated for $Eu(OH)_3(s)$ in the presence of acetate (a – b), phthalate (c – d) and urea (e) as a function of pH. Dashed lines stand for the speciation of Eu in equilibrium with the solid phase. Organic concentration fixed as 10^{-2} mol·L^{-1} (a – c) and 10^{-4} mol·L^{-1} (b – d). Calcium concentration fixed in all diagrams as 10^{-3} mol·L^{-1}. Note that for the urea scenario, Eu calculated solubility-speciation (e) is identical at 10^{-2} / 10^{-4} mol·L^{-1}.

In the studied pH conditions, from near neutral to alkaline pH, the effect of phenol over U is negligible (Figure 3-5). Contrary to the trends observed for acetate and phthalate, extremely high phenol concentrations (>$10^{-0.3}$ M) do not produce any influence on its chemistry (see Appendix II). This is not surprising given that thermodynamic data for phenol complexation with uranium selected in this work was obtained in acidic conditions. Similarly, our results indicate that complexation of Eu and U with urea is negligible in alkaline pH conditions (Figure 3-4, Figure 3-5 and Appendix II).

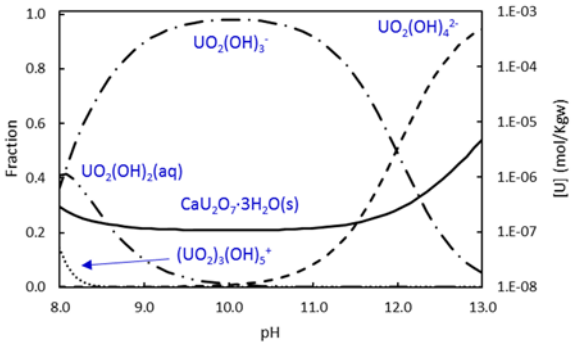

Figure 3-5. Solubility curve (black solid line) calculated for $CaU_2O_7 \cdot 3H_2O$(s) in the presence of acetate, phthalate and urea at 10^{-2} / 10^{-4} mol·L^{-1} as a function of pH. Dashed lines stand for the speciation of the different elements in equilibrium with the solid phase. Calcium concentration fixed in all diagrams as 10^{-3} mol·L^{-1}.

Based on the presented results, among the studied SPs degradation products, the most powerful complexing agent is phthalate, which exerts an important influence over Ni and Eu behaviour in slightly alkaline conditions (pH < 10). Overall, the complexation capacity shown by the different degradation products studied in this work could be ranked from the stronger to the weaker complexing agent as follows: phthalate > acetate > urea > phenol. As mentioned before the strongest complexing ligands, phthalate and acetate, are expected to form in deep repository conditions during the temperature transient period (~100 years); while the weakest ligands are expected to form at long-term. These findings clearly point out the importance of phthalate / acetate radionuclide complexation in repository conditions.

Is worth mentioning that U seems to be unaffected by any of the studied ligands in the conditions studied in this work. However, as previously highlighted, there is a general lack of data for the complexation of some of the studied organic ligands with radionuclides, specially at alkaline pH conditions. Thus, additional experiments are required to confirm the validity of the statements reflected here.

3.5 Conclusions

Superplasticizers present in concrete formulations may be altered in deep disposal conditions through several mechanisms: hydrolysis, temperature, ionizing radiation and microbial activity. Overall, few studies are available in the literature dealing with the alteration of superplasticizers; and specifically, there is an important lack of results for the degradation of PCE SPs.

Based on the literature review presented in this work, we can conclude that the alteration of superplasticizers may lead to the formation of small organic compounds that could be classified in three main categories: i) aromatic compounds, ii) aliphatic compounds, and iii) inorganic species. From those categories, four possible degradation products (representatives of different SPs types) have been selected (phthalic acid, adipic acid, phenol and urea) and their effect on radionuclide (Ni, Eu and U) behaviour has been addressed. Our calculations indicate that in alkaline pH conditions, the presence of these organic ligands up to concentrations of 10^{-2} M, will not affect the behaviour of any of the studied radionuclides.

However, in slightly alkaline systems (from pH 8 to 10), phthalic and acetic acids (up to concentrations of 10^{-2} M) could control the aqueous chemistry of both Ni and Eu. This chemical control produces an increase on Ni and Eu solubility, especially relevant in systems containing phthalic acid. Interestingly, U is not affected by any of the studied ligands in the conditions used in the present study. Nevertheless, this statement may be taken with caution given the scarcity of thermodynamic data found in the literature for the complexation of U with some of the studied organics in alkaline conditions.

For a better system comprehension, and to clearly ensure the safety of the radioactive waste disposal, additional superplasticizer degradation studies are required, especially for PCE SPs type. Moreover, specific radionuclide-organic complexation studies in alkaline pH conditions are desired to complement the available thermodynamic.

Chapter 4: DEGRADATION OF POLYCARBOXYLIC ETHER-BASED CEMENT SUPERPLASTICIZERS

4 Degradation of polycarboxylic ether-based cement superplasticizers

This chapter is dedicated to the experimental study of superplasticizers degradation. Given the lack of information on superplasticizer degradation processes highlighted in *Chapter* 3, the study detailed here aims to fill in this gap as well as to serve as a basis for future degradation studies.

4.1 Background of the study

As introduced in *Chapter* 3 and *Chapter* 5, concrete admixtures are materials added to concrete to alter its properties in its fresh and hardened states. Superplasticizers (SPs) are a type of organic admixtures used by manufacturers to improve concrete properties such as dispersion, hydration and workability [89]. For a detailed explanation of SPs properties and characteristics the reader is refereed to *Chapter* 1.

In previous *Chapters* (1, 3, 5) it has been already explained how those materials may be altered at the alkaline conditions prevailing under repository environments. However, as highlighted in *Chapter* 3 not just hydrolysis but temperature and radiation may induce important structural and chemical modifications over those compounds. The study presented below aims at investigating the degradation of polycarboxylic ether-based (PCE) SPs based on three different treatments: a) a hydrolysis treatment, b) a thermal treatment, and c) an irradiation treatment.

PCE SPs, see *Chapter* 1 and 3 for details, are last generation SPs currently included in the Belgian repository concept. Specifically, Glenium®27 (manufactured by BASF) superplasticizer is one of the possible materials that may be used in the construction of the future Belgian nuclear waste deep disposal facility [27]. The formulation of this component is under a patent protection but according with our characterisation results (see *Section* 2.1 and Appendix I) it's a long-chain polymer (with a length ranging from 15 to 20 units) mainly composed by ester and ether species. The presence of sulfonated groups in their composition has been also detected. However, besides the polymer itself such commercial cocktails use to have other unknow components in their formulations (i.e. pesticide, herbicides, etc.). In this work the degradation of Glenium®27 depending on the medium pH (from 10.5 to 13.0), the system temperature (from 100 to 250^{o}C) and the presence of radiation (from 100 Gy to 220 kGy) has been investigated. The experimental conditions used in the degradation experiments have been selected in agreement with the information found in the literature research performed in *Chapter* 3.

In parallel, and to simplify the system, the degradation of an in-house synthesized PCE SPs (see *Section* 2.4 for details about the synthesis) free from other components (i.e. pesticides, herbicides, etc.) has been done in similar conditions to that applied for Glenium®27 experiments.

4.2 Materials and methods

Based on the information previously presented, an experimental study including three possible SPs degradation mechanisms (hydrolysis, temperature, radiolysis) has been conducted with Glenium®27 and the in-house synthesized PCE SPs (see *Section* 2 and Appendix I for the entire characterisation of those materials).

4.2.1 Superplasticizer hydrolysis

Hydrolysis experiments were done by adding 0.1 g of the freeze-dried SPs, only Glenium®27 in these experiments, in 40 mL NaOH (Scharlau, Extra pure) solutions with pH ranging from 10.5 to 13.0. Samples were sealed and stored in polyethylene vials for one year at controlled temperature conditions, 25 ºC (Figure 4-1). Regularly, aliquots of the solution were taken and measured by using Raman spectroscopy. Additionally, for each aliquot the pH of the solution was measured (see *Section* 2.5 for experimental details regarding the analytical measurements).

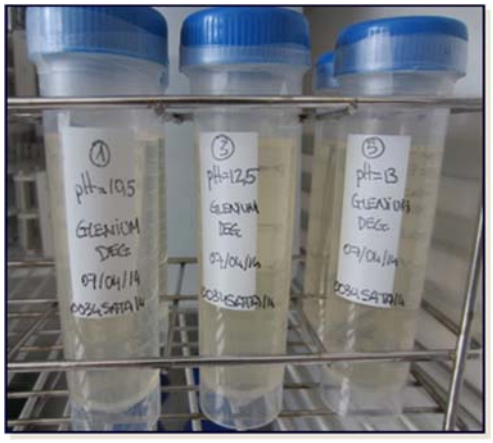

Figure 4-1. Glenium®27 hydrolysis experiments in hyperalkaline conditions.

4.2.2 Superplasticizer thermal treatment

Thermal experiments consisted in heating a freeze-dried portion of the SPs, Glenium®27 or the in-house synthesized PCE SPs, at different temperatures ranging from 100 to 250 ºC during different time intervals ranging from 1 to 2 hours. After the treatment, samples were stored in chromatographic sealed vials before being analysed by IR and H-NMR (see *Section* 2.5 for experimental details regarding the analytical measurements).

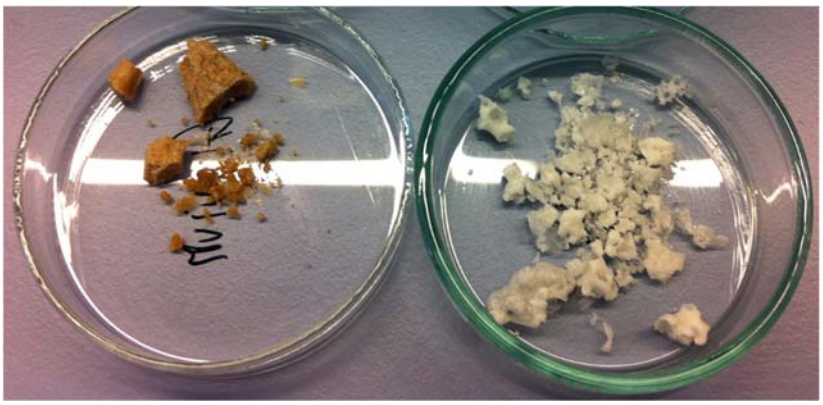

Figure 4-2. Visual aspect of the freeze-dried SPs, Glenium®27 (left side solid) and the in-house synthesized PCE SPs (right side solid), before the thermal treatment.

4.2.3 Superplasticizer irradiation

Selected freeze-dried fractions of Glenium®27 and the in-house synthesized PCE SPs were encapsulated in glass chromatographic vials to facilitate their irradiation. Then, three different methodologies were used to irradiate those samples:

- Irradiation with a very small dose (100 Gy), carried out in the Sant Pau Hospital using a "commercial" human irradiator in collaboration with UPC-INTE (Institute of Energy Technologies).
- Irradiation with a very high dose (220 kGy), carried out in Aragogamma S.L. by using a ^{60}Co gamma source.
- Systematic irradiation from 1 to 100 kGy, carried out in ARRONAX cyclotron by using a ^{137}Cs gamma source (manufactured by GSM medical gmbh).

After the treatment, samples were stored in the sealed vials before being analysed by IR, H-NMR and GPC (see *Section* 2.5 for experimental details regarding the analytical measurements).

Figure 4-3. ARRONAX cyclotron pictures (Courtesy of Guillaume Blain).

4.3 Results and discussion

4.3.1 Superplasticizer hydrolysis

Raman results are presented in Figure 4-4 for raw and hydrolysed Glenium®27 samples. Raw liquid and solid Raman spectra illustrate that the freeze-drying process do not alter the molecule signal, as the main bands could be observed for both materials.

The Raman hydrolysis results obtained for Glenium®27 are not conclusive. According to our results, the alteration of Glenium®27 structure is not confirmed at least in the studied pH range (10.5 - 13.0) given that Raman measurements do not shown any remarkable feature after 1 year of preservation in alkaline solutions. Note that the Raman spectra obtained at shorter contact times is identical to that obtained after 1 year and thus for simplification purposes these figures have not been included here. It is also obvious that the level of SPs used in this experiment was low (2.5 $g \cdot kg^{-1}$), but representative of the real concrete formulations used in *Chapter* 5 experiments (~3 $g \cdot kg^{-1}$), and unfortunately the Raman signal obtained from the samples was not as intensive as desired (dilution effect). To illustrate the dilution effect the Raman spectra of MilliQ water is also shown in Figure 4-4. The pH of the different aliquots taken from the original sample was almost constant during the last of the experiment, with variations included in the range of uncertainty. Overall, we did not find any signal indicating a possible modification of Glenium®27 SPs chemical structure and/or properties in alkaline media.

Note that given that results obtained for Glenium®27 were not conclusive we decided not to run hydrolysis experiments with the in-house synthesized superplasticizer moving forward to temperature and radiolysis treatments.

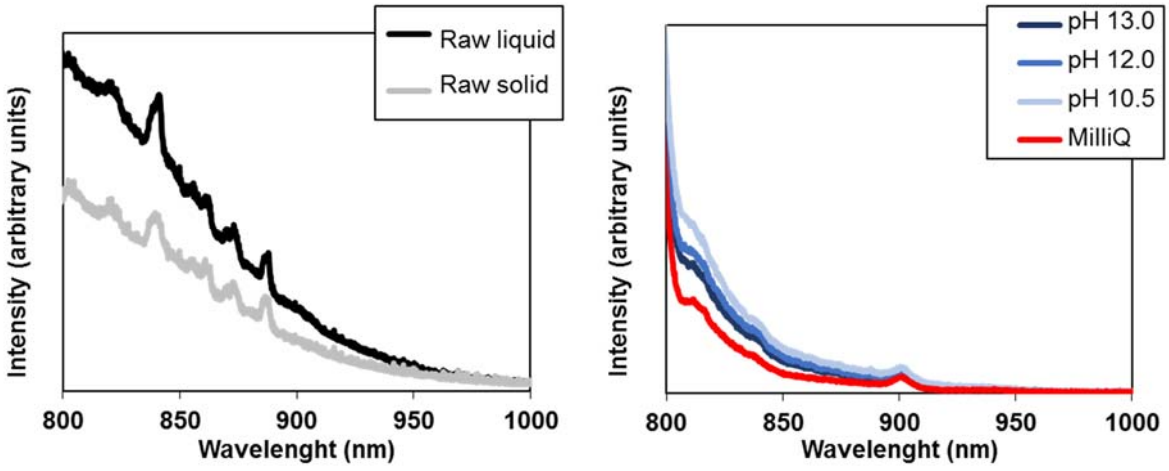

(a) **(b)**

Figure 4-4. Raman spectra obtained for (a) the raw and (b) the hydrolysed Glenium®27 samples after 1 year of contact. For comparative purposes MilliQ water spectra is also included in the figure.

4.3.2 Superplasticizer thermal treatment

Thermal treatment results are presented from Figure 4-7 to Figure 4-8. H-MNR spectra were acquired for samples treated at 100 and 200 ºC for 1 hour, while IR spectra were acquired for all treated samples. The reasoning behind these was because samples treated at 200 and 250 ºC for 4 and 1 hour, respectively, become non-soluble in the conditions used to acquire the H-MNR spectra (D_2O water media). Indeed, the most heated samples change their visual aspect becoming a rubber material (Figure 4-5).

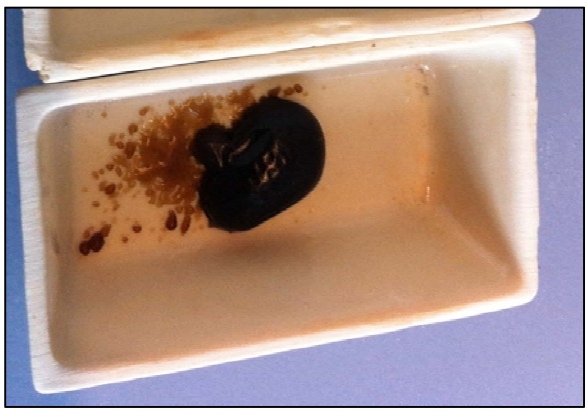

Figure 4-5. Visual aspect of Glenium®27 after the thermal treatment at 250 ºC.

IR spectra of Glenium®27 samples (Figure 4-6) shown a similar band profile independently of the thermal treatment applied. The most remarkable differences appear in the regions of 3000-2800 nm^{-1} and 1800-1400 nm^{-1}, in where the band intensity slightly changes. Those changes may be related with the

hydrolysis of the ester bond in the polyethyleneglicol (PEG) chain. So apparently, even the hardest thermal treatment did not modify the main chemical groups presents in the SPs structure.

As seen for the IR spectra, Glenium®27 H-NMR results (Figure 4-7) shown a similar band profile at 100 and 200ºC. Small chemical shifts could be seen in the H-NMR spectra but the signals remain almost unaltered, indicating that the material structure is preserved even at 200 ºC. Nevertheless, as mentioned before the samples heated with the most aggressive thermal treatment (i.e. 200 and 250 ºC for 1 and 4 hours, respectively) became insoluble in D_2O water fact that may indicate a structural modification of Glenium®27 in these conditions.

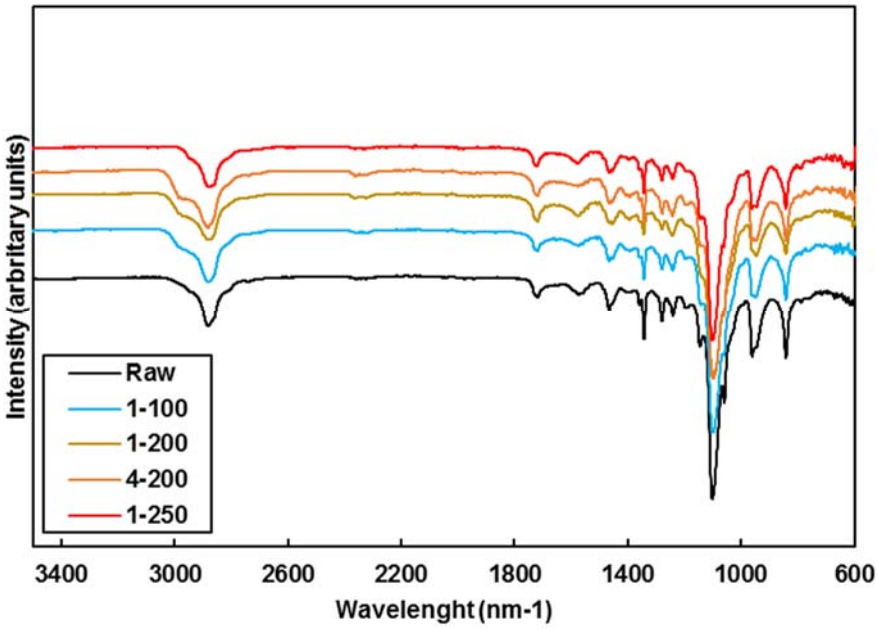

Figure 4-6. IR spectra of Glenium®27 samples exposed at a) samples 1-100, 1 hour at 100 ºC, b) samples 1-200, 1 hour at 200 ºC, c) samples 4-200, 4 hours at 200 ºC, and c) samples 1-250, 1 hour at 250 ºC. For comparative purposes the spectrum of the unaltered material is also included.

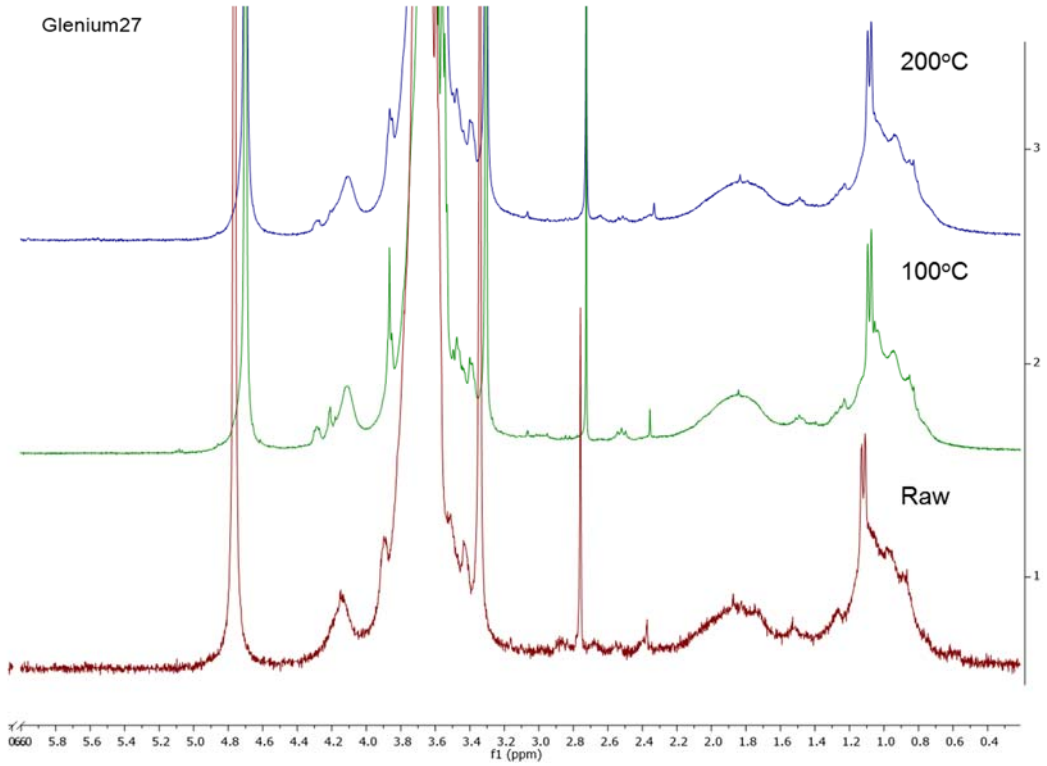

Figure 4-7. H-NMR spectra of Glenium®27 samples exposed at 100-200°C for 1 hour. For comparative purposes the spectrum of the unaltered material is also included.

IR and H-NMR results obtained for the in-house synthesized PCE (Figure 4-8 and Figure 4-9) are in line with those previously discussed for Glenium®27. Overall, the chemical groups within the SPs structure remain unaltered, even with the most aggressive thermal treatment, with minor modifications in the IR regions of 3000-2800 nm^{-1} and 1800-1400 nm^{-1}. On the contrary, H-NMR results, especially in the region from 2.0 to 0.5 ppm corresponding with H signals from the CH_3 and CH_2 units from the terminal SPs positions, shown a decrease in the bands intensity related with a possible restructuration (co-polymerization) of these units.

In general, the thermal treatment applied onto the SPs samples indicate that these materials structure remain almost unaltered up to 200 °C, at least in treatments that last 1 hour. Over this temperature (e.g. 250 °C) or after a long-time period at 200 °C (> 1 hr) the structure of these materials is not preserved directly affecting its performance. It is worth mentioning that such high temperatures are not expected in deep repository conditions which are designed to have a maximum thermal peak of approx. 100 °C [47].

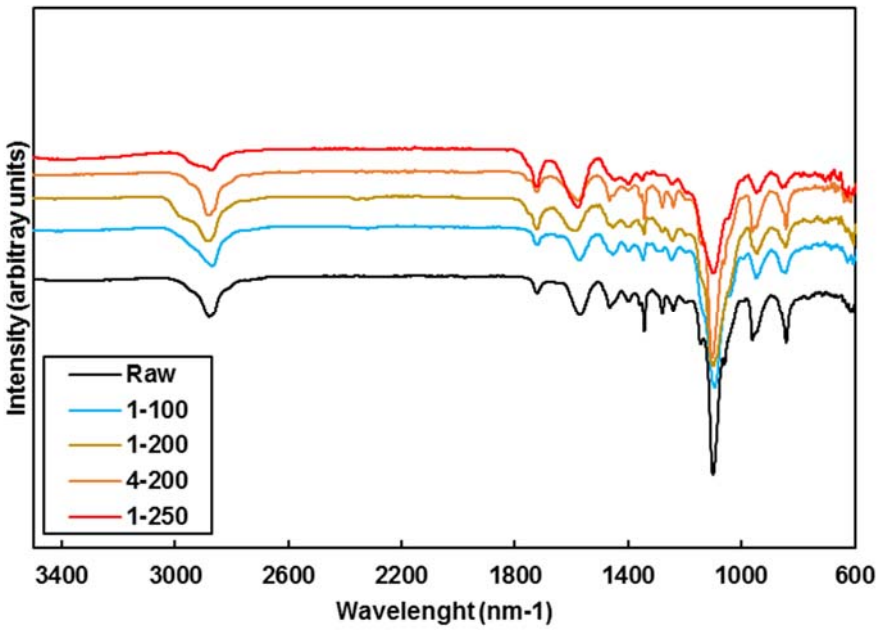

Figure 4-8. IR spectra of in-house synthesized PCE SPs exposed at a) samples 1-100, 1 hour at 100 ºC, b) samples 1-200, 1 hour at 200 ºC, c) samples 4-200, 4 hours at 200 ºC, and c) samples 1-250, 1 hour at 250 ºC. For comparative purposes the spectrum of the unaltered material is also included.

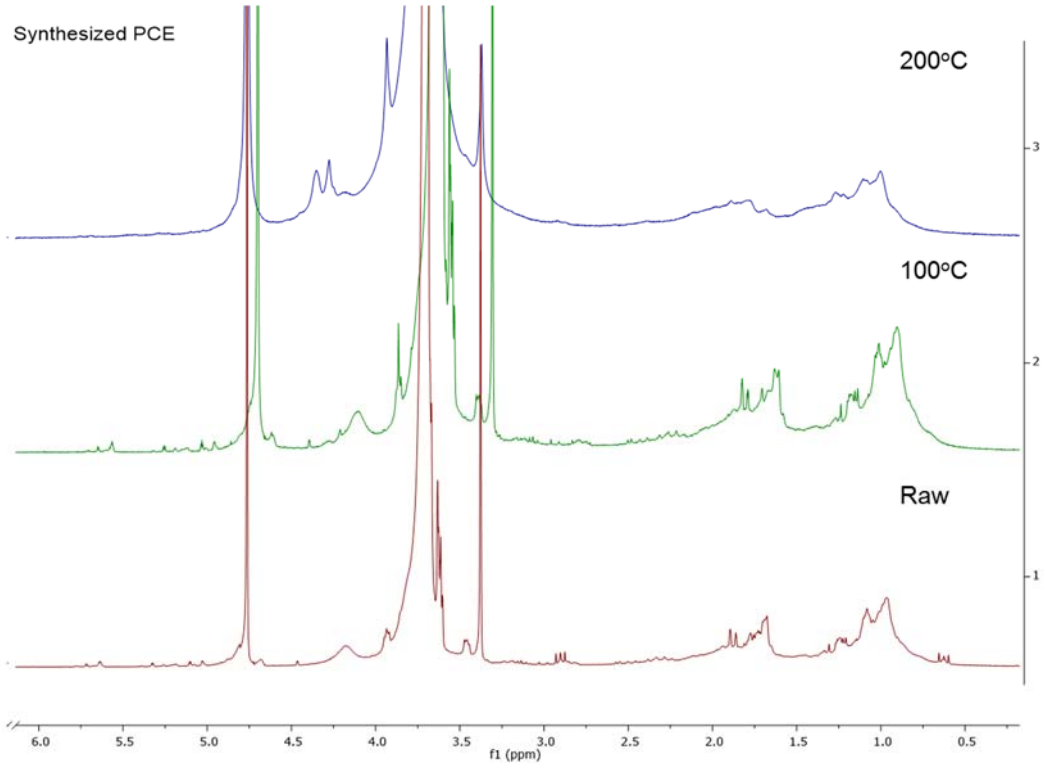

Figure 4-9. H-NMR spectra of the in-house synthesized PCE SPs samples exposed at 100-200 ºC for 1 hour. For comparative purposes the spectrum of the unaltered material is also included.

4.3.3 Superplasticizer irradiation

Results obtained for the SPs irradiated samples, Glenium®27 and the in-house synthesized PCE SPs, are shown from Figure 4-10 to Figure 4-17. Similarly, to the thermal treatment results, overall SPs materials

studied in this work remain almost unaltered up to radiation doses of 220KGy. It is worth mentioning that, contrary to the observations found in the thermal treatments, all irradiated samples were soluble in D_2O water and thus H-NMR measures were done to the whole set of samples. Results obtained at the lowest irradiation dose, 100 Gy, are not included in the figures because they do not shown any remarkable feature, being almost the raw material.

The IR spectra of both irradiated materials, Glenium®27 and the in-house synthesized PCE SPs, do not shown any remarkable feature that illustrate the degradation of the main chemical groups already in the SPs structure either the possible generation of new chemical groups. At first sight one can clearly see that the IR bands, corresponding to the vibration – rotation of the different bonds within the SPs, appear in the same spectra positions independently of the applied radiation dose (Figure 4-10 and Figure 4-11).

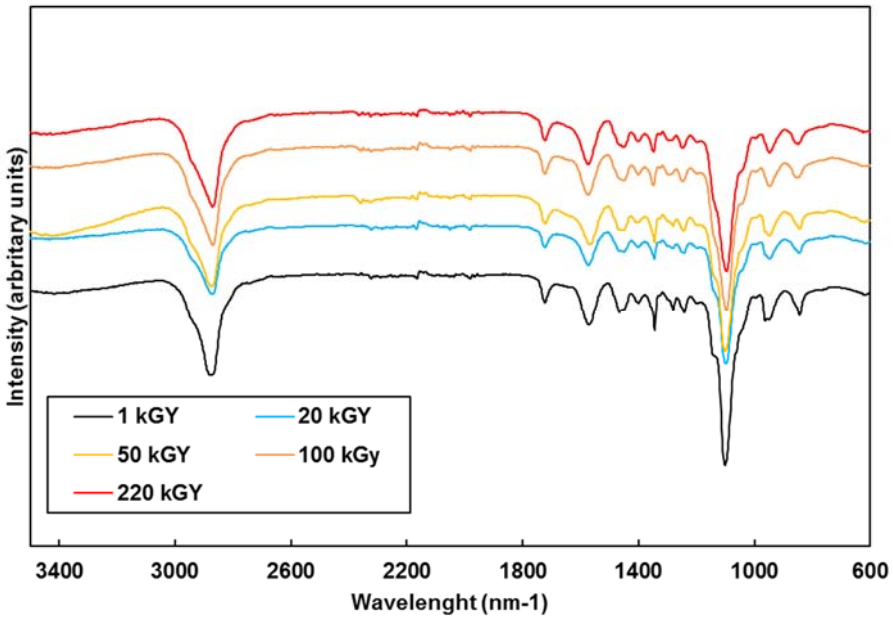

Figure 4-10. IR spectra of Glenium®27 samples exposed at 1-220 kGy.

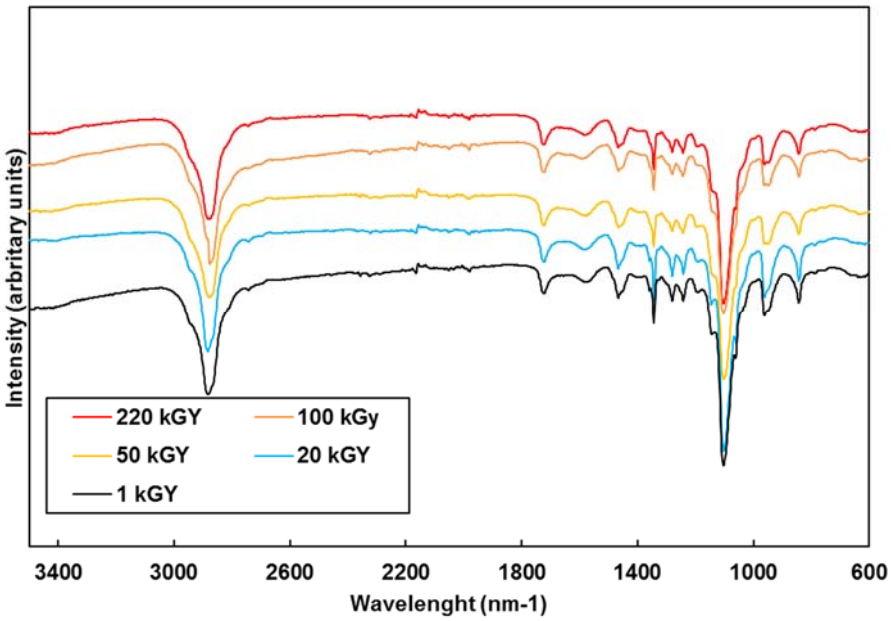

Figure 4-11. IR spectra of in-house synthesized PCE SPs samples exposed at 1-220 kGy.

In line with the IR results, H-NMR results for both studied materials (Figure 4-12 and Figure 4-13) did not show any special feature indicative of a possible material structural degradation even at the highest studied radiation doses. Small differences could be appreciated in the signals located approx. at 4 ppm, corresponding with the main polyethyleneglicol (PEG) chain, but it is hard to link this with a possible SPs structure modification.

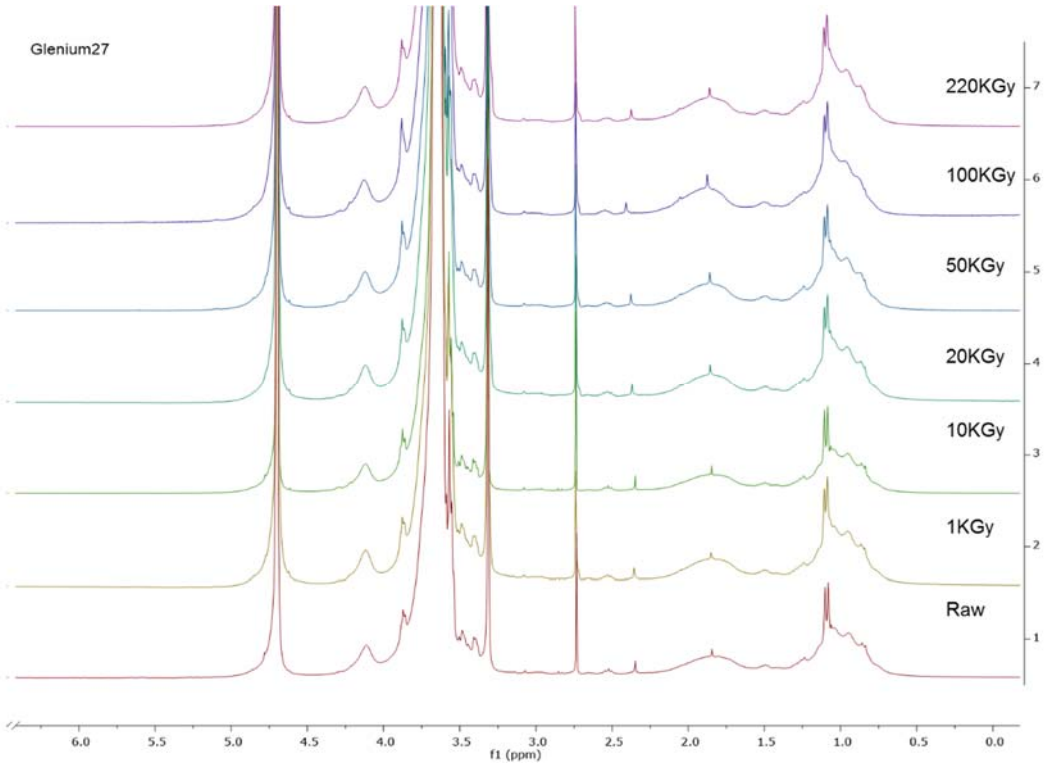

Figure 4-12. H-NMR spectra of Glenium®27 samples exposed at 1-220 kGy. For comparative purposes the spectrum of the unaltered material is also included.

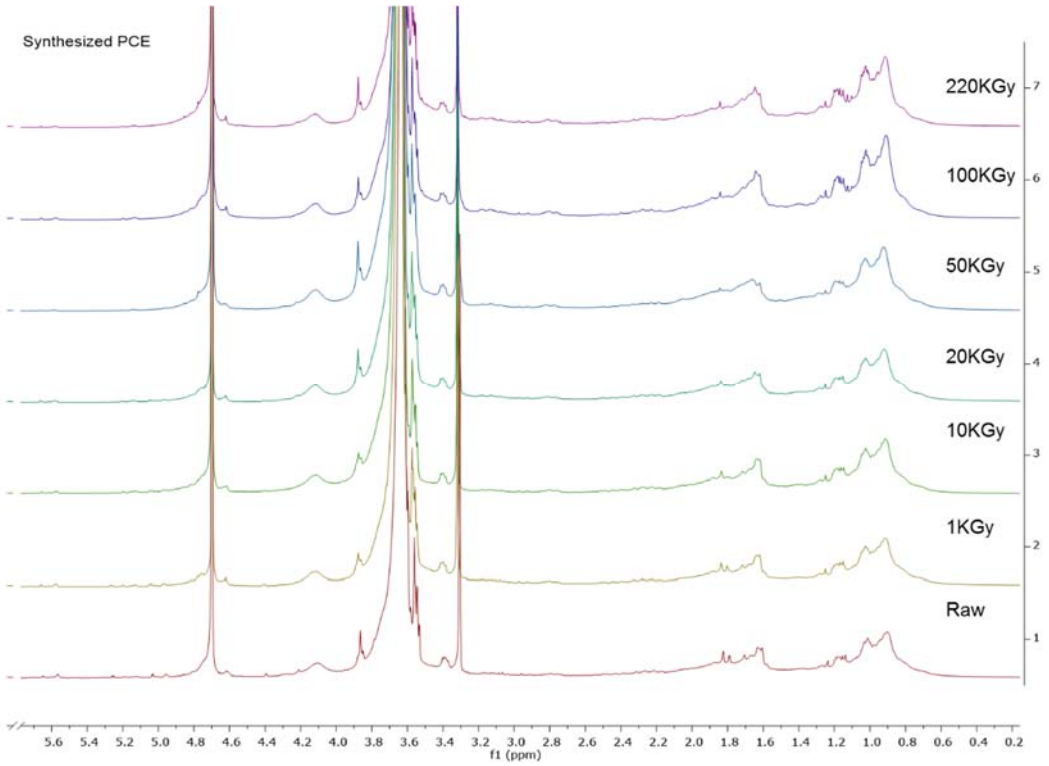

Figure 4-13. H-NMR spectra of the in-house synthesized PCE SPs samples exposed at 1-220 kGy. For comparative purposes the spectrum of the unaltered material is also included.

The irradiated samples were also analysed by means of GPC to determine not a total but a partial SPs degradation. The molar mass distribution (Figure 4-14 and Figure 4-15) and the polydispersity index (Figure 4-16 and Figure 4-17) of both, Glenium®27 and the in-house synthesized PCE SPs, clearly evolves as a function of the applied radiation dose.

From the molar mass distribution figures, we can see that Glenium®27 molar mass is characterised by a main band located between $10^{4/5}$ Da (corresponding to the polyethyleneglicol (PEG) chain) while the in-house synthesized PCE SPs presented a different profile with two main bands located between $10^{3/4}$ and approx. 10^5 Da, respectively. In the case of Glenium®27, increasing the samples irradiation implies a different molar mass distribution profile characterised by the formation of heavier compounds (i.e. > 10^6 Da). An important intensity decrease is also observed for the band at $10^{4/5}$ Da indicative of a decrease of the concentration of the main structural polyethyleneglicol (PEG) chain. These results indicate a partial Glenium®27 co-polymerization that are also in agreement with the polydispersity index evolution as a function of the irradiation dose (Figure 4-16).

GPC results obtained for the in-house synthesized PCE SPs (Figure 4-15) are more complex than that of Glenium®27. Apparently, up to 50 kGy the behaviour of this material is identical to that obtained for Glenium®27, heavier compounds are generated (i.e. >10^6 Da) with a decrease of the main bands corresponding to the original polyethyleneglicol (PEG) chain. The evolution of the polydispersity index (Figure 4-17) is also in line with the results obtained for Glenium®27 up to 50 kGy, suggesting that a co-polymerization process is occurring over the material. Results obtained for radiation doses up to 100 kGy

present a sharp molar mass distribution decrease, suggesting a probable polyethyleneglicol (PEG) chain restructuration in lower length members. However, at 220 kGy, we see again a partial material co-polymerization.

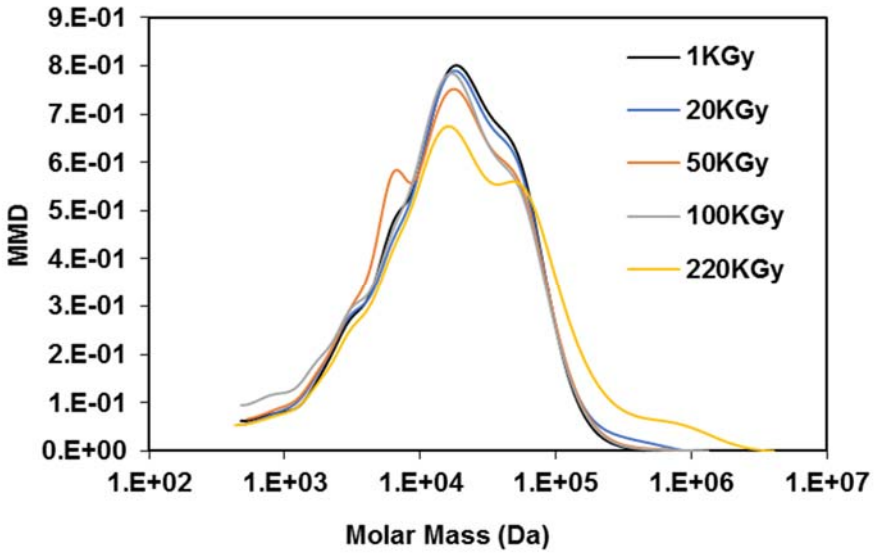

Figure 4-14. Glenium®27 molar mass distribution obtained with the GPC experiments.

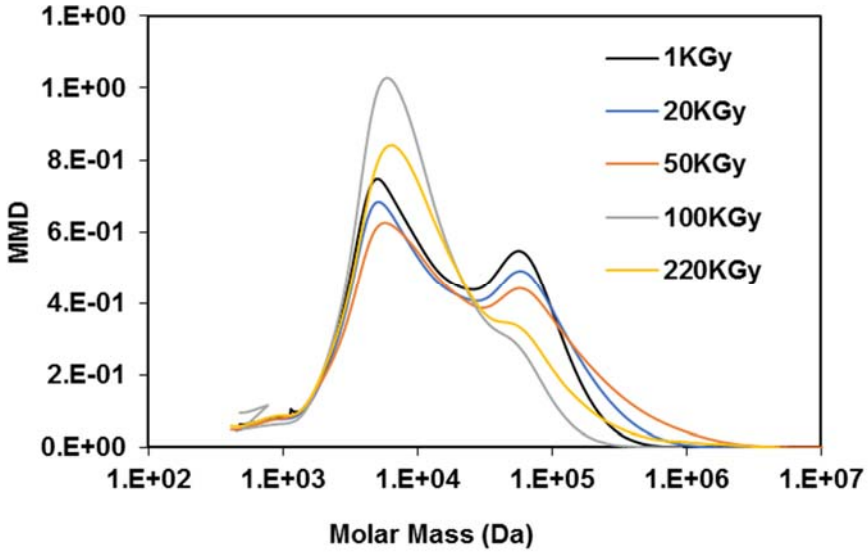

Figure 4-15. In-house synthesized PCE SPs molar mass distribution obtained with the GPC experiments.

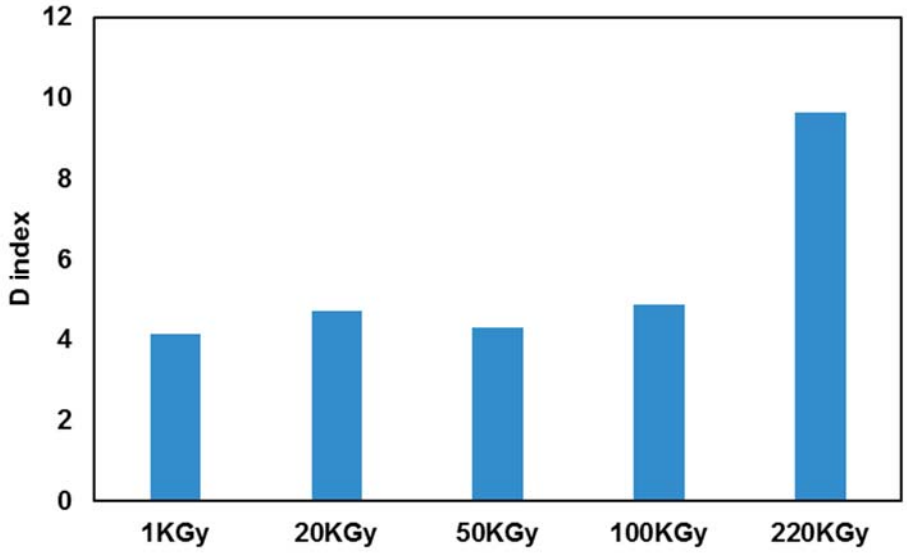

Figure 4-16. Polydispersity index for each irradiated Glenium®27 sample obtained with the GPC experiments.

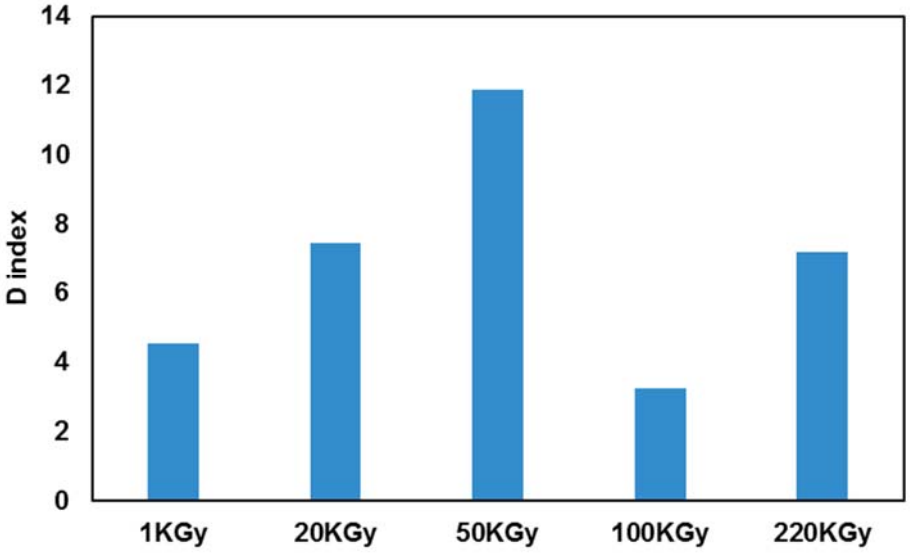

Figure 4-17. Polydispersity index for each irradiated in-house synthesized SPs PCE sample obtained with the GPC experiments.

Overall, our results indicate that the irradiation of Glenium®27 and the in-house synthesized PCE SPs, will generate a partial co-polymerization of these materials. However, the main chemical groups as well as the main SPs structure is preserved even in the samples treated with the highest radiation dose.

4.4 Conclusions

The degradation of polycarboxylate ether-based (PCE) superplasticizers (SPs) has been investigated in this work. Two materials, a commercial sample manufactured by BASF (Glenium®27) and an in-house synthesized PCE SPs, have been studied. The degradation studies consisted in three different chemical

treatments, hydrolysis, temperature and irradiation, that may induce the modification of the structure or functionalities of these materials.

Our results indicate that the studied SPs remain unaltered when exposed to hydrolysis processes, system pH keep constant during the last of the experiments, although those results are not conclusive given the weak signals obtained with the Raman spectroscopy. Alternative analytical methodologies for future experiments may be of great interest here in order to validate our results.

In the other hand, when these materials are exposed to high temperatures or radiation doses, important changes in the SPs structure have been observed although the main chemical groups remain unaltered. Temperatures over 200 ^{o}C produce a clear SPs alteration making the material water insoluble (i.e. structure alteration, co-polymerization) and thus affecting its performance. Fortunately, such high temperatures are not expected in repository conditions (maximum thermal peak expected at 100 ^{o}C). Therefore, according to our results none of the studied materials will be affected by thermal process under deep disposal conditions. Our results also indicate that small radiation doses will not affect the structure of the SPs. However, increasing the radiation doses up to 220 kGy will produce a partial SPs co-polymerization that finally may lead un-satisfactory material performance. As previously mentioned for the hydrolysis experiments, alternative analytical methodologies for future experiments may be of great interest here in order to validate our results. Moreover, the study of water radiolysis linked SPs degradation may be of utmost interest to re-confirm the stability of such materials under deep disposal conditions.

Overall, the results presented here indicate that PCE SPs are robust materials supporting their selection as reference SPs for being used in concrete formulations of future radioactive deep disposal facilities.

Chapter 5: EFFECT OF SUPERPLASTICIZERS ON Ni BEHAVIOUR IN CEMENTITIOUS ENVIRONMENTS

"The work presented in this Chapter has been published in Journal of Radioanalytical and Nuclear Chemistry (https://doi.org/10.1007/s10967-018-5837-x), and is included in Appendix IV of this thesis"

5 Effect of superplasticizers on Ni behaviour in cementitious environments

In the previous chapters the focus was on the degradation of cement superplasticizers, based on literature and also in experimental data, and the possible formation of small organics compounds that may affect the chemical behaviour of radionuclides in deep disposal conditions. The present chapter goes a step further with an experimental investigation on the effect of a commercial superplasticizer on the behaviour of nickel.

5.1 Overview of the case study

SuperPlasticizers (SPs), are common admixtures used in concrete formulations (no more than 5% of those materials by mass of cement [43]) to lower the mix water requirement of concrete [27]. As already mentioned in *Chapter* 1, Glenium®27 is one of the SPs currently defined as a reference material for being used in concrete formulations to build up different structures in the Belgian deep disposal facility for radioactive wastes (Figure 5-1).

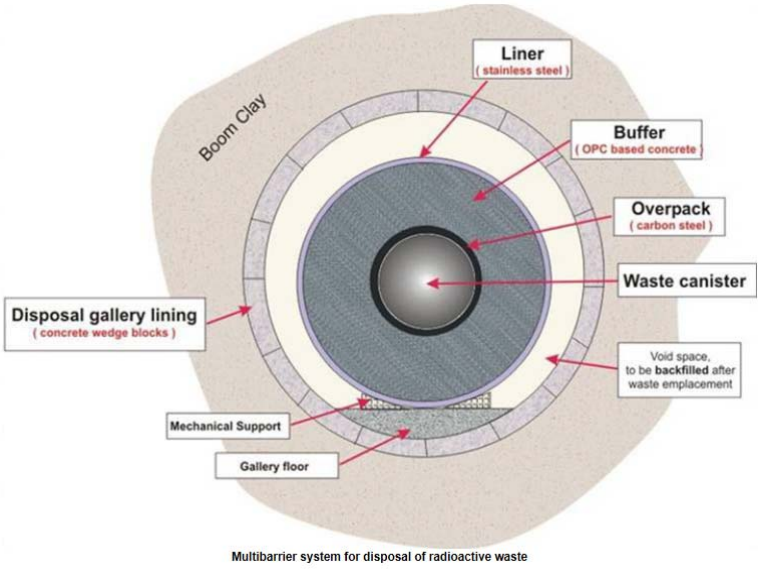

Figure 5-1. Multibarrier System for deep disposal of radioactive waste, Belgian disposal "supercontainer" concept [27].

Nickel is a constituent of repository construction materials (i.e. stainless steel) and thus expected to be encountered in the deep disposal conditions studied in this work [82].

On the other hand, cementitious materials reduce the mobility of radionuclides contributing to the long-term safety when the containment is lost and radionuclides start to move from the waste package due to water intrusion. Once containment is lost, intruding groundwater will be first in contact with the concrete barrier and later with the radioactive waste matrix and waste constituents (i.e. nickel activation products). Groundwater composition will therefore be conditioned by contact with concrete prior to contacting the waste [89]. In such conditions, polymeric SPs can be altered (see *Chapter* 3) with the subsequent production

of small organic compounds (i.e. gluconate, isosaccharinate, oxalate…) with different chemical properties [39]. Radionuclides form stable complexes with some small organic compounds ([8, 32] and references therein) of similar characteristics of those that may be originated from the alteration of SPs (Figure 5-2).

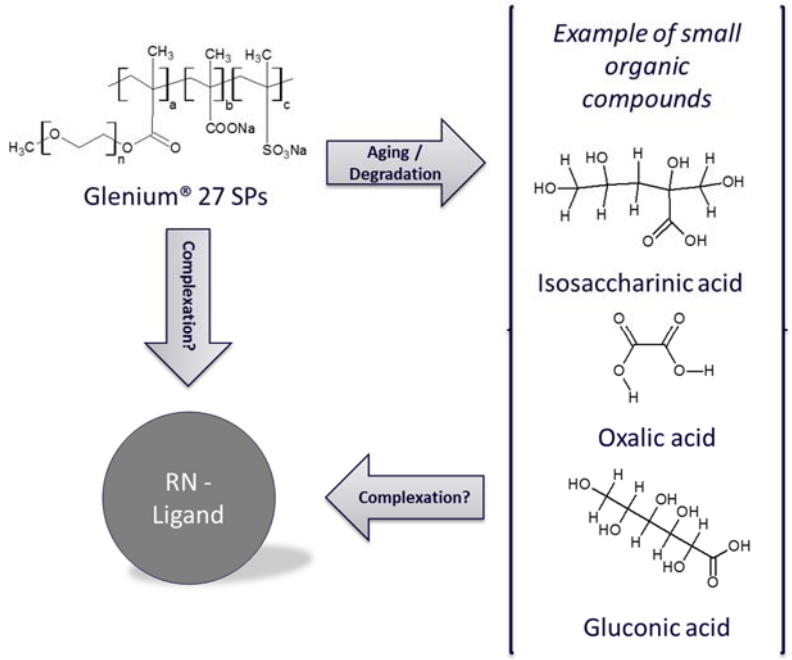

Figure 5-2. Tentative sketch of the Glenium®27, and small organics, behaviour towards radionuclides in the studied system.

The effect of gluconate, isosaccharinate and oxalate on the behaviour of several radionuclides have been extensively studied during the last years [6, 7, 10, 18-20, 24, 25, 29, 30, 32, 49-51, 75, 77-79, 88, 90-92, 97-102, 111]. The behaviour of Ni in the presence of these organics has been the focus of detailed sorption and solubility studies under different pH, temperature and ionic strength conditions [19, 29, 30, 49, 50, 75, 99, 101, 102]. Important effects on Ni behaviour have been observed due to the presence of these organics, especially at high organic concentrations. In near neutral and slightly alkaline conditions the formation of aqueous species with stoichiometries Ni-L (aq) and Ni-L_2 (aq) (where L stands for the organic ligand) has been reported [19, 29, 30, 99, 101, 102]; while in alkaline solutions the formation of ternary species including OH^- ions in the structure (i.e. Ni-OH-L) has been suggested [95]. Under these conditions, the stoichiometry of the formed species (i.e. mononuclear and/or polynuclear) remains uncertain and so do their associated stabilities.

Previous works [54, 110] pointed out that the direct addition of SPs (Rheobuild SP8LS manufactured by BASF [54] and ADVA Cast 551 manufactured by Grace [110]) to solution increases radionuclide solubility due to organic functional groups – radionuclide interaction. Nevertheless, once SPs are mixed with cement their effect on radionuclide solubility seems to be limited, probably due to a non-specific sorption mechanism of the SPs over the cement surface [54, 107]. Therefore, understanding the nature and

strength of the interactions between radionuclides and SPs present in concrete formulations (and their degradation/aging products) deserves focused studies.

In this chapter, we have studied the effect of a polycarboxylic ether-based (PCE) SPs on the solubility of $Ni(OH)_2(s)$. To this aim, solubility experiments have been set up by working from both, over and under-saturation conditions. The main goal of this study is to quantify the effect of a PCE-SPs on Ni, as well as to get some hints on the nature and mechanism of the interaction. Three different solution compositions were considered: 1) Concrete Synthetic PoreWater (CSPW) without organic compounds, 2) leachates of concrete samples without SPs, and 3) leachates of concrete samples (G and WG) containing SPS (Glenium®27 manufactured by BASF). Results are compared with thermodynamic calculations and available literature data to depict nickel behaviour in the studied conditions. The effect of Glenium®27 on the behaviour of Ni has been compared with that of other organics, i.e. isosaccharinate.

5.2 Materials and methods

5.2.1 Concrete solid samples

Concrete blocks were prepared following the European standard UNE-EN 196-1 [2]. The raw composition of the blocks is detailed in (Table 5-1), for additional details the reader is refereed to *Section* 2.2. Note that, as explained in *Section* 2.2, two different series were produced one containing Glenium®27 (G samples) and another one without Glenium®27 (WG samples).

Table 5-1. Amounts and materials used in concrete blocks preparation. G stands for samples with Glenium®27 addition while WG stands for samples without Glenium®27.

	kg of used raw material	
	Samples WG	**Samples G**
Cement	5.3	5.3
Filler	1.5	1.5
Aggregate 0/4	10.6	12.7
Aggregate 2/6	8.0	5.1
Aggregate 6/14	8.5	8.5
Glenium®27	-	0.1
Water	2.8	2.1
Water/Cement ratio (W/C)	0.5	0.4

5.2.2 Concrete porewaters

CSPW and concrete leachates were used in this work (Table 5-2). For details related with porewaters preparation the reader is refereed to *Section* 2.3.

Table 5-2. CSPW and real concrete leachates compositions obtained in this work. Note that CSPW, WG and G stands for Concrete Synthetic PoreWater, concrete leachates without Glenium®27 and concrete leachates with Glenium®27 respectively. For each of the leachates two different compositions are reported as a function of the grinding size (< 1 mm and 1-4 mm).

	CSPW	WG < 1 mm	WG 1-4 mm	G < 1 mm	G 1-4 mm
pH	13.3	12.4	12.4	12.5	12.4
			$mol \cdot L^{-1}$		
TIC	<LOD*	$1.7 \cdot 10^{-5}$	$3.2 \cdot 10^{-5}$	$1.7 \cdot 10^{-5}$	$2.3 \cdot 10^{-5}$
TOC	-	$5.2 \cdot 10^{-5}$	$4.7 \cdot 10^{-5}$	$1.2 \cdot 10^{-4}$	$1.2 \cdot 10^{-4}$
Na	$1.2 \cdot 10^{-1}$	$1.2 \cdot 10^{-4}$	$1.0 \cdot 10^{-4}$	$1.2 \cdot 10^{-4}$	$9.4 \cdot 10^{-5}$
K	$8.2 \cdot 10^{-2}$	$4.6 \cdot 10^{-4}$	$4.2 \cdot 10^{-4}$	$4.3 \cdot 10^{-4}$	$3.7 \cdot 10^{-4}$
Ca	$1.4 \cdot 10^{-3}$	$7.5 \cdot 10^{-3}$	$6.6 \cdot 10^{-3}$	$6.1 \cdot 10^{-3}$	$7.7 \cdot 10^{-3}$
SO_4	$1.8 \cdot 10^{-3}$	$5.9 \cdot 10^{-6}$	$7.7 \cdot 10^{-6}$	$8.2 \cdot 10^{-6}$	$8.3 \cdot 10^{-6}$
Fe	<LOD	<LOD	<LOD	<LOD	<LOD
Al	$7.7 \cdot 10^{-6}$	<LOD	$4.8 \cdot 10^{-6}$	<LOD	$4.8 \cdot 10^{-6}$
Cl	-	$2.1 \cdot 10^{-4}$	$2.3 \cdot 10^{-4}$	$1.7 \cdot 10^{-4}$	$1.5 \cdot 10^{-4}$
Si	$6.2 \cdot 10^{-6}$	<LOD	<LOD	<LOD	<LOD
Ni	<LOD	<LOD	<LOD	<LOD	<LOD

* <LOD. Below limit of detection

5.2.3 Solubility experiments

Solubility experiments (Figure 5-3) were set up in both, under- and oversaturation conditions under $N_2(g)$ atmosphere (Jacomex, GP[Concept]-II-S), as follows:

- Under-saturation experiments. Commercial $Ni(OH)_2(s)$ (ACROS, analysis grade) was used in the under-saturation experiments. Those experiments were set up by contacting 2 g of $Ni(OH)_2(s)$ with 50 mL of media (either CSPW or the leachates), S/L ratio of 40 $g \cdot L^{-1}$. This high S/L ratio was chosen to ensure the presence of unperturbed solid during the whole experiment duration. Solution pH was unaltered after the addition of the solid. The experiments were manually shaken daily over a period of 12 months.
- Oversaturation experiments. Oversaturation experiments consisted in mixing 4 mL of a 10^{-5} $mol \cdot L^{-1}$ $Ni(NO_3)_2$ solution (0.1 $mol \cdot L^{-1}$ HNO_3) with 40 mL of media (CSPW or the leachates). After few seconds, the formation of a characteristic green solid suspension was observed indicating the

formation of an amorphous nickel hydroxide that was later identified by Scanning Electron Microscopy - Energy Dispersive X-Ray spectroscopy (SEM-EDX; FE-SEM - ZEISS Ultraplus, X-Max EDX detector, from OXFORD Instruments) and X-Ray Diffraction (XRD; PANalytical X'Pert PRO MPD θ/θ powder diffractometer). XRD results are presented in Figure 5-4, note that two additional peaks appear in the in-situ precipitated sample related with the formation of calcium carbonate. In the case of the leachates, the pH of the solution in the oversaturation experiments was slightly acidified from ~12.3-12.4 to final pH values around 12.0. The reason behind this deviation was the addition of the acid Ni stock solution. On the contrary, pH was unaltered in oversaturation CSPW experiments after the acid Ni stock solution addition as the initial pH value in those samples (~13.27) was higher than in the leachates (12.3-12.4).

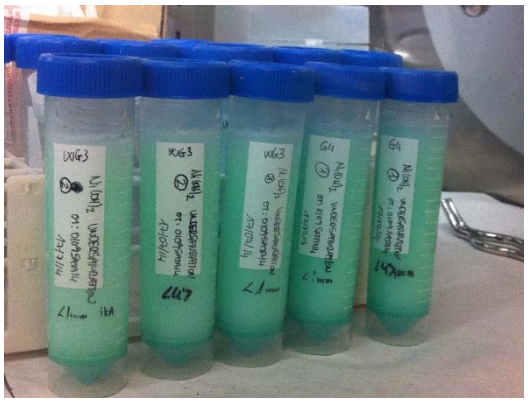

Figure 5-3. Nickel under-saturation solubility experiments in leachate solutions.

At given time intervals, aliquots of the samples were collected, filtered, acidified and analysed for Ni concentration by ICP-MS. The filtering process was done with Nylon syringe filters suitable for use in alkaline conditions. In order to check the possible formation of Ni colloid particles in these experiments two different filter meshes, 0.45 and 0.22 μm, were used.

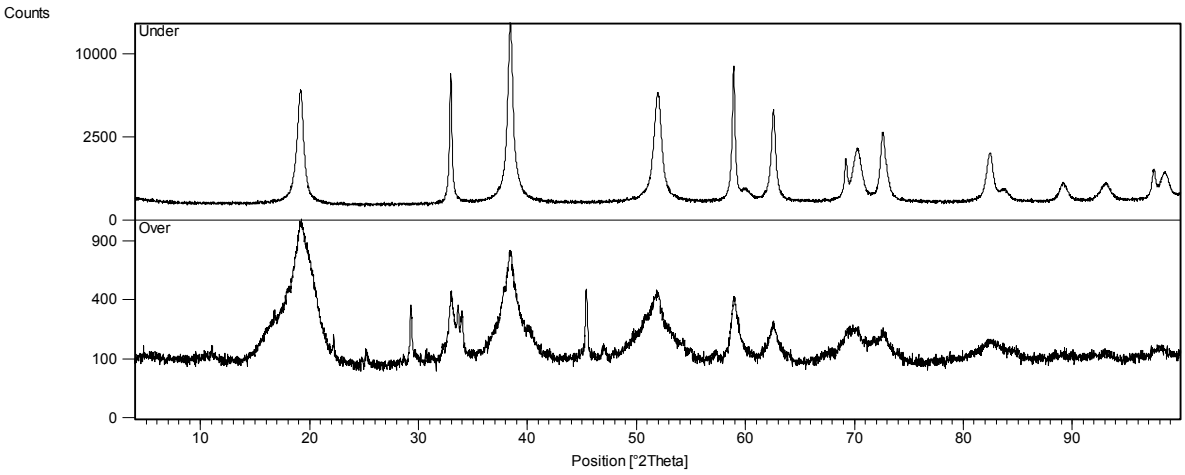

Figure 5-4. XRD pattern obtained from solids recovered after finishing the solubility experiments in both under- (commercial $Ni(OH)_2(s)$) and oversaturation (in-situ precipitated nickel hydroxide) conditions.

5.2.4 Thermodynamic calculations

The geochemical code PhreeqC [72] combined with the thermodynamic database ThermoChimie v.9 (*https://www.thermochimie-tdb.com/*) [37, 44] have been used in the calculations performed in this work. The Davies approach (eq. 1) has been used for ionic strength corrections. Thermodynamic calculations made in this work consisted mainly in solubility and speciation calculations as a function of different parameters like pH, organic concentration and time. The main purpose of these calculations was to get some hints on the behaviour of Ni in the different chemical scenarios studied in this work.

$$\log(\gamma_i) = -Az_i^2\left(\frac{\sqrt{I_m}}{1+\sqrt{I_m}} - 0.3I_m\right) \qquad \textbf{eq. 1}$$

5.3 Results and discussion

As seen in Table 5-2, concrete leachates and CSPW studied in this work presented a significantly different composition. CSPW was prepared for being representative of a fresh cement state, cement degradation state I (Figure 5-5), and thus its alkali content and pH are higher than in the case of leachates, where the alkali content has already been leached. Concrete leachates studied here are representative of a later cement degradation step governed by portlandite ($Ca(OH)_2$) dissolution (Figure 5-5) and thus presenting a lower pH (~ 12.5) and higher Ca concentrations in solution [55, 89].

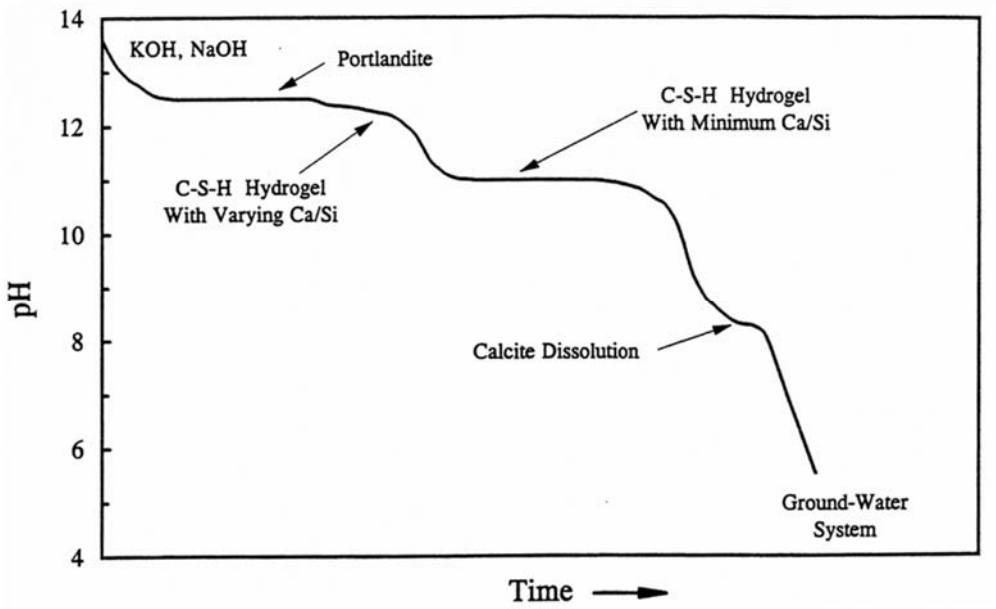

Figure 5-5. Schematic diagram illustrating the change of pore fluid pH resulting from the progressive aqueous dissolution of cement, taken from [55].

Ni solubility results obtained in this work are shown in Figure 5-6 and Figure 5-7. In CSPW media, equilibrium (i.e. measurements of different samples and replicates do not vary more than 10%) was always reached before 80 days of contact time (Figure 5-6). In the case of the solubility experiments with the leachates, whose composition is more complex than that of CSPW media (Table 5-2), equilibrium was not completely reached (measurements of different samples and replicates vary approx. half and order of magnitude) even after 120 days (Figure 5-7). In either the case, obtained results are in fair agreement with previous published studies [34, 59] (Figure 5-8). In addition, over and undersaturation trends cannot clearly seen in Figure 5-6 - Figure 5-7, indicating fast partial equilibrium in the system.

After 300 days of contact time, no relevant differences between solubility measurements in leachates of concrete samples with and without SPs in their formulations were observed, in agreement with the very similar TOC levels measured in both cases (Table 5-2). From this observation, it can be concluded that the release of small organic compounds from concrete, due to the SPs degradation or aging to the solution, is negligible after 300 days. This result is in good agreement with the predictions by Wieland and Van Loon [107] and results obtained by [3, 54] in similar systems using different radionuclides (Th, Am, etc.).

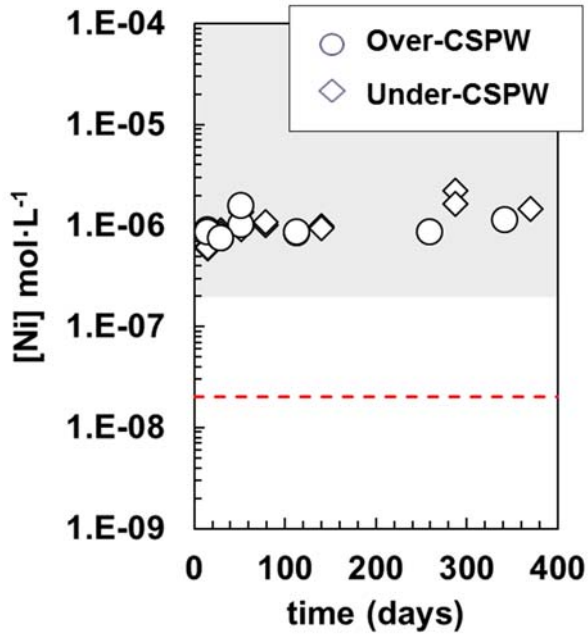

Figure 5-6. Ni (mol·L^{-1}) as a function of time (days) in over and under saturation experiments. Those results have been obtained in CSPW media, pH ~ 13.2. The grey shaded area stands for $Ni(OH)_2$ theoretical solubility range (including uncertainties) calculated with ThermoChimie at pH = 13.2. Red dashed line stands for the equipment Limit of Quantification (LOQ). Uncertainties stand for the standard deviation of at least two replicas, and are included within the point size.

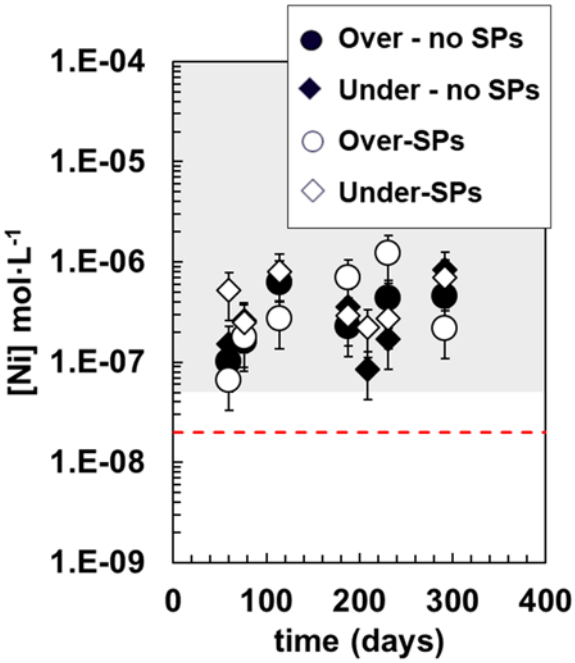

Figure 5-7. Ni (mol·L^{-1}) as a function of time (days) in over and under saturation experiments. Those results have been obtained in concrete leachates media, WG and G, pH from 12 to 13. The grey shaded area stands for $Ni(OH)_2$ theoretical solubility range (including uncertainties) calculated with ThermoChimie between pH 12-13 without organic presence in the system. Red dashed line stands for the LOQ. Uncertainties stand for the standard deviation of at least two replicas.

In CSPW media nickel aqueous concentrations are slightly higher than in leachates. This is because of the chemical hydrolysis of nickel as illustrated in Figure 5-8, where one can see a representation of the theoretical solubility of $Ni(OH)_2(s)$ as a function of pH and its underlying aqueous speciation. As seen from this figure the formation of the species $Ni(OH)_3^-$ at higher pH tends to increase Ni solubility. For illustrative purposes literature data obtained in similar conditions as well as data obtained in this work (up to 300 days) is plotted in Figure 5-8. As seen in this figure, data obtained in this work is in very good agreement with independent literature data, are slightly lower than the theoretical solubility predicted for $Ni(OH)_2(s)$ with ThermoChimie v.9, although fall within its uncertainty range. Note that the uncertainty associated with the formation of $Ni(OH)_3^-$ species is very large and, consequently the grey shaded zone accounting for the $Ni(OH)_2(s)$ solubility uncertainties in Figure 5-8 increases as a function of the participation of this species in Ni hydrolysis scheme. Recently published studies on $Ni(OH)_2(s)$ solubility [40] show no increase of the concentration of the solid under very alkaline pH values, indicating that the species $Ni(OH)_3^-$ might not be relevant under the studied conditions and that its stability could had been overestimated in the usual thermodynamic databases.

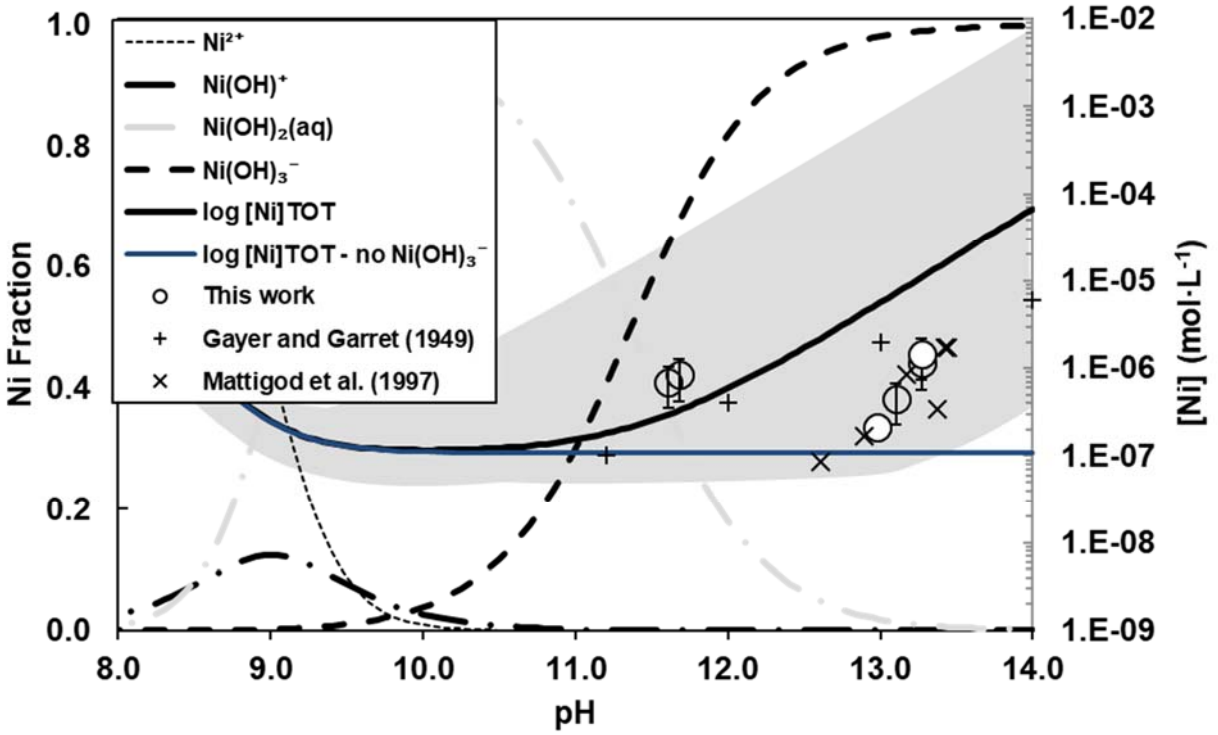

Figure 5-8. Theoretical solubility of $Ni(OH)_2(s)$, black solid line, as a function of pH. Circles stand for data obtained in this work up to 300 days in the different studied conditions. Cross and plus symbols stand for independent literature data [34, 59] obtained in similar conditions as the ones we worked with. Dashed lines stand for the fraction of the different Ni aqueous species in equilibrium with $Ni(OH)_2(s)$ in the studied conditions. The grey shaded area stands for $Ni(OH)_2(s)$ theoretical solubility uncertainties as a function of the hydrolysis species. For comparative purposes the solubility of $Ni(OH)_2(s)$ without considering the formation of $Ni(OH)_3^-$ species, blue solid line, has been included in this figure. Calculations done with PhreeqC and ThermoChimie v. 9.0 database.

Additional under-saturation solubility experiments with variable SPs spikes in aqueous solution were performed to decipher whether the studied SPs were able to affect the behaviour of nickel in a cementitious environment. Those experiments were done by using CSPW media, and thus following the same procedure previously detailed, but adding variable SPs dosage ranging from 0.05 to 1.0 mL from the original SPs raw solution. The selected SPs spikes gave TOC values in solution ranging from ~$1.6 \cdot 10^{-3}$ to $3.2 \cdot 10^{-2}$ mol·L^{-1}. Those TOC values are far from being representative of the standard concrete samples (e.g. G samples listed in Table 5-1) prepared in this work ($5.5 \cdot 10^{-5}$ mol·L^{-1}) but of interest to understand the interaction between nickel and the SPs. Figure 5-9 presents nickel hydroxide solubility results obtained at variable SPs spikes. From this figure one can deduce that the presence of SPs in solution clearly enhances nickel solubility in CSPW conditions. TOC values over $3 \cdot 10^{-3}$ mol·L^{-1} are required to observe an important increase of nickel solubility. Interestingly, at long term, increasing the TOC content from 1.6 to $3.2 \cdot 10^{-2}$ mol·L^{-1} does not seem to affect nickel behaviour, suggesting steady state conditions. An approximate increase of three orders of magnitude on Ni solubility is observed at the highest SPs spikes. In agreement with our findings here, a solubility increase effect has been also reported by others [41, 110] when studying U, Pu and Am behaviour in cementitious conditions with direct SPs addition in solution. More recently [63], an increase of the

solubility of Ni by three orders of magnitude has been found in cement equilibrated porewaters with different SP spikes. Those authors also reported an increase of two orders of magnitude for ^{241}Am and for ^{239}Pu solubilities while in the case of U similar concentrations were achieved with and without SP spikes. It must be notice that the cement equilibrated water used in [63] was obtained after squeezing the concrete samples and thus the authors believe that the agent responsible of controlling U behaviour was already present in the equilibrated water before adding the SP spike.

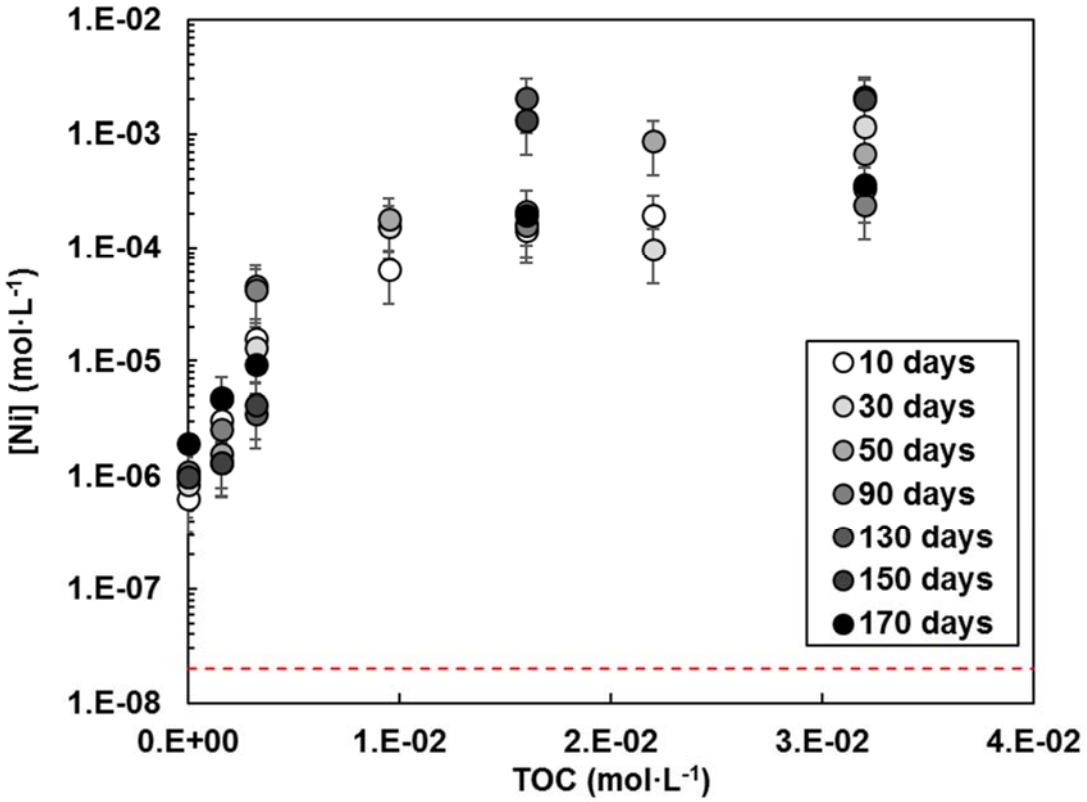

Figure 5-9. Ni (mol·L^{-1}) as a function TOC (mol·L^{-1}) at different times (10-170 days) in under saturation experiments. Those results have been obtained in CSPW media, pH ~ 13.2. Red dashed line stands for the LOQ. Uncertainties stand for the standard deviation of at least two replicas.

Small organics (i.e. isosaccharinic acid, gluconate, oxalate, etc.) have a great effect on Ni behaviour and may be used as surrogates to understand the effect of more complex materials like SPs. Kitamura and co-workers [54], studied gluconate as a simple surrogate to represent SPs complexing capacity when studying Th and Am solubilities in similar conditions as the ones presented in this work. The results presented by those authors overestimate Am and Th solubilities almost two or three orders of magnitude assuming gluconate as a SPs surrogate and using the JAEA thermodynamic database in their calculations. In their, study the authors used squeezed cement porewaters and thus as they discussed SPs could be strongly adsorbed in the cement phases preventing its release and its possible final effect on radionuclide behaviour. Considering Kitamura and co-workers [54] work as a reference, and using the TOC data obtained in our work, we have done a similar exercise. If we assume that all measured TOC content in our

samples is due to the presence of the organic ligand of interest (isosaccharinic acid, gluconate or oxalate) in solution, we can estimate what would be the concentration of the organic compound in our system through simple stoichiometry relationship (Table 5-3).

Table 5-3. Calculated concentrations of ISA, GLU and Oxalate, assuming TOC is completely originated by the presence of each one of the organic ligands in solution.

TOC ($mol \cdot L^{-1}$)	Isosaccharinic (ISA) ($mol \cdot L^{-1}$)	Gluconate (GLU) ($mol \cdot L^{-1}$)	Oxalate ($mol \cdot L^{-1}$)
$1.6 \cdot 10^{-3}$	$2.6 \cdot 10^{-4}$	$2.6 \cdot 10^{-4}$	$7.9 \cdot 10^{-4}$
$3.2 \cdot 10^{-3}$	$5.3 \cdot 10^{-4}$	$5.3 \cdot 10^{-4}$	$1.6 \cdot 10^{-3}$
$9.5 \cdot 10^{-3}$	$1.6 \cdot 10^{-3}$	$1.6 \cdot 10^{-3}$	$4.7 \cdot 10^{-3}$
$1.6 \cdot 10^{-2}$	$2.6 \cdot 10^{-3}$	$2.6 \cdot 10^{-3}$	$7.9 \cdot 10^{-3}$
$2.2 \cdot 10^{-2}$	$3.7 \cdot 10^{-3}$	$3.7 \cdot 10^{-3}$	$1.1 \cdot 10^{-2}$
$3.2 \cdot 10^{-2}$	$5.3 \cdot 10^{-3}$	$5.3 \cdot 10^{-3}$	$1.6 \cdot 10^{-2}$

Thermodynamic data for the complexation of Ni with ISA and oxalate ligands are included in ThermoChimie v9. A recent study [40] on Ni-ISA systems published different Ni-ISA stability constants that have been used in this work for comparative purposes. In the oxalate case, ternary species Ni-OH-Ox are expected to form at alkaline conditions [95]. Experimental data for the formation of these species are not yet available and thus not included in ThermoChimie v.9. It is possible to estimate an upper limit for the stability of these species taking into account that the hydrolysis of metal-ligand complexes is always somewhat weaker than the hydrolysis of the hydrated cation itself [95]. In this way, the following upper limits for log *K* values of formation of Ni-OH-Ox ternary species are obtained (r. 6 and r. 7).

$$Ni^{2+} + Ox^{2-} + H_2O \rightarrow Ni(OH)(Ox)^{-} + H^{+} \qquad \log K < -4.4 \qquad \text{r. 6}$$

$$Ni^{2+} + Ox^{2-} + 2H_2O \rightarrow Ni(OH)_2(Ox)^{2-} + 2H^{+} \qquad \log K < -12.6 \qquad \text{r. 7}$$

Ni gluconate complexation is not included in ThermoChimie v.9. Evans and co-workers [29, 30, 99, 100] studied this system in near-neutral and alkaline media (pH from 7 to 13) which is of interest for this work. The authors reported the formation of three different species as a function of the system pH. In the alkaline pH range of interest for the current study, the formation of a polynuclear species ($Ni_2(OH)_4(HGLU)^{-}$) with a log *K* of -24.6 at I = 0.3 $mol \cdot L^{-1}$ for r. 8 is expected according to Evans and co-workers studies.

$$2Ni^{2+} + GLU^{-} + 4H_2O \rightarrow Ni_2(OH)_4(HGLU)^{-} + 4H^{+} \qquad \text{r. 8}$$

Considering the organic concentration values listed in Table 5-3, the thermodynamic data for the Ni-organic species cited above together with the Ni solubility data obtained in this work, a prediction of Ni

concentration evolution as a function of the estimated organic content in samples have been done (Figure 5-10. a-c). The theoretical solubility of $Ni(OH)_2(s)$ calculated with ThermoChimie v.9 as a function of the total organic concentration (ISA, GLU or oxalate) as well as the aqueous speciation of nickel in equilibrium with the studied solid is also shown in these figures for comparative purposes. As seen from these figures, the increase of organic concentrations increases the solubility of $Ni(OH)_2(s)$ through the formation of different aqueous species depending on the studied organic ligand ($Ni(OH)_3(HISA)^{2-}$, $Ni_2(OH)_4(HGlu)^-$, $Ni(OH)_2(Ox)^{2-}$). The formation of these species occurs even at low organic concentrations ($1 \cdot 10^{-4}$ mol·L^{-1}) and controls the aqueous chemistry of nickel at organic levels above ~$1 \cdot 10^{-3}$ mol·L^{-1}.

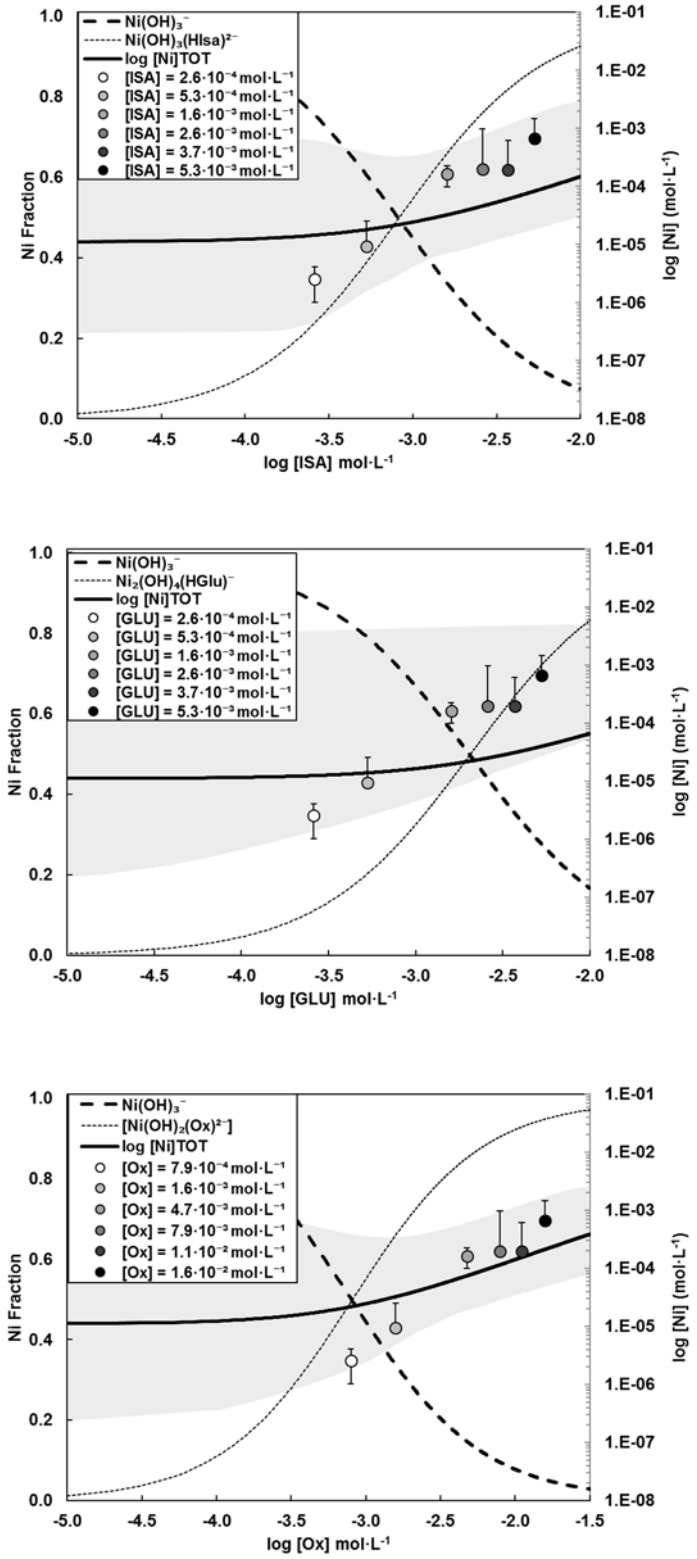

Figure 5-10. Theoretical solubility of $Ni(OH)_2(s)$, black solid line, as a function of organic ligand content ($mol \cdot L^{-1}$) in CSPW conditions. Black dashed lines stand for the fraction of Ni aqueous species in equilibrium with $Ni(OH)_2(s)$ in the studied conditions. Symbols stand for nickel solubility values measured in this work. The grey shaped area stands for $Ni(OH)_2(s)$ theoretical solubility uncertainties as a function of the hydrolysis species. ThermoChimie v. 9.0 together with Ni-OH-Ox ternary species and Ni-GLU data from [29] have been used in these calculations. Note that results obtained for Ni-ISA systems using Ni-ISA thermodynamic data from [40] are included in the uncertainty range.

Experimental Ni solubility data obtained in this work, symbols in Figure 5-10, follow the same trend as the theoretical $Ni(OH)_2(s)$ solubility in the presence of small organic ligands; this is Ni concentration increases as the level of organic increases in solution. Nevertheless, at the highest organic concentration there are some discrepancies between predicted and measured Ni concentrations for ISA and GLU systems. Assuming the formation of the ternary species Ni-OH-Ox results in a good fit of the experimental results at higher oxalate concentrations. Is worth mentioning that if we account for the uncertainties of the solid and aqueous Ni species in the system (grey shaped area in Figure 5-10. a-c), the experimental results may be explained by assuming the presence of either of the organics (ISA, GLU and oxalate) that have been studied here.

As previously explained, PCE SPs are mainly composed by a long carbon backbone and carboxylic acids terminations (Figure 5-2), besides different additives (pesticides, herbicides, etc.) added into the SPs cocktail solution to preserve its properties/functionalities. A direct relationship between SPs and ISA/GLU/Oxalate global structures is not straightforward (Figure 5-2 and Figure 5-11). A close comparison of "raw" SPs and small organic (ISA, GLU, Oxalate) structures points out that all those compounds have carboxylic or carboxylate terminations in their structure. ISA and GLU presented a similar structure with just one carboxylate member while oxalate is a relatively smaller molecule with two carboxylate terminations. From a chemical reactivity point of view this means that oxalate is a more labile molecule than ISA and GLU. This observation agrees well with the blind predictions presented in Figure 5-10, where it was shown that oxalate presented the higher complexing capacity towards Ni.

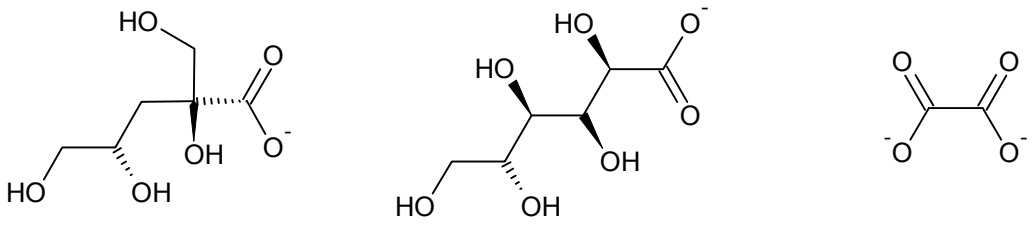

(a) **(b)** **(c)**

Figure 5-11. Sketch of a) ISA, b) GLU and c) oxalate structures.

5.4 Conclusions

The solubility of nickel in cementitious environments and the effect of Glenium®27, a PCE superplasticizer, on its solubility has been studied in this work. To this aim two different aqueous media were selected, a synthetic porewater representative of a fresh cement and leachate porewaters accounting for an aged cementitious system.

Nickel solubility values obtained in solution in the absence of superplasticizers are in fair agreement with previous published studies. Results obtained with the direct addition of Glenium®27 into the samples indicate that if this polymer is released to the solution, it could cause an important enhancement of Ni solubility in cementitious systems. This effect has also been observed by others in similar systems for a variety of radionuclides (U, Th, Pu, Am). In the case of leachates, our results indicate that, once SPs is included in the concrete formulation, this polymeric material is stabilized (e.g. adsorbed into the cement phases) and negligible mobilization effects on the behaviour of a trace radionuclide like Ni could be observed.

Thermodynamic calculations carried out in this work suggest that, for this specific system, oxalate may be used as a SPs surrogate to reproduce the experimental trends obtained for $Ni(OH)_2(s)$ solubility at variable superplasticizer dosages. Nevertheless, considering the high uncertainty of some of the thermodynamic data used in this exercise, either gluconate or isosaccharinate may be consider as alternative SPs surrogates. In future works the focus should be on characterising SPs structure as well as possible aging/degradation products in cementitious systems for a better process representation.

In summary, the results presented here indicate that in realistic systems Glenium®27 is stabilized (e.g. adsorbed into the cement phases) and thus its effect on radionuclide mobility will be negligible. Moreover, the amount of Glenium®27 used in the cement formulations is relatively low (TOC ~ $5 \cdot 10^{-5}$ mol·L^{-1}), and in the unlikely event of a total Glenium®27 release from the cementitious system, TOC values over $3 \cdot 10^{-3}$ mol·L^{-1} are required to observe an important increase of nickel solubility; which is far from the real samples measures. The results presented in this work support the selection of Glenium®27 as a reference SPs for being used in concrete formulations of future radioactive deep disposal facilities.

Chapter 6: CONCLUSIONS

6 Conclusions

In this study the characterisation, stability as well as the reactivity of polycarboxylate ether-based superplasticizers has been investigated in the frame of radioactive waste disposal. Specifically, Glenium®27 has been chosen in this work as it is one of the reference materials selected by the Belgian authorities for building up the future waste repository. In addition, an in-house synthesized polycarboxylate ether-based superplasticizer free from impurities (i.e. free from pesticides, herbicides, etc.) has been studied within the stability experiments for comparative purposes. Our stability studies have been mainly based in three processes (i.e. hydrolysis, temperature, irradiation) expected to have some impact on superplasticizers chemical evolution under deep disposal conditions. Reactivity of the studied superplasticizer towards Nickel has been investigated here through solubility studies in different porewater conditions representative of a variety of repository scenarios.

The results gathered from different analytical techniques led us to conclude that both, Glenium®27 as well as the in-house synthesized material, presented a polyethyleneglicol carbon-backbone chain with n members, n ranging from 15 to 23, and different terminal chemical groups including polycarboxylate and sulfonated species. Mainly, methacrylic acid has been found as a polycarboxylate species within the superplasticizers, although other non-identified species have been also found in Glenium®27 cocktail. Those elements, the polyethyleneglicol back-bone and the terminal functional groups, confer the superplasticizer with a great plasticity as well as good hydro and hygrophobic properties suitable for their use in concrete formulations.

Overall, we have found that temperature and radiation processes, at repository optimal levels, will not have an important impact on the structure and/or the chemical composition of such materials. However, a more aggressive treatment, will promote a structural material transformation that may have an important impact on the performance of the material under deep disposal conditions. As an example, superplasticizer co-polymerization has been found to occur at temperature over 250^{o}C, limiting thus the plasticity of the material under such conditions. The study of superplasticizer irradiation in aqueous solutions is envisaged as a possible degradation pathway through interactions with the $OH^{\bullet}$ radical that must be further study to ensure the safety of the radioactive waste disposal.

Not conclusive results have been obtained from our hydrolysis experiments. Superplasticizer hydrolysis has not been observed in our batch tests as the system pH remained constant after one-year contact time. Raman measurements were not able to confirm whether the superplasticizer was hydrolysed / modified. Devoted hydrolysis experiments using more sophisticated analytical techniques such as mass NMR to characterise the final products are envisaged as a good solution to confirm or to discard the extension of superplasticizer hydrolysis.

According to our results, once mixed with the different concrete primary components, Glenium®27 do not come back into solution keeping retained into the cementitious surfaces. Ni solubility studies, carried

out with different concrete leachates as well as with synthetic cementitious porewater, have confirmed this finding. Our results show that the inclusion of Glenium®27 into concrete formulations does not affect Ni behaviour under the dosages used in concrete preparation. However, adding directly the Glenium®27 cocktail (at dosages higher than the standard used in concrete formulations) into the cementitious porewater (without cement / concrete presence) substantially increases the concentration of Ni in solution. Interestingly, at high Glenium®27 concentration, a plateau is observed on Ni solubility indicating possible steady-state conditions or perhaps the formation of big Ni-Glenium®27 complexes that have been retained within the filters. The complexation capacity offered by the Glenium®27 towards Ni has been found to be similar to the complexation capacity of other small organic compounds such as oxalate, isosaccharinate or gluconate.

In summary, our results indicate that under standard deep disposal conditions Glenium®27 will be stable, and not altered by temperature, radiolysis and/or hydrolysis processes. This means that the generation of labile small organics compounds, that may complex radionuclides from the disposed wastes increasing their mobility, due to superplasticizers degradation will be almost negligible. This is a key argument to support the use of superplasticizers as a concrete admixture for building up the future nuclear waste disposal facilities.

Chapter 7: REFERENCES

7 References

[1] AENOR. Characterization of waste. Leaching. Compliance test for leaching of granular waste materials and sludges. Part 2: One stage batch test at a liquid to solid ratio of 10 L/Kg for materials with particle size below 4 mm (without or with size reduction). UNE-EN 12457-2, 2003.

[2] AENOR. Methods of testing cement - Part 1: Determination of strength. UNE-EN-196, 2005.

[3] S. Aggarwal, M.J. Angus, R.C. Hibbert, and A. Tyson. Radionuclide concentration in cementitious pore-fluids extracted under high pressure. Technical Report AEAT/R/ENV/0231, AEA Technology, 2001.

[4] A. Aignesberger and P. Bornmann. Verfahren zur herstellung von loesungen sulfitmodifizierter melaminharze. DE Patent: DE1745441 A1, 1975.

[5] A. Albrecht, S. Altmann, S. Buschaert, D. Coelho, M.O. Gallerand, E. Giffaut, and E. Leclerc-Cessac. Dossier 2005 Argile. Réferentiel du comportement des radionucléides et des toxiques chimiques d'un stockage dans le Callovo-Oxfordien jusq'à l'homme. Site de Meuse/Haute-Marne. Tome 1/2., 2005.

[6] S. Allard. *Investigations of a-D-isosaccharinate: Fundamental Properties and Complexation*. PhD thesis, Chalmers University of Technology, 2005.

[7] S. Allard and Ch. Ekberg. Complexing properties of alpha-isosaccharinate: Thorium. *Radiochimica Acta*, 94:537–540, 2006.

[8] M. Andersson, H. Ervanne, M.A. Glaus, S. Holgersson, H. Laine, B. Lothenbach, I. Puigdomenech, B. Schwyn, M. Snellman, H. Ueda, M. Vuorio, E. Wieland, and T. Yamamoto. Development of methodology for evaluation of long-term safety aspects of organic cement paste components. *POSIVA Working report*, 28:2008, 2008.

[9] Andra. Dossier 2005 Argile. Synthesis: Evaluation of the feasibility of a geological repository in an argillaceous formation. Technical Report Andra 226 VA, Andra, 2005.

[10] S. Bagawde, V. Ramakrishna, and S. Patil. Oxalate complexing of tetravalent actinides. *Journal of Inorganic and Nuclear Chemistry*, 38:1669–1672, 1976.

[11] I. Balakrishnan and M.P. Reddy. Homolytic hydroxylation of naphthalene in oxygenated aqueous solutions by gamma radiolysis at higher temperatures. *The Journal of Physical Chemistry*, 72(13):4609–4613, 1968.

[12] F. Bart, C. Cau-di Coumes, F. Frizon, and S. Lorente. *Cement-based materials for nuclear waste storage*. Springer Science & Business Media, 2012.

[13] M. Bartušek and L. Sommer. On the complex forming tendency of phenolic hydroxyl with UO_2^{2+}. *Journal of Inorganic and Nuclear Chemistry*, 27(11):2397–2412, 1965.

[14] M.E. Bedessem, N.G. Swoboda-Colberg, and P.J.S. Colberg. Naphthalene mineralization coupled to sulphate reduction in aquifer-derived enrichments. *FEMS Microbiology Letters*, 152(2):213–218, 1997.

[15] J.J.P. Bel, S.M. Wickham, and R.M.F. Gens. Development of the Supercontainer design for deep geological disposal of high-level heat emitting radioactive waste in Belgium. In *MRS Proceedings*, volume 932, pages 122–1. Cambridge Univ Press, 2006.

[16] A. Berckmans, D. Boulanger, S. Brassinnes, M. Capouet, C. Depaus, E. Dorado Lopez, A. Gambi, R. Gens, X. Sillen, H. Van Baelen, M. Van Geet, P. Van Marcke, Wacquier W., L. Wouters, L Harvey, S. Wickham, and V. Pirot. ONDRAF/NIRAS Research, Development and Demonstration (RD&D) plan for the geological disposal of high-level and/or long-lived radioactive waste including irradiated fuel if considered as waste. State-of-the-art report as of December 2012. Technical Report NIROND-TR 2013-12 E, ONDRAF/NIRAS, 2013.

[17] M.A. Boggs, W. Dong, B. Gu, and N.A. Wall. Complexation of Tc(IV) with acetate at varying ionic strengths. *Radiochimica Acta*, 98(9-11):583–587, 2010.

[18] M. Borkowski, G.R. Choppin, and R.C. Moore. Thermodynamic modelling of metal-ligand interactions in high ionic strength Nacl solutions: The Co^2+-oxalate system. *Radiochimica Acta*, pages 599–602, 2000.

[19] M. Borkowski, G.R. Choppin, and R.C. Moore. Thermodynamic modelling of metal–ligand interactions in high ionic strength NaCl solutions: the Ni^2+-oxalate system. *Radiochimica Acta*, 91(3):169, 2003.

[20] M. Borkowski, R.C. Moore, M.G. Bronikowski, J. Chen, O.S. Pokrovsky, Y. Xia, and G.R. Choppin. Thermodynamic modelling of actinide complexation with oxalate at high ionic strength. *Journal of Radioanalytical and Nuclear Chemistry*, 248(2):467–471, 2001.

[21] M. Brebu, G. Cazacu, and O. Chirila. Pyrolysis of lignin a potential method for obtaining chemicals and/or fuels. *Cellulose Chemistry and Technology*, 45(1):43, 2011.

[22] M. Brebu and C. Vasile. Thermal degradation of lignin a review. *Cellulose Chemistry & Technology*, 44(9):353, 2010.

[23] M. Castellote, C. Andrade, and A. Castillo. Characterisation of cementitious matrices for a surface disposal of LLW. Technical report, Centro Superior de Investigaciones Científicas - Instituto de Ciencias de la Construccion Eduardo Torroja (CSIC-ICCEJ), 2009.

[24] G. Choppin and J.F. Chen. Complexation of Am(III) by oxalate in $NaClO_4$ media. page 105, 1995.

[25] E. Colàs Anguita. *Complexation of Th (IV) and U (VI) by polyhydroxy and polyamino carboxylic acids*. PhD thesis, Universitat Politècncia de Catalunya, 2014.

[26] L. Costa and G. Camino. Thermal behaviour of melamine. *Journal of thermal analysis*, 34(2):423–429, 1988.

[27] B. Craeye, G. De Schutter, H. Van Humbeeck, and A. Van Cotthem. Early age behaviour of concrete supercontainers for radioactive waste disposal. *Nuclear Engineering and Design*, 239(1):23–35, 2009.

[28] A.D. English, D.B. Chase, and H.J. Spinelli. Structure and degradation of an intractable polymeric system: melamine formaldehyde crosslinked acrylic coatings. *Macromolecules*, 16(9):1422–1427, 1983.

[29] N. Evans, S. Antón-Gascón, S. Vines, and M. Felipe-Sotelo. Effect of competition from other metals on nickel complexation by alpha-isosaccharinic, gluconic and picolinic acids. *Mineralogical Magazine*, 76(8):3425–3434, 2012.

[30] N. Evans, P. Warwick, M. Felipe-Sotelo, and S. Vines. Prediction and measurement of complexation of radionuclide mixtures by a-isosaccharinic, gluconic and picolinic acids. *Journal of Radioanalytical and Nuclear Chemistry*, 293:725–730, 2012.

[31] A.I. Finkel'Shtein. Optical investigation of the molecular structure of s-triazine derivatives. IV. infrared absorption spectra of compounds with condensed nuclei of s-triazine derivatives of cyameluric acid. *Optics and Spectroscopy*, 6:17, 1959.

[32] X. Gaona, V. Montoya, E. Colàs, M. Grivé, and L. Duro. Review of the complexation of tetravalent actinides by ISA and gluconate under alkaline to hyperalkaline conditions. *Journal of Contaminant Hydrology*, 102(3):217–227, 2008.

[33] M. Gascoyne. Influence of grout and cement on groundwater composition. Technical Report 2002-07, Posiva, 2002.

[34] K.H. Gayer and A.B. Garrett. The equilibria of nickel hydroxide, $Ni(OH)_2$, in solutions of hydrochloric acid and sodium hydroxide at 25ºC. *Journal of the American Chemical Society*, 71(9):2973–2975, 1949.

[35] J.L. Gerlock, M.J. Dean, T.J. Korniski, and D.R. Bauer. Formaldehyde release from acrylic/melamine coatings during photolysis and the mechanism of photoenhanced cross-link hydrolysis. *Industrial & Engineering chemistry product research and development*, 25(3):449–453, 1986.

[36] F.G.F. Gibb. High-temperature, very deep, geological disposal: a safer alternative for high-level radioactive waste? *Waste Management*, 19(3):207 – 211, 1999.

[37] E. Giffaut, M. Grivé, Ph. Blanc, Ph. Vieillard, E. Colàs, H. Gailhanou, S. Gaboreau, N. Marty, B. Madé, and L. Duro. Andra thermodynamic database for performance assessment: ThermoChimie. *Applied Geochemistry*, 49:225–236, 2014.

[38] M.A. Glaus and L.R. Van Loon. Cellulose degradation at alkaline conditions: Long-term experiments at elevated temperatures. Technical Report PSI Report Nr. 04-01, PSI, 2004.

[39] M.A. Glaus and L.R. Van Loon. A generic procedure for the assessment of the effect of concrete admixtures on the retention behaviour of cement for radionuclides: concept and case studies. Technical Report PSI Report Nr. 04-02, PSI, 2004.

[40] M.R. González-Siso, X. Gaona, L. Duro, M. Altmaier, and J. Bruno. Thermodynamic model of Ni (II) solubility, hydrolysis and complex formation with ISA. *Radiochimica Acta*, 106(1):31–45, 2018.

[41] B.F. Greenfield, D.J. Ilett, M. Ito, R. McCrohon, T.G. Heath, C.J. Tweed, S.J. Williams, and M. Yui. The effect of cement additives on radionuclide solubilities. *Radiochimica acta*, 82(s1):27–32, 1998.

[42] I. Grenthe and I. Puigdomenech. *Modelling in aquatic chemistry*. OECD Publishing, 1997.

[43] A. Griesser. *Cement-Superplasticizer Interactions at Ambient Temperatures*. PhD thesis, ETH, 2002.

[44] M. Grivé, L. Duro, E. Colàs, and E. Giffaut. Thermodynamic data selection applied to radionuclides and chemotoxic elements: An overview of the ThermoChimie-TDB. *Applied Geochemistry*, 55:85–94, 2015.

[45] A. Haars and A. Huttermann. Macromolecular mechanism of lignin degradation by Fomes annosus. *Naturwissenschaften*, 67(1):39–40, 1980.

[46] S.A. Haveman, S. Stroes-Gascoyne, and C.J. Hamon. Biodegradation of a sodium sulphonated naphthalene formaldehyde condensate by bacteria naturally present in granitic groundwater. Technical Report TR-721, AECL, 1996.

[47] W.L. Hawkins. *Polymer degradation and stabilization*, volume 8. Springer Science & Business Media, 1984.

[48] A. Heller, A. Barkleit, G. Bernhard, and J.-U. Ackermann. Complexation study of Europium(III) and Curium(III) with urea in aqueous solution investigated by time-resolved laser-induced fluorescence spectroscopy. *Inorganica Chimica Acta*, 362(4):1215–1222, 2009.

[49] S. Holgersson and Y. Albinsson. Effects of gluco-isosaccharinate on Cs, Ni, Pm and Th sorption onto, and diffusion into cement. *Journal of Radiochimica Acta*, 82(3):393–398, 1998.

[50] S. Holgersson, Y. Albinsson, B. Allard, H. Boren, I. Pavasars, and I. Engkvist. Effects of gluco-isosaccharinate on Cs, Ni, Pm and Th sorption onto, and diffusion into cement. *Radiochimica Acta*, 82:393–398, 1998.

[51] W. Hummel, G. Anderegg, L. Rao, I. Puigdomènech, and O. Tochiyama. *Chemical thermodynamics of compounds and complexes of U, Np, Pu, Am, Tc, Se, Ni and Zr with selected organic ligands*, volume 9. Elsevier Science, 2005.

[52] K. Jutzi, A. M Cook, and R. Hütter. The degradative pathway of the s-triazine melamine. The steps to ring cleavage. *Biochemical Journal*, 208(3):679–684, 1982.

[53] S. Kanodia, V. Madhaven, and R.H. Schuler. Oxidation of naphthalene by radiolytically produced OH radicals. *International Journal of Radiation Applications and Instrumentation. Part C. Radiation Physics and Chemistry*, 32(5):661–664, 1988.

[54] A. Kitamura, K. Fujiwara, M. Mihara, M. Cowper, and G. Kamei. Thorium and americium solubilities in cement pore water containing superplasticiser compared with thermodynamic calculations. *Journal of Radioanalytical and Nuclear Chemistry*, 298(1):485–493, 2013.

[55] K.M. Krupka and Bradbury J.B. Serne, R.J. Effects on radionuclide concentrations by cement/groundwater interactions in support of the performance assessment of low-level radioactive waste disposal facilities. Technical Report NUREG/CR-6377 PNNL-11408, U.S. Regulatory Commission, 1998.

[56] A. Lair, C. Ferronato, J.-M. Chovelon, and J.-M. Herrmann. Naphthalene degradation in water by heterogeneous photocatalysis: an investigation of the influence of inorganic anions. *Journal of Photochemistry and Photobiology A: Chemistry*, 193(2):193–203, 2008.

[57] J.G. Mark. Concrete and hydraulic cement. US Patent: 2141570, 1938.

[58] R. Marsac, M. Davranche, G. Gruau, M. Bouhnik-Le Coz, and A. Dia. An improved description of the interactions between rare earth elements and humic acids by modelling: PhreeqC-Model VI coupling. *Geochimica et Cosmochimica Acta*, 75(19):5625–5637, 2011.

[59] S.V. Mattigod, D. Rai, A.R. Felmy, and L. Rao. Solubility and solubility product of crystalline $Ni(OH)_2$. *Journal of solution Chemistry*, 26(4):391–403, 1997.

[60] J.R. McKelvie, D.R. Korber, and G.M. Wolfaardt. *Microbiology of the Deep Subsurface Geosphere and Its Implications for Used Nuclear Fuel Repositories*, pages 251–300. Springer, 2016.

[61] J.R. Mihelcic and R.G. Luthy. Microbial degradation of acenaphthene and naphthalene under denitrification conditions in soil-water systems. *Applied and Environmental Microbiology*, 54(5):1188–1198, 1988.

[62] J.R. Mihelcic and R.G. Luthy. Sorption and microbial degradation of naphthalene in soil-water suspensions under denitrification conditions. *Environmental Science & Technology*, 25(1):169–177, 1991.

[63] NDA. Solubility studies in the presence of polycarboxylate ether superplasticisers. Technical Report NDA DRP LOT 2: Integrated Waste Management WP/B2/7, NDA, 2015.

[64] NEA. International conference on geological repositories 2016. Technical Report NEA No. 7345, OECD, 2017.

[65] C.F. Novak, M. Borkowski, and G.R. Choppin. Thermodynamic modelling of neptunium (V)-acetate complexation in concentrated NaCl media. *Radiochimica acta*, 74(s1):111–116, 1996.

[66] J.A. Onwudili and P.T. Williams. Reaction mechanisms for the decomposition of phenanthrene and naphthalene under hydrothermal conditions. *The Journal of Supercritical fluids*, 39(3):399–408, 2007.

[67] A. Osman, G. Geipel, A. Barkleit, and G. Bernhard. Uranium(VI) binding forms in selected human body fluids: Thermodynamic calculations versus spectroscopic measurements. *Chemical research in toxicology*, 28(2):238–247, 2015.

[68] A. Osman, G. Geipel, and G. Bernhard. Interaction of Uranium(VI) with bioligands present in human biological fluids: the case study of urea and uric acid. *Radiochimica Acta International journal for chemical aspects of nuclear science and technology*, 101(3):139–148, 2013.

[69] N. Öztekin, F.B. Erim, and B. Basaran. Stability constants of complexes of Thorium(IV) with phenolate ions. *Microchemical journal*, 53(2):164–167, 1996.

[70] J.D. Palmer and G.A. Fairhall. The radiation stability of ground granulated blast furnace slag/ordinary Portland cement grouts containing organic admixtures. In *MRS Proceedings*, volume 294, page 285. Cambridge Univ Press, 1992.

[71] K.K. Park, T.R. Kwon, Y.J. Park, E.C. Jung, and W.H. Kim. Ternary complex formation of Eu(III) with phthalate in aquatic solutions. In *Transactions of the Korean Nuclear Society Meeting (Autumn, 2006)*, 2006.

[72] D.L. Parkhurst and C.A.J. Appelo. *Groundwater, Book 6, Modelling Techniques. Techniques and Methods 6–A43*, chapter 43 of Section A. Description of Input and Examples for PhreeqC Version 3 – A Computer Program for Speciation, Batch-reaction, One-dimensional Transport, and Inverse Geochemical Calculations. USGS, 2013.

[73] H. Pathak, D. Kantharia, A. Malpani, and D. Madamwar. Naphthalene degradation by Pseudomonas sp. HOB1: in vitro studies and assessment of naphthalene degradation efficiency in simulated microcosms. *Journal of Hazardous Materials*, 166(2):1466–1473, 2009.

[74] K. Pedersen. Investigations of subterranean bacteria in deep crystalline bedrock and their importance for the disposal of nuclear waste. *Canadian Journal of Microbiology*, 42(4):382–391, 1996.

[75] J. Peñuela, D. Martinez, M. L. Araujo, F. Brito, G. Lubes, M. Rodriguez, and V. Lubes. Speciation of the Nickel(II) complexes with oxalic and malonic acids studied in 1.0 $mol \cdot dm^{-3}$ NaCl at 25ºC. *Journal of Coordination Chemistry*, 64(15):2698–2705, 2011.

[76] J. Plank, K. Pöllmann, N. Zouaoui, P.R. Andres, and C. Schaefer. Synthesis and performance of methacrylic ester based polycarboxylate superplasticizers possessing hydroxy terminated poly (ethylene glycol) side chains. *Cement and Concrete Research*, 38(10):1210–1216, 2008.

[77] D. Rai. The influence of isosaccharinic acid on the solubility of Np(IV) hydrous oxide. *Radiochimica Acta*, 83:8–13, 1998.

[78] D. Rai, L. Rao, and D.A. Moore. The influence of isosaccharinic acid on the solubility of Np(IV) hydrous oxide. *Radiochimica Acta*, 83(1):9–13, 1998.

[79] D. Rai, M. Yui, D.A. Moore, and L. Rao. Thermodynamic model for ThO_2(am) solubility in isosaccharinate solutions. *Journal of Solution Chemistry*, 38(12):1573–1587, November 2009.

[80] T.F. Rees and S.R. Daniel. Complexation of Neptunium(V) by salicylate, phthalate and citrate ligands in a pH 7.5 phosphate buffered system. *Polyhedron*, 3(6):667–673, 1984.

[81] K.J. Rockne, J.C. Chee-Sanford, R.A. Sanford, B.P. Hedlund, J.T. Staley, and S.E. Strand. Anaerobic naphthalene degradation by microbial pure cultures under nitrate-reducing conditions. *Applied and Environmental Microbiology*, 66(4):1595–1601, 2000.

[82] O. Rosskopfová, M. Galamboš, and P. Rajec. Determination of ^{63}Ni in the low level solid radioactive waste. *Journal of Radioanalytical and Nuclear Chemistry*, 289(1):251–256, 2011.

[83] S. Ruckstuhl, M.J.-F. Suter, H.-P. E Kohler, and W. Giger. Leaching and primary biodegradation of sulfonated naphthalenes and their formaldehyde condensates from concrete superplasticizers in groundwater affected by tunnel construction. *Environmental science & technology*, 36(15):3284–3289, 2002.

[84] K. Schmeide, S. Sachs, M. Bubner, T. Reich, K.H. Heise, and G. Bernhard. Interaction of uranium(VI) with various modified and unmodified natural and synthetic humic substances studied by EXAFS and FTIR spectroscopy. *Inorganica chimica acta*, 351:133–140, 2003.

[85] D.R. Shelton, J.S. Karns, G.W. McCarty, and D.R. Durham. Metabolism of melamine by Klebsiella terragena. *Applied and environmental microbiology*, 63(7):2832–2835, 1997.

[86] Z. Song, S.R. Edwards, and R.G. Burns. Biodegradation of naphthalene-2-sulfonic acid present in tannery wastewater by bacterial isolates Arthrobacter sp. 2AC and Comamonas sp. 4BC. *Biodegradation*, 16(3):237–252, 2005.

[87] T. Stumpf, J. Tits, C. Walther, E. Wieland, and T. Fanghänel. Uptake of trivalent actinides (Curium(III)) by hardened cement paste: a time-resolved laser fluorescence spectroscopy study. *Journal of colloid and interface science*, 276(1):118–124, 2004.

[88] M. Svensson, M. Berg, K. Ifwer, R. Sjoblom, and H. Ecke. The effect of isosaccharinic acid (ISA) on the mobilization of metals in municipal solid waste incineration (MSWI) dry scrubber residue. *Journal of hazardous materials*, 144(1-2):477–484, June 2007.

[89] H.F.W. Taylor. *Cement Chemistry*. Thomas Telford Ed., 1997.

[90] P. Thakur, J.N. Mathur, C.J. Dodge, A.J. Francis, and G.R. Choppin. Thermodynamics and the structural aspects of the ternary complexes of Am(III), Cm(III) and Eu(III) with Ox and EDTA + Ox. *Dalton transactions*, pages 4829–4837, October 2006.

[91] J. Tits, M. Bradbury, P. Eckert, A. Schaible, and E. Wieland. The uptake of Eu(III) and Th(IV) by calcite under hyperalkaline conditions: The influence of gluconic and isosaccharinic acid. Technical Report ISSN 1015-2636, Nagra, 2002.

[92] J. Tits, E. Wieland, and M. H. Bradbury. The effect of isosaccharinic acid and gluconic acid on the retention of Eu(III), Am(III) and Th(IV) by calcite. *Applied Geochemistry*, 20(11):2082–2096, 2005.

[93] G.R. Tucker. Amine salts of aromatic sulphonic acids. US Patent: US2052586A, 1936.

[94] G. Van der Plaats, H. Soons, and R. Snellings. The thermal behaviour of melamine. In *Proceedings of Second European symposium on thermal analysis. London: Heyden*, pages 215–7, 1981.

[95] L.R. Van Loon and W. Hummel. *The radiolytic and chemical degradation of organic ion exchange resins under alkaline conditions: effect on radionuclide speciation*, volume TR 95-08. Paul Scherrer Institute, 1995.

[96] G.J. Vazquez, C.J. Dodge, and A.J. Francis. Interaction of Uranium(VI) with phthalic acid. *Inorganic chemistry*, 47(22):10739–10743, 2008.

[97] K. Vercammen. *Complexation of Calcium, Thorium and Europium by a-Isosaccharinic Acid under Alkaline Conditions*. PhD thesis, Swiss Federal Institute of Technology Zurich, 2000.

[98] K. Vercammen, M. A. Glaus, and L. R. Van Loon. Complexation of Th(IV) and Eu(III) by alpha-isosaccharinic acid under alkaline conditions. *Radiochimica Acta*, 89:393–401, 2001.

[99] P. Warwick, N. Evans, T. Hall, and S. Vines. Complexation of Ni(II) by a-isosaccharinic acid and gluconic acid from pH 7 to pH 13. *Radiochimica Acta*, 91:233–240, 2003.

[100] P. Warwick, N. Evans, T. Hall, and S. Vines. Stability constants of Uranium(IV)-alpha-isosaccharinic acid and gluconic acid complexes. *Radiochimica Acta*, 92:897–902, 2004.

[101] P. Warwick, N. Evans, and S. Vines. Studies on some divalent metal a-isosaccharinic acid complexes. *Radiochimica Acta*, 94:363–368, June 2006.

[102] P. Warwick, N. Evans, and S. Vines. Studies on some divalent metal alpha-isosaccharinic acid complexes. *Radiochimica Acta*, 94:363–368, 2006.

[103] S.H. Watkins. Bacterial degradation of lignosulfonates and related model compounds. *Water Pollution Control Federation*, pages R47–R56, 1970.

[104] J.M. West. A review of progress in the geomicrobiology of radioactive waste disposal. *Radioactive Waste Management and Environmental Restoration*, 19:263–283, 1995.

[105] J.M. West and I.G. McKinley. The geomicrobiology of nuclear waste disposal. In *MRS Proceedings*, volume 26, page 487. Cambridge Univ Press, 1983.

[106] E. Wieland, B. Lothenbach, M.A. Glaus, T. Thoenen, and B. Schwyn. Influence of superplasticizers on the long-term properties of cement pastes and possible impact on radionuclide uptake in a cement-based repository for radioactive waste. *Applied Geochemistry*, 49:126–142, 2014.

[107] E. Wieland and L.R. Van Loon. Cementitious near-field sorption data base for performance assessment of an ILW repository in Opalinus Clay. Technical report, Paul Scherrer Institute, 2003.

[108] S.A. Wood, D.J. Wesolowski, and D.A. Palmer. The aqueous geochemistry of the rare earth elements: IX. A potentiometric study of Nd^{3+} complexation with acetate in 0.1 molal NaCl solution from 25° C to 225° C. *Chemical Geology*, 167(1):231–253, 2000.

[109] V.T. Yilmaz, M. Odabasoglu, H. Icbudak, and H. Ölmez. The degradation of cement superplasticizers in a high alkaline solution. *Cement and Concrete Research*, 23(1):152 – 156, 1993.

[110] A.J. Young. *The stability of cement superplasticiser and its effect on radionuclide behaviour*. PhD thesis, University of Loughborough, 2012.

[111] K. P. Zhernosekov, E. Mauerhofer, G. Getahun, P. Warwick, and F. Rosch. Complex formation of Tb^3+ with glycolate, D-gluconate and alpha-isosaccharinate in neutral aqueous perchlorate solutions. *Radiochimica Acta*, 91:599–602, 2003.

Appendixes

Appendix I

Material characterisation

Raw cementitious materials were characterised by X-Rray diffraction and acid digestions (HF and Aqua regia) followed by ICP-OES / ICP-MS (see *Section* 2.5 for experimental details) metals analysis. XRD and solid digestion results are shown in Table A 1 and from Figure A 1 to Figure A 5. As expected, Ca and Si were found as the major elements within the analysed materials. Indeed, calcium carbonate solid phases (Calcite and Dolomite) and Quartz were detected as main solid phases in the aggregates. CEM I solid phase composition was in the range of other literature reported data [89].

Raw Glenium®27 material presented neutral pH values (6.44) and an extremely high TOC signal (9.5 ppm, dilution 1:10000 in MilliQ water). The UV-vis spectra of the raw superplasticizer is shown in Appendix I and Figure A 6. The absorption maximum is observed around 200 nm and could be associated with an n- * transition in the polyether chains or a transition in the C=O groups. The UV-vis spectra is in agreement with the results obtained for a similar superplasticizer, Glenium®51, by Andersson and co-workers [8].

IR spectra of both, Glenium®27 and the in-house synthesized superplasticizer, are detailed in Figure A 7 and Figure A 8. As could be seen there are important features in both spectra, but most importantly both materials presented similar characteristics:

- The peak at ~ 2.900 nm, which is related with C-H bond tensions, is well observed in both samples.
- In both spectra the peak at ~ 1.700 – 1.500 nm, related with the tension of the C=O and C=C bond, could be well observed.
- In both spectra the peak at ~ 1.200 nm, related with the tension of the S=O bond, could be well observed.
- Finally, it is also interesting to observe that the peak at ~ 1.000 nm, which could be related with alcohols, carboxylic acids or esters, is well observed in both spectra.

Based on the IR spectra of both materials the following organic chemical groups could be expected: alkane, alcohol, carbonyls, sulfones, carboxylic acids and esters.

Results from HPLC-HRMS are presented from Figure A 9 to Figure A 13. As seen in these figures the presence of methacrylic acid and metal-PEG chains with different n members, from 3 to 30, has been confirmed in Glenium®27 sample in large quantities. Other non-identified PEG derivatives have been also found in the sample.

TGA analysis of the freeze-dried superplasticizer (Figure A 14) shows two different mass loss regions: i) from 20 to 100^{o}C and ii) from 350 to 400^{o}C. The first mass loss, 8% of the total sample amount, could

be associated with the dehydration (crystallization waters) of the samples. The second and most important mass loss, around 85% of the sample material, is mainly observed at 400ºC and is related with the decomposition of organic compounds.

H-NMR are results for both, Glenium®27 and the in-house synthesized superplasticizer, are presented in Figure A 15 and Figure A 16. As seen in those figures, both materials presented a similar spectrum. Two regions could be clearly seen: the first one going approximately from 4.0 to 3.0 ppm with two main signals at 3.6 and 3.3 corresponding to CH_2 and the terminal CH_3 from the polyethylene glycol (PEG) chain respectively, and a second one from 2.0 to 0.5 with to signals corresponding with the H from the CH_3 and CH_2 units from the terminal positions (see PCE structure in Figure 2-7). The signal found at approx. 2.7 ppm in Glenium®27 have not been properly identified and has not been found in the in-house synthesized superplasticizer spectrum.

As mentioned in *Section* 2.2, concrete blocks were characterised by means of XRD, SEM-EDX and TGA (see *Section* 2.5 for details). Results are presented from Figure A 17 to Figure A 21. XRD results shown the presence of the standard crystalline cementitious hydrates as Larnite (Ca_2SiO_4) and calcium hydroxide ($Ca(OH)_2$) as well as the presence of primary components as calcium carbonate ($CaCO_3$) and quartz (SiO_2). Similarly, SEM images shown the presence of cementitious hydrates as calcium hydroxide ($Ca(OH)_2$), C-S-H gels and ettringite ($Ca_6Al_2(SO_4)_3(OH)_{12}\cdot 26H_2O$). TGA results shown mainly two peaks at approx. 400 and 800ºC, corresponding to calcium hydroxide ($Ca(OH)_2$) and calcium carbonate ($CaCO_3$). Overall, results indicate that concrete blocks have a standard composition [89] and that the presence of Glenium®27 do not affect the formation of cementitious hydrates.

Table A 1. ICP-OES (Na, K, Ca) and ICP-MS (Mg, Al, Si) results from samples acid digestion results.

	Aqua Regia	HF
Aggregate 0/4 (mg/g material)		
Na	1.3	34.0
K	1.0	7.3
Ca	360.4	1.0
Mg	2.6	<LOD*
Si	1.5	152.0
Al	0.2	1.6
Aggregate 2/6 (mg/g material)		
Na	0.9	27.6
K	0.4	5.0
Ca	368.7	0.8
Mg	3.7	<LOD
Si	0.8	119.8
Al	0.1	1.0
Aggregate 6/14 (mg/g material)		
Na	0.9	21.2
K	0.4	4.4
Ca	386.8	7.4e-1
Mg	3.2	<LOD
Si	0.6	91.9
Al	0.1	0.7

	Aqua Regia	HF
Filler(mg/g material)		
Na	1.8	23.5
K	1.5	3.9
Ca	375.3	<LOD
Mg	2.0	<LOD
Si	0.3	95.9
Al	$2.1 \cdot 10^{-2}$	0.7
Cement (mg/g material)		
Na	1.7	15.9
K	5.4	7.4
Ca	542.6	1.5
Mg	6.3	1.2
Si	4.5	83.8
Al	2.1	0.8

*LOD: Limit of detection.

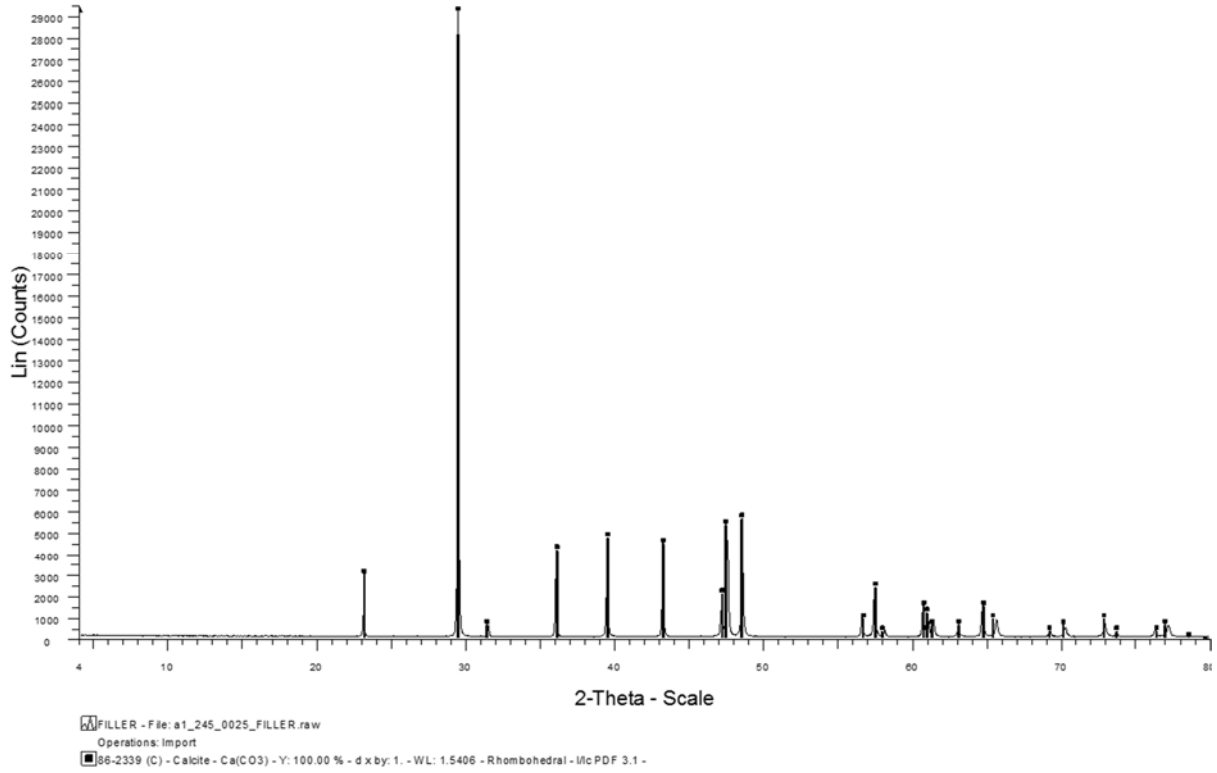

Figure A 1. XRD pattern obtained for the raw filler.

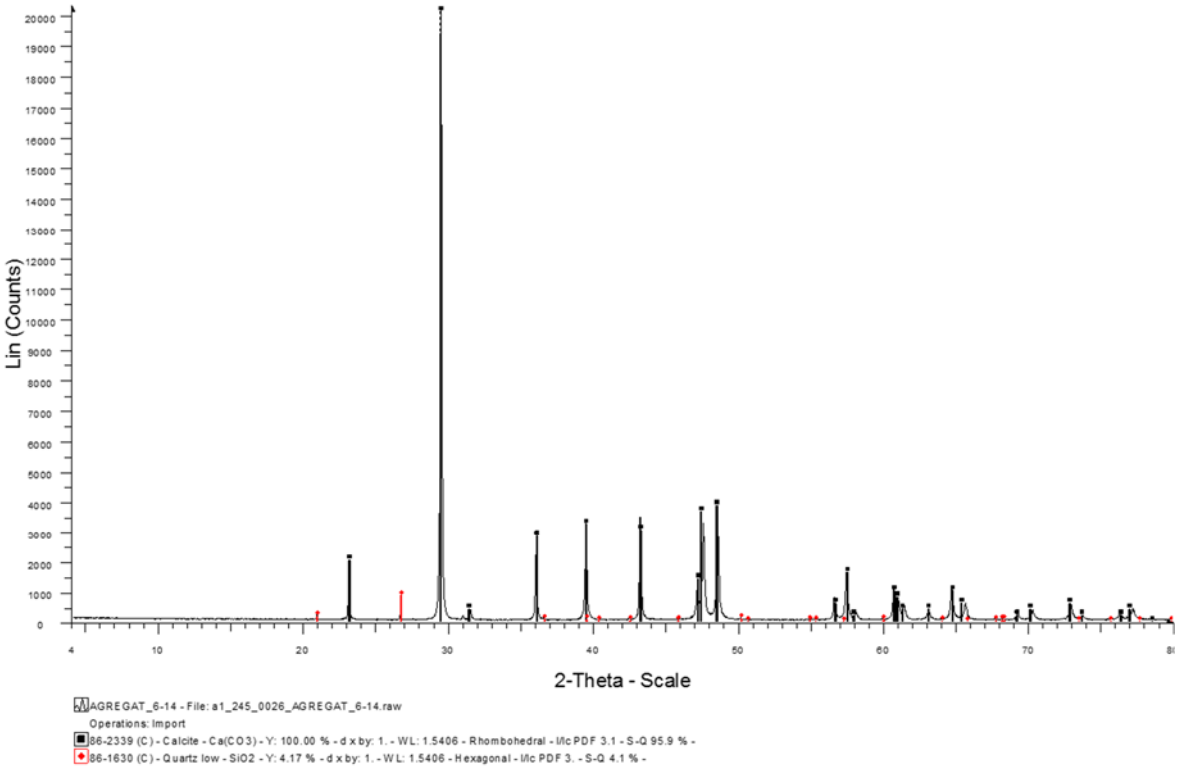

Figure A 2. XRD pattern obtained for the raw aggregate 6/14.

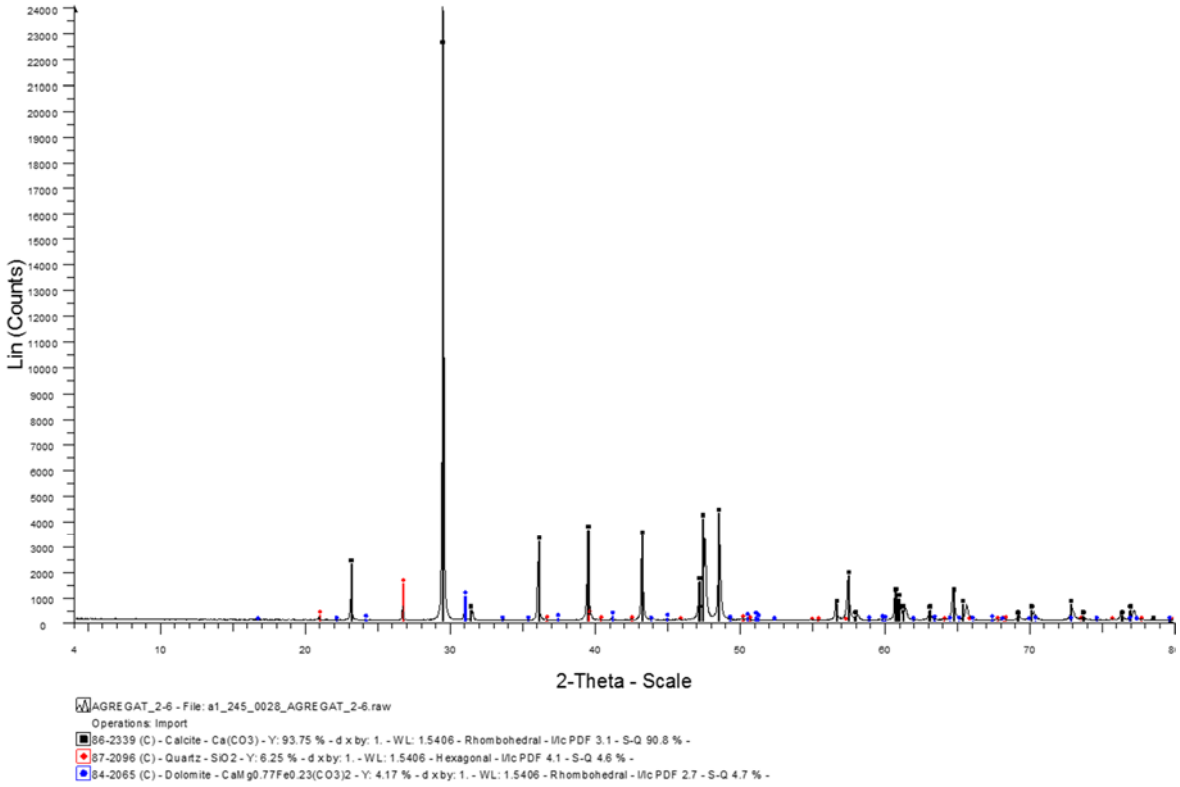

Figure A 3. XRD pattern obtained for the raw aggregate 2/6.

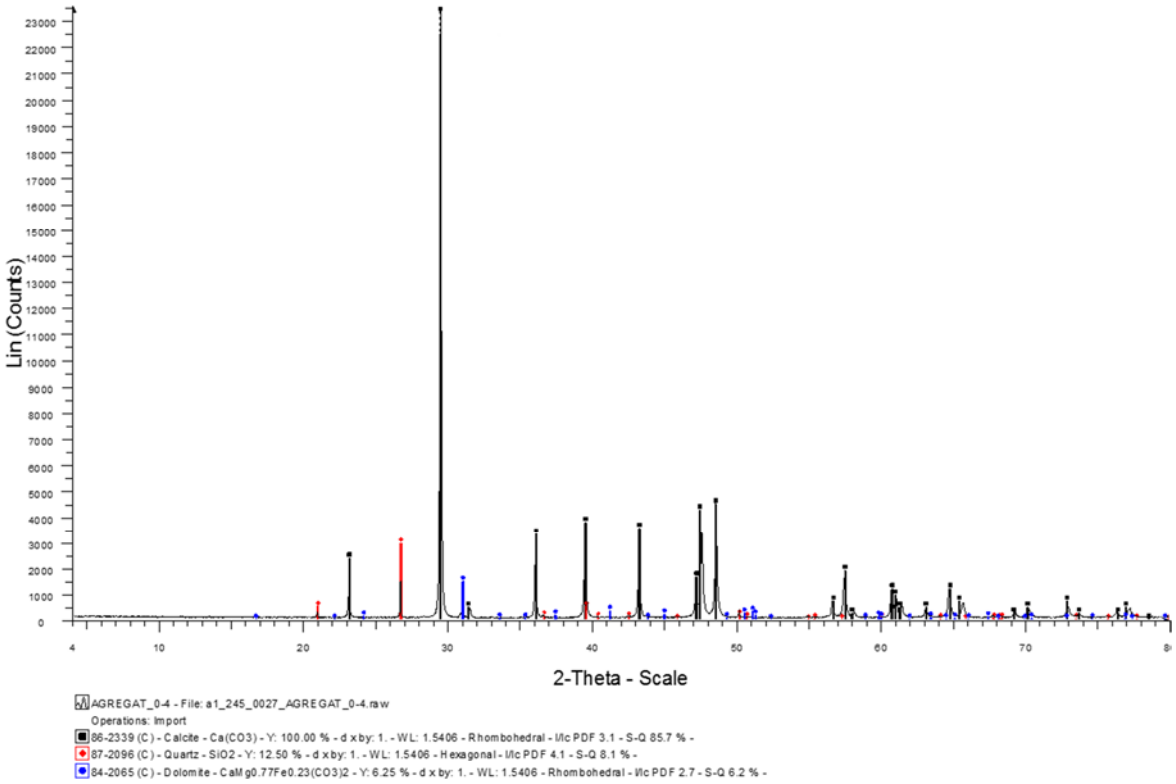

Figure A 4. XRD pattern obtained for the raw sand 0/4.

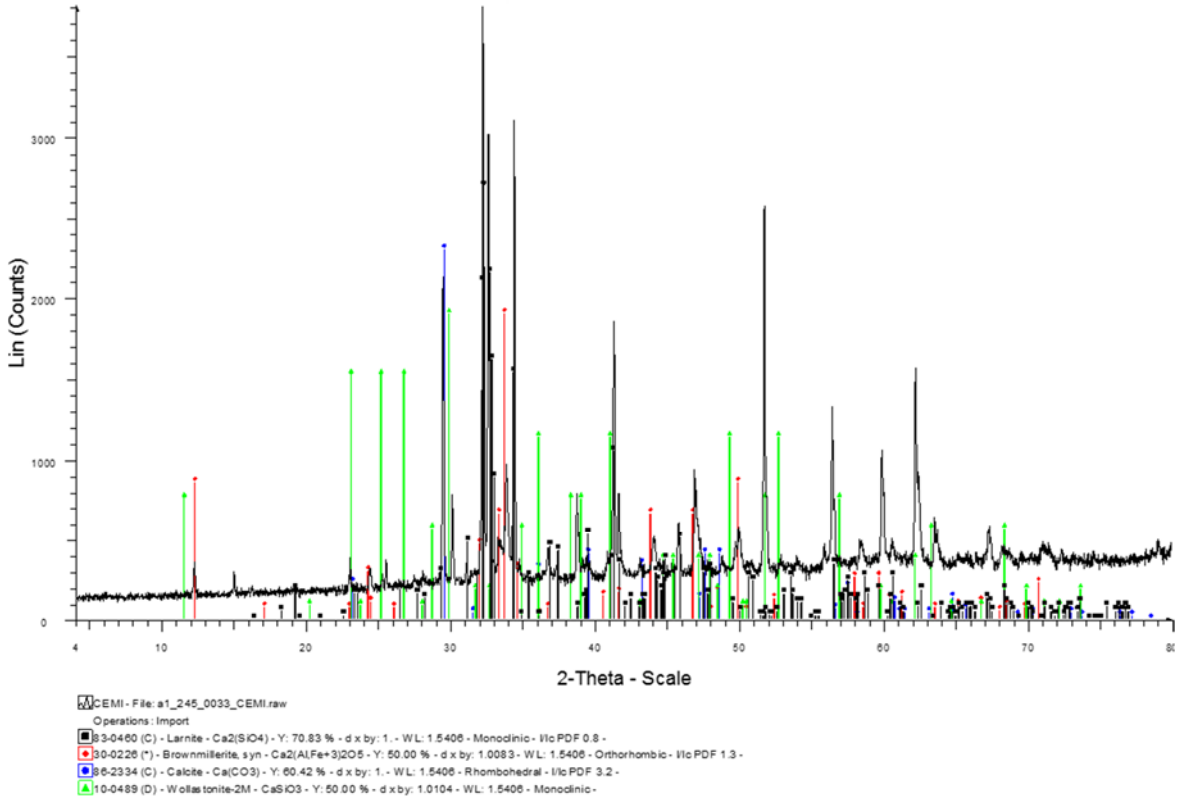

Figure A 5. XRD pattern obtained for the raw CEM I.

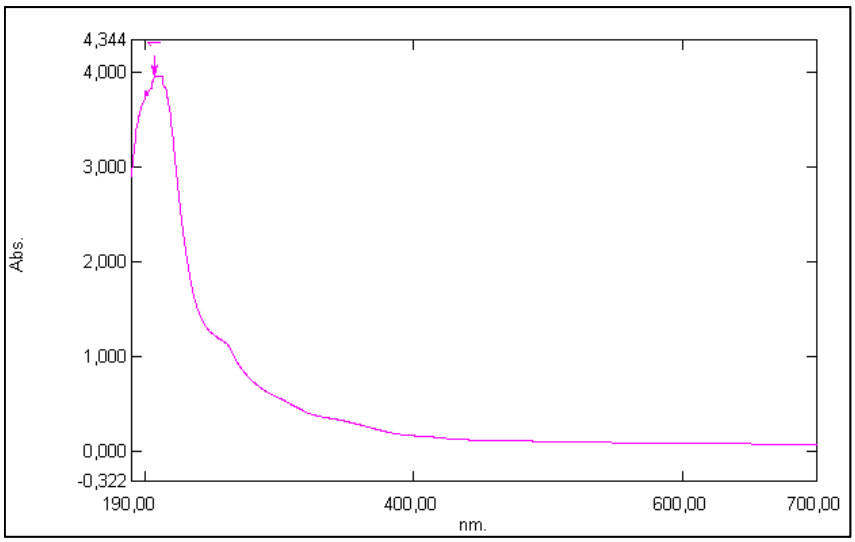

Figure A 6. UV-vis spectra of the raw superplasticizer (dilution 0.1/3 in MilliQ water).

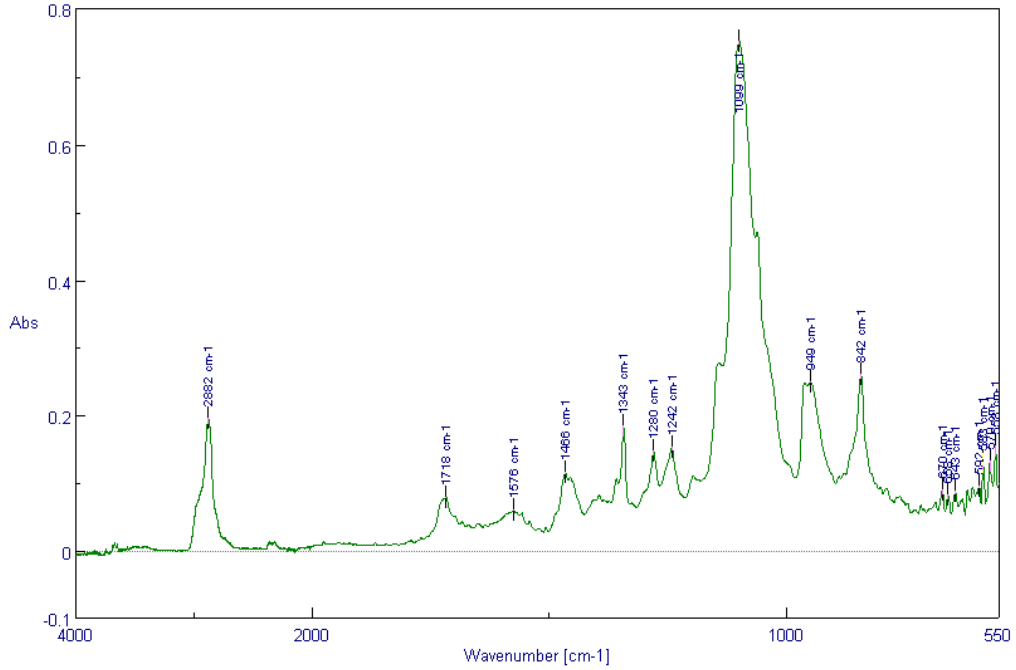

Figure A 7. IR spectra of the freeze-dried Glenium®27 superplasticizer. Spectra obtained in ATR (Attenuated Total Reflectance) mode.

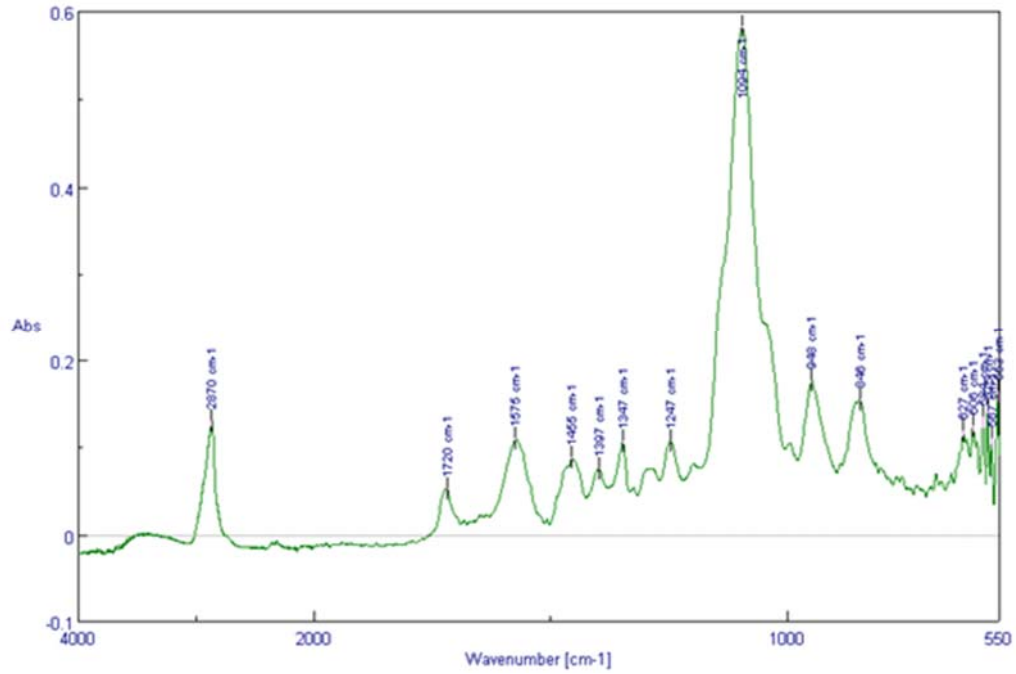

Figure A 8. IR spectra of the freeze-dried in-house synthesized superplasticizer. Spectra obtained in ATR (Attenuated Total Reflectance) mode.

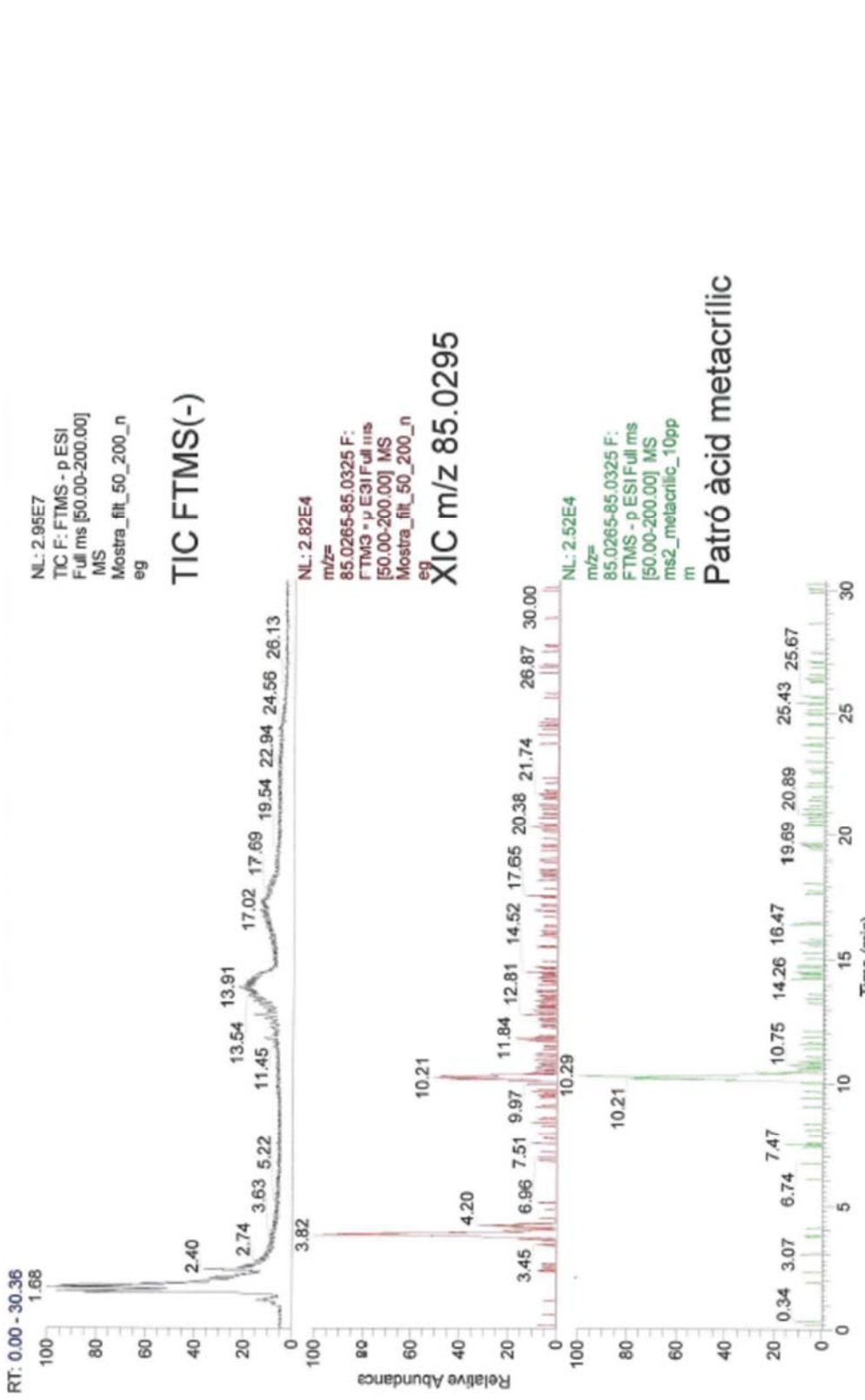

Figure A 9. Total Ion Current (TIC) obtained for Glenium®27 sample in positive polarity, as well as eXtracted Ion Chromatogram (XIC) for the ion m/z 85.0295. For comparative purposes the XIC obtained for a methacrylic acid standard is shown in the figure.

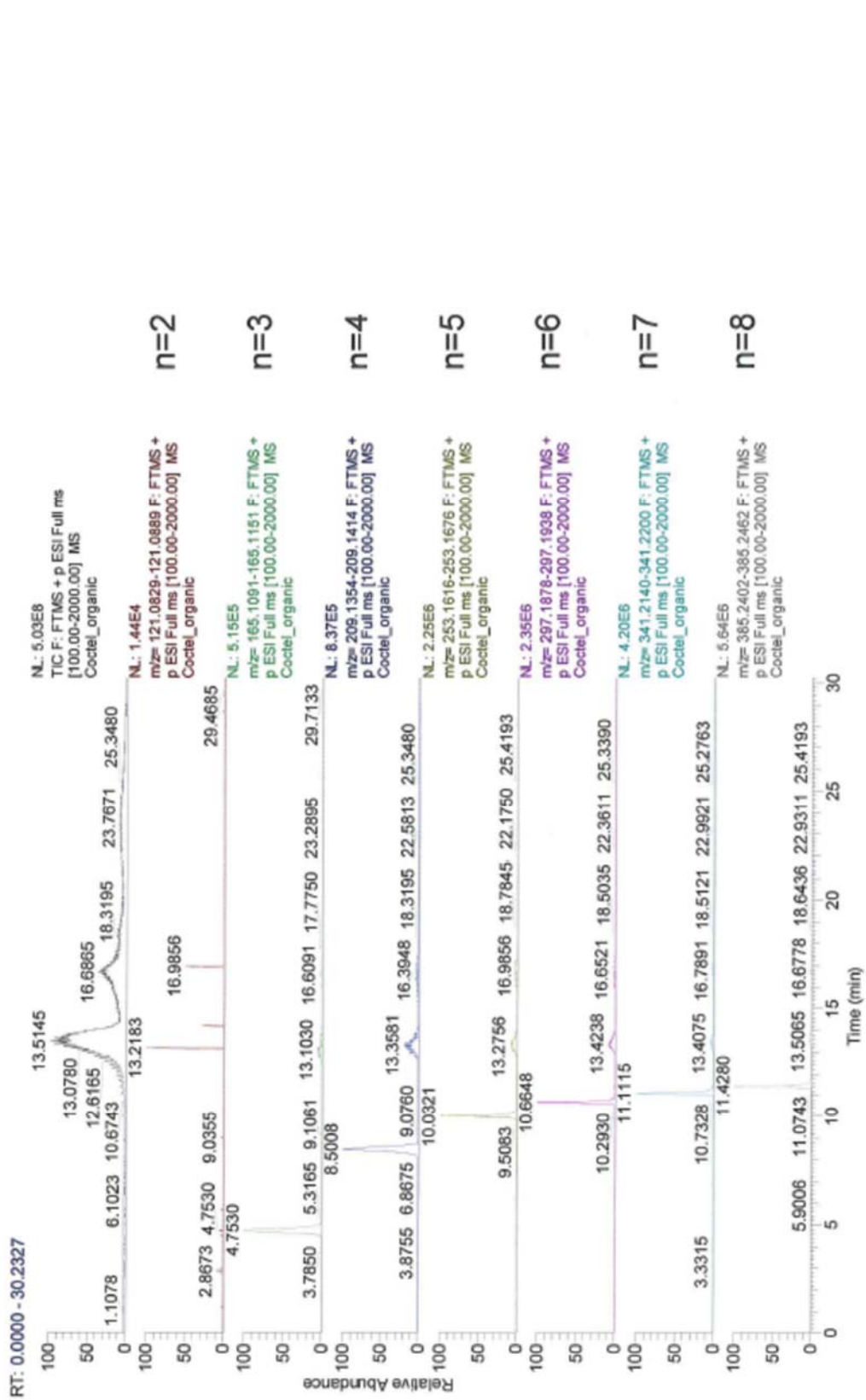

Figure A 10. Total Ion Current (TIC) obtained for Glenium®27 sample in positive polarity. Calculated ion chromatogram for different metal-PEG chains with variable n members from 2 to 8.

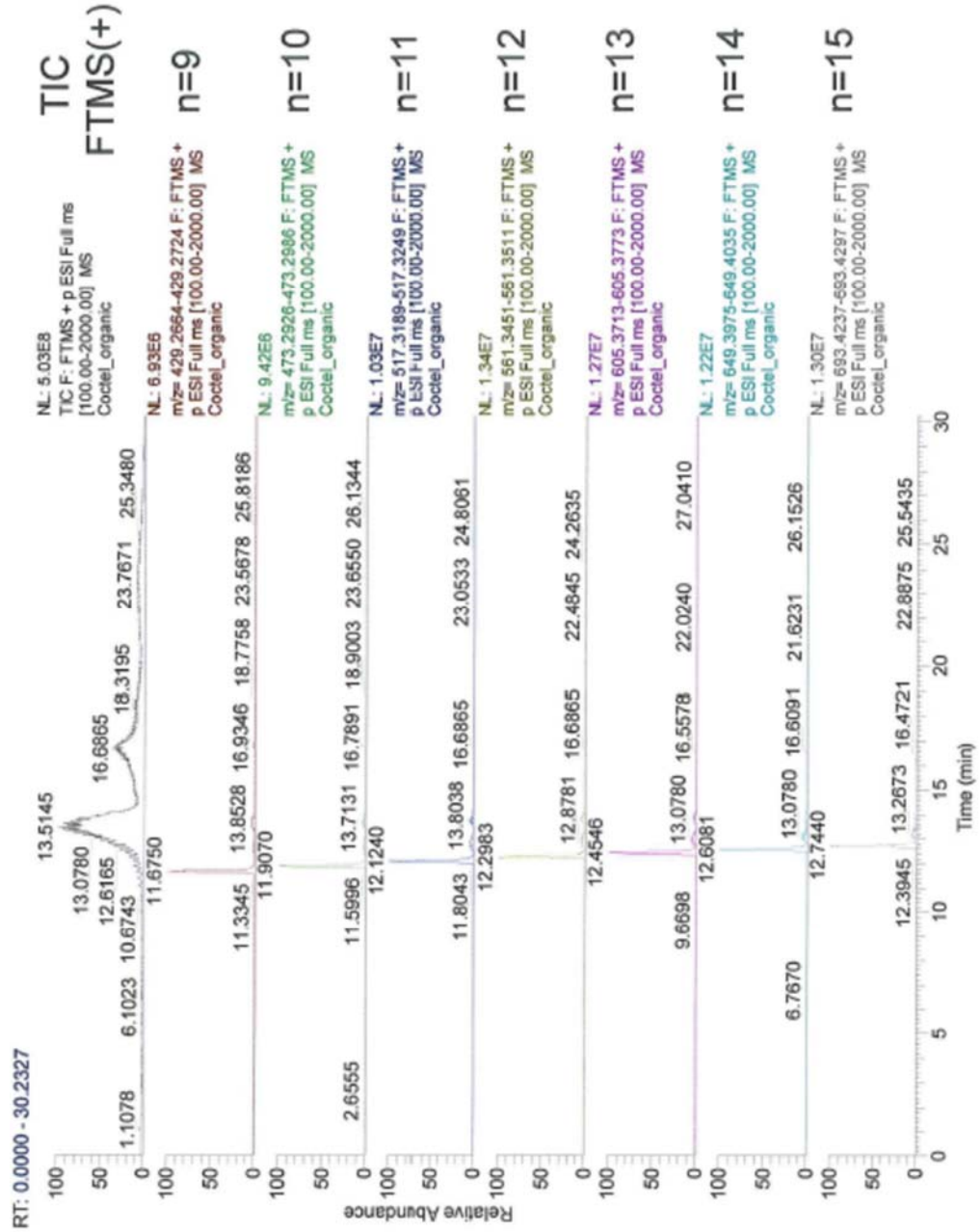

Figure A 11. Total Ion Current (TIC) obtained for Glenium®27 sample in positive polarity. Calculated ion chromatogram for different metal-PEG chains with variable n members from 9 to 15.

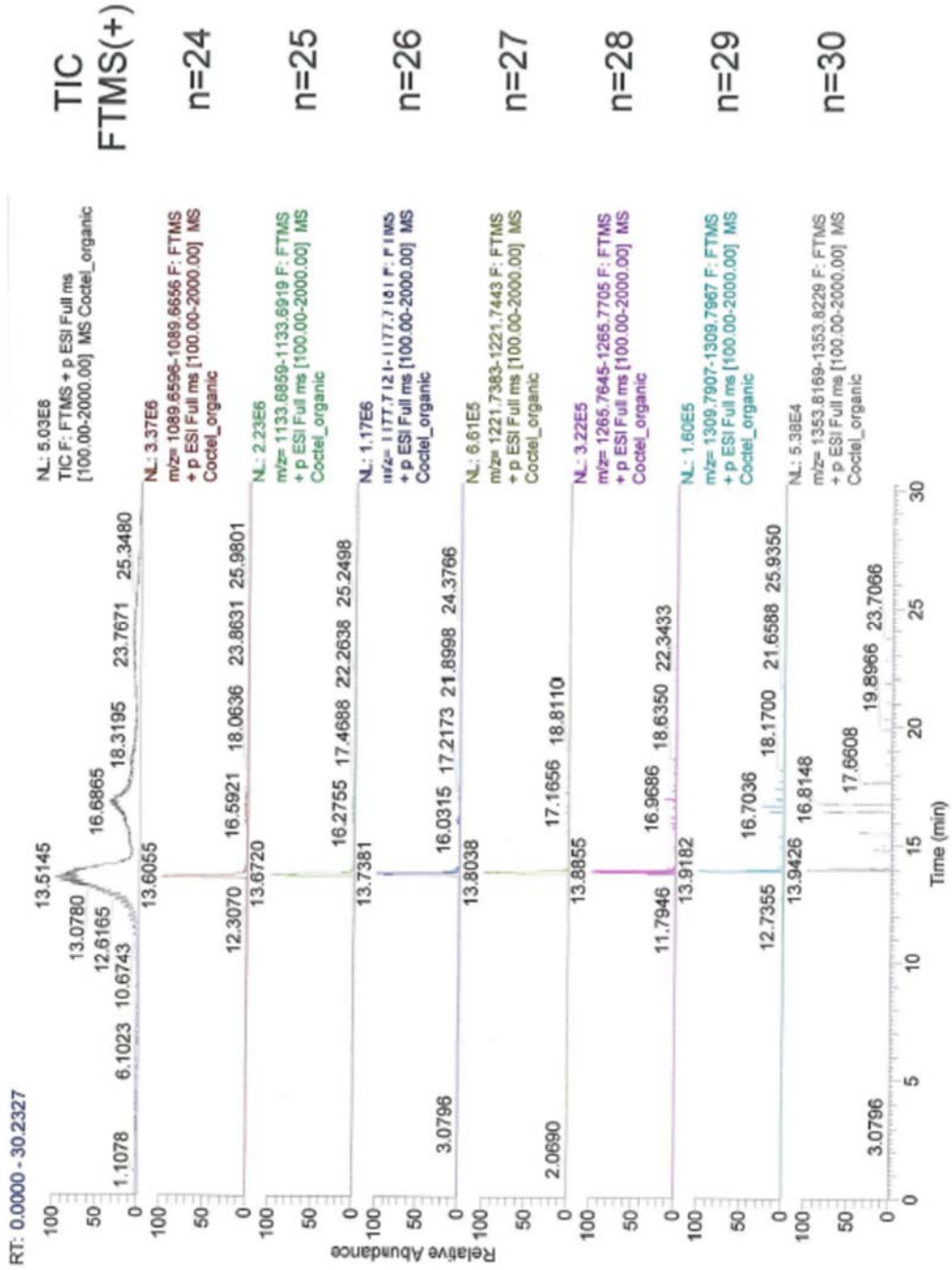

Figure A 12. Total Ion Current (TIC) obtained for Genium®27 sample in positive polarity. Calculated ion chromatogram for different metal-PEG chains with variable n members from 24 to 30.

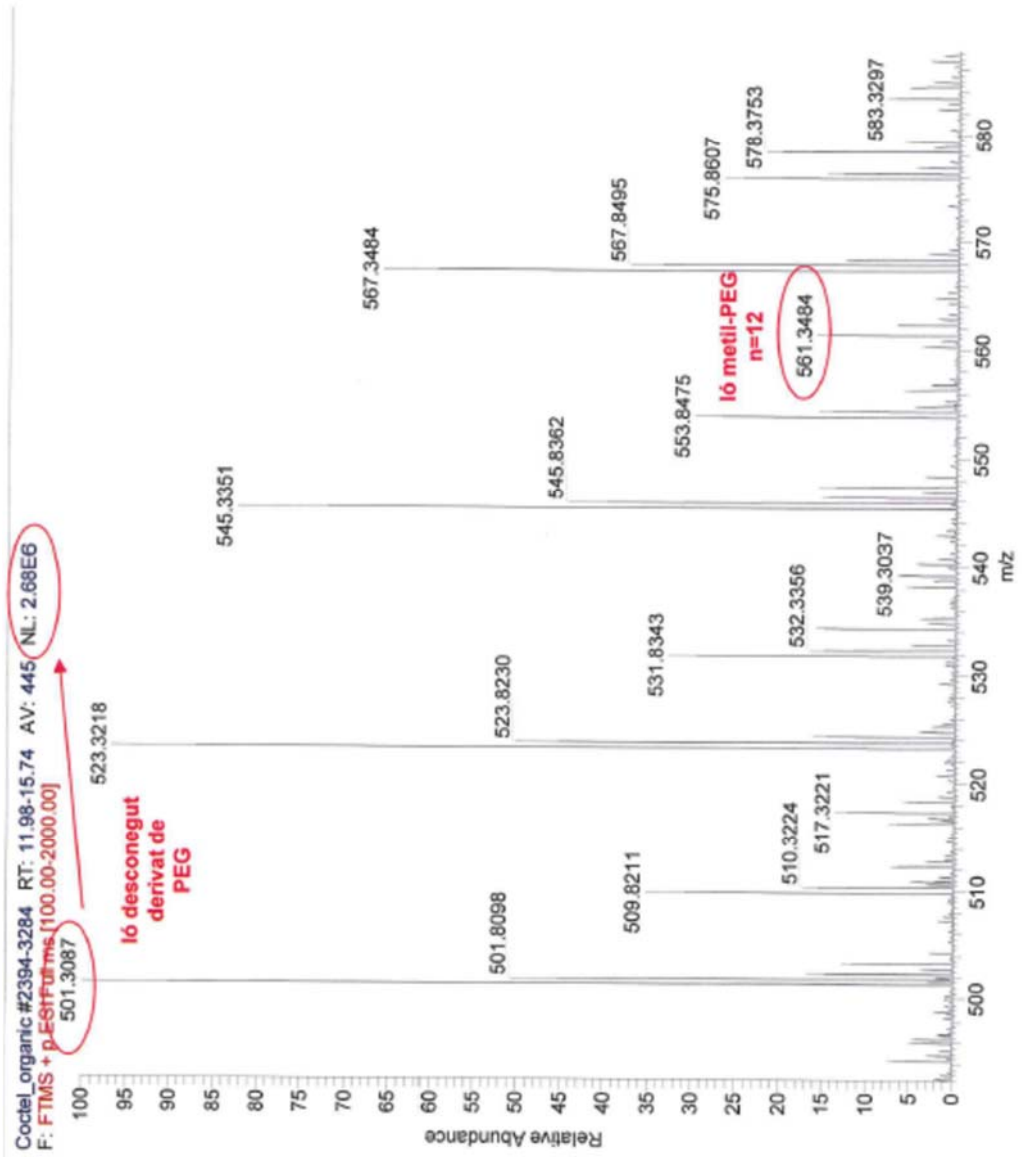

Figure A 13. Intensity of the different ions m/z obtained for Glenium®27 sample.

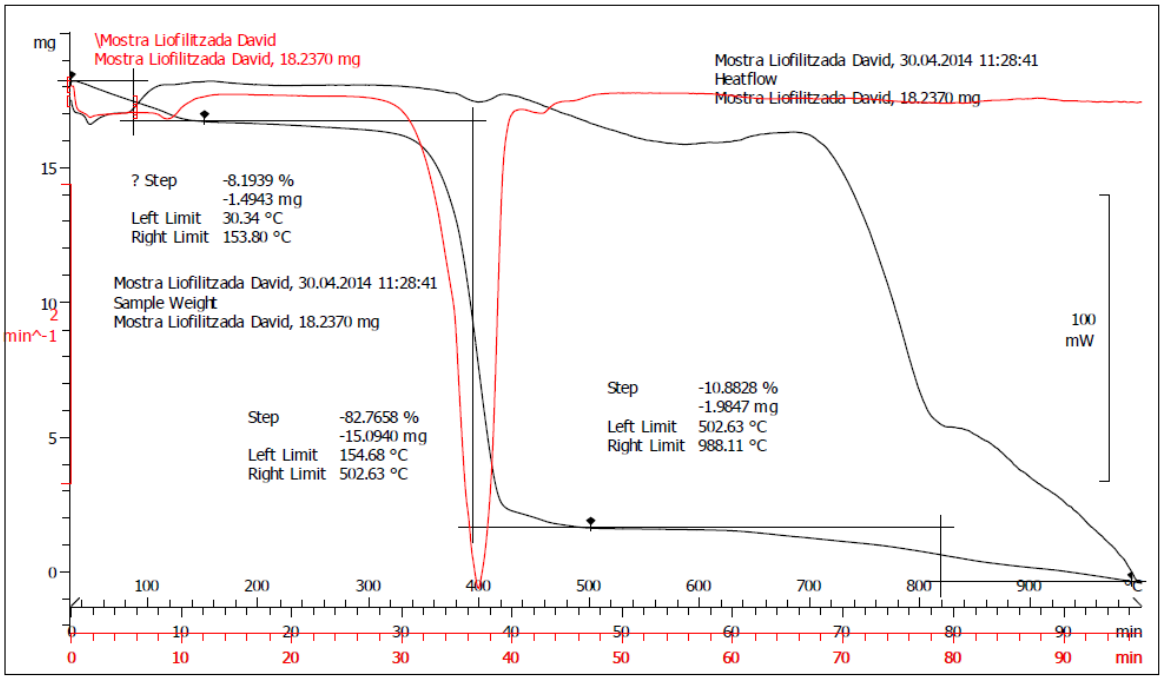

Figure A 14. TGA results obtained for the freeze-dried Glenium®27. Black line stands for the continuous decrease of mass as a function of time, while the red line stands for the integration of the mass lost.

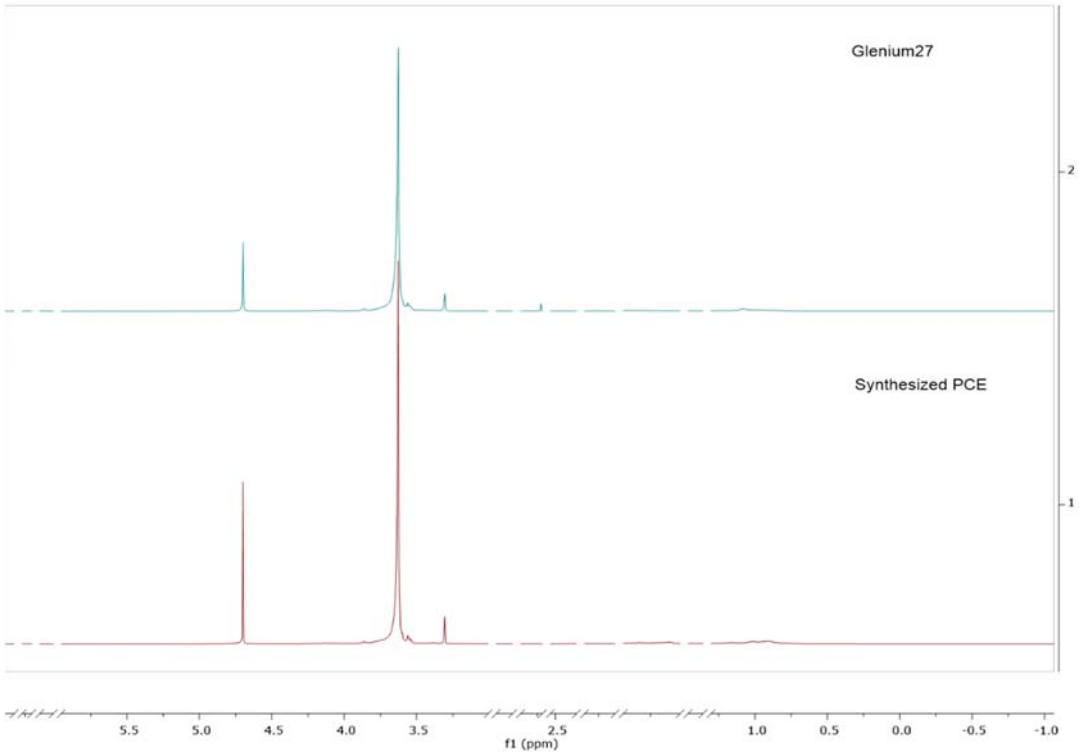

Figure A 15. H-NMR results obtained for both, Glenium®27 and the in-house synthesized, superplasticizers.

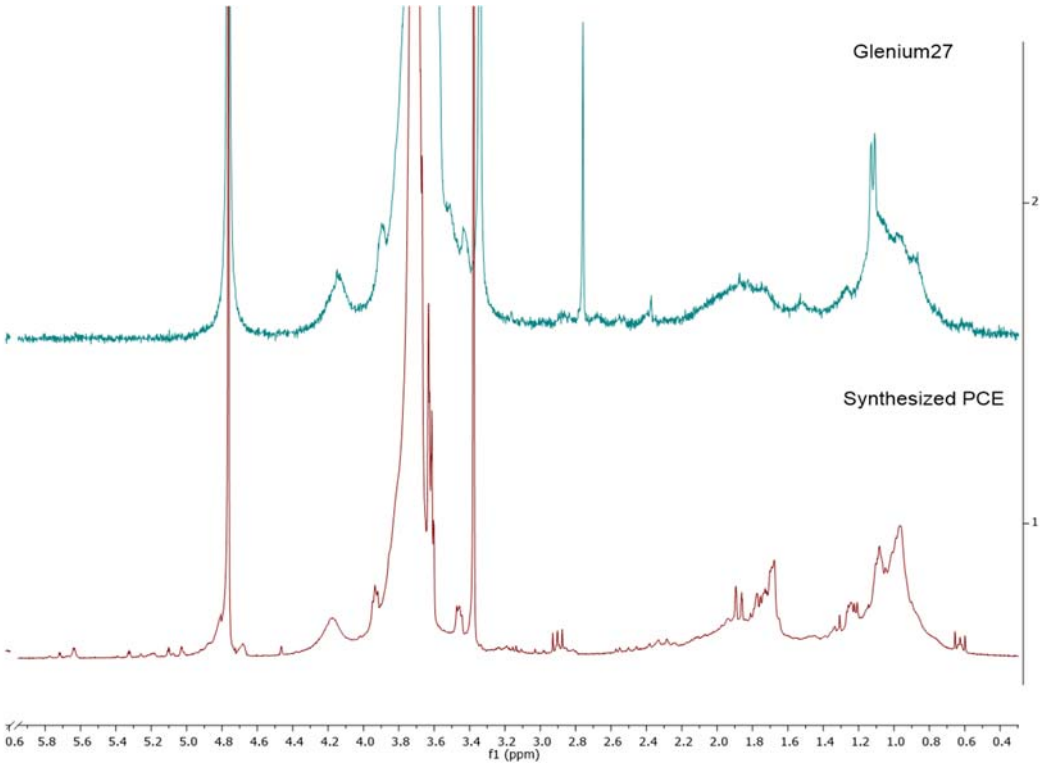

Figure A 16. Zoom-in of the H-NMR results obtained for both, Glenium®27 and the in-house synthesized, superplasticizers.

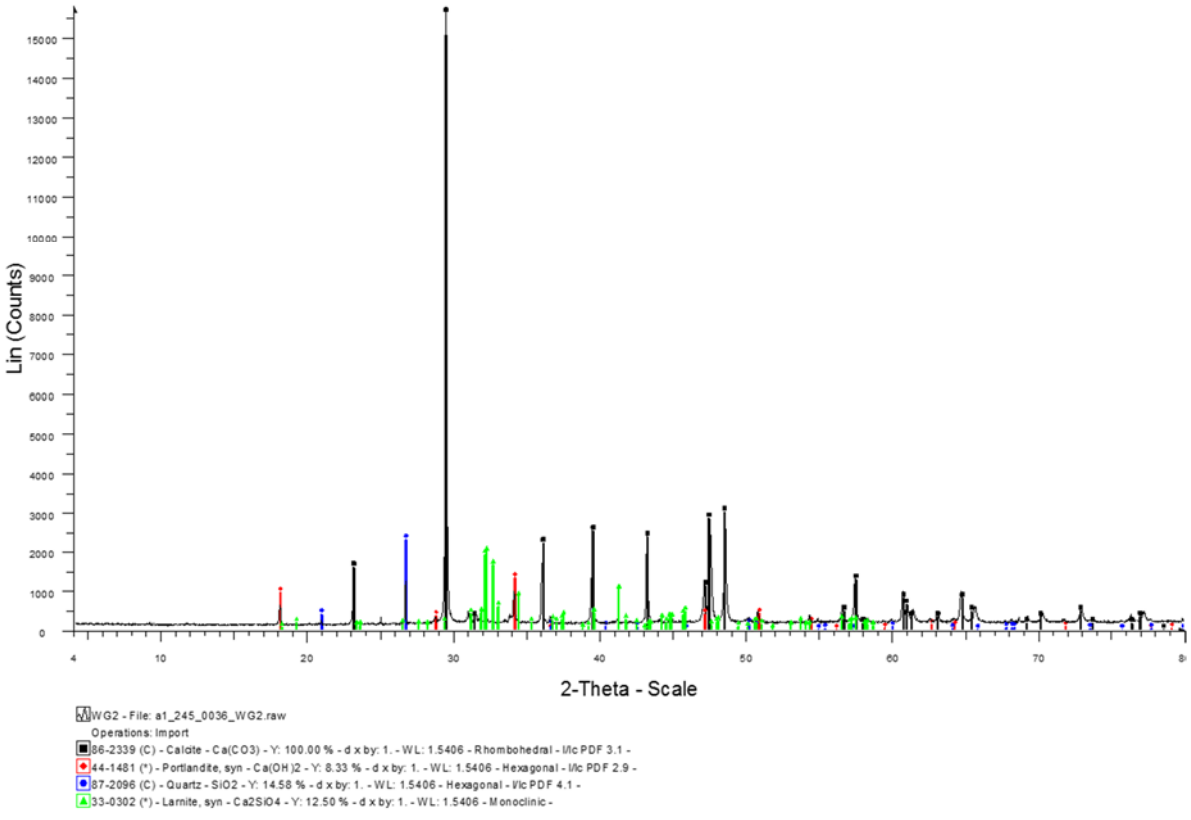

Figure A 17. XRD pattern obtained for the concrete sample non-containing Glenium®27 in the formulation (WG sample).

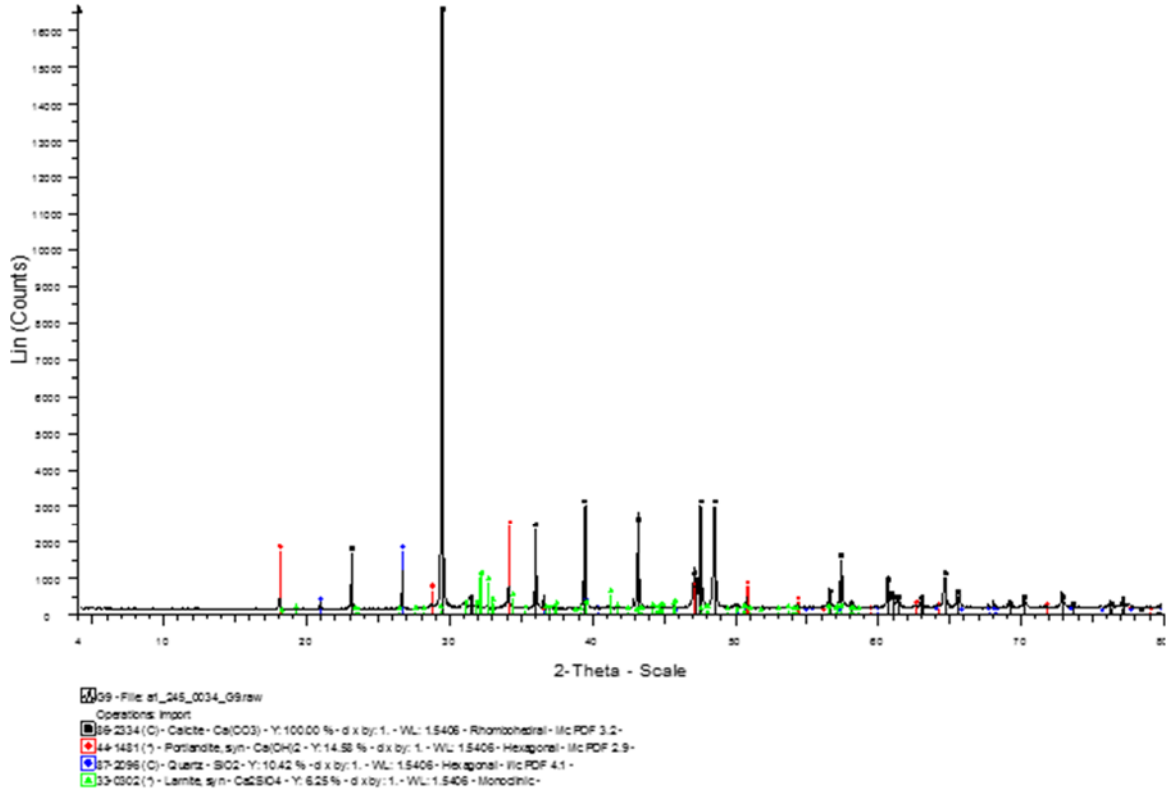

Figure A 18. XRD pattern obtained for the concrete sample containing Glenium®27 in the formulation (G sample).

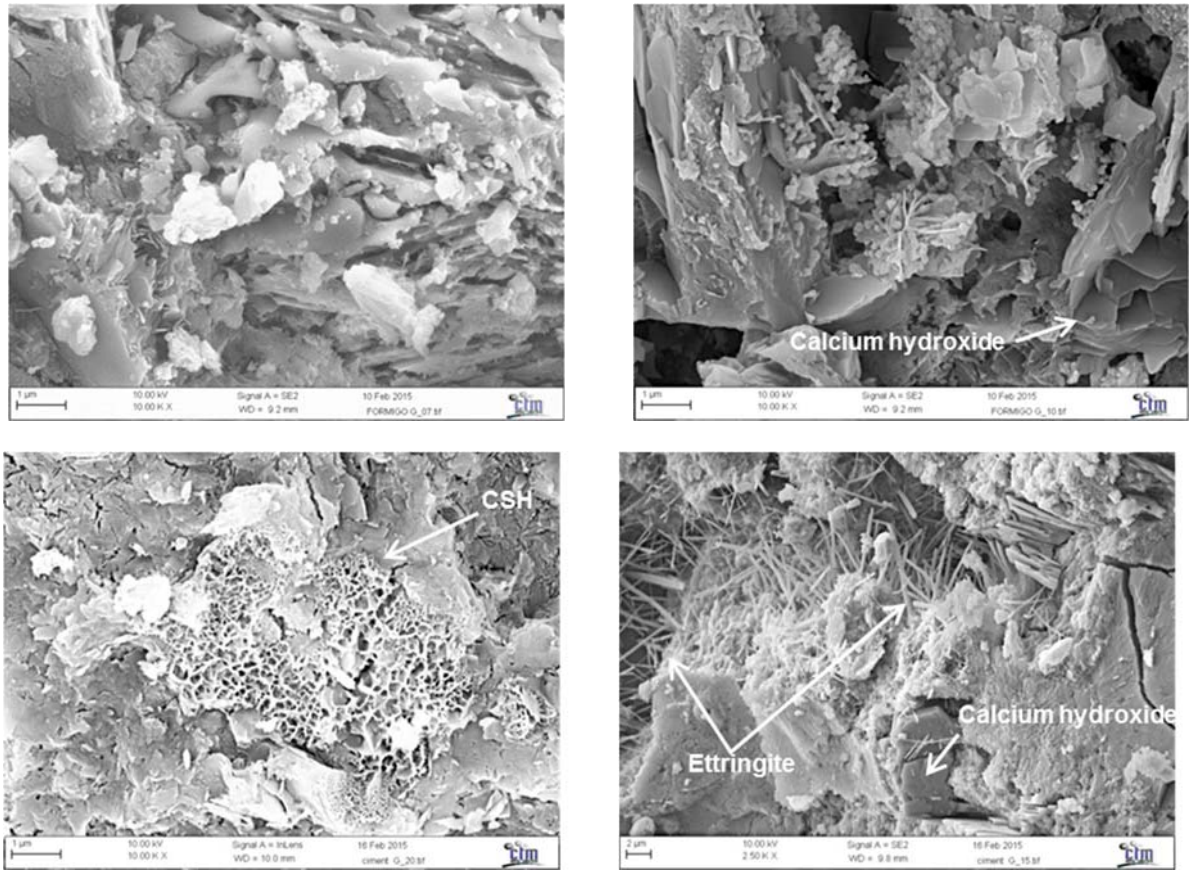

Figure A 19. SEM images obtained for the concrete sample containing and non-containing Glenium®27 in the formulation. The images shown the presence of different cementitious hydrated phases, i.e. calcium hydroxide, ettringite, C-S-H gels.

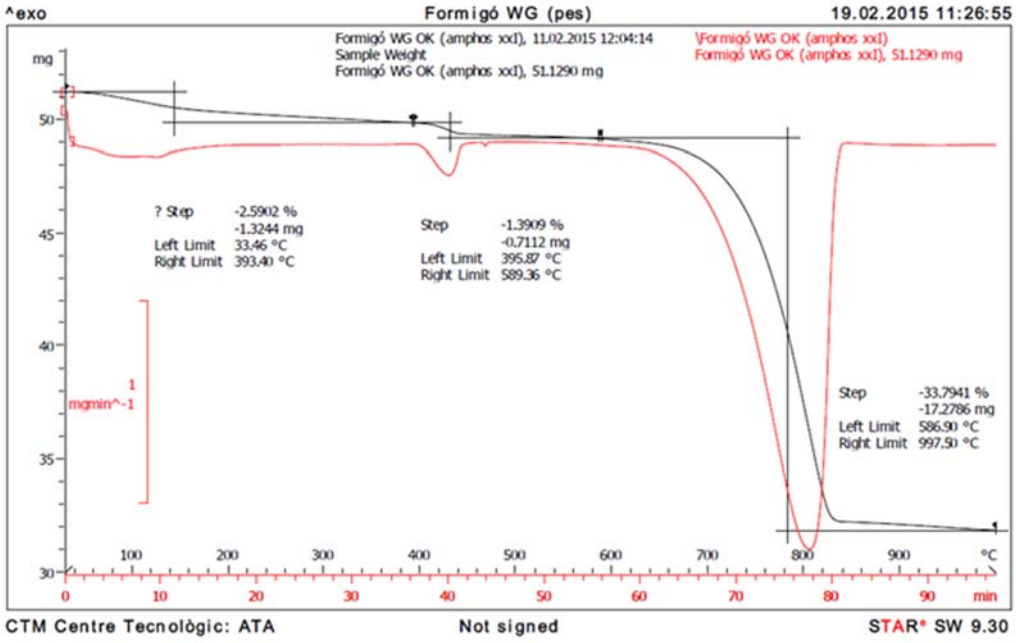

Figure A 20. TGA results obtained for the concrete samples non-containing Glenium®27 in the formulation (WG samples). Black line stands for the continuous decrease of mass as a function of time, while the red line stands for the integration of the mass lost.

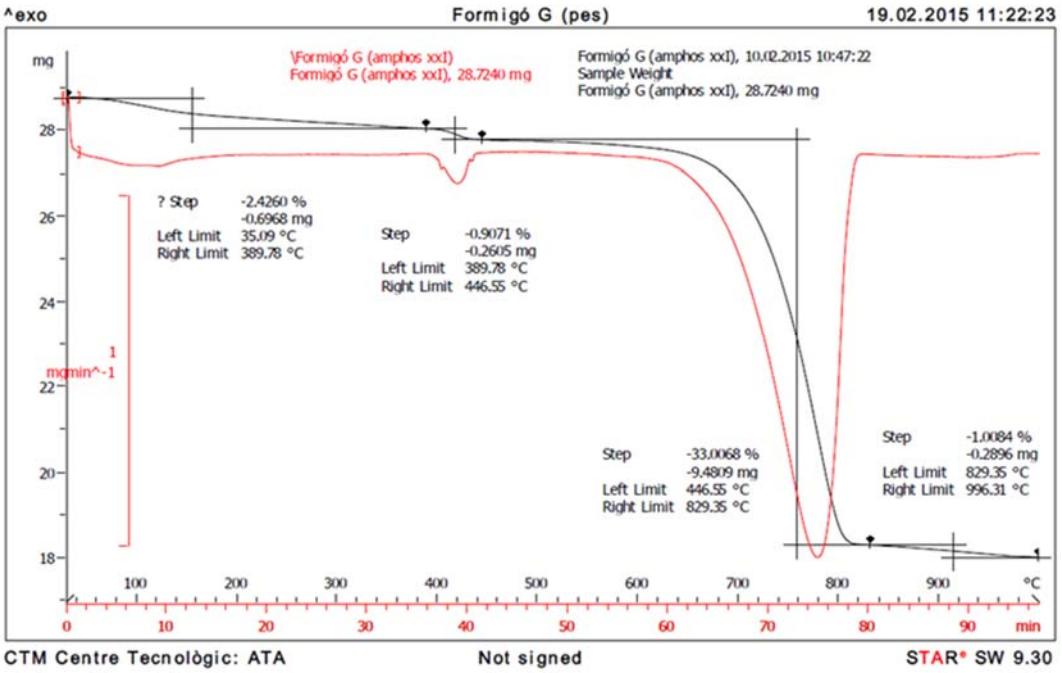

Figure A 21. TGA results obtained for the concrete samples containing Glenium®27 in the formulation (G samples). Black line stands for the continuous decrease of mass as a function of time, while the red line stands for the integration of the mass lost.

Appendix II

Supplementary material for Chapter 3

Table A 2. Summary of organic SPs (or proxy organics) degradation products found in the literature review.

	SPs source	Degradation product		Reference
		Structure	*Name*	
Aromatic Compounds	Melamine based SPs	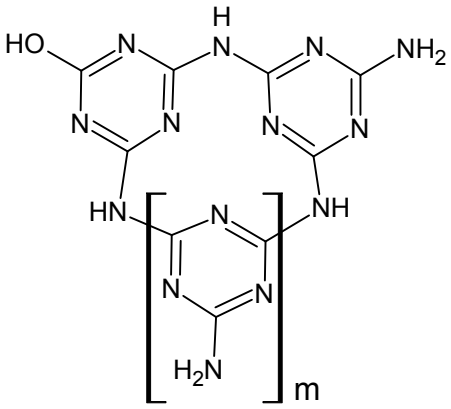	"melem"	[26]
	Naphthalene based SPs	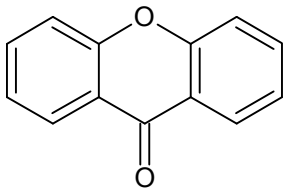	Xanthose	[66]
	Naphthalene based SPs	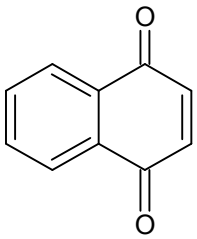	Naphthoquinone	[66]
	Naphthalene based SPs	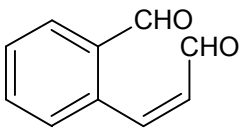	2-Formylcinnamaldehyde	[56]
	Naphthalene based SPs	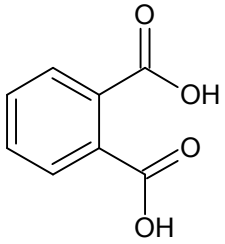	Phthalic Acid	[66]

	SPs source	Degradation product		Reference
		Structure	*Name*	
Aromatic Compounds	Naphthalene based SPs	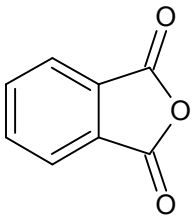	Phthalic anhydride	[66]
	Naphthalene based SPs	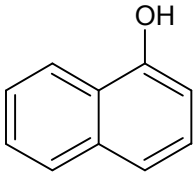	1-Naphthalenol	[11, 14, 53, 56, 66]
	Lignosulfonate based SPs	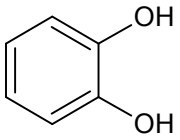	Pyrocatechol	[21]
	Naphthalene based SPs	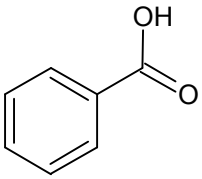	Benzoic acid	[66]
	Melamine based SPs	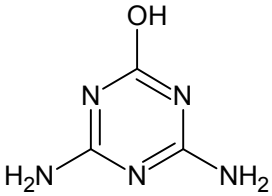	Ammeline	[52, 85]
	Melamine based SPs	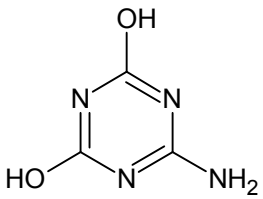	Ammelide	[52, 85]
	Melamine based SPs	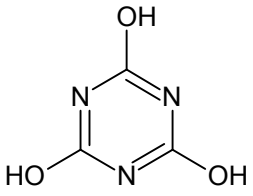	Cyanuric acid	[52, 85]

	SPs source	Degradation product		Reference
		Structure	*Name*	
Aromatic Compounds	Naphthalene based SPs	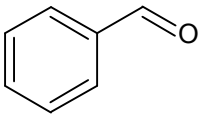	Benzaldehyde	[66]
	Naphthalene and lignosulfonate based SPs,	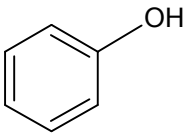	Phenol	[45, 66]
Aliphatic Compounds	Naphthalene based SPs	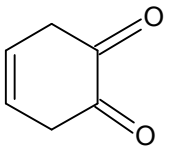	1,2-Benzoquinone	[66]
	Naphthalene based SPs	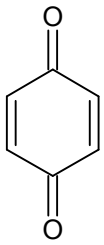	1,4-Benzoquinone	[66]
	Naphthalene based SPs	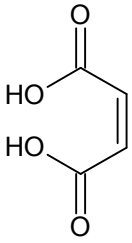	1,4-But-2-enoic acid	[66]
	Melamine based SPs	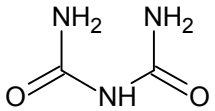	Biuret	[85]
	Naphthalene based SPs	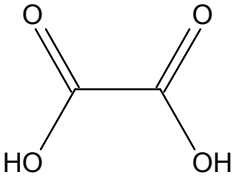	Oxalic acid	[66]
	Naphthalene based SPs	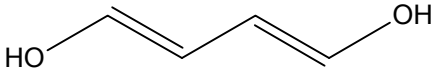	1,4-But-1,3-diol	[66]

	SPs source	Degradation product		Reference
		Structure	*Name*	
Aliphatic compounds	Naphthalene based SPs	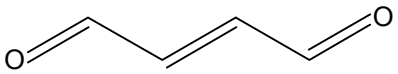	1,4-But-2-dienal	[66]
	Naphthalene based SPs	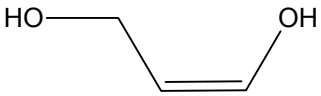	2-propendiol	[66]
	Naphthalene based SPs	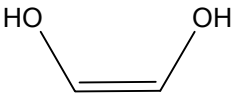	Ethene-1,2-diol	[66]
	Melamine based SPs	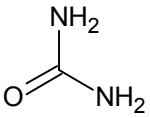	Urea	[85]
	Naphthalene based SPs	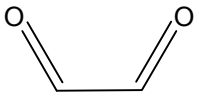	1,2-Dialdehyde	[66]
	Naphthalene based SPs	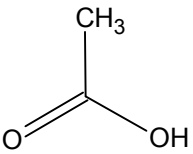	Acetic acid	[66]
Inorganic Compounds	Lignosulfonate and melamine based SPs	NH_3	Ammonia	[21, 26]
	Lignosulfonate based SPs	SO_2	Sulphur dioxide	[21]

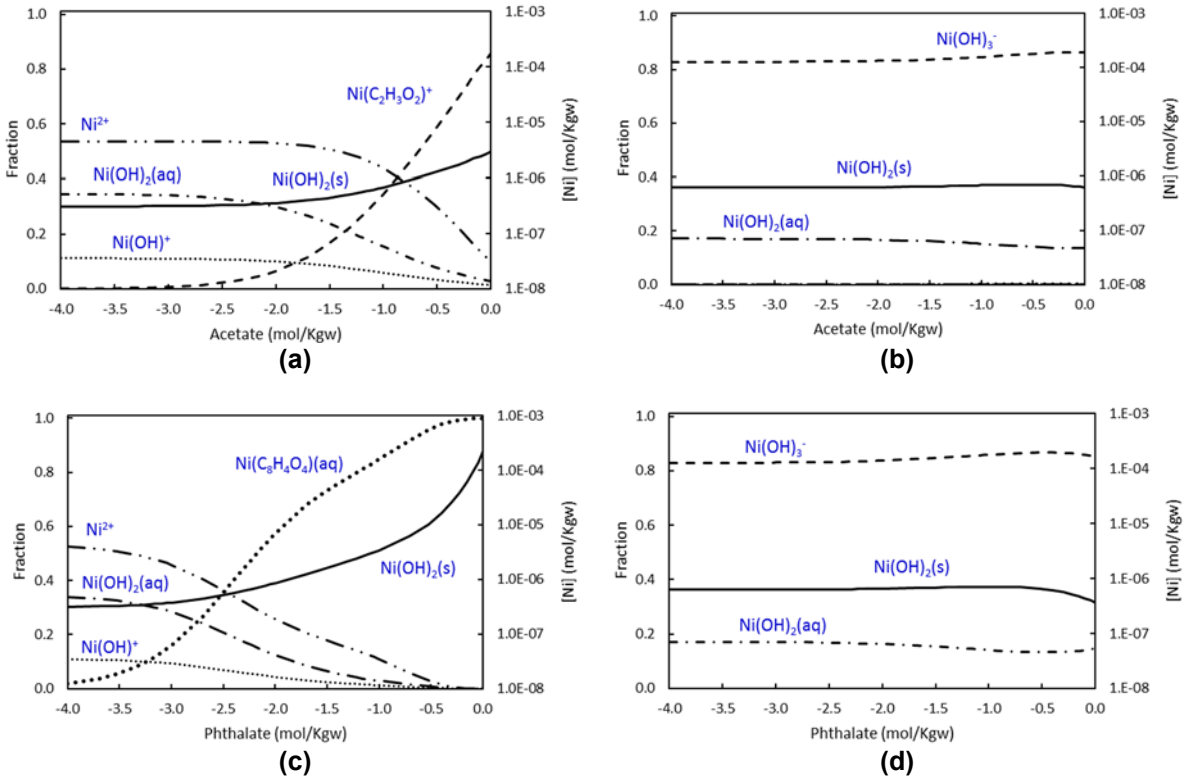

Figure A 22. Solubility curve (black solid lines) calculated for $Ni(OH)_2(s)$ in the presence of acetate (a – b) and phthalate (c – d) as a function of the organic concentration. Dashed lines stand for the speciation of Ni in equilibrium with the solid phase. pH fixed as 9 (a – c) and as 12 (b – d). Calcium concentration fixed in all diagrams as 10^{-3} mol·L^{-1}.

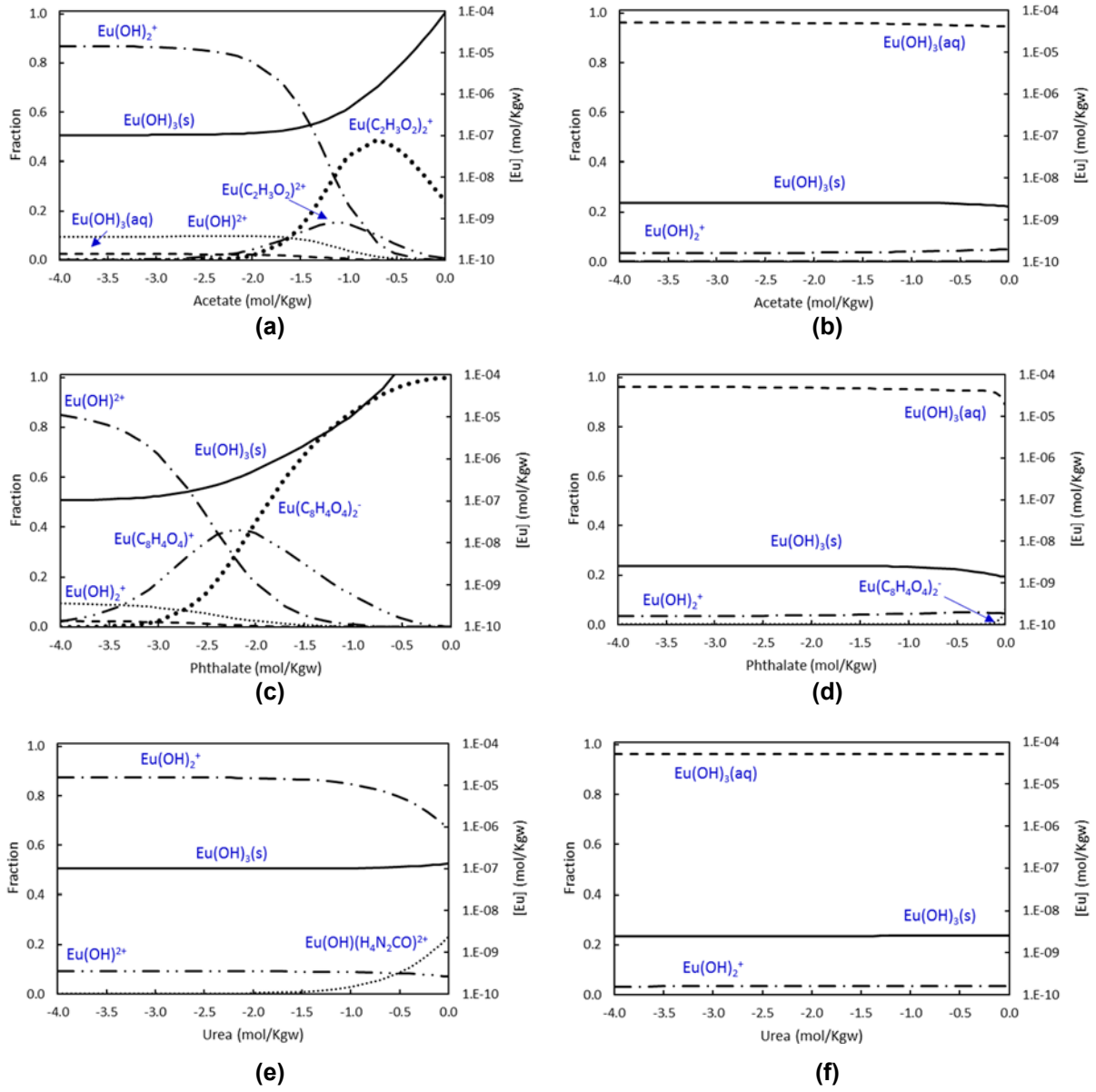

Figure A 23. Solubility curve (black solid lines) calculated for $Eu(OH)_3(s)$ in the presence of acetate (a – b), phthalate (c – d) and urea (e – f) as a function of the organic concentration. Dashed lines stand for the speciation of Eu in equilibrium with the solid phase. pH fixed as 9 (a – c – e) and 12 (b – d – f). Calcium concentration fixed in all diagrams as 10^{-3} mol·L^{-1}.

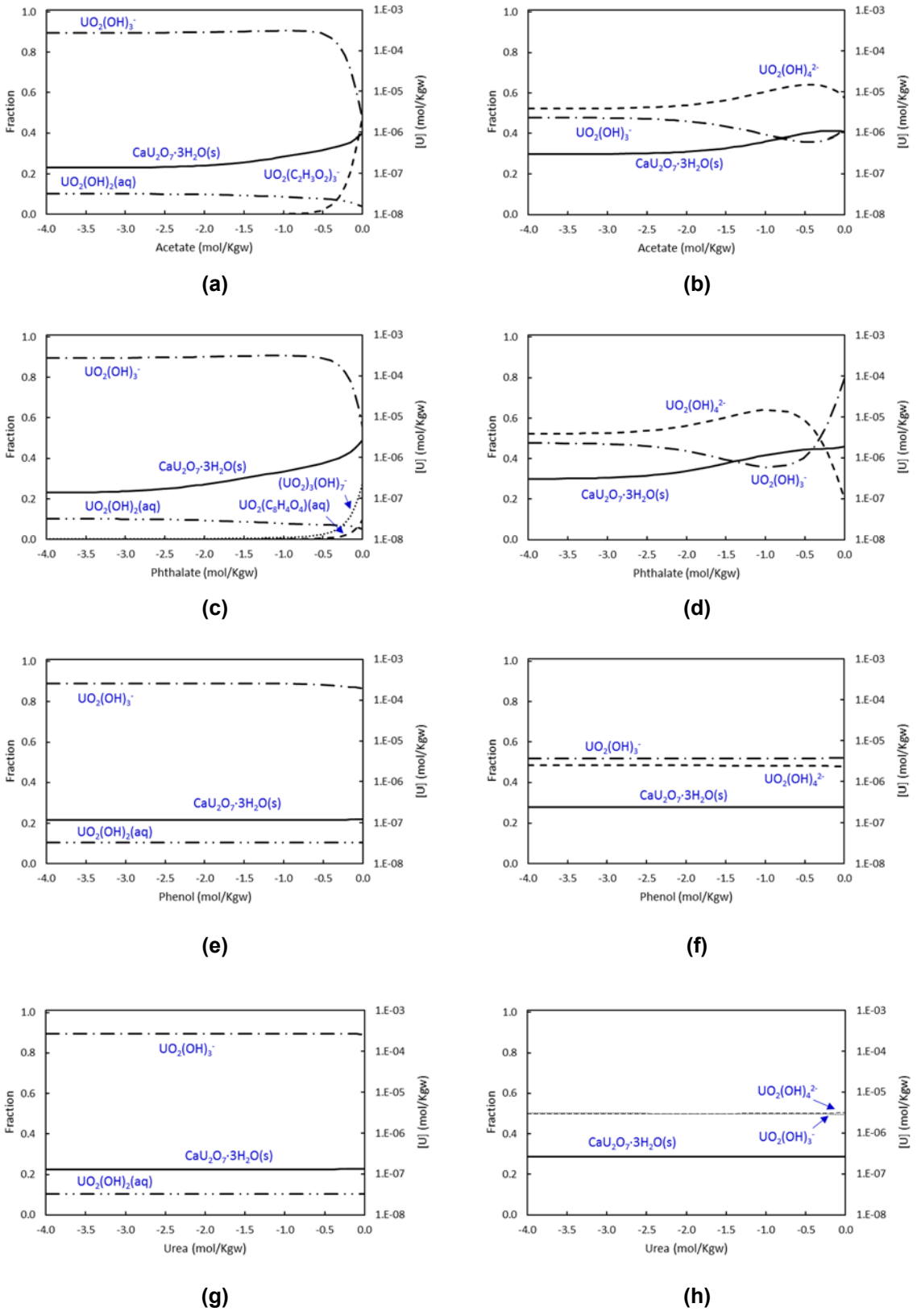

Figure A 24. Solubility curve (black solid lines) calculated for $CaU_2O_7{\cdot}3H_2O$(s) in the presence of acetate (a – b), phthalate (c – d), phenol (e – f) and urea (g – h) as a function of the organic content. Dashed lines stand for the speciation of U in equilibrium with the solid phase. pH fixed as 9 (a – c – e – g) and 12 (b – d – f – h). Calcium concentration fixed in all diagrams as 10^{-3} mol·L^{-1}.

Appendix III

"The work presented in this Chapter has been submitted for publication in Applied Geochemistry, 16th International Conference on the Chemistry and Migration Behaviour of Actinides and Fission Products in the Geosphere, Special Issue Volume"

The potential role of superplasticizers and their degradation products on radionuclides mobilization

David García[a], Mireia Grivé[a], Lara Duro[a], Stéphane Brassinnes[b], Joan de Pablo[c]

[a.] Amphos21, Passeig de Garcia i Fària 49-51, 08019, Barcelona, Spain

[b.] Belgian Agency for Radioactive Waste and Enriched Fissile materials (ONDRAF/NIRAS), Avenue des Arts 14, 1210, Brussels, Belgium

[c.] CTM Centre Tecnològic, Plaça de la Ciència, 2,08243, Manresa, Spain

Abstract

Superplasticizers added into cement can degrade due to hydrolytic, thermal, radiolytic and microbial effects. Short-chain organic compounds such as acetate, phthalate, oxalate, phenol, urea, etc., have been confirmed as a possible superplasticizers degradation products. This work presents a state-of-the-art of the degradation process of superplasticizers and a thermodynamic study on the effect that model compounds considered as proxy for their degradation products have on the mobility of several radionuclides (Ni, Eu, U). Our results indicate that the complexation capacity of the proxy superplasticizers degradation products considered (i.e. acetate, phthalate, phenol and urea) towards Ni Eu and U is almost negligible in alkaline conditions, while relatively important in the near-neutral pH range.

Keywords

Superplasticizers, radionuclides, mobility, cement, chemical degradation

THE POTENTIAL ROLE OF SUPERPLASTICIZERS AND THEIR DEGRADATION PRODUCTS ON RADIONUCLIDES MOBILIZATION

David García[a,*], Mireia Grivé[a], Lara Duro[a], Stéphane Brassinnes[b], Joan de Pablo[c]

[a.] Amphos21, Passeig de Garcia i Fària 49-51, 08019, Barcelona, Spain

[b.] Belgian Agency for Radioactive Waste and Enriched Fissile materials (ONDRAF/NIRAS), Avenue des Arts 14, 1210, Brussels, Belgium

[c.] CTM Centre Tecnològic, Plaça de la Ciència, 2,08243, Manresa, Spain

Abstract

Superplasticizers added into cement can degrade due to hydrolytic, thermal, radiolytic and microbial effects. Short-chain organic compounds such as acetate, phthalate, oxalate, phenol, urea, etc., have been confirmed as a possible superplasticizers degradation products. This work presents a state-of-the-art of the degradation process of superplasticizers and a thermodynamic study on the effect that model compounds considered as proxy for their degradation products have on the mobility of several radionuclides (Ni, Eu, U). Our results indicate that the complexation capacity of the proxy superplasticizers degradation products considered (i.e. acetate, phthalate, phenol and urea) towards Ni Eu and U is almost negligible in alkaline conditions, while relatively important in the near-neutral pH range.

Keywords

Superplasticizers, radionuclides, mobility, cement, chemical degradation

* Corresponding author: David García, Ph.D Candidate in a collaborative project between Amphos 21, ONDRAF-NIRAS and CTM. E-mail: david.garcia@amphos21.com. +34 935 830 500

Glossary of terms

C_6H_5OH	Phenol
$C_2H_3O_2^-$	Acetate
$C_8H_4O_4^{2-}$	Phthalate
H_4N_2CO	Urea
GC-MS	Gas Chromatography – Mass Spectrometry
IR	Infrared
NMR	Nuclear magnetic resonance
PCE	Polycarboxylate ether-based
SMF	Sulfonated Melamine Formaldehyde
SN	Sulfonated naphthalene
SNF	Sulfonated Naphthalene Formaldehyde
SNFC	Sulfonated naphthalene formaldehyde condensate
SP/SPs	Superplasticizer

1. Introduction

In nuclear waste disposal facilities concrete is used as a construction material (construction and stabilisation of galleries and tunnels shotcrete), as a confinement matrix to immobilize some type of wastes but also as a safety barrier to reduce the mobility of radionuclides in the eventual scenario of radionuclide release (Bart et al., 2012).

Superplasticizers (SPs) are a type of organic chemical admixtures used by manufacturers to improve dispersion, hydration and workability properties of concrete (Taylor, 1997). During the last century, SPs industry has been continuously evolving. In overall, four different SPs categories (Figure 1) can be defined: (a) naphthalene-sulfonate based SPs (Tucker, 1936), (b) melamine-sulfonate based SPs (Aignesberger and Bornmann, 1975), (c) lignosulfonate based SPs (Mark, 1938), and (d) polycarboxylate ether-based SPs. (a), (b), and (c) SPs type were widely used in the past century being also named as 1st and 2nd SPs generation. (d) SPs type were described in the 90's, the so called 3rd SPs generation, being widely used in the cement industry nowadays.

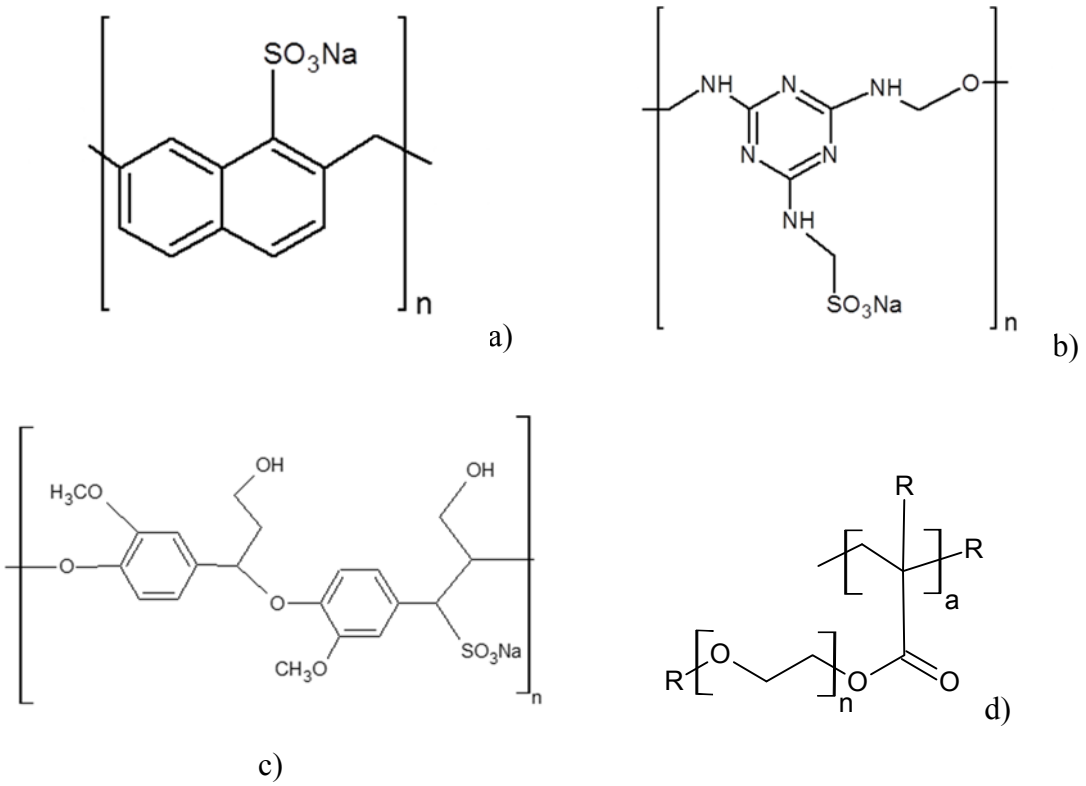

Figure 1. a) Naphthalene sulfonate SPs type structure, b) Melamine sulfonate SPs type structure, c) lignosulfonate, and d) polycarboxylate ether-based SPs type structure.

Glenium® 27 is a polycarboxylate ether-based (PCE) SPs, (d) SPs type, defined as a reference material for being used in concrete formulations to build up different structures in the Belgian deep disposal facility for radioactive wastes. In contrast with the older SPs generation this kind of SPs improves the dispersion of cement particles by electro-steric repulsions (Figure 2). The chemical structure of these type of SPs is formed by a long hydrophobic chain (i.e. polyethyleneglicol chain) and one or several hydrophilic groups linked through an ester bound.

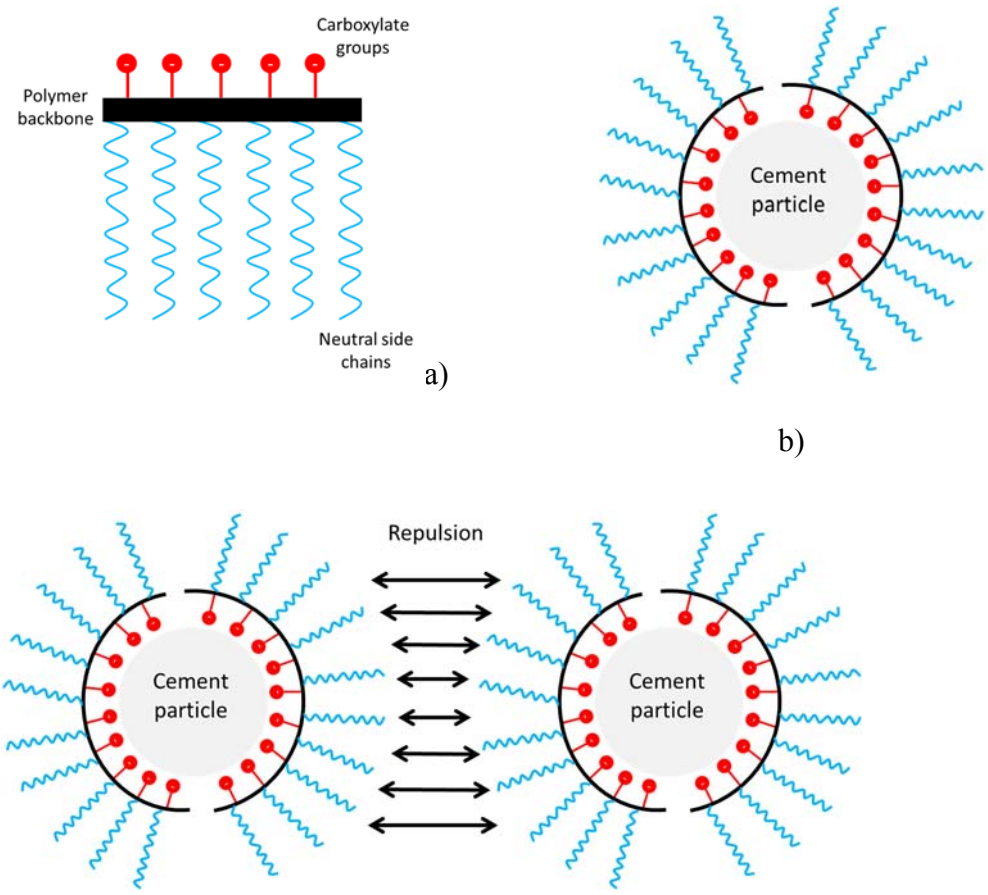

Figure 2. a) Simplified sketch of a PCE SPs, b) representation of cement particle and PCE SPs interaction, and c) repulsion between cement particles surrounded by PCE SPs.

Little information is available regarding the degradation of SPs in cementitious systems (Gascoyne, 2002), although the interest on this topic has recently increased (Wieland et al., 2014). It is well recognized that hyperalkaline conditions developed in cementitious environments can cause chemical transformations of organic substances, i.e. polymeric SPs, (degradation, aging, etc.) with the subsequent production of small organic compounds with new chemical properties (Glaus and Van Loon, 2004a, Glaus and Van Loon, 2004b, Yilmaz et al., 1993).

It is also known the influence that organic substances may have on the behaviour and mobility of several radionuclides (Andersson et al., 2008, Colàs Anguita, 2014, Gaona et al., 2008, Wieland et al., 2014). The role of SPs degradation processes on radionuclide

mobility through the near and far field of a radioactive waste repository is therefore a matter of concern for performance assessment of radioactive waste repositories. This work aims at investigating to which extent the degradation of SPs may affect radionuclide behaviour in concrete environments.

2. Superplasticizers degradation: Literature survey

In this section, a literature research focused on SPs hydrolytic, thermal, radiological and microbial degradation is provided. Overall there is an important lack of SPs degradation studies. To complement the literature research, studies focused on main organic SPs groups' (i.e., naphthalene, melamine, etc.) degradation have been also reviewed.

To the best of our knowledge studies dealing with the degradation of PCE SPs are not available yet. Therefore, specific degradation products from PCE SPs degradation have not been found.

2.1 Hydrolytic degradation

Cementitious environments promote highly alkaline systems due to the dissolution-precipitation processes occurring within a cementitious matrix in contact with water. Overall, four pH ranges may be defined depending on the cement degradation state: (i) fresh or degradation state I, characterized by a high alkaline pH range (>13) produced by the dissolution of Na and K alkalis, (ii) degradation state II, in where portlandite ($Ca(OH)_2$) dissolution controls the evolution of the system, buffering the pH around values of 12.5, (iii) degradation state III, after total dissolution of portlandite, C-S-H gels dissolve buffering the system from pH 12.3 to 10.5 as a function of the Ca/Si ratio within the C-S-H gel, and, finally (iv) degradation state IV, where the formation of calcite within the cement matrix buffers the system pH at values <10 (Taylor, 1997). For the current

research, only studies in which pH values higher than 10.5 are reported have been considered in order to magnify SPs hydrolysis.

Yilmaz and co-workers (Yilmaz et al., 1993) studied the degradation of Sulfonated Naphthalene Formaldehyde (SNF) and Sulfonated Melamine Formaldehyde (SMF) SPs. According to their results, SNF SPs were not altered in alkaline solutions (1 M KOH) while solid precipitation was observed in SMF solutions at similar pH values. Analysis of the precipitated product confirmed the alteration of the original SMF chemistry. However, the chemical characterization of the precipitated solid was not entirely clear and thus the authors did not report conclusive SPs degradation pathways.

Naphthalene degradation based on photocatalysis was studied by Lair and co-workers (Lair et al., 2008). The authors investigated different parameters affecting naphthalene degradation, among others the system pH (from 2 to 12). From their results (Lair et al., 2008) concluded that an increase of the system pH increased the degradation rate of naphthalene. A possible explanation for this phenomenon reported by the authors is that the increase of OH^- ions in solution increase the presence of OH• radicals favouring naphthalene degradation. Intermediate degradation products were determined by GC-MS (Gas Chromatography – Mass Spectrometry) analyses; dozens of compounds were identified being 2-formylcinnamaldehyde and 1-naphtalenol the most abundant (see Appendix I).

Melamine Formaldehyde-Acrylic coatings degradation were studied by (English et al., 1983) with different analytical techniques (^{13}C NMR, IR). Under standard weathering conditions, only accounting for hydrolysis at atmospheric conditions, the degradation reaction reported by the authors was r. **1**. This reaction involved the substitution of the terminal methyl by water releasing formaldehyde. No modifications of the melamine

back-bone were found by the authors. Later (Gerlock et al., 1986) confirmed the same degradation pathway by using photo-enhanced hydrolysis.

$$\text{Melamine-}CH_2OCH_3 + H_2O \Leftrightarrow \text{Melamine-}CH_2OH + CH_3OH \quad \text{r. 1}$$

2.2 Thermal degradation

Temperature elevations (around 100ºC) in the surroundings of a high-level waste repository are expected by the exothermic wastes (Bel et al., 2006, Gibb, 1999). In order to minimize the effect of temperature on the repository performance, in the current facilities waste management organizations designed repositories to ensure a temperature below 100ºC in the internal package surfaces and below 90ºC in the host rock (Andra, 2005). Thermal organic polymer degradation mostly occurs at temperatures above 100ºC (Hawkins, 1984) and thus for a better temperature degradation analysis in the following survey studies at higher temperatures (>100ºC) have been also included.

Lair et al., 2008) studied the effect of temperature (from 10 to 40ºC) on photocatalytic naphthalene degradation. They could not draw clear conclusions on the temperature effect, as volatilization of naphthalene could affect the results. Nevertheless, in agreement with what was mentioned in section 2.1, the authors identified 2-formylcinnamaldehyde and 1-naphtalenol as the most abundant intermediates during naphthalene degradation (see Appendix I).

Onwudili and Williams (Onwudili and Williams, 2007) investigated the reaction mechanisms of phenanthrene and naphthalene hydrothermal degradation from 350 to 380ºC. The authors used sealed reactors reaching highly pressurized systems (170-225 bar). Weak naphthalene decomposition was reported to occur after 1h at 380ºC, 90% of naphthalene remained in solution. In such temperature conditions, the presence of a large excess of oxidant in solution (hydrogen peroxide) favours naphthalene degradation.

Naphthalene decomposition products were determined by GC-MS. The reaction path mechanism shown in Figure 3 was proposed for the oxidative degradation of naphthalene.

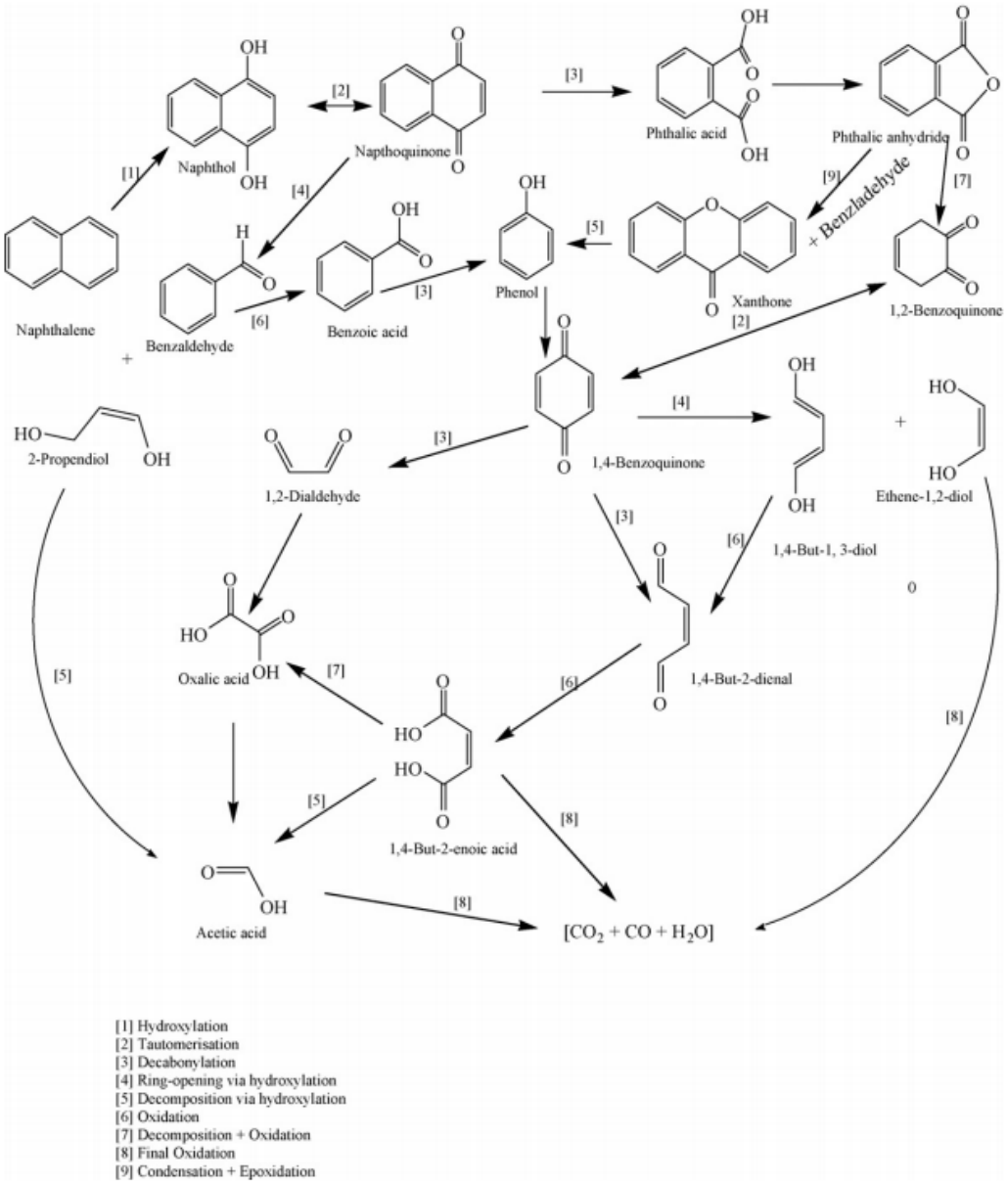

Figure 3. Naphthalene degradation reaction mechanism proposed by (Onwudili and Williams, 2007) under hydrothermal conditions.

Brebu and Vasile (Brebu and Vasile, 2010), published a literature survey on lignin thermal degradation products. Those authors reported lignin degradation to start between 200 and 275ºC, the main process occurring around 400ºC, yielding a variety of organic compounds (i.e. aromatic hydrocarbons, phenolics, hydroxyphenolics and

guaiacyl/syringil-type compounds). Pyrolysis up to 340ºC of three different lignin-based compounds (lignosulfonate among others) was done by (Brebu et al., 2011). Degradation products were characterized by thermogravimetric and chromatographic analysis. The authors reported the formation of ammonia and sulphur dioxide around 250ºC (see Appendix I) followed by derivatives of the structural compounds in lignin (i.e. phenols derivatives as pyrocatechol).

Deamination followed by condensation was reported by (Costa and Camino, 1988) in their melamine thermal study. According to their thermogravimetric results, the authors suggests the formation of ammonia in a temperature range between 350-400ºC. Analysis of the residual product by IR showed the presence of unreacted solid, melamine, and the formation of a water-insoluble product coming from melamine condensation. The identification of this water-insoluble product was not clearly defined in the study although the authors claimed the formation of "melem", an organic molecule formed by different cyameluric rings (Finkel'Shtein, 1959, Van der Plaats et al., 1981).

2.3 Radiolytic or radiolytic induced degradation

Ionizing radiation released by nuclear waste may lead to the alteration of the different elements present in storage conditions (i.e. water radiolysis and subsequent generation of $OH^{\bullet}$).

Palmer and Fairhall (Palmer and Fairhall, 1992), examined the production of gas due to the irradiation of small OPC cylinders and blast furnace slag grouts containing sulfonated naphthalenes formaldehyde condensates (Na-SNFC) and sulfonated melamine formaldehyde condensate (SMFC) SPs. The radiation field was 104 Gy/hr and total dose applied over the samples was up to 9 MGy. The results showed that both CO_2 (g) and H_2

(g) were generated by irradiation (up to 6.7 mL gas/g superplasticizer). The authors commented that the radiation did not appear to affect the strength or stability of the grout.

Naphthalene degradation was accounted for by Kanodia and co-workers (Kanodia et al., 1988) by means of radiolitically produced OH• radicals. An oxidative process was then favoured yielding the conversion of naphthalene to naphthalenol. The same degradation product was found by Balakrishnan and Reddy (Balakrishnan and Reddy, 1968) in aqueous γ irradiated solutions containing naphthalene at high temperatures (see Appendix I).

2.4 Microbial degradation

Microbiology within nuclear waste disposal has been a matter of important studies during the last five decades. Biogeochemical effects on the chemistry and the long-term evolution of repository materials as well as on the transport of radionuclides have been extensively studied (McKelvie et al., 2016, Pedersen, 1996, West and McKinley, 1983). Among others process mediated by microbes, biodegradation of bituminized waste forms (West, 1995) yielding small organic compounds, is a comparable case as the once studied here involving SPs biodegradation.

Haveman and co-workers (Haveman et al., 1996) studied Disal (a naphthalene based SPs) degradation in the presence of Pseudonomas bacteria. The authors reported an increase of bacteria population in anaerobic conditions and in the presence of an electron acceptor as nitrate. Although results of this study were not conclusive, the degradation of naphthalene under denitrifying conditions or coupled to sulphate reductions have been reported by others (Bedessem et al., 1997, Mihelcic and Luthy, 1988, Mihelcic and Luthy, 1991, Rockne et al., 2000, Song et al., 2005). In all those studies (Bedessem et al., 1997, Mihelcic and Luthy, 1988, Mihelcic and Luthy, 1991, Rockne et al., 2000, Song et al.,

2005) naphthalene mineralization is observed but some authors (Bedessem et al., 1997) also reported naphthalenol as an intermediate product during naphthalene degradation (see Appendix I).

Ruckstuhl and co-workers (Ruckstuhl et al., 2002) studied the leaching and biodegradation of SN and SNFC from concrete materials used in tunnel constructions. Those authors reported that in-situ biodegradation, mediated by the microorganism presents in the studied samples, was the most effective mechanism to remove SNFC components from groundwater. Total depletion of mono-sulfonated monomers was quickly observed while the di-sulfonated analogues were proven to be persistent. Unfortunately, no information about possible degradation products was detailed by the authors indicating a possible mineralization of the original SPs.

Pseudomonas sp. HOB1 bacterium was used by Pathak and co-authors (Pathak et al., 2009) in their naphthalene degradation studies. The authors reported total naphthalene mineralization indicating that temperatures about 35-37ºC and alkaline pH favoured naphthalene degradation. No intermediate products were detected by those authors.

The metabolism of melamine degradation by Klebsiella terragena was studied in detail by (Shelton et al., 1997). The authors reported a deamination pathway (Figure 4) of the triazine ring through hydrolytic reactions mediated by the studied bacteria yielding the following degradation products: ammeline, ammelide, cyanuric acid, biuret and urea (see Appendix I). Early in the 80's (Jutzi et al., 1982) proposed a similar degradative pathway using Pseudonomas sp. Strain A.2 bacteria.

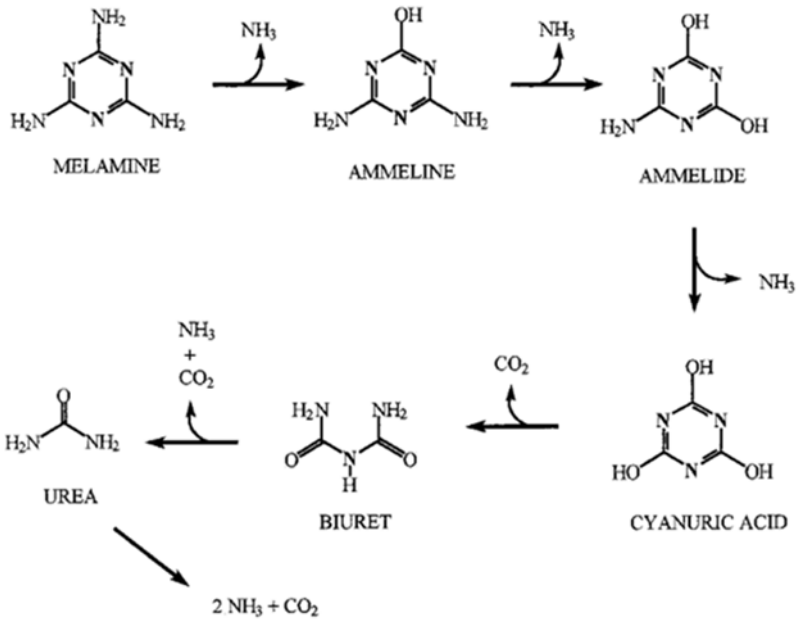

Figure 4. Melamine degradation reaction mechanism proposed by (Shelton et al., 1997) under microbial mediated conditions.

The degradation of lignin through the fungus Formes annosus was studied in the 80's by Haars and Hüttermann (Haars and Huttermann, 1980). Although not much detail is provided in that work phenolic derivatives were detected by the authors in the presence of the so-called fungus. Early in the 70's (Watkins, 1970) reported that lignosulfonates were more resistant that lignin to microbial decomposition due to a) the sulfonation of side chains of aromatic monomers, and b) the hydrolysis of the ether linkages and the formation of new carbon-carbon bonds between aromatic rings.

The list of possible superplasticizer degradation products detailed in Appendix I could be divided in three categories: i) aromatic compounds, ii) aliphatic compounds, and iii) inorganic species. The first (i) and the second (ii) categories include degradation products coming from naphthalene and melamine based SPs, while in the third (iii) category species coming from lignosulfonate and/or melamine based SPs degradation are included. Overall, aromatic compounds are more reactive than aliphatic species. However, the

presence of carboxylic terminations in the aliphatic compounds included in Table S1 (see Appendix I) may increase the reactivity of those species, producing thus quite reactive aliphatic degradation products.

Although no specific degradation studies on PCE SPs have been found in the literature, aliphatic organic compounds specified previously can be taken as a proxy for PCE SPs degradation products.

3. Discussion

In the previous section an extensive list of possible SPs degradation products has been compiled based on independent literature reported data (Table S1). Considering the information within this table four degradation products have been selected to study their possible effect on radionuclides aqueous chemistry, including both aromatic and aliphatic organic compounds, representative of possible PCE SPs degradation):

- Phthalic and acetic acids, formed during naphthalene (proxy for SNF structure) hydrothermal degradation. It is well recognized that both acids have a powerful capacity to interact with a variety of radionuclides (Boggs et al., 2010, Novak et al., 1996, Park et al., 2006, Rees and Daniel, 1984, Vazquez et al., 2008, Wood et al., 2000). Given that those species are generated through a thermal process, the formation of those species is expected to occur during the temperature transient period (~100 years) under repository conditions.
- Phenol, formed during the biodegradation of both lignin and naphthalene (proxy for SMF and SNF structures, respectively). In general little is known about phenol interaction with radionuclides although some authors reported strong affinity towards actinides (Bartušek and Sommer, 1965, Öztekin et al., 1996, Schmeide et al., 2003). The formation of this species in deep repository conditions through

SPs polymers degradation is expected to occur only through microbially-mediated mechanisms. In deep repository conditions microbes will be first fed by small organics, already present in the system from other sources, and later by big polymers like SPs. Thus, phenol formed due to lignin or naphthalene biodegradation is expected to appear in the repository in a long-time scale.

- Urea, formed during melamine (proxy for a SMF structure) biodegradation. The Interaction between lanthanides and urea has recently been a matter of concern and some authors reported relatively weak affinities among them (Heller et al., 2009, Osman et al., 2013). Like phenol, urea generated due to melamine biodegradation is expected to appear in the repository in the long-term.

Ni, Eu(III) and U(VI) have been selected as radionuclides of interest for this exercise. Nickel is a constituent of repository construction materials (i.e. stainless steel) and its corresponding activation products are expected to be encountered in the deep disposal conditions studied in this work. Eu(III), as representative of the trivalent lanthanides, constitute the major fraction of the minor lanthanides/actinides present in the high-level liquid waste generated during the reprocessing of spent nuclear fuel and thus the understanding of its chemical interactions with organics is of utmost importance to ensure the repository safety. Finally, U(VI) constitutes the major component spent fuel, being a good representative of heavy the actinides.

In order to study the possible effect of those organics on radionuclides chemistry, it is of the outmost importance to have a consistent and reliable set of thermodynamic data. Thus, before performing specific thermodynamic calculations a data selection has been done and is presented in the following section.

3.1 Thermodynamic data selection

3.1.1 Phthalic and acetic acid

The interaction of those organics with several radionuclides is well described in ThermoChimie database (Giffaut et al., 2014) being available at https://www.thermochimie-tdb.com/. ThermoChimie database was created by the French National Waste Management agency (ANDRA) to address geochemical modelling and performance assessment tasks; being the included thermodynamic data self-consistent and reliable.

Thermodynamic data for Ni, Eu and U complexation with both organics, acetate ($C_2H_3O_2^-$) and phthalate ($C_8H_4O_4^{2-}$), included in ThermoChimie and considered in this work is listed in Table 1.

3.1.1 Phenol

There is a general lack of data for the complexation of phenol with rare earth elements (Marsac et al., 2011). The only data on the complexation of uranyl (VI) ion with phenol come from the potentiometric titrations of Bartušek and Sommer (Bartušek and Sommer, 1965). The authors suggested the formation of 1:1 metal-ligand complex in acidic conditions (pH<3), which is easily hydrolysed to polynuclear species at pH 4-5. The Log *K* value calculated by the authors according to eq. 1 is -3.56 ±0.1 (*I*=0.1M $NaClO_4$), and is the one selected in this work (Table 1).

$$UO_2^{2+} + C_6H_5OH \leftrightarrow UO_2(C_6H_5O)^+ + H^+ \qquad \text{eq. 1}$$

To the best of our knowledge, thermodynamic data for the complexation of phenol with Ni and Eu are not available in the open literature.

3.1.1 Urea

As in the case of phenol, little is known about the complexation of urea with Ni, Eu and U. Osman and co-workers (Osman et al., 2015, Osman et al., 2013), studied the complexation of urea and uric acid with uranium in acid conditions (pH<4), and proposed the formation of a 1:1 week complex ($UO_2(H_4N_2CO)^{2+}$). The authors reported a stability constant of 2.12 ± 0.18 (*I*=0.1M $NaClO_4$) according to eq. 2.

$$UO_2^{2+} + H_4N_2CO \leftrightarrow UO_2(H_4N_2CO)^{2+} \quad \text{eq. 2}$$

Similarly, Heller and co-workers (Heller et al., 2009), studied the complexation of trivalent Eu and Cm with urea in aqueous solution. The authors reported stability constants for two Eu – urea weak complexes, $Eu(H_4N_2CO)^{3+}$ and $Eu(OH)(H_4N_2CO)^{2+}$, -0.12 ± 0.05 and -6.86 ± 0.15 (*I*=0.1M $NaClO_4$) respectively.

$$Eu^{3+} + H_4N_2CO \leftrightarrow Eu(H_4N_2CO)^{3+} \quad \text{eq. 3}$$

$$Eu^{3+} + H_4N_2CO + H_2O \leftrightarrow Eu(OH)(H_4N_2CO)^{2+} + H^+$$

To the best of our knowledge, thermodynamic data for the complexation of urea with Ni is not available in the open literature. Selected data for the studied urea – radionuclide systems is detailed in Table 1.

Table 1. Relevant thermodynamic data used in this work.

Reaction	Log K^0	Reference
$Ni^{2+} + C_2H_3O_2^- <=> Ni(C_2H_3O_2)^+$	1.34 ± 0.11	ThermoChimie database
$Eu^{3+} + C_2H_3O_2^- <=> Eu(C_2H_3O_2)^{2+}$	2.90 ± 0.50	
$Eu^{3+} + 2C_2H_3O_2^- <=> Eu(C_2H_3O_2)_2^+$	4.80 ± 0.20	
$Eu^{3+} + 3C_2H_3O_2^- <=> Eu(C_2H_3O_2)_3(aq)$	5.60 ± 0.20	
$Ni^{2+} + C_8H_4O_4^{2-} <=> Ni(C_8H_4O_4)(aq)$	3.00 ± 1.00	
$Eu^{3+} + C_8H_4O_4^{2-} <=> Eu(C_8H_4O_4)^+$	4.96 ± 0.30	
$Eu^{3+} + 2C_8H_4O_4^{2-} <=> Eu(C_8H_4O_4)_2^-$	7.34 ± 0.50	
$UO_2^{2+} + C_6H_5OH <=> UO_2(C_6H_5O)^+ + H^+$	-3.77* ± 0.10	(Bartušek and Sommer, 1965)
$UO_2^{2+} + H_4N_2CO <=> UO_2(H_4N_2CO)^{2+}$	2.12* ± 0.18	(Osman et al., 2013)
$Eu^{3+} + H_4N_2CO <=> Eu(H_4N_2CO)^{3+}$	-0.12* ± 0.05	(Heller et al., 2009)
$Eu^{3+} + H_4N_2CO + H_2O <=> Eu(OH)(H_4N_2CO)^{2+} + H^+$	-7.28* ± 0.15	

*Values corrected to I=0 using Davies ionic strength corrections.

3.2 Thermodynamic calculations

Calculations presented in this section have been done with the PhreeqC geochemical code (Parkhurst and Appelo, 2013). As mentioned in the previous section, thermodynamic data used in the calculations have been taken from ThermoChimie database and from other literature sources if not available in ThermoChimie. All calculations were performed at 25ºC and ionic strength corrections have been applied by using the Davies approach (Grenthe and Puigdomenech, 1997). In agreement with the solid phase selection in Albrecht et al. (Albrecht et al., 2005) the effect of the organic complexes has been calculated on the solubility of the following solid phases: $Ni(OH)_2(s)$, $Eu(OH)_3(s)$ and $CaU_2O_7 \cdot 3H_2O(s)$.

Solubility diagrams obtained in the presence of acetate as a function of pH are shown in Figure 5, Figure 6 and Figure 7. The underlying chemical speciation of each element is

shown in the same figures. According to these results, organic ligand concentrations higher than 10^{-4} M are required to see some effects on Ni and Eu chemistry (Figure 5 and Figure 6). For both elements, acetate complexation only occurs from pH 8 to 9.5, increasing ¼ order of magnitude the solubility of both $Ni(OH)_2(s)$ and $Eu(OH)_3(s)$. In alkaline pH conditions, the hydrolysis of Ni and Eu is strong enough to avoid the binding with acetate up to organic concentrations of 10^{-2} M. Increasing the acetate concentration up to 10^{-2} M does not affect the aqueous chemistry of U in the whole studied pH range (8 – 13) (Figure 7). Unrealistic Acetate concentrations as high as $10^{-0.3}$ M (see Appendix II), are needed to observe an important effect on U behaviour in near neutral pH conditions. The same is true for phthalate (see Figure 7 and Appendix II). As with acetate, phthalate affects Ni and Eu chemistry only at concentrations over 10^{-2} M (Figure 5 and Figure 6). Phthalate complexation with Ni and Eu is relatively stronger than acetate complexation, prevailing up to pH ~10. This is notorious in near neutral pH conditions, where the solubility of both $Ni(OH)_2(s)$ and $Eu(OH)_3(s)$ increase more than one order of magnitude when increasing phthalate aqueous concentration from 10^{-2} M to 10^{-4} M. Overall, the effect of acetate and phthalate on the chemistry of Ni, Eu and U will be negligible in the alkaline pH region but certainly important in near-neutral conditions (i.e. clay barriers or clay host-rock present in some repository designs) (see Appendix II). It is worth mentioning that in clay conditions the effect of carbonate, major system species, will partially hinder the effect of acetate and phthalate on radionuclides behaviour.

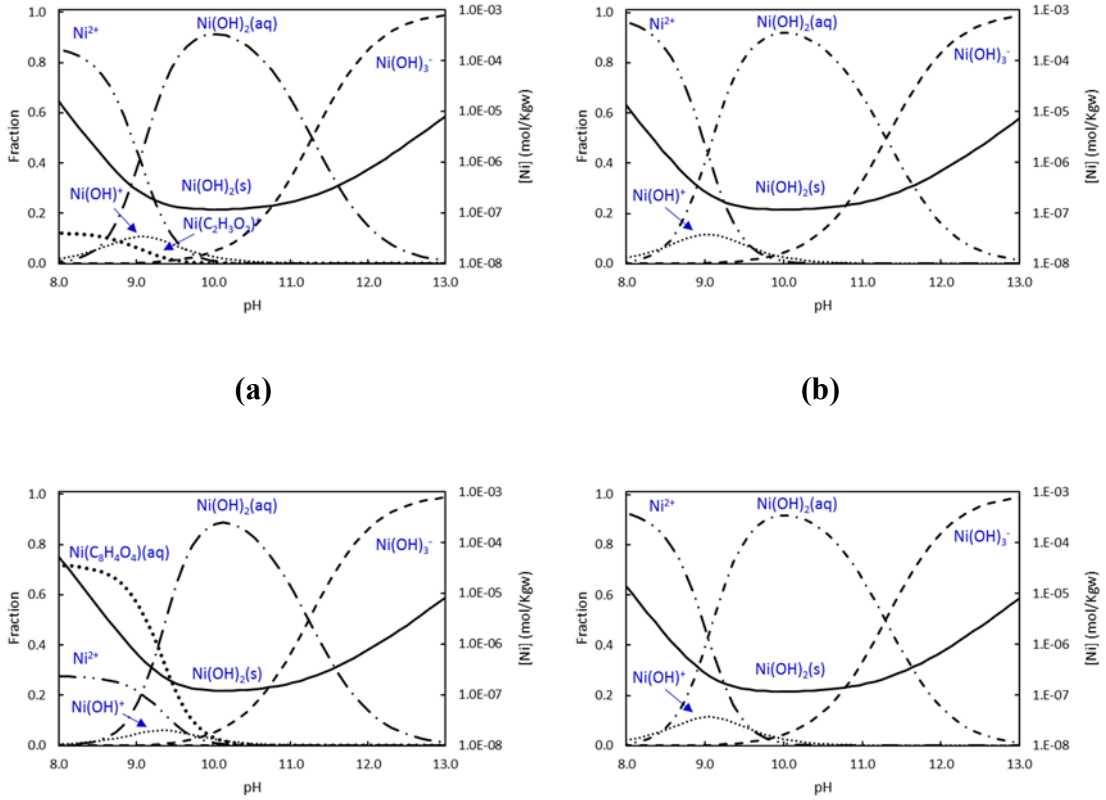

Figure 5. Solubility curve (black solid line) calculated for $Ni(OH)_2(s)$ in the presence of acetate (a – b) and phthalate (c – d) as a function of pH. Dashed lines stand for the speciation of Ni in equilibrium with the solid phase. Organic concentration fixed as 10^{-2} M (a – c) and 10^{-4} M (b – d). Calcium concentration fixed in all diagrams as 10^{-3} M in agreement with the expected Ca concentrations in state II cement degradation conditions.

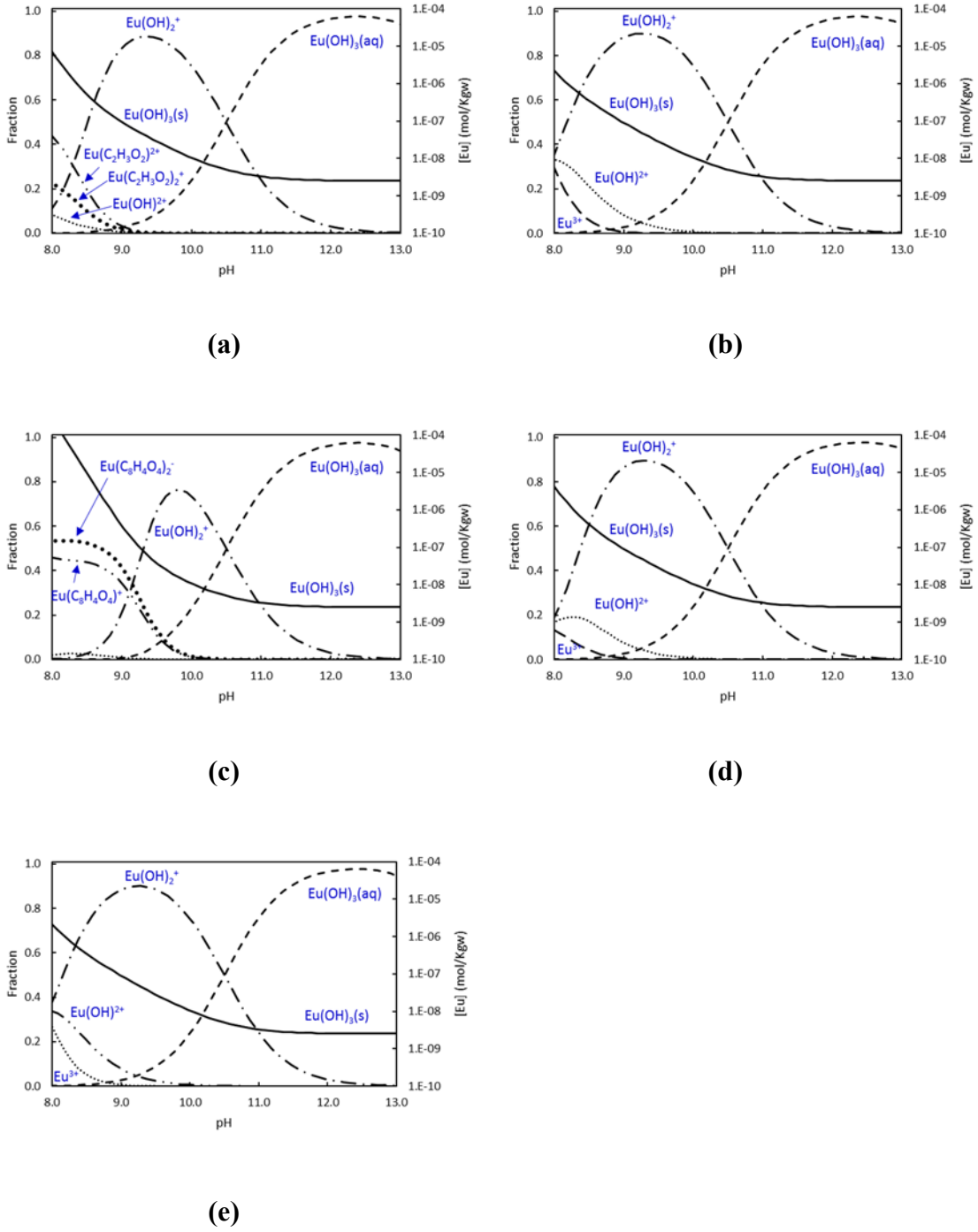

Figure 6. Solubility curve (black solid lines) calculated for $Eu(OH)_3(s)$ in the presence of acetate (a – b), phthalate (c – d) and urea (e) as a function of pH. Dashed lines stand for the speciation of Eu in equilibrium with the solid phase. Organic concentration fixed as 10^{-2} M (a – c) and 10^{-4} M (b – d). Calcium concentration fixed in all diagrams as 10^{-3}

M. Note that for the urea scenario, Eu calculated solubility-speciation (e) is identical at 10^{-2} / 10^{-4} M.

In the studied pH conditions, from near neutral to alkaline pH, the effect of phenol over U is negligible (Figure 7). Contrary to the trends observed for acetate and phthalate, extremely high phenol concentrations (>$10^{-0.3}$ M) do not produce any influence on its chemistry (see Appendix II). This is not surprising given that thermodynamic data for phenol complexation with uranium selected in this work was obtained in acidic conditions. Similarly, our results indicate that complexation of Eu and U with urea is negligible in alkaline pH conditions (Figure 6, Figure 7 and Appendix II).

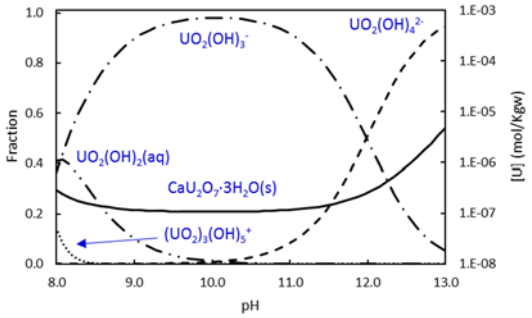

Figure 7. Solubility curve (black solid line) calculated for $CaU_2O_7 \cdot 3H_2O(s)$ in the presence of acetate, phthalate and urea at 10^{-2} / 10^{-4} M as a function of pH. Dashed lines stand for the speciation of the different elements in equilibrium with the solid phase. Calcium concentration fixed in all diagrams as 10^{-3} M.

Based on the presented results, among the studied SPs degradation products, the most powerful complexing agent is phthalate exerting an important control over Ni and Eu behaviour in slightly alkaline conditions. Overall, the complexation capacity shown by the different degradation products studied in this work could be ordered from the stronger to the weaker complexing agent as follows: phthalate > acetate > urea > phenol. As

mentioned before the strongest complexing ligands, phthalate and acetate, are expected to form in deep repository conditions during the temperature transient period (~100 years); while the weakest ligands are expected to form at long-term. These findings clearly point out the importance of phthalate / acetate radionuclide complexation in repository conditions.

Is worth mentioning that U seems to be unaffected by any of the studied ligands in the conditions studied in this work. However, as previously highlighted, there is a general lack of data for the complexation of some of the studied organic ligands with radionuclides, specially at alkaline pH conditions. Thus, additional experiments are required to confirm the validity of the statements reflected here.

4. Conclusions

Superplasticizers present in concrete formulations may be altered in deep disposal conditions through several mechanisms: hydrolysis, temperature, ionizing radiation and microbial activity. Overall, few studies are available in the literature dealing with the alteration of superplasticizers; and specifically, there is an important lack of results for the degradation of PCE SPs.

Based on the literature review presented in this work, we can conclude that the alteration of superplasticizers may lead to the formation of small organic compounds that could be classified in three main categories: i) aromatic compounds, ii) aliphatic compounds, and iii) inorganic species. From those categories, four possible degradation products (representatives of different SPs types) have been selected (phthalic acid, adipic acid, phenol and urea) and their effect on radionuclide (Ni, Eu and U) behaviour has been calculated. Our results indicate that in alkaline pH conditions, the presence of these organic ligands up to concentrations of 10^{-2} M, will not affect the behaviour of any of the

studied radionuclides. However, in slightly alkaline systems (from pH 8 to 10), phthalic and acetic acids (up to concentrations of 10^{-2} M) could control the aqueous chemistry of both Ni and Eu. This chemical control produces an increase on Ni and Eu solubility, especially relevant in systems with phthalic acid presence. Interestingly, U is not affected by any of the studied ligands in the conditions used in the present study. Nevertheless, this statement may be taken with caution given the scarcity of thermodynamic data found in the literature for the complexation of U with some of the studied organics in alkaline conditions.

For a better system comprehension, and to clearly ensure the safety of the radioactive waste disposal, additional superplasticizer degradation studies are required, especially for PCE SPs type. Moreover, specific radionuclide-organic complexation studies in alkaline pH conditions are desired to complement the available thermodynamic.

Acknowledgments

The research leading to these results has been funded by the Belgian Agency for Radioactive Waste and Enriched Fissile materials (Ondraf-Niras).

References

Aignesberger, A. and Bornmann, P. (1975). Verfahren zur herstellung von loesungen sulfitmodifizierter melaminharze. DE Patent: DE1745441 A1

Albrecht, A., Altmann, S., Buschaert, S., Coelho, D., Gallerand, M., Giffaut, E., and Leclerc-Cessac, E. (2005). Dossier 2005 Argile. Réferentiel du comportement des radionucléides et des toxiques chimiques d'un stockage dans le Callovo-Oxfordien jusq'à l'homme. Site de Meuse/Haute-Marne. Tome 1/2.

Andersson, M., Ervanne, H., Glaus, M., Holgersson, S., Laine, H., Lothenbach, B., Puigdomenech, I., Schwyn, B., Snellman, M., Ueda, H., Vuorio, M., Wieland, E., and Yamamoto, T. (2008). Development of methodology for evaluation of long-term safety aspects of organic cement paste components. *POSIVA Working report*, 28:2008.

Andra (2005). Dossier 2005 Argile. Synthesis: Evaluation of the feasibility of a geological repository in an argillaceous formation. Technical Report Andra 226 VA, Andra.

Balakrishnan, I. and Reddy, M. (1968). Homolytic hydroxylation of naphthalene in oxygenated aqueous solutions by. gamma. radiolysis at higher temperatures. *The Journal of Physical Chemistry*, 72(13):4609–4613.

Bart, F., Cau-di Coumes, C., Frizon, F., and Lorente, S. (2012). *Cement-based materials for nuclear waste storage*. Springer Science & Business Media.

Bartušek, M. and Sommer, L. (1965). On the complex forming tendency of phenolic hydroxyl with UO_2^{2+}. *Journal of Inorganic and Nuclear Chemistry*, 27(11):2397–2412.

Bedessem, M., Swoboda-Colberg, N., and Colberg, P. (1997). Naphthalene mineralization coupled to sulfate reduction in aquifer-derived enrichments. *FEMS Microbiology Letters*, 152(2):213–218.

Bel, J., Wickham, S., and Gens, R. (2006). Development of the Supercontainer design for deep geological disposal of high-level heat emitting radioactive waste in Belgium. In *MRS Proceedings*, volume 932, pages 122–1. Cambridge Univ Press.

Boggs, M., Dong, W., Gu, B., and Wall, N. (2010). Complexation of Tc (IV) with acetate at varying ionic strengths. *Radiochimica Acta*, 98(9-11):583–587.

Brebu, M., Cazacu, G., and Chirila, O. (2011). Pyrolysis of lignin a potential method for obtaining chemicals and/or fuels. *Cellulose Chemistry and Technology*, 45(1):43.

Brebu, M. and Vasile, C. (2010). Thermal degradation of lignin a review. *Cellulose Chemistry & Technology*, 44(9):353.

Colàs Anguita, E. (2014). *Complexation of Th (IV) and U (VI) by polyhydroxy and polyamino carboxylic acids*. PhD thesis, Universitat Politècncia de Catalunya.

Costa, L. and Camino, G. (1988). Thermal behaviour of melamine. *Journal of thermal analysis*, 34(2):423–429.

English, A., Chase, D., and Spinelli, H. (1983). Structure and degradation of an intractable polymeric system: melamine formaldehyde crosslinked acrylic coatings. *Macromolecules*, 16(9):1422–1427.

Finkel'Shtein, A. (1959). Optical investigation of the molecular structure of s-triazine derivatives. IV. Infrared absorption spectra of compounds with condensed nuclei of s-triazine derivatives of cyameluric acid. *Optics and Spectroscopy*, 6:17.

Gaona, X., Montoya, V., Colàs, E., Grivé, M., and Duro, L. (2008). Review of the complexation of tetravalent actinides by ISA and gluconate under alkaline to hyperalkaline conditions. *Journal of Contaminant Hydrology*, 102(3):217–227.

Gascoyne, M. (2002). Influence of grout and cement on groundwater composition. Technical Report 2002-07, Posiva.

Gerlock, J., Dean, M., Korniski, T., and Bauer, D. (1986). Formaldehyde release from acrylic/melamine coatings during photolysis and the mechanism of photoenhanced cross-

link hydrolysis. *Industrial & Engineering chemistry product research and development*, 25(3):449–453.

Gibb, F. (1999). High-temperature, very deep, geological disposal: a safer alternative for high-level radioactive waste? *Waste Management*, 19(3):207 – 211.

Giffaut, E., Grivé, M., Blanc, P., Vieillard, P., Colàs, E., Gailhanou, H., Gaboreau, S., Marty, N., Madé, B., and Duro, L. (2014). Andra thermodynamic database for performance assessment: ThermoChimie. *Applied Geochemistry*, 49:225–236.

Glaus, M. and Van Loon, L. (2004a). Cellulose degradation at alkaline conditions: Long-term experiments at elevated temperatures. Technical Report PSI Report Nr. 04-01, PSI.

Glaus, M. and Van Loon, L. (2004b). A generic procedure for the assessment of the effect of concrete admixtures on the retention behaviour of cement for radionuclides: concept and case studies. Technical Report PSI Report Nr. 04-02, PSI.

Grenthe, I. and Puigdomenech, I. (1997). *Modelling in aquatic chemistry*. OECD Publishing.

Haars, A. and Huttermann, A. (1980). Macromolecular mechanism of lignin degradation by Fomes annosus. *Naturwissenschaften*, 67(1):39–40.

Haveman, S., Stroes-Gascoyne, S., and Hamon, C. (1996). Biodegradation of a sodium sulphonated naphthalene formaldehyde condensate by bacteria naturally present in granitic groundwater. Technical Report TR-721, AECL.

Hawkins, W. (1984). *Polymer degradation and stabilization*, volume 8. Springer Science & Business Media.

Heller, A., Barkleit, A., Bernhard, G., and Ackermann, J.-U. (2009). Complexation study of europium (III) and curium (III) with urea in aqueous solution investigated by time-resolved laser-induced fluorescence spectroscopy. *Inorganica Chimica Acta*, 362(4):1215–1222.

Jutzi, K., Cook, A. M., and Hütter, R. (1982). The degradative pathway of the s-triazine melamine. The steps to ring cleavage. *Biochemical Journal*, 208(3):679–684.

Kanodia, S., Madhaven, V., and Schuler, R. (1988). Oxidation of naphthalene by radiolytically produced OH radicals. *International Journal of Radiation Applications and Instrumentation. Part C. Radiation Physics and Chemistry*, 32(5):661–664.

Lair, A., Ferronato, C., Chovelon, J.-M., and Herrmann, J.-M. (2008). Naphthalene degradation in water by heterogeneous photocatalysis: an investigation of the influence of inorganic anions. *Journal of Photochemistry and Photobiology A: Chemistry*, 193(2):193–203.

Mark, J. (1938). Concrete and hydraulic cement. US Patent: 2141570.

Marsac, R., Davranche, M., Gruau, G., Bouhnik-Le Coz, M., and Dia, A. (2011). An improved description of the interactions between rare earth elements and humic acids by modeling: PhreeqC-Model VI coupling. *Geochimica et Cosmochimica Acta*, 75(19):5625–5637.

McKelvie, J., Korber, D., and Wolfaardt, G. (2016). *Microbiology of the Deep Subsurface Geosphere and Its Implications for Used Nuclear Fuel Repositories*, pages 251–300. Springer.

Mihelcic, J. and Luthy, R. (1988). Microbial degradation of acenaphthene and naphthalene under denitrification conditions in soil-water systems. *Applied and Environmental Microbiology*, 54(5):1188–1198.

Mihelcic, J. and Luthy, R. (1991). Sorption and microbial degradation of naphthalene in soil-water suspensions under denitrification conditions. *Environmental Science & Technology*, 25(1):169–177.

Novak, C., Borkowski, M., and Choppin, G. (1996). Thermodynamic modeling of neptunium (V)-acetate complexation in concentrated NaCl media. *Radiochimica acta*, 74(s1):111–116.

Onwudili, J. and Williams, P. (2007). Reaction mechanisms for the decomposition of phenanthrene and naphthalene under hydrothermal conditions. *The Journal of supercritical fluids*, 39(3):399–408.

Osman, A., Geipel, G., Barkleit, A., and Bernhard, G. (2015). Uranium (VI) binding forms in selected human body fluids: Thermodynamic calculations versus spectroscopic measurements. *Chemical research in toxicology*, 28(2):238–247.

Osman, A., Geipel, G., and Bernhard, G. (2013). Interaction of uranium (VI) with bioligands present in human biological fluids: the case study of urea and uric acid. *Radiochimica Acta International journal for chemical aspects of nuclear science and technology*, 101(3):139–148.

Öztekin, N., Erim, F., and Basaran, B. (1996). Stability constants of complexes of thorium (IV) with phenolate ions. *Microchemical journal*, 53(2):164–167.

Palmer, J. and Fairhall, G. (1992). The radiation stability of ground granulated blast furnace slag/ordinary Portland cement grouts containing organic admixtures. In *MRS Proceedings*, volume 294, page 285. Cambridge Univ Press.

Park, K., Kwon, T., Park, Y., Jung, E., and Kim, W. (2006). Ternary complex formation of Eu (III) with phthalate in aquatic solutions. In *Transactions of the Korean Nuclear Society Meeting (Autumn, 2006)*.

Parkhurst, D. and Appelo, C. (2013). *Groundwater, Book 6, Modelling Techniques. Techniques and Methods 6–A43*, chapter 43 of Section A. Description of Input and Examples for PhreeqC Version 3 – A Computer Program for Speciation, Batch-reaction, One-dimensional Transport, and Inverse Geochemical Calculations. USGS.

Pathak, H., Kantharia, D., Malpani, A., and Madamwar, D. (2009). Naphthalene degradation by Pseudomonas sp. HOB1: in vitro studies and assessment of naphthalene degradation efficiency in simulated microcosms. *Journal of hazardous materials*, 166(2):1466–1473.

Pedersen, K. (1996). Investigations of subterranean bacteria in deep crystalline bedrock and their importance for the disposal of nuclear waste. *Canadian Journal of Microbiology*, 42(4):382–391.

Rees, T. and Daniel, S. (1984). Complexation of neptunium (V) by salicylate, phthalate and citrate ligands in a pH 7.5 phosphate buffered system. *Polyhedron*, 3(6):667–673.

Rockne, K., Chee-Sanford, J., Sanford, R., Hedlund, B., Staley, J., and Strand, S. (2000). Anaerobic naphthalene degradation by microbial pure cultures under nitrate-reducing conditions. *Applied and Environmental Microbiology*, 66(4):1595–1601.

Ruckstuhl, S., Suter, M.-F., Kohler, H.-P. E., and Giger, W. (2002). Leaching and primary biodegradation of sulfonated naphthalenes and their formaldehyde condensates from concrete superplasticizers in groundwater affected by tunnel construction. *Environmental science & technology*, 36(15):3284–3289.

Schmeide, K., Sachs, S., Bubner, M., Reich, T., Heise, K., and Bernhard, G. (2003). Interaction of uranium (VI) with various modified and unmodified natural and synthetic humic substances studied by EXAFS and FTIR spectroscopy. *Inorganica chimica acta*, 351:133–140.

Shelton, D., Karns, J., McCarty, G., and Durham, D. (1997). Metabolism of melamine by Klebsiella terragena. *Applied and environmental microbiology*, 63(7):2832–2835.

Song, Z., Edwards, S., and Burns, R. (2005). Biodegradation of naphthalene-2-sulfonic acid present in tannery wastewater by bacterial isolates Arthrobacter sp. 2AC and Comamonas sp. 4BC. *Biodegradation*, 16(3):237–252.

Taylor, H. (1997). *Cement Chemistry*. Thomas Telford Ed.

Tucker, G. (1936). Amine salts of aromatic sulphonic acids. US Patent: US2052586A.

Van der Plaats, G., Soons, H., and Snellings, R. (1981). The thermal behavior of melamine. In *Proceedings of Second European symposium on thermal analysis. London: Heyden*, pages 215–7.

Vazquez, G., Dodge, C., and Francis, A. (2008). Interaction of uranium (VI) with phthalic acid. *Inorganic chemistry*, 47(22):10739–10743.

Watkins, S. (1970). Bacterial degradation of lignosulfonates and related model compounds. *Water Pollution Control Federation*, pages R47–R56.

West, J. (1995). A review of progress in the geomicrobiology of radioactive waste disposal. *Radioactive Waste Management and Environmental Restoration*, 19:263–283.

West, J. and McKinley, I. (1983). The geomicrobiology of nuclear waste disposal. In *MRS Proceedings*, volume 26, page 487. Cambridge Univ Press.

Wieland, E., Lothenbach, B., Glaus, M., Thoenen, T., and Schwyn, B. (2014). Influence of superplasticizers on the long-term properties of cement pastes and possible impact on radionuclide uptake in a cement-based repository for radioactive waste. *Applied Geochemistry*, 49:126–142.

Wood, S., Wesolowski, D., and Palmer, D. (2000). The aqueous geochemistry of the rare earth elements: IX. A potentiometric study of Nd^{3+} complexation with acetate in 0.1 molal NaCl solution from 25° C to 225° C. *Chemical Geology*, 167(1):231–253.

Yilmaz, V., Odabasoglu, M., Icbudak, H., and Ölmez, H. (1993). The degradation of cement superplasticizers in a high alkaline solution. *Cement and Concrete Research*, 23(1):152 – 156.

Appendix I

Table S1. Summary of organic SPs (or proxy organics) degradation products found in the literature review.

	SPs source	Degradation product		Reference
		Structure	*Name*	
Aromatic Compounds	Melamine based SPs	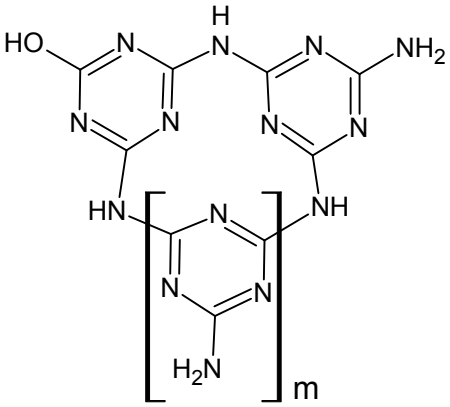	"melem"	(Costa and Camino, 1988)
	Naphthalene based SPs	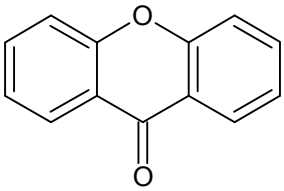	Xanthose	(Onwudili and Williams, 2007)
	Naphthalene based SPs	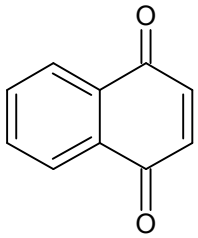	Naphthoquinone	(Onwudili and Williams, 2007)
	Naphthalene based SPs	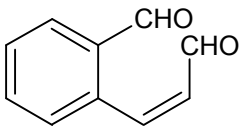	2-Formylcinnamaldehyde	(Lair et al., 2008)

	SPs source	Degradation product		Reference
		Structure	*Name*	
Aromatic Compounds	Naphthalene based SPs	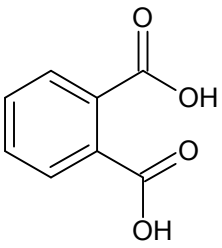	Phthalic Acid	(Onwudili and Williams, 2007)
	Naphthalene based SPs	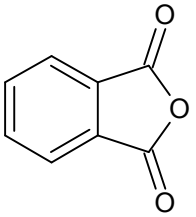	Phthalic anhydride	(Onwudili and Williams, 2007)
	Naphthalene based SPs	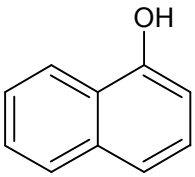	1-Naphthalenol	(Balakrishnan and Reddy, 1968, Bedessem et al., 1997, Kanodia et al., 1988, Lair et al., 2008, Onwudili and Williams, 2007)
	Lignosulfonate based SPs	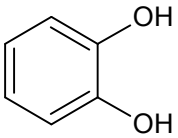	Pyrocatechol	(Brebu et al., 2011)
	Naphthalene based SPs	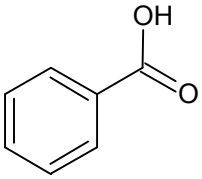	Benzoic acid	(Onwudili and Williams, 2007)

	SPs source	Degradation product		Reference
		Structure	*Name*	
Aromatic compounds	Melamine based SPs	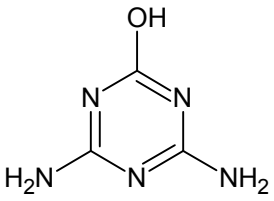	Ammeline	(Jutzi et al., 1982, Shelton et al., 1997)
	Melamine based SPs	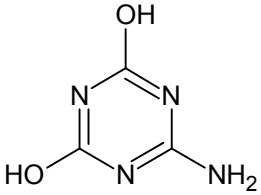	Ammelide	(Jutzi et al., 1982, Shelton et al., 1997)
	Melamine based SPs	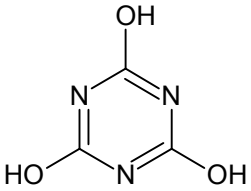	Cyanuric acid	(Jutzi et al., 1982, Shelton et al., 1997)
	Naphthalene based SPs	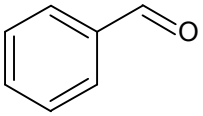	Benzaldehyde	(Onwudili and Williams, 2007)
	Naphthalene and lignosulfonate based SPs,	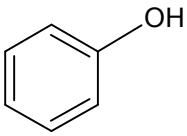	Phenol	(Haars and Huttermann, 1980, Onwudili and Williams, 2007)

	SPs source	Degradation product		Reference
		Structure	*Name*	
Aliphatic Compounds	Naphthalene based SPs	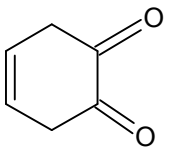	1,2-Benzoquinone	(Onwudili and Williams, 2007)
	Naphthalene based SPs	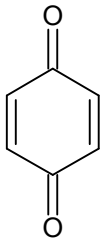	1,4-Benzoquinone	(Onwudili and Williams, 2007)
	Naphthalene based SPs	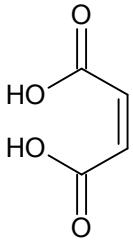	1,4-But-2-enoic acid	(Onwudili and Williams, 2007)
	Melamine based SPs	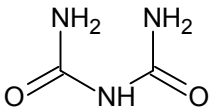	Biuret	(Shelton et al., 1997)
	Naphthalene based SPs	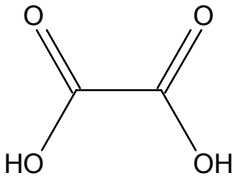	Oxalic acid	(Onwudili and Williams, 2007)
	Naphthalene based SPs	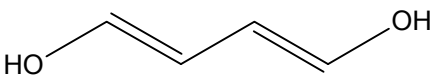	1,4-But-1,3-diol	(Onwudili and Williams, 2007)
	Naphthalene based SPs	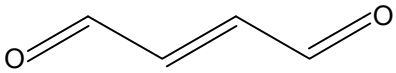	1,4-But-2-dienal	(Onwudili and Williams, 2007)

	SPs source	Degradation product		Reference
		Structure	*Name*	
Aliphatic compounds	Naphthalene based SPs	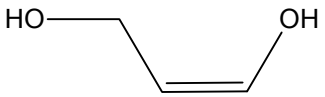	2-propendiol	(Onwudili and Williams, 2007)
	Naphthalene based SPs	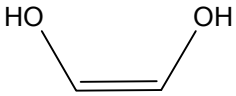	Ethene-1,2-diol	(Onwudili and Williams, 2007)
	Melamine based SPs	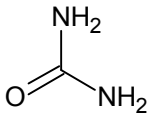	Urea	(Shelton et al., 1997)
	Naphthalene based SPs	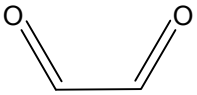	1,2-Dialdehyde	(Onwudili and Williams, 2007)
	Naphthalene based SPs	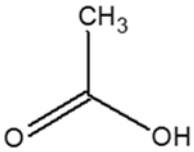	Acetic acid	(Onwudili and Williams, 2007)
Inorganic Compounds	Lignosulfonate and melamine based SPs	NH_3	Ammonia	(Brebu et al., 2011, Costa and Camino, 1988)
	Lignosulfonate based SPs	SO_2	Sulphur dioxide	(Brebu et al., 2011)

Appendix II

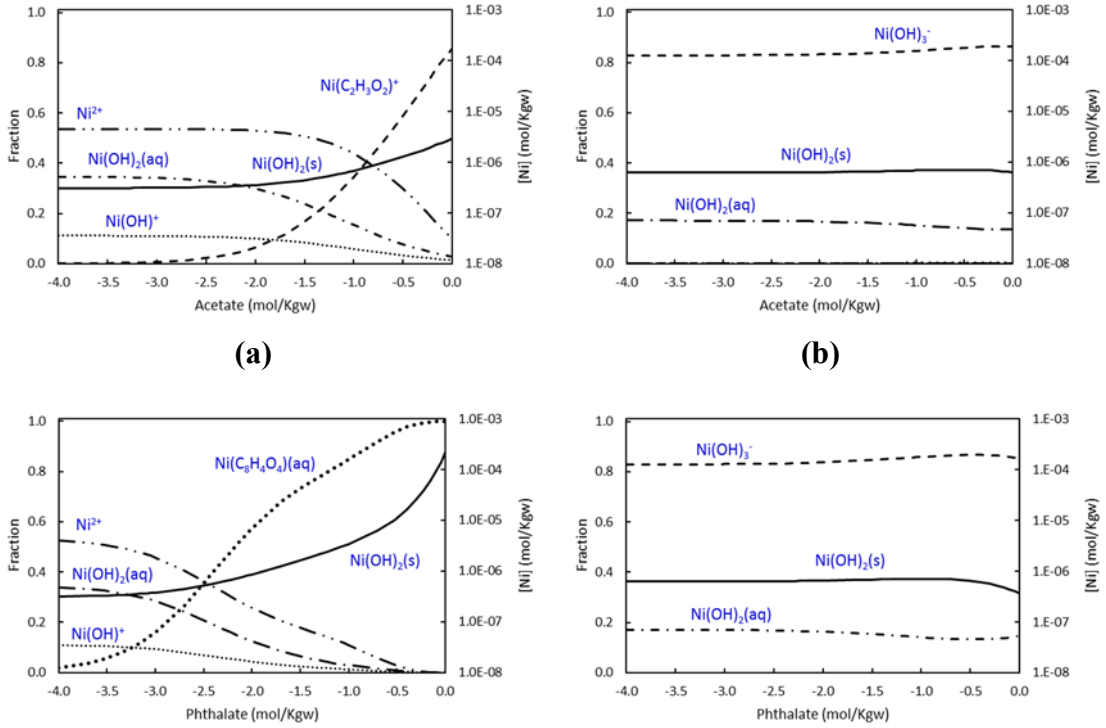

Figure S1. Solubility curve (black solid lines) calculated for $Ni(OH)_2(s)$ in the presence of acetate (a – b) and phthalate (c – d) as a function of the organic concentration. Dashed lines stand for the speciation of Ni in equilibrium with the solid phase. pH fixed as 9 (a – c) and as 12 (b – d). Calcium concentration fixed in all diagrams as 10^{-3} M.

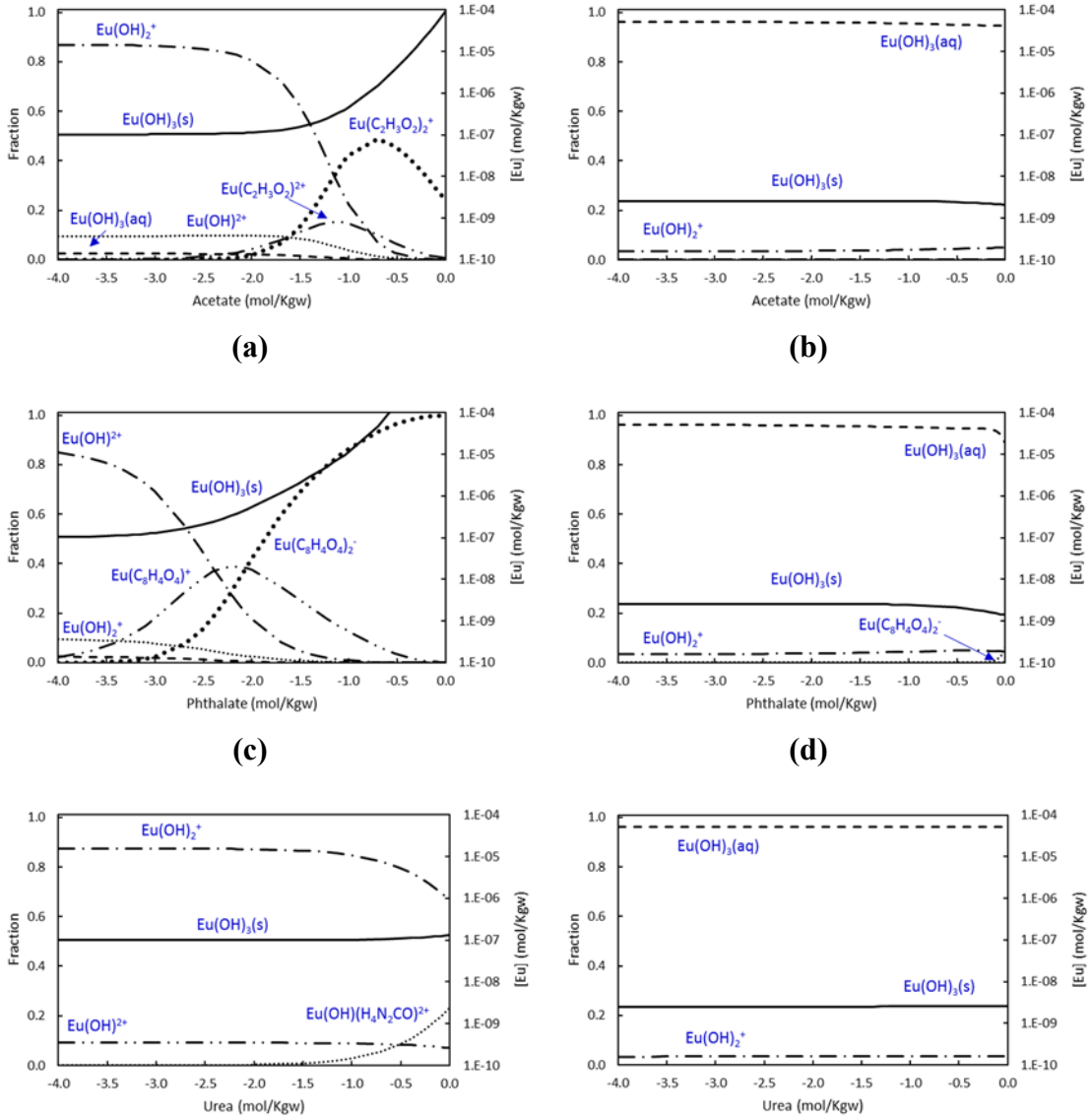

Figure S2. Solubility curve (black solid lines) calculated for $Eu(OH)_3(s)$ in the presence of acetate (a – b), phthalate (c – d) and urea (e – f) as a function of the organic concentration. Dashed lines stand for the speciation of Eu in equilibrium with the solid phase. pH fixed as 9 (a – c – e) and 12 (b – d – f). Calcium concentration fixed in all diagrams as 10^{-3} M.

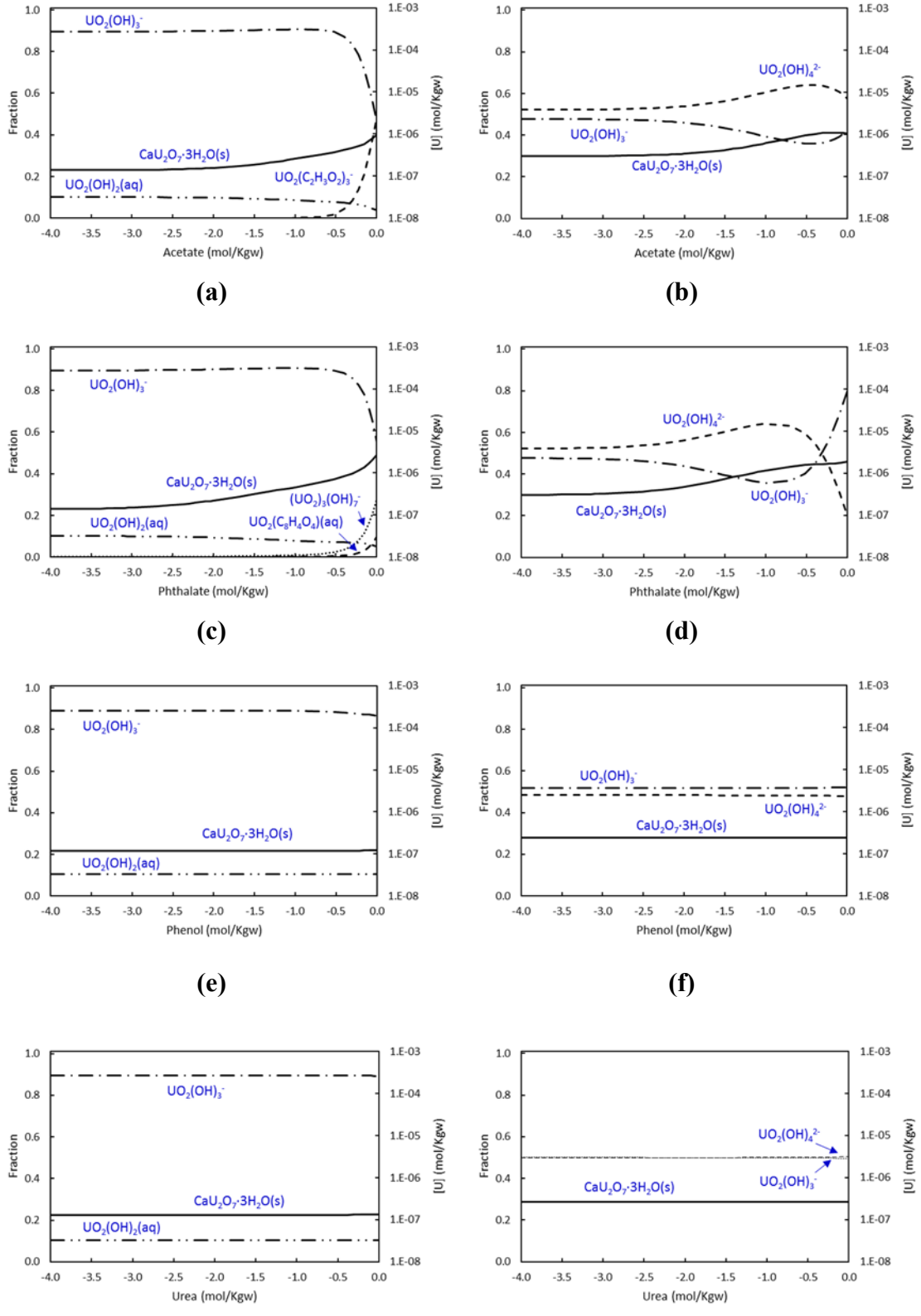

Figure S3. Solubility curve (black solid lines) calculated for $CaU_2O_7 \cdot 3H_2O(s)$ in the presence of acetate (a – b), phthalate (c – d), phenol (e – f) and urea (g – h) as a function of the organic content. Dashed lines stand for the speciation of U in equilibrium with the

solid phase. pH fixed as 9 (a – c – e – g) and 12 (b – d – f – h). Calcium concentration fixed in all diagrams as 10^{-3} M.

Appendix IV

Effect of superplasticizers on Ni behaviour in cementitious environments

David García, Mireia Grivé, Lara Duro, Stéphane Brassinnes & Joan de Pablo

Journal of Radioanalytical and Nuclear Chemistry
An International Journal Dealing with All Aspects and Applications of Nuclear Chemistry

ISSN 0236-5731

J Radioanal Nucl Chem
DOI 10.1007/s10967-018-5837-x

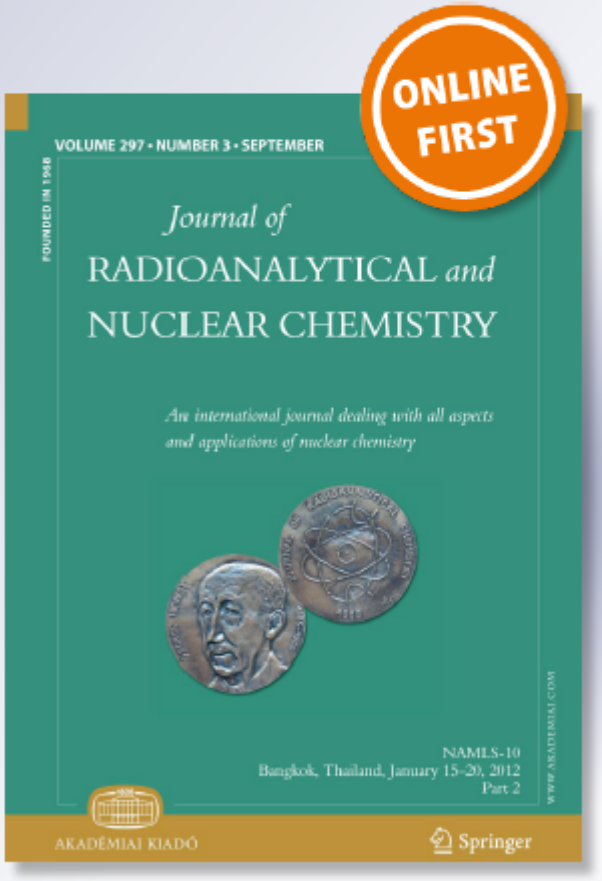

Springer

Journal of Radioanalytical and Nuclear Chemistry
https://doi.org/10.1007/s10967-018-5837-x

Effect of superplasticizers on Ni behaviour in cementitious environments

David García[1] · Mireia Grivé[1] · Lara Duro[1] · Stéphane Brassinnes[2] · Joan de Pablo[3]

Received: 6 February 2018

Abstract
Nickel hydroxide solubility has been studied in this work in different cementitious systems. Our results indicate that once Glenium® 27, cement superplasticizer admixture, is added to water and then mixed with cement, this polymeric material is stabilized and not released back to the aqueous solution, with negligible effects on the mobility of nickel. Contrary to that, when Glenium® 27 is added directly in solution at high dosages, an important effect is observed on nickel behaviour. Thermodynamic calculations indicate that the effect of such component on Ni is likely the effect that other small organics could have over this element.

Keywords Solubility · Nickel · Superplasticizer · Waste disposal

Introduction

SuperPlasticizers (SPs), are common admixtures used in concrete formulations (no more than 5% of those materials by mass of cement [1]) to lower the mix water requirement of concrete [2]. Glenium® 27 is one of the SPs currently defined as a reference material for being used in concrete formulations to build up different structures in the Belgian deep disposal facility for radioactive wastes (Fig. 1). Glenium® 27 is a last generation polymer, also named 3rd SPs generation, composed by a long carbon backbone and carboxylic acids terminations. In contrast with the old generation SPs (Naphthalene-sulfonate, melamine-sulfonate, lignosulfonate, etc.), this kind of SPs improves the dispersion of cement particles by electro-steric repulsions [3].

Nickel is a constituent of repository construction materials (i.e. stainless steel) and thus expected to be encountered in the deep disposal conditions studied in this work [4].

Cementitious materials reduce the mobility of radionuclides contributing to the long-term safety when the containment is lost and radionuclides start to move from the waste package. Once containment is lost, intruding groundwater will be first in contact with the concrete barrier and later with the radioactive waste matrix and waste constituents (i.e. nickel activation products, mainly ^{63}Ni). Groundwater composition will therefore be conditioned by contact with concrete prior to contacting the waste. It is well recognized that cementitious environments produce highly alkaline conditions [5]. Polymeric SPs can be altered under these conditions (degradation, aging, etc.) with the subsequent production of small organic compounds (i.e. gluconate, isosaccharinate, oxalate…) with different chemical properties [6]. Radionuclides form stable complexes with some small organic compounds ([7, 8] and references therein) of similar characteristics of those that may be originated from the alteration of SPs (Fig. 2).

The effect of gluconate, isosaccharinate and oxalate on the behaviour of several radionuclides have been extensively studied during the last years [7–32]. The behaviour of Ni in the presence of these organics has been the focus

✉ David García
david.garcia@amphos21.com

[1] Amphos21, Passeig de Garcia i Fària 49-51, 08019 Barcelona, Spain

[2] Belgian Agency for Radioactive Waste and Enriched Fissile Materials (ONDRAF/NIRAS), Brussels, Belgium

[3] Fundació CTM Centre Tecnològic, Environmental Technology Area, Plaça de la Ciència, 2, 08243 Manresa, Spain

Published online: 30 March 2018

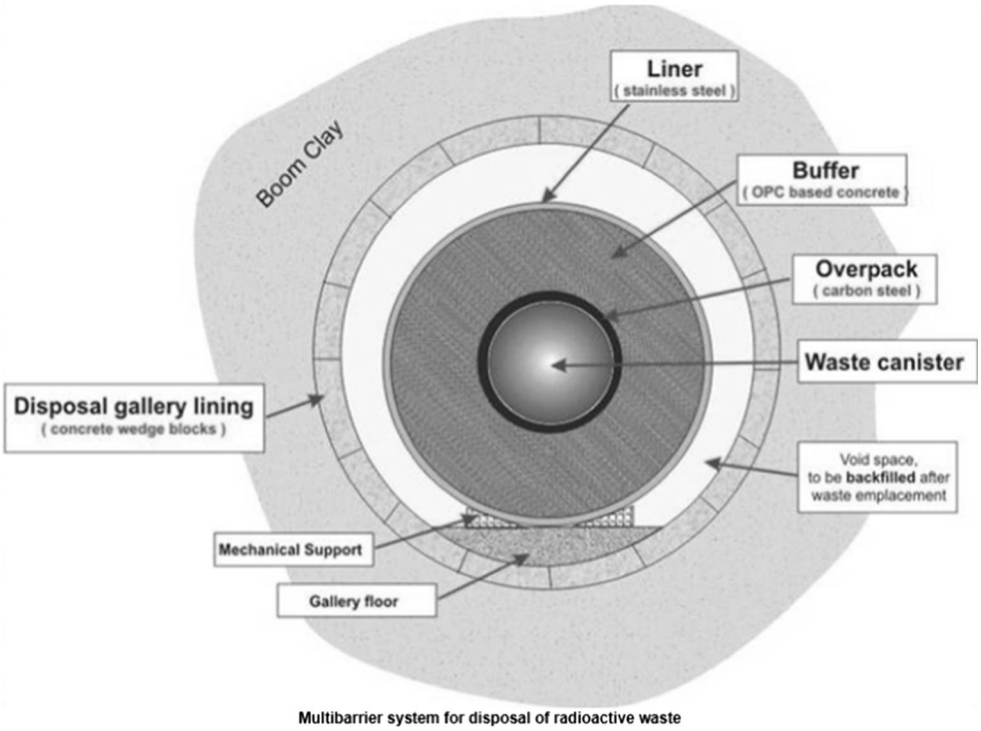

Fig. 1 Multibarrier system for deep disposal of radioactive waste, Belgian disposal "supercontainer" concept [2]

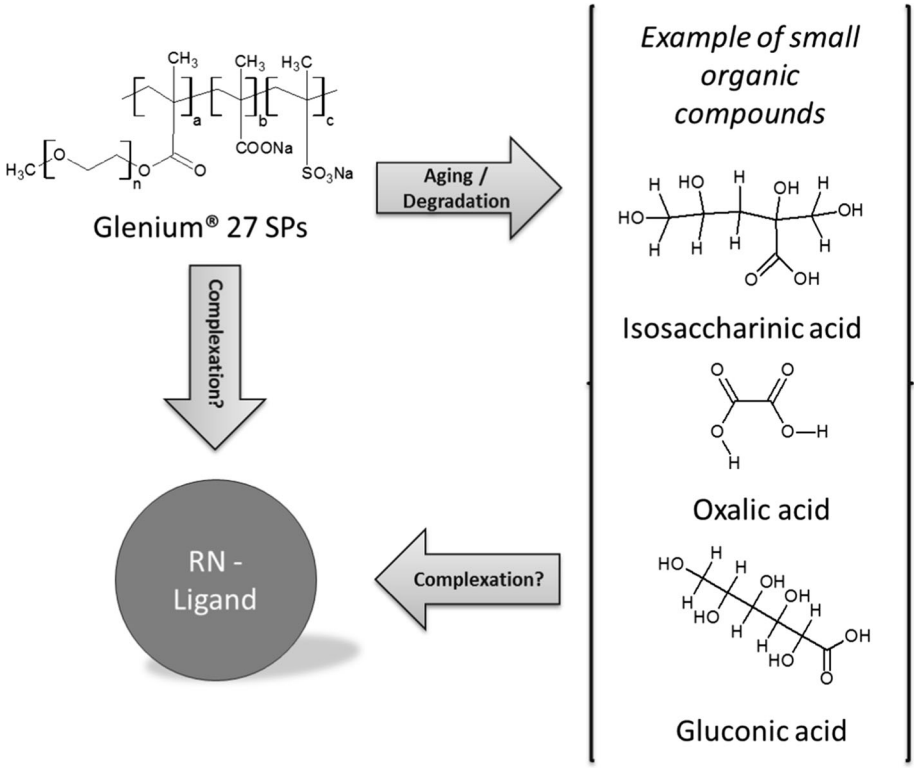

Fig. 2 Tentative sketch of the Glenium® 27, and small organics, behaviour towards radionuclides in the studied system

of detailed sorption and solubility studies under different pH, temperature and ionic strength conditions [12, 14–16, 23, 27, 33]. Important effects on Ni behaviour have been observed due to the presence of these organics, especially at high organic concentrations. In near neutral and slightly alkaline conditions the formation of aqueous species with stoichiometry Ni–L (aq) and Ni–L_2 (aq) (where L stands for the organic ligand) has been reported [14–16, 23, 27]; while in alkaline solutions the formation of ternary species including OH ions in the structure (i.e.,

Ni–OH–L) has been suggested [34]. Under these conditions, the stoichiometry of the formed species (i.e. mononuclear and/or polynuclear) remains uncertain and so do their associated stability constants.

Previous works [35, 36] pointed out that the direct addition of SPs (Rheobuild SP8LS manufactured by BASF [35] and ADVA Cast 551 manufactured by Grace [36]) into solution (i.e. cementitious porewater) increases radionuclide solubility due to organic functional groups—radionuclide interaction. Nevertheless, once SPs are mixed with cement their effect on radionuclide solubility seems to be limited, probably due to a non-specific sorption mechanism of the SPs over the cement surface [35, 37]. Therefore, understanding the nature and strength of the interactions between radionuclides and SPs present in concrete formulations (and their degradation/aging products) deserves focused studies.

In this work, we have studied the effect of a polycarboxylic ether-based (PCE) SPs on the solubility of $Ni(OH)_2(s)$. To this aim, solubility experiments have been set up by working from both, over and under-saturation conditions. The main goal of this study is to quantify the effect of a PCE-SPs on Ni, as well as to get some hints on the nature and mechanism of the interaction. Three different solution compositions were considered: (1) concrete synthetic porewater (CSPW) without organic compounds, (2) leachates of concrete samples without SPs, and (3) leachates of concrete samples containing SPs (Glenium® 27 manufactured by BASF). Results are compared with thermodynamic calculations and available literature data to depict nickel behaviour in the studied conditions. The effect of Glenium® 27 on the behaviour of Ni has been compared with that of other organics, i.e. isosaccharinate.

Experimental

Concrete solid samples

Concrete blocks were prepared following the European standard UNE-EN 196-1 [38]. Raw materials used to do so were (a) cement, CEM I-42.5 manufactured by Holcim Dannes, (b) filler, a limestone material manufactured by Premiacal, (c) aggregates, inert granular materials such as sand, gravel, or crushed stone mainly formed by calcium carbonate and quartz, (d) superplasticizer, Glenium® 27 manufactured by BASF, and (e) water (Table 1). Briefly, raw materials were mixed and left to a solidification period of 24 h at atmospheric conditions (open atmosphere). Two different series (Table 1) were produced one containing Glenium® 27 (G samples) and another one without Glenium® 27 (WG samples). For each of the series, 9 cast of $\sim$ 4 kg per sample were produced. After the solidification period, and according to the European standard UNE-EN 196-1 [38], samples were unmoulded and stored for curing in a climatic chamber for 28 days at 25 °C and 100% of humidity. This time period is necessary to transform raw materials into cement hydrates providing samples with a necessary compressive strength. Once the curing process was over, samples were hand-crushed and sieved at two different size fractions, between 1–4 mm and < 1 mm. Contamination of the samples with metal particles from the crushing materials was prevented in order to avoid unwanted experimental artefacts in the experiments.

Table 1 Amounts and materials used in concrete blocks preparation

	Kg of used raw material	
	Samples WG	Samples G
Cement	5.3	5.3
Filler	1.5	1.5
Aggregate 0/4	10.6	12.7
Aggregate 2/6	8.0	5.1
Aggregate 6/14	8.5	8.5
Glenium® 27	–	0.1
Water	2.8	2.1
Water/Cement ratio (W/C)	0.5	0.4

Concrete porewaters

CSPW was prepared according to [39]. Briefly, the necessary quantities of KOH (Scharlau, Extra pure), NaOH (Scharlau, Extra pure), $Na_2SiO_3{\cdot}9H_2O$ (Sigma, 98% pure), Calcite (Scharlau, Extra pure) and Portlandite (Scharlau, Extra pure) were mixed and left in orbital agitation for 3 weeks. After that time, the solution was filtered through 0.22 μm Nylon filters suitable for use in alkaline conditions. Finally, Na_2SO_4 (Scharlau, reagent grade) and $Al_2(SO_4)_3{\cdot}10H_2O$ (Scharlau, Extra pure) were added to the solution. All handling during CSPW preparation was done in glove box conditions (Jacomex, GP[Concept]-II-S) to avoid $CO_2(g)$ presence.

Concrete leachates with and without Glenium® 27 (henceforth named respectively as G and WG) were obtained after contacting the hand-crushed concrete (1–4 mm and < 1 mm fractions) with MilliQ water for 30 days at a fixed solid/liquid ratio of 10 g L^{-1} according to the granular material leaching standard UNE-EN 12457-2 [40].

CSPW and concrete leachates compositions detailed in Table 2 were in the range of values reported in the literature for similar systems [41]. Ni concentrations in all prepared initial waters were below the limit of detection.

Table 2 CSPW and real concrete leachates compositions obtained in this work

	CSPW	WG < 1 mm	WG 1–4 mm	*G* < 1 mm	*G* 1–4 mm
pH	13.3	12.4	12.4	12.5	12.4
	mol L^{-1}				
TIC	< LOD	1.7×10^{-5}	3.2×10^{-5}	1.7×10^{-5}	2.3×10^{-5}
TOC	–	5.2×10^{-5}	4.7×10^{-5}	1.2×10^{-4}	1.2×10^{-4}
Na	1.2×10^{-1}	1.2×10^{-4}	1.0×10^{-4}	1.2×10^{-4}	9.4×10^{-5}
K	8.2×10^{-2}	4.6×10^{-4}	4.2×10^{-4}	4.3×10^{-4}	3.7×10^{-4}
Ca	1.4×10^{-3}	7.5×10^{-3}	6.6×10^{-3}	6.1×10^{-3}	7.7×10^{-3}
SO_4	1.8×10^{-3}	5.9×10^{-6}	7.7×10^{-6}	8.2×10^{-6}	8.3×10^{-6}
Fe	< LOD	< LOD	< LOD	< LOD	< LOD
Al	7.7×10^{-6}	< LOD	4.8×10^{-6}	< LOD	4.8×10^{-6}
Cl	–	2.1×10^{-4}	2.3×10^{-4}	1.7×10^{-4}	1.5×10^{-4}
Si	6.2×10^{-6}	< LOD	< LOD	< LOD	< LOD
Ni	< LOD	< LOD	< LOD	< LOD	< LOD

Note that CSPW, WG and G stands for Concrete Synthetic PoreWater, concrete leachates without Glenium® 27 and concrete leachates with Glenium® 27 respectively. For each of the leachates two different compositions are reported as a function of the grinding size (< 1 and 1–4 mm)

< *LOD* Below limit of detection

As shown in Table 2 no differences in leachate compositions were observed as a function of the samples grinding size and thus the effect of this parameter in the studied conditions will not be further discussed.

Solubility experiments

Solubility experiments were set up in both, under- and oversaturation conditions under N_2(g) atmosphere (Jacomex, GP[Concept]-II-S), as follows:

- Under-saturation experiments. Commercial $Ni(OH)_2$ (s) (ACROS, analysis grade) was used in the under-saturation experiments. Those experiments were set up by contacting 2 g of $Ni(OH)_2$(s) with 50 mL of media (either CSPW or the leachates), S/L ratio of 40 g L^{-1}. This high S/L ratio was chosen to ensure the presence of unperturbed solid during the whole experiment duration. Solution pH was unaltered after the addition of the solid. The experiments were daily manually shaken over a period of 12 months.
- Oversaturation experiments. Oversaturation experiments consisted in mixing 4 mL of a 10^{-5} M $Ni(NO_3)_2$ solution (0.1 M HNO_3) with 40 mL of media (CSPW or the leachates). After few seconds, the formation of a characteristic green solid suspension was observed indicating the formation of an amorphous nickel hydroxide that was later identified by Scanning Electron Microscopy—Energy Dispersive X-ray spectroscopy (SEM–EDX) and X-Ray Diffraction (XRD). In the case of the leachates, the pH of the solution in the oversaturation experiments was slightly acidified from ~ 12.3–12.4 to final pH values around 12.0. The reason behind this deviation was the addition of the acid Ni stock solution. On the contrary, pH was unaltered in oversaturation CSPW experiments after the acid Ni stock solution addition as the initial pH value in those samples (~ 13.27) was higher than in the leachates (12.3–12.4). The experiments were daily manually shaken over a period of 12 months as in the case of the under-saturation samples.

At given time intervals, weekly sampling at the beginning and monthly sampling when equilibrium was attained, aliquots of the samples were collected, filtered, acidified and analysed for Ni concentration. The filtering process was done with Nylon syringe filters suitable for use in alkaline conditions. In order to check the possible formation of Ni colloid particles in these experiments two different filter meshes, 0.45 and 0.22 μm, were used.

Instrumentation

All prepared waters, CSPW and real leachates generated in this work as detailed in Table 2, were characterised in terms of cations (ICP-OES Thermo Scientific, iCap 6000 series and ICP-MS Agilent Technologies, 7500 CX) and anions (IC, Dionex, model ICS 2000). Total Inorganic Carbon (TIC) and Total Organic Carbon (TOC) were determined with a Multi N/C 3100 equipment manufactured by Analytik Jena. The solution pH was measured with a Crison model GLP 22 pH-meter employing a 52-22

electrode, the system has an associate error of ≤ 0.1. The equipment was calibrated with buffer solutions at pH 11 (Scharlab, Boric acid/Sodium hydroxide/Potassium chloride), 12 (Scharlab, di-Sodium hydrogen phosphate/Sodium hydroxide) and 13 (Scharlab, Potassium chloride/Sodium hydroxide).

Solid samples characterization within this work was carried out by SEM–EDX (FE-SEM—ZEISS Ultraplus, X-Max EDX detector, from OXFORD Instruments) and XRD (PANalytical X'Pert PRO MPD θ/θ powder diffractometer). For XRD, an X-Ray generator formed by a Copper anode and a Wolfram cathode which worked at 40–45 kV and 40 mA. PIXcel and X'Celerator detectors were used for the different samples using monochromator in continuous scanning within a 2-θ range from 4° to 100°.

Thermodynamic calculations

The geochemical code PhreeqC [42] combined with the thermodynamic database ThermoChimie v.9 (https://www.thermochimie-tdb.com/) [43, 44] have been used in the calculations performed in this work. The Davies approach (Eq. 1) has been used for ionic strength corrections

$$\log(\gamma_i) = -Az_i^2\left(\frac{\sqrt{I_m}}{1+\sqrt{I_m}} - 0.3I_m\right) \quad (1)$$

where A is a constant with a value of 0.5 $M^{-1/2}$, z_i stands for the ion valence and I_m stands for the system ionic strength.

Thermodynamic calculations made in this work consisted mainly in solubility and speciation calculations as a function of different parameters like pH, organic concentration and time. The main purpose of these calculations was to get some hints on the behaviour of Ni in the different chemical scenarios studied in this work.

Results and discussion

XRD results

XRD results are presented in Fig. 3 and Table 3, note that two additional peaks appear in the in situ precipitated sample related with the formation of calcium carbonate. Overall, XRD results confirmed that both solids, from over and under-saturation experiments, correspond fairly well in between.

Solubility experiments

As seen in Table 2, concrete leachates and CSPW studied in this work presented a significantly different composition. CSPW was prepared for being representative of a fresh cement state, cement degradation state I [45], and thus its alkali content and pH are higher than in the case of leachates, where the alkali content has already been leached. Concrete leachates studied here are representative of a later cement degradation step governed by portlandite ($Ca(OH)_2$) dissolution and thus presenting a lower pH ($\sim$ 12.5) and higher Ca concentrations in solution [5, 45].

Ni solubility results obtained in this work are shown in Figs. 4 and 5. In CSPW media, equilibrium (i.e. measurements of different samples and replicates do not vary more than 10%) was always reached before 20 days of contact time (Fig. 4). In the case of the solubility experiments with the leachates, whose composition is more complex than that of CSPW media (Table 2), equilibrium was not completely reached (measurements of different samples and replicates vary approx. half and order of magnitude) even after 120 days (Fig. 5). In either the case, obtained results are in fair agreement with previous published studies [46, 47] (Fig. 6). In addition, there are not clear differences between over and under-saturation results, Figs. 4 and 5, indicating fast partial equilibrium in the system.

After 300 days of contact time, no relevant differences between solubility measurements in leachates of concrete samples with (G) and without SPs (WG) in their formulations were observed, in agreement with the very similar TOC levels measured in both cases at the beginning (Table 2) and at the end of the experiments ($10^{-4/5}$ mol L^{-1}). From this observation, it can be concluded that the release of small organic compounds from concrete, due to the SPs degradation or aging to the solution, is negligible after 300 days. This result is in good agreement with the predictions by [37] and results obtained by [35, 48] in similar systems using different radionuclides (Th, Am, etc.).

In CSPW media nickel aqueous concentrations are slightly higher than in leachates. This is presumably because of the chemical hydrolysis of nickel as illustrated in Fig. 6, where one can see a representation of the theoretical solubility of $Ni(OH)_2(s)$ as a function of pH and its underlying aqueous speciation. As seen from this figure the formation of the species $Ni(OH)_3^-$ at higher pH tends to increase Ni solubility. For illustrative purposes literature data obtained in similar conditions as well as data obtained in this work (up to 300 days) is plotted in Fig. 6. As seen in this figure, data obtained in this work is in very good agreement with independent literature data, are slightly lower than the theoretical solubility predicted for $Ni(OH)_2(s)$ with ThermoChimie v.9, although fall within its uncertainty range. Note that the uncertainty associated with the formation of $Ni(OH)_3^-$ species is very large and, consequently the grey shaped zone accounting for the $Ni(OH)_2(s)$ solubility uncertainties in Fig. 6 increases as a function of the participation of this species in Ni hydrolysis scheme. Very recent results in the literature [49] seem to

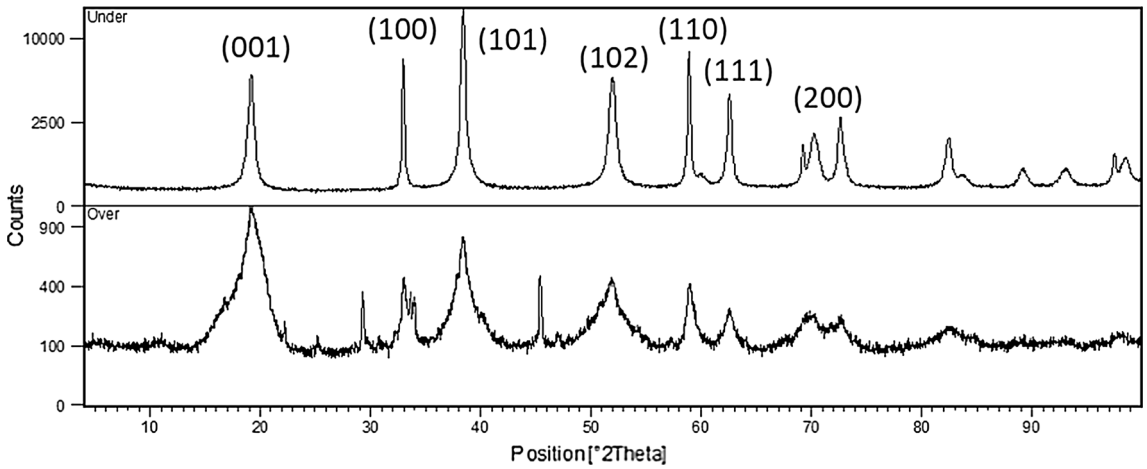

Fig. 3 XRD pattern obtained from solids recovered after finishing the solubility experiments in both under- (commercial $Ni(OH)_2(s)$) and oversaturation (in situ precipitated nickel hydroxide) conditions

Table 3 XRD parameters of the solids recovered after finishing the solubility experiments in both under- (commercial $Ni(OH)_2(s)$) and oversaturation (in situ precipitated nickel hydroxide) conditions

	$2\theta_{CuK\alpha}$ (°)	d (Å)
(001)	19.2	4.6
(100)	33.0	2.7
(101)	38.5	2.3
(102)	52.0	1.7
(110)	59.0	1.5
(111)	62.6	1.4
(200)	72.6	1.3

Diffraction angles are listed for Cu K_α (λ = 1.542 Å) X-ray sources

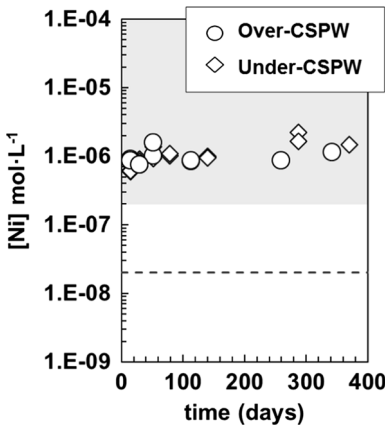

Fig. 4 Ni (mol L^{-1}) as a function of time (days) in over and under saturation experiments. Those results have been obtained in CSPW media, pH 13.2. The grey shaped area stands for $Ni(OH)_2$ theoretical solubility range (including uncertainties) calculated with ThermoChimie at pH 13.2. Dashed line stands for the equipment Limit of Quantification (LOQ). Uncertainties stand for the standard deviation of at least two replicas, and are included within the point size

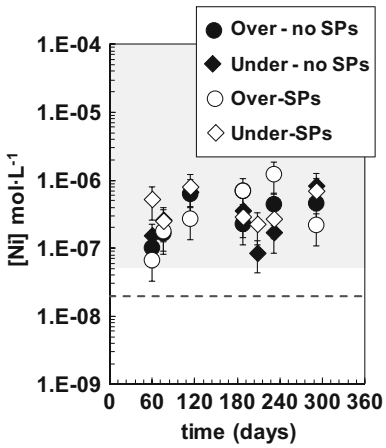

Fig. 5 Ni (mol L^{-1}) as a function of time (days) in over and under saturation experiments. Those results have been obtained in concrete leachates media, WG and G, pH from 12 to 13. The grey shaped area stands for $Ni(OH)_2$ theoretical solubility range (including uncertainties) calculated with ThermoChimie between pH 12–13 without organic presence in the system. Dashed line stands for the LOQ. Uncertainties stand for the standard deviation of at least two replicas

indicate that this species might not be relevant under the studied conditions and that its stability could had been overestimated in previous works.

Solubility experiments with SPs spikes

Additional under-saturation solubility experiments with variable SPs spikes in aqueous solution were performed to decipher whether the studied SPs was able to affect the behaviour of nickel in a cementitious environment. Those experiments were done by using CSPW media, and thus following the same procedure previously detailed, but adding variable SPs dosage ranging from 0.05 to 1.0 mL from the original SPs raw solution. The selected SPs spikes

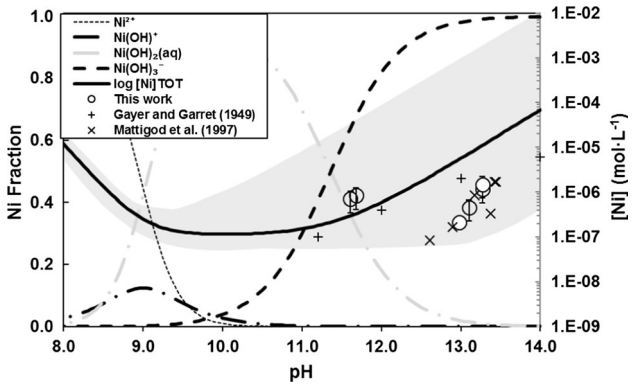

Fig. 6 Theoretical solubility of $Ni(OH)_2(s)$, black solid line, as a function of pH. Circles stand for data obtained in this work up to 300 days in the different studied conditions. Cross and plus symbols stand for independent literature data [46, 47] obtained in similar conditions as the ones we worked with. Dashed lines stand for the fraction of the different Ni aqueous species in equilibrium with $Ni(OH)_2(s)$ in the studied conditions. The grey shaped area stands for $Ni(OH)_2(s)$ theoretical solubility uncertainties as a function of the hydrolysis species. Calculations done with PhreeqC and ThermoChimie v. 9.0 database

gave TOC values in solution ranging from $\sim 1.6 \times 10^{-3}$ to 3.2×10^{-2} mol L^{-1}. Those TOC values are far from being representative of the standard concrete samples (e.g. G samples listed in Table 1) prepared in this work (5.5×10^{-5} mol L^{-1}) but of interest to understand the interaction between nickel and the SPs. Figure 7 presents nickel hydroxide solubility results obtained at variable SPs spikes as a function of the measured TOC. From this figure one can deduce that the presence of SPs in solution clearly enhances nickel solubility in CSPW conditions. TOC values over 3×10^{-3} mol L^{-1} are required to observe an important increase of nickel solubility. Interestingly, at long term, increasing the TOC content from 1.6

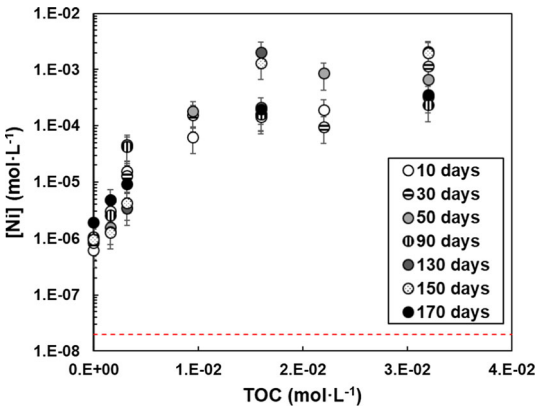

Fig. 7 Ni (mol L^{-1}) as a function TOC (mol L^{-1}) at different times (10–170 days) in under saturation experiments. Those results have been obtained in CSPW media, pH 13.2. Dashed line stands for the LOQ. Uncertainties stand for the standard deviation of at least two replicas

Table 4 Calculated concentrations of ISA, GLU and Oxalate, assuming TOC is completely originated by the presence of each one of the organic ligands in solution

TOC (mol L^{-1})	Isosaccharinic (ISA) (mol L^{-1})	Gluconate (GLU) (mol L^{-1})	Oxalate (mol L^{-1})
1.6×10^{-3}	2.6×10^{-4}	2.6×10^{-4}	7.9×10^{-4}
3.2×10^{-3}	5.3×10^{-4}	5.3×10^{-4}	1.6×10^{-3}
9.5×10^{-3}	1.6×10^{-3}	1.6×10^{-3}	4.7×10^{-3}
1.6×10^{-2}	2.6×10^{-3}	2.6×10^{-3}	7.9×10^{-3}
2.2×10^{-2}	3.7×10^{-3}	3.7×10^{-3}	1.1×10^{-2}
3.2×10^{-2}	5.3×10^{-3}	5.3×10^{-3}	1.6×10^{-2}

Note that these are individual absolute values, i.e. not assuming the presence of an organic cocktail but individual species

to 3.2×10^{-2} mol L^{-1} does not seem to affect nickel behaviour, suggesting steady state conditions. An approximate increase of three orders of magnitude on Ni solubility is observed at the highest SPs spikes. In agreement with our findings here, a solubility increase effect has been also reported by others [36, 50] when studying U, Pu and Am behaviour in cementitious conditions with direct SPs addition in solution. More recently [51], an increase of the solubility of Ni by three orders of magnitude has been found in cement equilibrated porewaters with different SP spikes. Those authors also reported an increase of two orders of magnitude for ^{241}Am and for ^{239}Pu solubilities while in the case of U similar concentrations were achieved with and without SP spikes. It must be notice that the cement equilibrated water used in [51] was obtained after squeezing the concrete samples and thus the authors believe that the agent responsible of controlling U behaviour was already present in the equilibrated water before adding the SP spike.

Nickel theoretical solubility as a function total organic concentration

Small organics (i.e. isosaccharinic acid, gluconate, oxalate, etc.) have a great effect on Ni behaviour and may be used as surrogates to understand the effect of more complex materials like SPs. Kitamura and co-workers [35] studied gluconate as a simple surrogate to represent SPs complexing capacity when studying Th and Am solubilities in similar conditions as the ones presented in this work. The results presented by those authors overestimate Am and Th solubilities almost two or three orders of magnitude assuming gluconate as a SPs surrogate and using the JAEA thermodynamic database in their calculations. In their, study the authors used squeezed cement porewaters and thus as they discussed SPs could be strongly adsorbed in the cement phases preventing its release and its possible

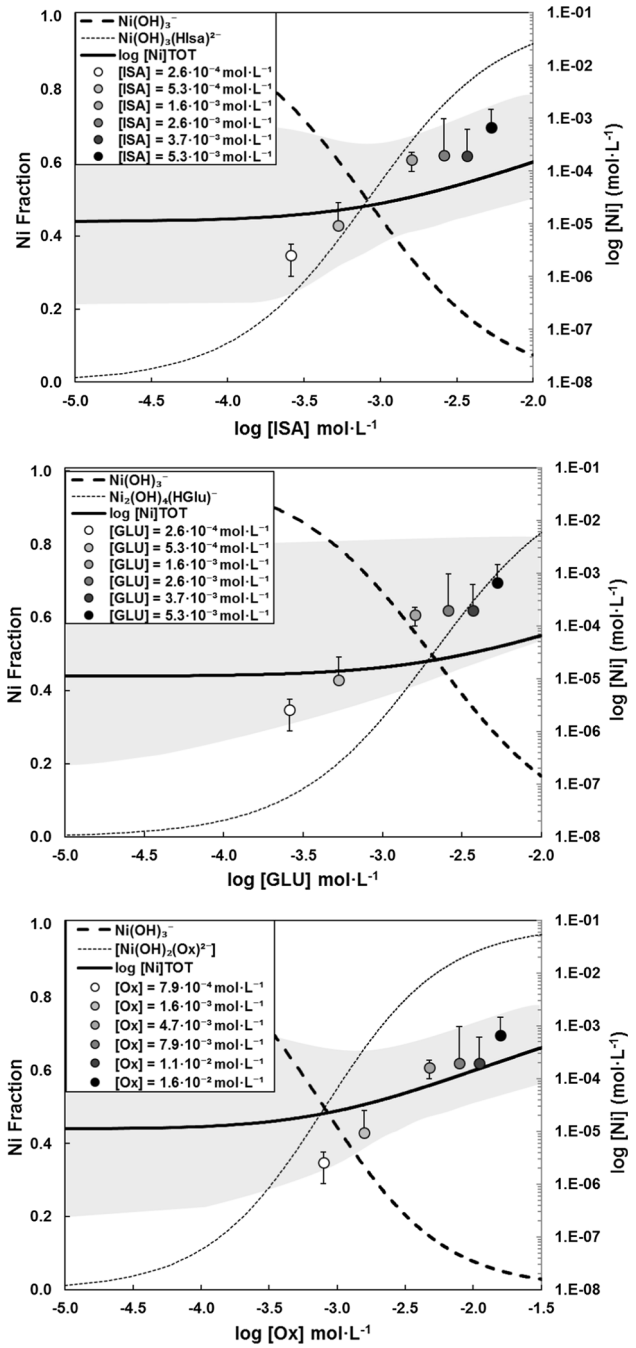

Fig. 8 Theoretical solubility of $Ni(OH)_2(s)$, black solid line, as a function of organic ligand content (mol L^{-1}) in CSPW conditions (pH 13.2). Black dashed lines stand for the fraction of Ni aqueous species in equilibrium with $Ni(OH)_2(s)$ in the studied conditions. Symbols stand for nickel solubility values measured in this work. The grey shaped area stands for $Ni(OH)_2(s)$ theoretical solubility uncertainties as a function of the hydrolysis species. ThermoChimie v. 9.0 together with Ni–OH–Ox ternary species and Ni-GLU data from [15] have been used in these calculations

final effect on radionuclide behaviour. Considering Kitamura et al. [35] work as a reference, and using the TOC data obtained in our work, we have done a similar exercise. If we assume that all measured TOC content in our samples is due to the presence of the organic ligand of interest (isosaccharinic acid, gluconate or oxalate) in solution, we can estimate what would be the concentration of each organic compound in our system through simple stoichiometry relationship (Table 4).

Thermodynamic data for the complexation of Ni with ISA and oxalate ligands is included in ThermoChimie v9. In the oxalate case, ternary species Ni–OH–Ox are expected to form at alkaline conditions [34]. Experimental data for the formation of these species are not yet available and thus not included in ThermoChimie v.9. It is possible to estimate an upper limit for the stability of these species taking into account that the hydrolysis of metal–ligand complexes is always somewhat weaker than the hydrolysis of the hydrated cation itself [34]. In this way, the following upper limits for log K values of formation of Ni–OH–Ox ternary species are obtained (r.1 and r.2).

$$Ni^{2+} + Ox^{2-} + H_2O \rightarrow Ni(OH)(Ox)^{-} + H^{+} \quad \log K < -4.4 \qquad (r.1)$$

$$Ni^{2+} + Ox^{2-} + 2H_2O \rightarrow Ni(OH)_2(Ox)^{2-} + 2H^{+} \quad \log K < -12.6 \qquad (r.2)$$

Ni gluconate complexation is not included in ThermoChimie v.9. Evans and co-workers [14, 15, 22, 23] studied this system in near-neutral and alkaline media (pH from 7 to 13) which is of interest for this work. The authors reported the formation of three different species as a function of the system pH. In the alkaline pH range of interest for the current study, the formation of a polynuclear species ($Ni_2(OH)_4(HGLU)^{-}$) with a log K of −24.6 at I = 0.3 M for r.3 is expected according to Evans and co-workers studies.

$$2Ni^{2+} + HGLU^{-} + 4H_2O \rightarrow Ni_2(OH)_4(HGLU)^{-} + 4H^{+} \qquad (r.3)$$

Considering the organic concentration values listed in Table 4, the thermodynamic data for the Ni-organic species cited above together with the Ni solubility data obtained in this work, a prediction of Ni concentration evolution as a function of the estimated organic content in samples have been done (Fig. 8a–c). The theoretical solubility of $Ni(OH)_2(s)$ calculated with ThermoChimie v.9 as a function of the total organic concentration (ISA, GLU or oxalate) as well as the aqueous speciation of nickel in equilibrium with the studied solid is also shown in these figures for comparative purposes. As seen from these figures, the increase of organic concentrations increases the solubility of $Ni(OH)_2(s)$ through the formation of different aqueous species depending on the studied organic ligand ($Ni(OH)_3(HISA)^{2-}$, $Ni_2(OH)_4(HGLU)^{-}$, $Ni(OH)_2(Ox)^{2-}$). The formation of these species occurs even at low organic

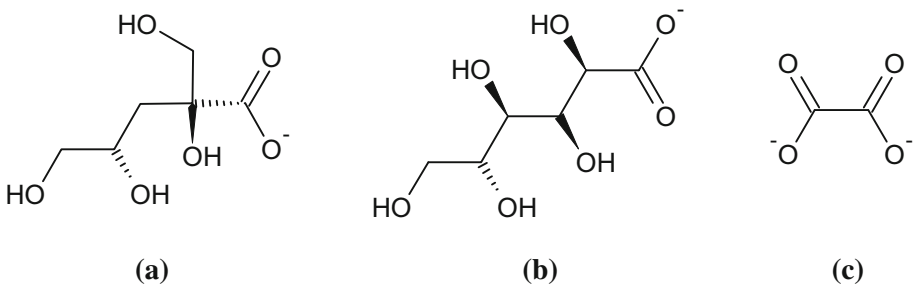

(a) (b) (c)

Fig. 9 Sketch of **a** ISA, **b** GLU and **c** oxalate structures

concentrations (1×10^{-4} mol L^{-1}) and controls the aqueous chemistry of nickel at organic levels above $\sim 1 \times 10^{-3}$ mol L^{-1}.

Experimental Ni solubility data obtained in this work, symbols in Fig. 8, follow the same trend as the theoretical $Ni(OH)_2(s)$ solubility in the presence of small organic ligands; this is Ni concentration increases as the level of organic increases in solution. Nevertheless, at the highest organic concentration there are some discrepancies between predicted and measured Ni concentrations for ISA and GLU systems. Assuming the formation of the ternary species Ni–OH–Ox results in a good fit of the experimental results at higher oxalate concentrations. Is worth mentioning that if we account for the uncertainties of the solid and aqueous Ni species in the system (grey shaped area in Fig. 8a–c), the experimental results may be explained by assuming the presence of either of the organics (ISA, GLU and oxalate) that have been studied here.

As previously explained, PCE SPs are mainly composed by a long carbon backbone and carboxylic acids terminations (Fig. 2), besides different additives (pesticides, herbicides, etc.) added into the SPs cocktail solution to preserve its properties/functionalities. A direct relationship between SPs and ISA/GLU/Oxalate global structures is not straightforward (Figs. 2, 9). A close comparison of "raw" SPs and small organic (ISA, GLU, Oxalate) structures points out that all those compounds have carboxylic or carboxylate terminations in their structure. ISA and GLU presented a similar structure with just one carboxylate member while oxalate is a relatively smaller molecule with two carboxylate terminations. From a chemical reactivity point of view this means that oxalate is a more labile molecule than ISA and GLU. This observation agrees well with the blind predictions presented in Fig. 8, where it was shown that oxalate presented the higher complexing capacity towards Ni.

Conclusions

The solubility of nickel in cementitious environments and the effect of Glenium® 27, a PCE superplasticizer, on its solubility has been studied in this work. The results presented in this work support the selection of Glenium® 27 as a reference SPs for being used in concrete formulations of future radioactive deep disposal facilities.

Nickel solubility values obtained in solutions in the absence of superplasticizers are in fair agreement with previous published studies. Results obtained with the direct addition of Glenium® 27 into the samples indicate that if this polymer is released to the solution, it could cause an important enhancement of Ni solubility in cementitious systems. In the case of leachates, our results indicate that, once SPs is included in the concrete formulation, this polymeric material is stabilized (e.g. adsorbed into the cement phases) and negligible mobilization effects on the behaviour of a trace radionuclide like Ni could be observed. The amount of Glenium® 27 used in the cement formulations is relatively low (TOC $\sim 5 \times 10^{-5}$ mol L^{-1}), and in the unlikely event of a total Glenium® 27 release from the cementitious system, TOC values over 3×10^{-3} mol L^{-1} are required to observe an important increase of nickel solubility; which is far from the real samples measures.

Thermodynamic calculations carried out in this work suggest that, for this specific system, oxalate may be used as a SPs surrogate to reproduce the experimental trends obtained for $Ni(OH)_2(s)$ solubility at variable superplasticizer dosages. In future works the focus should be on characterising SPs structure as well as possible aging/degradation products in cementitious systems for a better process representation.

Acknowledgements The research leading to these results has been funded by the Belgian Agency for Radioactive Waste and Enriched Fissile materials (Ondraf-Niras). Dra. Susanna Valls (UPC, Construction Engineering Department) is acknowledge for their support during concrete samples preparation. We thank two anonymous reviewers for helpful comments on earlier drafts of the manuscript.

References

1. Griesser A (2002) Cement-superplasticizer interactions at ambient temperatures. PhD Thesis, ETH
2. Craeye B, De Schutter G, Van Humbeeck H, Van Cotthem A (2009) Early age behaviour of concrete supercontainers for radioactive waste disposal. Nucl Eng Des 239:23–35

3. Plank J, Pöllmann K, Zouaoui N et al (2008) Synthesis and performance of methacrylic ester based polycarboxylate superplasticizers possessing hydroxy terminated poly (ethylene glycol) side chains. Cem Concr Res 38:1210–1216
4. Rosskopfová O, Galamboš M, Rajec P (2011) Determination of ^{63}Ni in the low level solid radioactive waste. J Radioanal Nucl Chem 289:251–256
5. Taylor HFW (1997) Cement chemistry, 2nd edn. Thomas Telford, London
6. Glaus MA, Van Loon LR (2004) A generic procedure for the assessment of the effect of concrete admixtures on the retention behaviour of cement for radionuclides: concept and case studies. PSI Nr. 04-02
7. Andersson M, Ervanne H, Glaus MA, et al (2008) Development of methodology for evaluation of long-term safety aspects of organic cement paste components. POSIVA Work Rep 2008-28
8. Gaona X, Montoya V, Colàs E et al (2008) Review of the complexation of tetravalent actinides by ISA and gluconate under alkaline to hyperalkaline conditions. J Contam Hydrol 102:217–227
9. Colàs Anguita E (2014) Complexation of Th(IV) and U (VI) by polyhydroxy and polyamino carboxylic acids. PhD Thesis, Universitat Politècncia de Catalunya
10. Allard S (2005) Investigations of α-D-isosaccharinate: fundamental properties and complexation. PhD Thesis, Chalmers University of Technology
11. Allard S, Ekberg C (2006) Complexing properties of alpha-isosaccharinate: thorium. Radiochim Acta 94:537–540
12. Holgersson S, Albinsson Y, Allard B et al (1998) Effects of gluco-isosaccharinate on Cs, Ni, Pm and Th sorption onto, and diffusion into cement. Radiochim Acta 82:393–398
13. Rai D, Rao L, Moore DA (1998) The influence of isosaccharinic acid on the solubility of Np(IV) hydrous oxide. Radiochim Acta 83:9–13
14. Evans N, Warwick P, Felipe-Sotelo M, Vines S (2012) Prediction and measurement of complexation of radionuclide mixtures by α-isosaccharinic, gluconic and picolinic acids. J Radioanal Nucl Chem 293:725–730
15. Evans N, Antón-Gascón S, Vines S, Felipe-Sotelo M (2012) Effect of competition from other metals on nickel complexation by α-isosaccharinic, gluconic and picolinic acids. Mineral Mag 76:3425–3434
16. Warwick P, Evans N, Vines S (2006) Studies on some divalent metal α-isosaccharinic acid complexes. Radiochim Acta 94:363–368
17. Svensson M, Berg M, Ifwer K et al (2007) The effect of isosaccharinic acid (ISA) on the mobilization of metals in municipal solid waste incineration (MSWI) dry scrubber residue. J Hazard Mater 144:477–484
18. Vercammen K (2000) Complexation of calcium, thorium and europium by α-isosaccharinic acid under alkaline conditions. PhD Thesis, Swiss Federal Institute of Technology Zurich
19. Vercammen K, Glaus MA, Van Loon LR (2001) Complexation of Th(IV) and Eu(III) by α-isosaccharinic acid under alkaline conditions. Radiochim Acta 89:393–401
20. Tits J, Bradbury M, Eckert P, et al (2002) The uptake of Eu(III) and Th(IV) by calcite under hyperalkaline conditions: the influence of gluconic and isosaccharinic acid. PSI Nr. 02-03
21. Tits J, Wieland E, Bradbury MH (2005) The effect of isosaccharinic acid and gluconic acid on the retention of Eu(III), Am(III) and Th(IV) by calcite. Appl Geochem 20:2082–2096
22. Warwick P, Evans N, Hall T, Vines S (2004) Stability constants of uranium (IV)-α-isosaccharinic acid and gluconic acid complexes. Radiochim Acta 92:897–902
23. Warwick P, Evans N, Hall T, Vines S (2003) Complexation of Ni(II) by α-isosaccharinic acid and gluconic acid from pH 7 to pH 13. Radiochim Acta 91:233–240
24. Rai D, Yui M, Moore DA, Rao L (2009) Thermodynamic model for ThO_2(am) solubility in isosaccharinate solutions. J Solut Chem 38:1573–1587
25. Zhernosekov KP, Mauerhofer E, Getahun G et al (2003) Complex formation of Tb^{3+} with glycolate, D-gluconate and alpha-isosaccharinate in neutral aqueous perchlorate solutions. Radiochim Acta 91:599–602
26. Bagawde S, Ramakrishna V, Patil S (1976) Oxalate complexing of tetravalent actinides. J Inorg Nucl Chem 38:1669–1672
27. Borkowski M, Choppin GR, Moore RC (2003) Thermodynamic modeling of metal-ligand interactions in high ionic strength NaCl solutions: the Ni^{2+}-oxalate system. Radiochim Acta 91:169–172
28. Borkowski M, Choppin GR, Moore RC (2000) Thermodynamic modeling of metal-ligand interactions in high ionic strength NaCl solutions: the Co^{2+}-oxalate system. Radiochim Acta 88:599–602
29. Borkowski M, Moore RC, Bronikowski MG et al (2001) Thermodynamic modeling of actinide complexation with oxalate at high ionic strength. J Radioanal Nucl Chem 248:467–471
30. Choppin G, Chen JF (1995) Complexation of Am(III) by oxalate in $NaClO_4$ media. In: V international conference on the chemistry and migration behaviour of actinides and fission products in the geosphere, Saint-Malo, France
31. Thakur P, Mathur JN, Dodge CJ et al (2006) Thermodynamics and the structural aspects of the ternary complexes of Am(III), Cm(III) and Eu(III) with Ox and EDTA + Ox. Dalton Trans 40:4829–4837
32. Hummel W, Andereeg G, Rao L et al (2005) Chemical thermodynamics of compounds and complexes of U, Np, Pu, Am, Tc, Se, Ni and Zr with selected organic ligands. Elsevier Science, Amsterdam
33. Peñuela J, Martinez D, Araujo ML et al (2011) Speciation of the nickel (II) complexes with oxalic and malonic acids studied in 1.0 mol·dm^{-3} NaCl at 25°C. J Coord Chem 64:2698–2705
34. Van Loon LR, Hummel W (1995) The radiolytic and chemical degradation of organic ion exchange resins under alkaline conditions: effect on radionuclide speciation. PSI Nr. 95-13
35. Kitamura A, Fujiwara K, Mihara M et al (2013) Thorium and americium solubilities in cement pore water containing superplasticiser compared with thermodynamic calculations. J Radioanal Nucl Chem 298:485–493
36. Young AJ (2012) The stability of cement superplasticiser and its effect on radionuclide behaviour. PhD Thesis, University of Loughborough
37. Wieland E, Van Loon LR (2003) Cementitious near-field sorption data base for performance assessment of an ILW repository in Opalinus Clay. PSI Nr. 03-06
38. AENOR (2005) Methods of testing cement—Part 1: determination of strength. UNE-EN-196
39. Stumpf T, Tits J, Walther C et al (2004) Uptake of trivalent actinides (Curium (III)) by hardened cement paste: a time-resolved laser fluorescence spectroscopy study. J Colloid Interface Sci 276:118–124
40. AENOR (2003) Characterization of waste. Leaching. Compliance test for leaching of granular waste materials and sludges. Part 2: One stage batch test at a liquid to solid ratio of 10 k/kg for materials with particle size below 4 mm (without or with size reduction). UNE-EN 12457-2
41. Castellote M, Andrade C, Castillo A (2009) Characterisation of cementitious matrices for a surface disposal of LLW. Report 19.171. Centro Superior de Investigaciones Científicas - Instituto de Ciencias de la Construccion Eduardo Torroja (CSIC-ICCEJ)
42. Parkhurst DL, Appelo CAJ (2013) Groundwater, book 6, modelling techniques. Techniques and methods 6 A43. USGS

43. Giffaut E, Grivé M, Blanc P et al (2014) Andra thermodynamic database for performance assessment: thermoChimie. Appl Geochem 49:225–236
44. Grivé M, Duro L, Colàs E, Giffaut E (2015) Thermodynamic data selection applied to radionuclides and chemotoxic elements: an overview of the ThermoChimie-TDB. Appl Geochem 55:85–94
45. Krupka KM, Serne JB, Bradbury RJ (1998) Effects on radionuclide concentrations by cement/ground-water interactions in support of the performance assessment of low-level radioactive waste disposal facilities. NUREG/CR-6377 PNNL-11408. U.S. Regulatory Commission
46. Gayer KH, Garrett AB (1949) The equilibria of nickel hydroxide, $Ni(OH)_2$, in solutions of hydrochloric acid and sodium hydroxide at 25°C. J Am Chem Soc 71:2973–2975
47. Mattigod SV, Rai D, Felmy AR, Rao L (1997) Solubility and solubility product of crystalline $Ni(OH)_2$. J Solut Chem 26:391–403
48. Aggarwal S, Angus MJ, Hibbert RC, Tyson A (2001) Radionuclide concentration in cementitious pore-fluids extracted under high pressure. AEA Technology PLC report (for UK Nirex), report number AEAT/R/ENV/0231
49. González-Siso MR, Gaona X, Duro L et al (2018) Thermodynamic model of Ni(II) solubility, hydrolysis and complex formation with ISA. Radiochim Acta 106:31. https://doi.org/10.1515/ract-2017-2762
50. Greenfield BF, Ilett DJ, Ito M et al (1998) The effect of cement additives on radionuclide solubilities. Radiochim Acta 82:27–32
51. NDA (2015) Solubility studies in the presence of polycarboxylate ether superplasticisers. NDA DRP LOT 2: integrated waste management WP/B2/7. NDA